Three Essays On Foreign Exchange Options

HANDING SUN

Three Essays On Foreign Exchange Options

Handing Sun

Durham University Business School

Durham University

A thesis submitted for the degree of

Doctor of Philosophy

2019

Abstract

Over-the-counter (OTC) foreign exchange (FX) option market is the fourth largest derivatives market in the world. However, the extant literature on their pricing is noticeably thin, especially for less actively traded contacts, including FX options on pegged currency pairs.

To price these FX options, firstly I propose a new discrete time exponential-affine model in Chapter 3, with multiple estimation strategies and pricing confidence intervals for the resulting synthetic volatility surface. Then I test the various specifications out-of-sample on five liquid currencies versus the dollar. My specification can be estimated directly from spot FX and deposit rate quotes without recourse to quoted volatility surfaces. Results indicate that both short and long tenor OTC FX options can be accurately priced with minimal calibration.

I further extend the model to allow autoregressive conditional Poisson jumps and multiple factors in the interest rates to handle the latent interest factors in Chapter 4. I propose to adjust the discrete time-step size to price FX options with different tenors, because this adjustment helps preserve the volatility surface dynamic of longer maturity options. In the empirical test on G7 currencies, the model is calibrated

against market FX option quotes to extract the hidden factors in both the domestic and foreign interest rates. Results show that these hidden factors have strong persistence property and certain correlation with the spot variance.

In order to price FX options on pegged FX rates, I propose to capture the trading and realignment uncertainties embedded in the forward FX rate deviation by a jump diffusion model in Chapter 5. Given the fact that transactions of FX option on such currency pairs are currently rare with very limited data available, I design a novel approach to estimate the model parameters. I then apply the proposed approach on four representative pegged currency pairs (EURDKK, USDSAR, USDQAR and USDNGN) and provide option quotes under the market convention. Distinguishing from traditional option pricing model based on historical information, the proposed model is based on forward looking information. These forward price deviation and synthetic volatility surfaces offer an alternative way to manage the FX rate risk for pegged currency pairs.

Declaration

I, Handing Sun, hereby declare that this is entirely my own work unless referenced to the contrary in the text. No part of this thesis has previously been submitted else where for any other degree or qualification in this or any other university.

I would like to dedicate this thesis to my loving parents.

Acknowledgements

This thesis would not have been possible without the help from many great and brilliant people, who generously contributed to this work from all aspects.

First and foremost, I would like to thank my supervisor Professor Julian Williams, for all his support of my Ph.D study and research. He and his enthusiasm, motivation and immense knowledge set an excellent role model for me as a successful researcher and leader. Spending a lot of time working on our projects together, I learned not only academic knowledge and systematically planning, but also positive attitude towards difficulties, discipline and integrity.

Many thanks also to my second supervisor Professor Dennis Philip for his encouragement, insightful comments and guidance. His valuable advices and insights improves my work significantly and broadened my horizons.

Special gratitude goes to Mr. Julian Cook and Fenics Software Inc., BGC Partners. Fenics generously provided funding (RF350084) for my research project, and offered me opportunities to cooperate with their experienced developer team in New York. These experiences strengthen my understanding of the real market and industry. Mr.

Julian Cook gave me valuable advice as an expert in the market. I appreciate his patience and immeasurable amount of support.

I would like to thank my fellow colleagues, Dr. Jing Nie, Dr. Yang Zhang and Xiao Liang for the discussions, for the encouragements, and for the fun we have had in the last few years. The colleagues and friends in PGR DUBS, especially my room-mate Yaodong Liu, have played a substantial role in my academic success and the assistance they offered at critical times is greatly appreciated.

My life has been colourful thanks to Yuebo He. I am charmed by her personality, and shared happiness and sadness in life with her.

Last but not least, I would like to thank my parents for their love and support. They having been giving me the best education they can offer through out my life. I learned how to be a nice and decent person from their daily behaviours.

Contents

List of Figures

Nomenclature

Abbreviations

ACP	Autoregressive conditional Poisson
AD	Affine diffusion model
AJD	Affine jump diffusion model
ASTSV	Affine stochastic term structure with stochastic volatility
ATM	At-the-money
BS	Black-Scholes
BF	Butterfly
BIS	Bank for International Settlements
BV	Bipower variation
c.d.f	Cumulative density function
CF	Characteristic function
CIR	Cox-Ingersoll-Ross process
FX	Foreign exchange
GARCH	The generalized autoregressive conditional heteroskedasticity
GMM	Generalized method of moments
GMT	Greenwich mean time
HN	Heston-Nandi
IMF	International Monetary Fund
LSV	Local stochastic volatility
ME	Mean error
MGF	Moment generating function
MLE	Maximum likelihood estimation
NDF	Non-deliverable forward
ODE	Ordinery differencial equation
OTC	Over-the-counter
OTM	Out-of-the-money
ON	Over night

p.d.f	Probability density function
RMSE	Root mean squared error
RR	Risk reversal
RV	Realized volatility
SW	Spot week
TP	Tripower quarticity
1W/M/Y	One week/month/year tenor

Non-greeks Conventions

$\mathbb{C}$	Complex number
$\mathbb{R}$	Real number
$\widetilde{AT}$	At-the-money, delta neutral straddle
$\widetilde{BF}_{25/10}$	Butterfly at 25/10-delta level
$\widetilde{RR}_{25/10}$	Risk reversal at 25/10-delta level
Ω	Event space
$\mathcal{F}$	σ space
$\mathcal{F}_t$	Filtration
$\mathbb{P}$	Physical probability measure
$\mathbb{Q}$	Risk neutral probability measure
$N(\cdot)$	Standard normal cumulative distribution function
F	Forward rate
c	Call option indicator
p	Put option indicator
$P_c(\cdot)$	Call option dollar price
$P_p(\cdot)$	Put option price
K	Strike price
S	Asset price
x	Logarithm asset price
R	Return
h	GARCH variance
$r_{d/f}$	Domestic/foreign interest rate
J	Poisson process, jumps
$\mathbf{W}$	Brownian motion
t	Time stamp at spot
T	Time stamp at mature date
V	Value of a contingent claim
$\mathbf{H}$	Hessian matrix
$\mathbb{E}$	Expectation

$\mathcal{N}(\cdot)$	Normal distribution
$f(\cdot)$	Characterstic function
$\mathcal{L}$	Likelihood
$\Re(\cdot)$	Real part of a complex number
$\Im(\cdot)$	Imaginary part of a complex number
$D_{t,T}$	Spot rate bias
N_t	Counting process

Greeks Conventions

τ	Tenor
$\Psi(\cdot)$	Characteristic function
σ	Volatility
Δ	Black-Scholes implied delta
μ	Drift
θ	Parameter vector
ϖ	Call/put option indicator
η	Increment

Currencies

AUD	Australian dollar
CAD	Canadian dollar
CHF	Swiss franc
CNY	Chinese yuan
DKK	Danish krone
EUR	Euro
GBP	UK pound
JPY	Japanese yen
NGN	Nigerian naira
NZD	New Zealand dollar
QAR	Qatari riyal
SAR	Saudi riyal
USD	US dollar
XAG	Silver
XAU	Gold

Chapter 1

Introduction

Trader A (Thomson Reuters Dealing message)

''Please, EURUSD 6M 25D fly in 300.''

Broker B (message)

''0.218, 0.318.''

Trader A (message)

''0.318 pls, spot ref 1.1523.''

Broker B (message)

''OK, vol for atm 7.612.''

1.1 Background on the foreign exchange options market

The snippet of conversation above provides a window into the daily life of a foreign exchange (hereafter FX or forex) option trader, with a lot of abstract terminology in the conversation. These traders/brokers are involved in one of the most active and important over-the-counter (OTC) derivatives market, the FX option market.

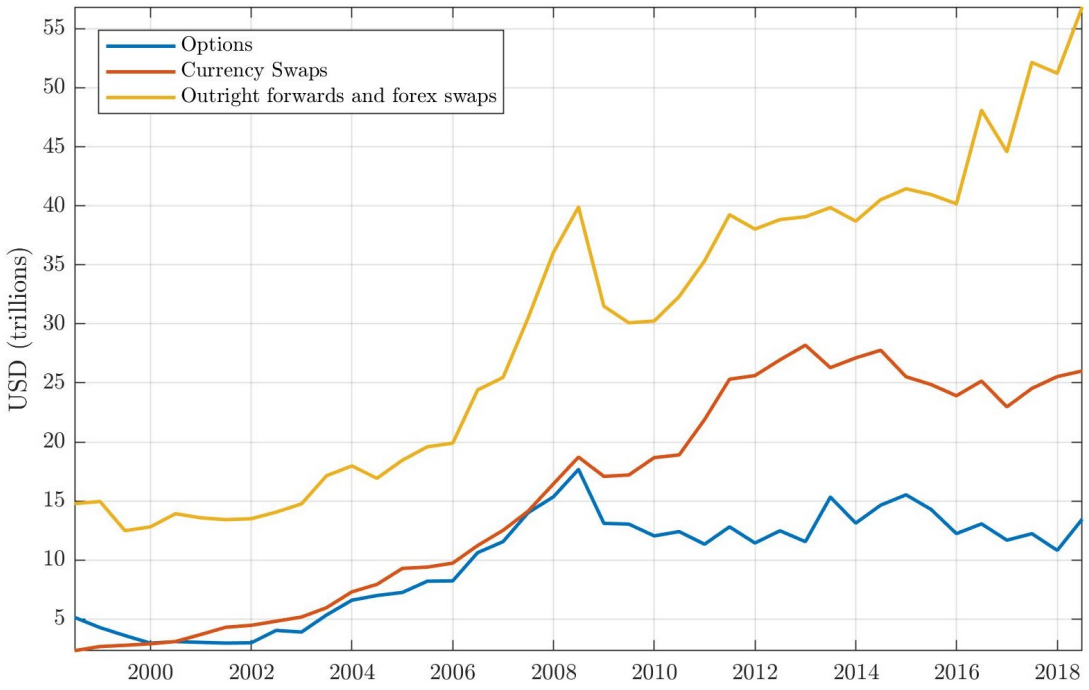

Figure 1.1: BIS OTC FX derivatives notional amount outstanding

Notes: This figure presents the notional amount outstanding (in USD trillions) of OTC FX derivatives, including gold[2], reported by BIS from 1998 to 2018. BIS categorize FX derivatives into options, currency swaps and outright forwards and FX swaps.

According to Bank for International Settlements (BIS)[1], the overall OTC FX derivatives outstanding notional amount (including gold) in 2018 has grown up to \$96 trillion from \$22 trillion in 1998. In Fig. 1.1, we can see that option is a smaller part of the FX derivatives market as a whole. However, FX option market is still comparatively large compared to non FX financial instruments. For instance in the first half year of 2018, the FX option market has outstanding notional amounts of \$13.455 trillion, compared with the OTC credit default swaps (CDS) market being \$8.346 trillion, US equity market being only \$3.027 trillion

[1]Source: Bank of International Settlements OTC derivatives outstanding. URL: https://www.bis.org/statistics/.

and commodity derivatives being around $2.133 trillion.

FX option is a common tool to hedge or to speculate the FX rate risk and shares similar characters with options on other types of underlying assets, such as equity options. As the development of this market, FX option forms its unique trading properties to fit its underlying currency market. The first feature for the forex spot or derivatives trading is that the underlying asset, the currency exchange rate, involves two currencies that both have the potential to be numéraires. It would be ambiguous for both sides of a trade to quote without a set of agreements in advance, such as which currency is the denominator and which currency should be paid as the option premium.

Another character of FX option distinguishing from that of options on other assets is the quotation style. Most options, like equity option, quote dollar value price as strike or moneyness and quote option premium also in the dollar amount. This is the nature quoting style considering most models regard option dollar price as a function of dollar value strike price. However in the FX option market, options are quoted in terms of Black-Scholes implied volatility, and the moneyness of a option is represented by delta, the sensitivity of options to spot FX rate. It is worth noting that for a specified option price, there exists an unique delta and Black-Scholes implied volatility. Thus implied volatility is then a function of delta and time to maturity. Under that Black-Scholes assumption, this function should be flat that implied volatility is constant and not change according to delta and maturity. But what we observe from the market shows that the implied volatility is different for different moneyness. And this forms a volatility surface. Therefore

[2]Gold is included in the data because these precious metals' price are often regarded as "FX" rates, and options on gold and silver can be transacted on the FX option market.

Table 1.1: OTC FX option notional amounts outstanding by currency (in trillion USD)

	Total	USD	EUR	JPY	GBP	CHF	CAD	SEK	Other
H1 2018	13.307	11.165	4.773	2.700	1.037	0.469	0.402	0.212	5.854
H2 2017	10.679	9.003	3.649	2.214	0.894	0.413	0.330	0.212	4.643
H1 2017	12.088	10.606	3.812	2.427	1.074	0.421	0.341	0.180	5.313
H2 2016	11.533	10.384	3.329	2.830	0.798	0.392	0.331	0.211	4.791
H1 2016	12.913	11.499	3.405	2.726	1.332	0.459	0.437	0.164	5.803
H2 2015	12.093	10.683	3.860	2.329	0.845	0.561	0.367	0.144	5.398
H1 2015	14.157	12.464	4.776	3.270	1.019	0.693	0.454	0.097	5.541
H2 2014	15.333	13.604	4.383	3.952	0.880	0.968	0.405	0.100	6.374
H1 2014	14.473	12.289	4.089	3.211	0.987	0.763	0.550	0.136	6.921

Notes: This table presents the notional amounts outstanding of OTC FX option market by currency for the last five years from 2014 to 2018 (half-annually). Data also from BIS OTC derivatives statistics.

the FX options are traded based on an implied volatility surface system, which I will introduce in detail in Chapter 2.

In addition, the following Table 1.1 reports the notional amounts outstanding of OTC FX option market by currency for the last five years. From the table we can observe that most of the options are trading on US dollar (USD) involved currency pairs. For example in the first half year of 2018, 83.9% of the market is trading on USD. Further more, euro (EUR), Japanese yen (JPY) and UK pound (GBP) account for 64.0% of the market. As a result, most of the liquidity of this market concentrates on few currency pairs, leaving the majority of currency pairs very sparsely traded.

Given the characters of this OTC FX option market as presented above, it is natural to bring out the following questions studied in this thesis.

1.2 Main research questions

In this thesis, I will focus on the following questions:

1. (RQ1) For currency pairs with floating exchange rates, is it possible to accurately quote FX option volatility surfaces, when there are only limited option market quotes to calibrate against?

2. (RQ2) Do OTC FX option price and its dynamic contain information that is not fully reflected in the spot FX rate and interest rate? Is there a hidden interest rate factor structure determining yield curves and FX option price?

3. (RQ3) How to price an FX option on a pegged currency pair, particularly when there is no active option market for such currency pairs?

RQ1 comes from the fact that current popular models are not applicable to all the currency pairs. At the moment, the industry standard pricing engine for FX options is local stochastic volatility model (LSV), which combines local volatility models and stochastic volatility models. LSV models are able to generate promising volatility surface but they require actively traded volatility quotes to calibrate their parameters because of the moving market conditions as discussed by Carr and Wu [2016]. This is feasible for about 70 currency pairs that have frequently updated option market. However for any other currency pairs it is then unrealistic to query market quotes for calibration. Due to the demand for trading less active FX pairs, I thereby raise RQ1: how to generate FX quotes when options have been sparsely traded before?

There are a number of techniques that can estimate parameters for processed with latent state variables non-parametrically from spot asset price dynamic,

such as Aït-Sahalia et al. [2015], Andersen et al. [2015] and recent Jacod et al. [2018]. However, the OTC FX option market does not necessarily reflect the same distribution forecast as spot market, therefore the expected return does not align with risk-free interest return as described by the covered interest parity. Previous empirical literature have shown that OTC FX options contains unique information. Beber et al. [2010] point out the implied volatility surface's level, shape, risk premium are affected by different beliefs of the underlying. And the volatility surface shape is also affected by buying pressure based on Bollen and Whaley [2004]'s test. Similarly Hanke et al. [2018] demonstrate that FX options contain betting information on future exchange rates. An important finding by Du et al. [2018] is that, even for G10 currencies, the covered interest parity have been systematically violated since 2008 and as a result forward contracts on these major currencies contains extra information than spot FX rate and risk-free rates.

RQ2 then comes with the observation from practitioners: iIs it possible to accurately price FX option only based on the spot FX rate and interest rates? To be more specific, will the introduction of hidden interest rate factors help improve the pricing performance of models? I will try to answer this question by designing a model that allows multiply interest factors to represent the hidden dynamics embedded in the option price and check the property of these extracted factors.

In contrast to most assets, in the FX market there are a number of currencies that are pegged to other currencies, which means the exchange rates between two pegged currencies is fixed or controlled to maintain the exchange rate within specific margins, substantially altering both the physical and risk-neutral dynamics. Even though the pegged currency rate seems stable, investors holding assets

denominated by such currency are still exposed to currency risk because the authority can change their currency regime under different political or economic environments. However the existing option pricing models are not applicable for pegged FX rates. Not only because there is no option quotes data available in the market for these model to calibrate the parameters, but also the underlying spot process itself has no observed dynamic thus barely contains useful information. Therefore it is impossible to extract future spot rate's distribution information from option or spot markets. And this is RQ3 concerned by this thesis: how to price an option on a pegged FX rate? Where can we find information that infers the distribution of the pegged FX rate in the future?

1.3 Contribution of the thesis

This thesis contributes to the literature by designing FX option pricing models for currency pairs that are sparsely or not traded. These models generalized previous models in the literature and are applied to the less focused assets. These models can then benefit the market makers by expanding the existing market currency pairs coverage. This thesis also investigates the unique factors that drives drift terms of the the FX options.

To answer RQ1, I have proposed and implemented a discrete time model with generalized autoregressive conditional heteroskedasticity (GARCH) type stochastic variance, this model is carefully derived and presented in Chapter 3. I contribute to the literature by modifying the work of Heston and Nandi [2000] to fit the FX settings. This model takes both domestic and foreign interest rates as stochastic factors with N-GARCH type variance processes. This model also has

the potential to include arbitrary number of factors with same structure.

The most important advantage of this discrete time model is that all the parameters can be easily estimated from the spot rates only, without the requirement of option data. This immediately allows option pricing on float currency pairs that are not traded before. For FX option contracts that do have quoting activities, I also provide empirical evidence that given very few market option quotations, the proposed model can be calibrated to have consistently good performance of predicting the volatility level. In addition, I present an error bound calculation algorithm based on delta method. This algorithm can be used to impute sensitivity of the final volatility quotation to the parameter estimation procedure.

Building on the work in Chapter 3 as a foundation, I then extend the discrete model to include autoregressive conditional Poisson (ACP) jump process in the spot return dynamic, and introduce multiple factors in both domestic and foreign interest rates in Chapter 4. These factors are discrete time autoregressive and contain both unique increments and increments correlated with the spot return and spot variance. I then categorize these factors into observed interest rates and hidden factors, which even though are not observed from the market interest rates, but also affect the money account rates of return. I calibrate the model to market FX option quotes to extract the hidden factors in the empirical part of this chapter, and find that for the G7 currency pairs (EURUSD, GBPUSD, AUDUSD, USDJPY, USDCAD, USDCHF), the dynamic of the hidden factors in drift terms tend to have strong autoregressive property and certain correlation with the spot variances.

In this chapter, I also propose to apply the model on different time-step size

corresponding to the time to maturity. This adjustment of time-step is similar to the approach mentioned in Chapter 3 where I use daily data for contracts with tenor shorter or equal to 1Y and monthly data for tenor long than 1Y, but with a more flexible adjustment rule. This change in time-step size compensates the over mean reverting property of the variance process especially when tenor is large and requires large number of iterations. Thus the proposed method keeps more variance dynamic for long maturity options.

I fill a gap in the literature of option pricing for pegged FX rates in Chapter 5. By observing the forward FX rate market for the pegged currency rates, I identify the synthetic spot FX rates and spot rate bias. To capture the dynamic of these identified processes, I then propose an simply but effective affine jump diffusion model and provide an approach to estimate the model based on different types of spot rate bias. Because the model is calibrated against the forward-looking forward FX rate market, it contains the market's outlook of the future information instead of the traditional backward-looking model estimation based on historical prices. Here I specify two types of risks for pegged currencies, trading uncertainty captured by the diffusion part of the model, and currency arrangement realignment uncertainty modelled by the jump part of the model. Finally I adjust the risk neutral probability measure to include the spot rate bias and match the real market forward FX rates, and provide the closed form option price under this measure. I test the model on four classic pegged currency pairs, i.e. EURDKK, USDSAR, USDQAR and USDNGN, in the empirical part of this chapter. The model implied synthetic volatility surface contributes to the literature by offering an alternative risk measure for these "ignored" currency pairs.

1.4 Structure of the thesis

The reminder of this thesis is structured as follows. I firstly present some essential knowledge of the FX option market conventions in Chapter 2. Chapter 3 introduces and modifies the existing GARCH type discrete option pricing model to the FX option market and tests its performance given few market FX option quotes in the empirical experiments. In Chapter 4, I derive a closed form solution to the proposed discrete FX option model with ACP jumps and multi-factor interest rates. The character of hidden factors in interest rates is studied in the empirical part based on the G7 currencies. In Chapter 5, I design a model to price FX options on pegged currency rates and test its performance on four sets of pegged currency pairs. Chapter 6 concludes this thesis. All chapters are self-contained and can be read independently of each other.

Chapter 2

Market Conventions and Relative Models

The exchange rate (FX) is the amount of currency required to buy 1 unit of another currency. So the exchange transaction involves buying/selling one target currency and selling/buying the other currency at the same time. Based on the trader's point of view, we call one leg of this pair domestic currency, and the other one foreign currency. Sercu and Uppal [1995] provides definitions of various concepts in the area and Backus et al. [2001] presents an mathematical description of the economy and exchange rate movements. In the last section of this chapter, I will introduce briefly about several important existing models.

2.1 FX spot market conventions

A simple contract can have two quotation styles, domestic currency per foreign currency or foreign currency per domestic currency, because there are two money

Table 2.1: Currency pair quotation conventions example

	GBP	USD	JPY	CHF	AUD	CAD	NZD
EUR	EURGBP	EURUSE	EURJPY	EURCHF	EURAUD	EURCAD	EURNZD
GBP	-	GBPUSD	GBPJPY	GBPCHF	GBPAUD	GBPCAD	GBPNZD
USD	-	-	USDJPY	USDCHF	AUDUSD	USDCAD	NZDUSD
JPY	-	-	-	CHFJPY	AUDJPY	CADJPY	NZDJPY
CHF	-	-	-	-	AUDCHF	CADCHF	NZDCHF
AUD	-	-	-	-	-	AUDCAD	AUDNZD
CAD	-	-	-	-	-	-	NZDCAD

Note: In the table, I list the conventions for some main currency pairs' quotation. Normally the market convention tends to order the two currencies in a way that the resulting FX rate is larger than one.

market accounts as numeraires in one FX transaction. The terms of domestic and foreign here can be ambiguous in the sense that the two counterparts would both naturally think they are the domestic investor. In this market, it is purely market convention to call one of the leg domestic currency and not the other way around. To be more clear, we list some of the currency pair quotation conventions in Table 2.1.

Transaction settlement time is also an important rule in FX market. The payment of the two side of the trade generally are made on a later date which is often known as the spot date, which is later than when transaction is agreed. For most of the cases, FX trades settle two business days after the initial trade date, known as T+2 settlement. Exceptions as T+1 settlement can also be found, such as for USDCAD, USDTRY, USDRUB, EURTRY, EURRUB, CADTRY, CADRUB and TRYRUB. "Two business days" here can also refer to different duration for a global transaction. This period takes the holidays and other non-trading days from both domestic and foreign countries into consideration, thus varies from one trade to another. The character of arbitrary settlement time introduces more FX risk into the transactions.

Table 2.2: Volatility surface of EURUSD on October 19th, 2018

	$\widetilde{AT}$	$\widetilde{RR}_{25}$	$\widetilde{BF}_{25}$	$\widetilde{RR}_{25}$	$\widetilde{BF}_{10}$
1D	4.340/5.630	-1.135/-0.235	-0.170/0.470	-1.910/-0.365	-0.110/0.920
1W	6.925/7.525	-1.075/-0.655	-0.005/0.295	-1.845/-1.125	0.155/0.635
1M	7.000/7.200	-0.980/-0.840	0.095/0.195	-1.680/-1.440	0.310/0.470
6M	7.455/7.655	-1.315/-1.175	0.240/0.340	-2.310/-2.070	0.775/0.866
1Y	7.605/7.805	-1.340/-1.200	0.300/0.400	-2.385/-2.145	1.020/1.180
18M	7.825/8.035	-1.230/-1.080	0.300/0.405	-2.180/-1.930	1.015/1.185
2Y	7.940/8.165	-1.175/-1.020	0.305/0.415	-2.090/-1.820	1.065/1.245

Note: This table presents volatility surface data of EURUSD on October 19th, 2018. It includes the volatility bid and ask quotes with tenor from one day up to 2 years. $\widetilde{AT}$ is the al-the-money volatility, $\widetilde{RR}$ is the risk reversal and $\widetilde{BF}$ is the butterfly. These quotes describe the shape of the volatility surface, and I will introduce them later in this chapter.

2.2 FX option quotation style

The OTC FX option market displays quotes in a way that is quite different to the equity or bond option markets and further transformations of the option price are needed to allow comparison with market quotes. Overall, FX option prices are displayed in the form of five quotes that can be used to form the European volatility surface. Table 2.2 is a snapshot of EURUSD volatility surface data on October 19th, 2018. Here $\widetilde{AT}$ is the al-the-money volatility, $\widetilde{RR}$ is the risk reversal and $\widetilde{BF}$ is the butterfly. These quotes represent the relative level of volatilities at certain moneyness points and describe the shape of the volatility surface. I will introduce the calculation of these quotes in Section 2.2.1, Section 2.2.3 and Section 2.2.2.

In each case the quote is given in the units of Black-Scholes implied volatilities. For equity options, the volatility smile describes that implied volatility is a function of strike price. However for FX options, the options are also not quoted

by strike, but by one of the Greeks, delta. Hence the quoted European surface for OTC FX option is formed over five deltas, 10- and 25-delta put and call and the at the money delta. Thus the steps to calculate an option price for a particular tenor are as follows. Collect five quotes from the market, giving a 10- and 25-delta butterfly ($\widetilde{BF}_{25}, \widetilde{BF}_{10}$), a 10- and 25-delta risk reversal ($\widetilde{RR}_{25}, \widetilde{RR}_{10}$) and an at-the-money ($\widetilde{AT}$) volatility. Using the quotes we have then compute the European volatilities for five points (10-delta and 25-delta puts and calls and the at-the-money). Based on these quotes, the conventional dollar value strike price and option premium can be calculated correspondingly. I will introduce butterfly, risk reversal and at-the-money in detail in later sub-sections.

A client taking a bid or ask position in the OTC FX option can then compute the strike and option premium by applying their particular discount rate using the volatility surface computed from the quoted prices. Whilst all quotes are based on Black-Scholes-Merton implied volatilities, this should not be confused for the actual process presumed to drive the market. The Black-Scholes-Merton implied volatilities actually act as a device for presenting a normalised price that can easily be compared across tenors and deltas. The relative values of the risk reversals and butterflies provide guidance on the anticipated skew and kurtosis of the market.

Common industrial practice (for instance the approach used in the most popular pricing software) is to use a spline (such as a cubic spline), or SABR model, to fill in the gaps between the 10-delta call and the 10-delta put. Pricing options at put and call deltas of less than 10-delta is problematic. Polynomial extrapolation can lead to nonsensical negative volatilities or explosive values that result in uncomputable call prices. The parametric structure of polynomial extrapolation

can go to infinite to quickly.

Before discuss the volatility, we should firstly understand the delta that FX option uses. Delta is the first order derivative of the option price with respect to the changes in the currency price. So different types of quotation for the price will lead to different types of delta. In essence OTC FX options use volatility as a normalised price, when a firm quotes a volatility the individual price that a counter-party will pay, will vary slightly depending on a variety of specific factors, notably any counter-party valuation adjustments and this is not part of the baseline pricing structure.

For domestic investors, when the premium is expressed and actually exchanged in domestic currency, the premium is itself risk free and adds no further complexity to their risk portfolio. Thus no premium adjustment is needed under this circumstance. But for a foreign investor who has to accept the domestic currency as the premium, the premium is no longer risk free and constitutes an extra currency risk. As a result, they will calculate the premium adjusted delta.

For a given currency pair, whether to adjust the premium or not and hence use pips or percentage delta depends on the choice of premium currency. The premium adjustment and percentage delta are applied when the premium is expressed in foreign currency, for example as most developing currencies versus US dollar.

The at-the-money and 25- and 10-delta put and calls are the five benchmark points required to build the FX volatility surfaces. We will denote these five points as $\sigma_j(\Delta)$, where $j \in \{p, c\}$ and $\Delta \in \{50, 25, 10\}$ respectively represent put or call options and their corresponding delta. Another characteristic of the FX option is that the market does not directly quote the volatility implied by a

single European option as above, but the volatility describing specific strategies instead. We denote the strikes corresponding to the strategies as $K_j(\mathscr{Q})$, where $\mathscr{Q} \in [\widetilde{AT}, \widetilde{BF}_{25}, \widetilde{BF}_{10}, \widetilde{RR}_{25}, \widetilde{RR}_{10}]'$ indicates the vector of quote types at their deltas. In our notation $\Delta_j(K, \sigma)$ denotes that delta Δ is a function of strike price K and volatility σ.

With the observed option quotes, one should be able to construct the volatility surface that has volatility as a function of the delta value. Then for a target delta, a unique dollar value strike price can be found through one of the equations: $\Delta_{S;pips} = \varpi \exp(-r_f \tau) N(\varpi d_1)$, $\Delta_{S;\%} = \varpi \exp(-r_d \tau) \frac{K}{S(t)} N(\varpi d_2)$, $\Delta_{f;pips} = \varpi N(\varpi d_1)$, or the $\Delta_{f;\%} = \varpi \frac{K}{F_{0,T}} N(\varpi d_2)$ where σ is the corresponding volatility and Δ is the target moneyness delta. The choice of delta equation depends on the convention of the relative currency pairs. Then the option premium that the trader should pay in this deal is simply the value that plugging the strike price and corresponding volatility into the Black-Scholes option pricing engine, as the normal equity options.

2.2.1 At-the-money, $\widetilde{AT}$

For $\widetilde{AT}$, the at-the-money strike can be interpolated as either the forward price or the strike for building a delta neutral straddle. The first case is straightforward, as

$$K(\widetilde{AT}) \equiv F(t, T).$$

This convention is used only when the currency pair is USD against a currency from a Latin American emerging market.

In the second case, at-the-money refers to the quoted volatility $\widetilde{AT}$ and its

corresponding strike $K(\widetilde{AT})$, which can be used to construct a straddle that eliminates delta, whereby

$$\Delta_p(K(\widetilde{AT}), \widetilde{AT}) + \Delta_c(K(\widetilde{AT}), \widetilde{AT}) = 0,$$

which is the quotes delta-neutral straddle. This straddle is most actively traded product since it is the purest way to buy a volatility at the middle level of strikes. For a straight Black-Scholes-Merton quoted forward pips delta, $\widetilde{AT} = \sigma(50)$.

2.2.2 $1vol$-butterfly, $2vol$-butterfly, $\widetilde{BF}$

The term 'Butterfly' in the market quotation refers to a single approximated volatility premium, which if added to the at-the-money volatility can be used to price a market strangle that longs out-of-the-money put and call options at the same delta level. In the preceding academic literature this market strangle is usually approximated by butterfly. The market quotation convention is confusing here. Commonly the OTC FX option tickers for market strangles are BF or B10 for 25- and 10-delta quotes respectively. Unfortunately, for heavily smirked European surfaces the straight forward $2vol$-butterfly can diverge substantially from the $1vol$ butterfly market strangle. This kind of approximation is based on the assumption that the skewness of the volatility smile is neglected. Note that the strikes of the put and call options can be calculated by equalling delta to 0.25 or -0.25 with a constant volatility $(\widetilde{AT} + \widetilde{BF}_{25-1vol})$. So we have

$$\begin{aligned}\Delta_p(K_p(\widetilde{BF}_{25-1vol}), \widetilde{AT} + \widetilde{BF}_{25-1vol}) &= -0.25 \\ \Delta_c(K_c(\widetilde{BF}_{25-1vol}), \widetilde{AT} + \widetilde{BF}_{25-1vol}) &= +0.25.\end{aligned}$$

Note that here we apply the same volatility premium $\widetilde{BF}_{25-1vol}$ to both call and put options. For brevity we term this butterfly a $1vol$-butterfly and this is the

quotation in the FX option market.

The way to calculate $1vol$-butterfly is somehow complicated. In most of the academic literature, we would use another way to quote butterfly, which demonstrates the volatility surface shape more intuitively. This is denoted as a $2vol$-butterfly to correspond to the actual skew volatility surface. The $2vol$-butterfly is defined as the average volatility of the 25/10-delta call and 25/10-delta put, expressed as a premium over the at-the-money volatility:

$$\widetilde{BF}_{25/10-2vol} = (\sigma_c(25/10) + \sigma_p(25/10))/2 - \widetilde{AT}.$$

Even though this is the actual butterfly derived directly from the volatility surface, the market quotations are always in the form of a $1vol$-butterfly (market strangle). As such, we then need to compute the $1vol$-butterfly to generate the right market quotation after we build the volatility surface. Notice that the volatility smile is generally not symmetric; therefore the assumption of $1vol$-butterfly that 25-delta call and 25-delta put have the same quote $\widetilde{AT} + \widetilde{BF}_{25-1vol}$ is not supported. However, the aggregate market strangle price under the actual volatility smile should be identical to the equivalent aggregate price for the same market strangle instrument, under the biased assumption.

2.2.3 Risk reversal, $\widetilde{RR}$

Risk reversal is used by market participants to understand the anticipated skewness of the terminal distribution by tenor, and is relatively easy to compute as the difference in the volatilities of call and put options with the same delta. Hence

the 25-delta risk reversal (henceforth referred to as $\widetilde{RR}$) is computed from:

$$\widetilde{RR}_{25} = \sigma_c(25) - \sigma_p(25),$$

and $\widetilde{RR}_{10}$ apparently follow the same rule.

2.3 Quoting volatility

From the previous section we can see that in the FX option market options are quoting in terms of implied volatilities, and replacing strike prices with delta of the option. This quotation style may be difficult to understand for someone who is new to the market, but this is actually a smart and efficient way of quoting, especially in such a mature OTC market for professional participants. Once the implied volatility and delta has been decided, the dollar value strike price and option premium can be calculated given the spot FX rate and interest rates based on the standard Black-Scholes option model and delta formula.

Quoting in this way allows the traders not to worry about the fluctuation of the FX spot rates while negotiating about the deal. Because the counterparts agree on delta and volatility on a deal, not strike price or option dollar price, the real strike level and option price are not determined before closing the deal. Only after the agreement is made, the absolute strike and option price will then be calculated based on the market convention and BS model. Also traders in this market tend to construct delta-hedged, gamma-hedged or Vega-hedged portfolio positions instead of single put or call option. A trader can be sure about his or her position is correctly hedged under this quotation style.

2.4 Computing option quotes from the FX volatility surface

Building a European volatility surface from market quotes is straight-forward and thoroughly covered in the practitioner literature; see for instance Clark [2011] and Castagna and Mercurio [2007] for an overview of this procedure. However, 'bottom-up' computation of the surface and identification of the error bounds is completely absent in the literature and not entirely straightforward. We also need to make use of the delta method once more to determine the actual error bounds on the quotes given the noisy preceding estimation.

As mentioned in sections above, there are five important quotes (two butterflies, two risk-reversals and the at-the-money straddle) over a range of deltas. With the delta/volatility combination, strike prices and options prices can be easily recovered using the Black-Scholes formula. Some data vendors such as Thomson–Reuters provide cubic spline interpolated European surfaces by delta by polling quotes from the major broker dealers. For deltas outside of the 10-put to 10-call range, fitting a structural model such as a one- or two-factor Heston, the SABR or the local stochastic volatility models by tenor provides a useful approximation.

Overall, the task proceeds as follows: generate a smooth surface for the option price as a function of strike from the model parameters; compute the implied volatility for each point on the surface and then the resulting delta; interpolate the deltas at the desired market quotes to generate the volatility by delta; and then use these tuples to build the quotes.

I start with the options prices by strike from our preceding model specification

and then compute the options prices by Black-Scholes volatility and delta. I presume that the spot price, relevant discount factors and tenor are background variables and hence constant here for simplicity, and therefore concentrate on the variables of interest: the strike price (K), option price (P_{ϖ}), delta (Δ) and implied volatility (σ). Let $\mathscr{S}(\Delta;\varpi)$ be the at least twice-differentiable function such that $\mathscr{S} : [-1,1] \to \mathbb{R}^{+}$. The critical points to evaluate are of course the pivotal market quotes at $\Delta = \{\pm 10, \pm 25, 50\}$. Recall that ϖ provides the switch from put (-1) to call (+1).

I now specify two operators, $\mathscr{D}_{\varpi} : \mathbb{R}^{+} \to [-1,1]$ and $\mathscr{V}_{\varpi} : \mathbb{R}^{+} \to \mathbb{R}^{+}$, which return the Black-Scholes delta and Black-Scholes implied volatility for a given combination of implied volatility σ and strike price K for the former and European option price P_{ϖ} and strike price K. Finally, we have the pricing function for the option from the structural model $P_{\varpi} = \mathscr{H}(\sigma, K; \varpi)$, such that $\mathscr{H} : \mathbb{R}^{+} \to \mathbb{R}^{+}$. Hence we have the following sequence of non-linear equations:

$$\sigma = \mathscr{S}(\Delta;\varpi), \quad \Delta = \mathscr{D}_{\varpi}(\sigma, K), \quad \sigma = \mathscr{V}_{\varpi}(P_{\varpi}, K), \quad P_{\varpi} = \mathscr{H}(\sigma, K; \varpi). \quad (2.1)$$

Our objective is to identify the form of $\sigma = \mathscr{S}(\Delta;\varpi)$ from $P_{\varpi} = \mathscr{H}_{\varpi}(\sigma, K; \varpi)$. However, several practical issues occur that make this process slow.

First and foremost, the operator $\mathscr{V}_{\varpi}(P_{\varpi}, K)$ must be numerically evaluated, and the accuracy of the numerical procedure is dependent on problem-specific factors such as moneyness, tenor and the prevailing discount factor. Using the delta convention, operator $\mathscr{D}_{\varpi}(\sigma, K)$ can be one of the forms $\Delta_{S;pips} = \varpi \exp(-r_f \tau) N(\varpi d_1)$, $\Delta_{S;\%} = \varpi \exp(-r_d \tau) \frac{K}{S(t)} N(\varpi d_2)$, $\Delta_{f;pips} = \varpi N(\varpi d_1)$, or the $\Delta_{f;\%} = \varpi \frac{K}{F_{0,T}} N(\varpi d_2)$ for a given K and σ. The market convention imposes

the use of the Black-Scholes-Merton delta with Garmen-Kohlhagen's adjustment for the FX option quotes.

To find the pivotal points at $\Delta = \{\pm 10, \pm 25, 50\}$ (the 5 most important points of the implied volatility surface), I generate a dense grid of strike prices and then compute the option price and implied volatility at each point. For each strike I compute the put and call deltas (based on the four market convention combinations, pips/percentage and forward/spot) from the strike and implied volatility combination. A cubic spline is then used to recover the market quotation points as vector pairs $\{\Delta, \sigma\}$. This gives us the corresponding implied volatility of the option at the pivotal Δ. Volatility for the at-the-money strangle is straightforwardly $\widetilde{AT}$. Risk reversal is then the difference between the volatilities of call and put options with the same delta $\widetilde{RR}_{\Delta} = \sigma_c(\Delta) - \sigma_p(\Delta)$. It is worth noting that the market quotes to model is much more straight forward. In this case volatility and delta (and hence the strike by simple numerical analysis) are given with precision. As such, the analyst just needs to compute the option pricing model that recovers the market volatility five pivot strikes.

The $2vol$-butterfly is defined as $\widetilde{BF}_{\Delta-2vol} = 0.5\sigma_c(\Delta) + 0.5\sigma_p(\Delta) - \widetilde{AT}$, but we need to transfer this to $1vol$-butterfly for the market quotation. Solving the equation numerically, we find the market quoted $\widetilde{BF}_{\Delta-1vol}$, which its corresponding strike price $K_j(\widetilde{BF}_{\Delta-1vol})$ renders $\Delta_j(K_j(\widetilde{BF}_{\Delta-1vol}),\ \widetilde{AT} + \sigma(\widetilde{BF}_{\Delta-1vol})) = \{\pm 0.25, \pm 0.1\}$, and with this strike price, both of the volatilities at Δ_j and the $1vol$-butterfly adjusted volatility can be used to construct a strangle at the same

price

$$\begin{aligned}&\mathscr{H}_c(\widetilde{AT}+\widetilde{BF}_{\Delta-1vol},K_c(\widetilde{BF}_{\Delta-1vol}))+\mathscr{H}_p(\widetilde{AT}+\widetilde{BF}_{\Delta-1vol},K_p(\widetilde{BF}_{\Delta-1vol}))\\=&\mathscr{H}_c(\sigma_c(25),K_c(\widetilde{BF}_{\Delta-1vol}))+\mathscr{H}_p(\sigma_p(25),K_c(\widetilde{BF}_{\Delta-1vol})).\end{aligned}\tag{2.2}$$

The solution to this equation yields the market quotation convention. In Section 3.4 of next chapter, I will provide a figure example to demonstrate the volatility surface building process together with the error bound calculation.

2.5 Relative models

In this section, I will present some fundamental models that this thesis is built on. These well-known models have important implementation and impact on both the academia and industry works.

2.5.1 The Black-Scholes model

Under the risk neutral measure, risk-free portfolios should have return the same as risk-free rate, the spot price S_t is described by a geometric Brownian motion

$$dS_t = rS_t dt + \sigma S_t dW_t,$$

where r is the risk-free rate, σ is the volatility and dW_t is Wiener process that $dW_t \sim \mathcal{N}(0, dt)$. The closed form call option price based on such process is

$$C = S_0 N(d_1) - Ke^{-rT} N(d_2),$$

where T is the maturity, K is the strike price, $N(\cdot)$ is the cumulative distribution function of normal distribution and

$$d_{1,2} = \frac{\ln(S_0/K) + (r \pm \frac{1}{2}\sigma^2)T}{\sigma\sqrt{T}}.$$

The implied volatility is then the σ that makes the model option price C equals to the market observed option price.

2.5.2 The Heston model

The most significant disadvantage of Black-Scholes model is its constant volatility σ. The Heston [1993] improves the model by allowing the variance also being a stochastic process. Therefore the Heston model has the following form

$$dS_t = rS_t dt + \sqrt{v_t} S_t dW_t^s,$$
$$dv_t = \kappa(\theta - v_t)dt + \sigma\sqrt{v_t} dW_t^v.$$

Here the random shocks allow to have correlation $[dW_t^s, dW_t^v] = \rho dt$. The variance process is a Cox-Ingersoll-Ross process, which has the property that it will remain positive if $v_0 > 0$ and the Feller condition is satisfied $2\kappa\theta > \sigma^2$.

The Heston model is able to generatei implied volatility surface with desired skewness and kurtosis characters. The model parameter ρ, which is the correlation between the spot rate and variance processes, significantly affects the skewness of the surface, and the volatility of volatility parameter θ affects the level of the volatility surface.

2.5.3 The Heston Nandi model

The Heston Nandi model is a discrete time model introduced by Heston and Nandi [2000] based on Non-linear GARCH process. The mean return of spot price $R(t)$ and variance process are

$$R(t+1) = r + \lambda h(t+1) + \sqrt{h(t+1)}Z(t+1),$$
$$h(t+1) = \omega + \beta h(t) + \alpha(Z(t) - \gamma\sqrt{h(t)})^2,$$

where the idiosyncratic shock $Z(t) \sim \mathcal{N}(0,1)$. This process remains stationary if $\beta + \alpha\gamma^2 < 1$. The most important advantage of discrete time model over continuous time model is the process parameters can be easily estimated from spot price observation using maximum likelihood estimation.

2.5.4 The Cox-Ingersoll-Ross model

The Cox-Ingersoll-Ross model (CIR) was designed by Cox et al. [1985] as a short rate model to capture the term structure of the interest rate. It is defined as

$$dr_t = \kappa(\theta - r_t)dt + \sigma\sqrt{r_t}dW_t, \tag{2.3}$$

where dW_t is a Wiener process. κ corresponds to the mean reverting speed, θ corresponds to the long term mean level and σ corresponds to volatility level. The good property of a CIR process is that it remains positive as long as $2\kappa\theta > \sigma^2$. This property allows it to be applied to modelling volatility movements as mentioned above. The CIR has a non-central Chi-squared distribution and I will use this for parameter estimation in Chapter 5.

2.5.5 Option pricing based on characteristic function

All of the three models in previous subsections (the Black-Scholes model, the Heston model and the Heston Nandi model) can have closed form option price using their characteristic function, denoted as $\Psi(\phi) = \mathbb{E}[e^{i\phi x}]$ and $x = \ln S_T$. We can see that the characteristic function is the Fourier transformed probability density function, $f(x)$

$$\Psi(\phi) = \mathbb{E}[e^{i\phi x}] = \int_{-\infty}^{\infty} e^{i\phi x} f(x) dx,$$

where $i = \sqrt{-1}$. Once a characteristic function is derived, the probability density function of the terminal logarithm spot rate can be calculated by the inverse Fourier transformation

$$f(x) = \frac{1}{2} \int_{-\infty}^{\infty} e^{i\phi x} \Psi(\phi) d\phi.$$

The Gil-Pelaez theorem uses this to derive the in-the-money probability

$$Pr(\ln S_T > \ln K) = \frac{1}{2} + \frac{1}{\pi} \int_0^{\infty} \Re[\frac{e^{-iu \ln K} \Psi(iu)}{iu}] du.$$

Then the option price can be derived from this probability. Details of the derivation can be found in the following chapters.

Chapter 3

Recovering Foreign Exchange Option Prices from Spot Price Dynamics

3.1 Discrete time asset pricing models

The prices of European foreign exchange options reflect the market participants view of the stochastic structure of the global economy. The largest market of this kind is the over-the-counter (OTC) variant and these options are commonly quoted in terms of the shape of a European volatility surface, which is based on the Garman and Kohlhagen [1983] foreign exchange adjustment to the standard Black-Scholes model. Typically this surface is calibrated against option quotes from broker-dealers. However, there is an open question as to how to generate volatility surfaces synthetically from historical spot exchange rates and deposit rates. The word "synthetic" here emphasis that the implied volatility surface is

hard to be observed from the market quotes and need to be generated without directly implied from option quotes. Indeed, this is part of a more general question in financial econometrics on the forecasting performance of models based on spot data versus those recovered from the market price of derivative securities.

I outline a new multi-factor option pricing model that can be fitted from spot data, adjusted and re-calibrated from any observable options data and nested using an arbitrary number of factors. The attractive feature of my approach is that an arbitrary number of observed or latent factors can be added and this framework effectively generalises the approach suggested in Engle and Mustafa [1992], Duan [1995] and Heston and Nandi [2000].

Options on FX rates are one of the most common hedging and speculating tools to either reduce spot FX risk or leverage exposure to it. Trading in FX options is dominated by the over-the-counter market. The OTC FX options is in fact, by notional volume, the fourth largest derivatives market in the world behind various types of money market swaps and interest rate futures.[1] It is also one of the fastest growing derivatives markets post the 2008/9 global financial crisis; yet the body of research addressing the structural asset pricing analysis of the OTC FX option market is noticeable sparse. Two studies are of note, [Carr and Wu, 2007; Du, 2013], both use market quotes to illustrate calibrations of structural models, no systematic statistical testing of asset pricing effectiveness was conducted on the options themselves, indeed in both cases the models could not be calibrated to spot-only data. A Deutsche Bank study by Jain and Stafford [2006] provides some coverage of the factors underlying one type of market quote

[1]Source: Bank of International Settlements Derivatives Market Statistics 2015. URL: http://www.bis.org/statistics/d5_1.pdf, last accessed January 30, 2017.

for five currencies for a one year tenor. However, no structural model is proposed other than a series of observations on the relationship between risk reversals and spot variation.

Undoubtedly, one of the reasons for this lack of research on OTC FX options is the relatively opaque nature of the market data and certain acute properties of OTC FX options. First, the term structure, OTC FX option contracts typically have tenors dated from overnight to beyond five years, indeed, for certain Asian contracts versus the dollar tenors can run beyond 15 years. Very few of the currently popular models provide good fit over all tenors for the same parameters.

Second, for a given currency pair, to price a complete OTC FX option pricing surface would require five ticker codes, knowledge of the pricing conventions for the particular currency pair and a structural model of the European volatility surface. As such the pricing of OTC FX options is embedded in volatility adjustments to the standard Black and Scholes [1973] model. Additionally, many further market-specific statistical adjustments (such as the forward convention and quoting factors) are required when inferring implied volatilities for non-quoted strikes or maturities, which presents a challenge for the consistent determination of the different implied volatilities. For instance, previous papers use an approximation of the functional form for quoted butterflies (the average of the put and call volatilities at the same Black–Scholes delta minus the at-the-money straddle volatility); however, this approximation only works in certain cases (see for instance Carr and Wu [2007]; Du [2013] and Dupoyet [2006] for examples). For certain shapes of the implied volatility surface, the correct market strangle needs to be computed from the equivalent butterfly to recover an accurate quote. Careful appreciation of these types of issues reduces many of the implementation

errors associated with pricing FX options.

Pricing of FX options in the prior literature is generally based on continuous time derivatives of models such as the Heston [1993] stochastic volatility model, the SABR model developed by Hagan et al. [2002] and the local stochastic volatility model versions of these, see Pagliarani and Pascucci [2012]; Reghai et al. [2012]; Shiraya and Takahashi [2013]. However, such models assume the existence of an option market surface to actively calibrate against. In the presence of sparse options information, as is the case for many currency pairs, there is a pressing need in the industry for structural asset pricing models that can be estimated directly from the underlying spot data and requires limited knowledge of the FX option European surface for calibration. Early empirical work on pricing FX options maybe found in Melino and Turnbull [1990] and Shastri and Tandon [1986]. However, both cases review exchange traded options and directly price quoted puts and calls. OTC FX options have a quite different quotation mechanism and I will demonstrate that propagation of errors from the prices to the European surface can result in quite significant errors and unpredictable error dynamics.

My contribution is threefold. First, I specify a multi-factor option pricing model in the affine GARCH type family. This model is unique in the practitioner and academic literature and may be calibrated in exactly the same manner as a standard Heston or SABR type model or, more usefully, fitted directly from spot data, by adjusting the physical, observed measure to the risk neutral measure using a simple exponential affine model of interest rates with discrete time stochastic volatility. The time series properties of the GARCH family of models are particularly flexible at multiple time-scales. From high frequency Engle et al.

[1990] to very long memory Ding et al. [1993]. There is an extensive literature on in- and out- of sample forecasting of spot integrated variance using GARCH types models, see Engle and Ishida [2002] and Barone-Adesi et al. [2008] for some classic examples amongst many.

Second, I outline in detail how to build actual market quotes from the parameterised form of this model and compute confidence bounds from the error structure of the underlying estimators. These quotes can then be used to calibrate the parameters and compared directly with the market data for performance evaluation and show the ability to expand the existing market by providing option pricing tool for more currency pairs.

Finally, we provide empirical strategies to parameterise this model from spot FX rates data at both high and low frequencies, ranging from daily to monthly data.

One of the major issues in OTC FX option is that volatility surfaces are regularly quoted from overnight/same week (ON/SW) all the way out to 5+ years. This makes option pricing from discrete-time models computationally very intensive, even when a closed form solution exists. Hence we outline a daily and a monthly version of my model to cater for both short and long tenor option pricing. These models are then fitted to spot data for five actively traded currency pairs. I find that a) inclusion of stochastic short rates improves out-of-sample long horizon fitting significantly (in most cases by an order of magnitude) for long horizon option b) joint calibration to a modest sample of option data improves the model fit by up to two orders of magnitude.

With small adjustments to the model, it can be used to price both short and very long maturity options. Indeed, my analysis stretches out to the five-year

tenor options. As such, the model is easily fitted from spot data via standard maximum likelihood estimation (MLE) and this allows for a very useful comparative asset pricing analysis. For instance, using spot only data we are able to impute the effectiveness of the pricing of the model versus market quotes. Also, using an asymptotic expansion we can determine the anticipated pricing error from the spot estimation procedure and whether the observed quotes sit within the resulting error bounds, both through the term structure and across quoted deltas.

At present, the OTC FX option market is effectively designed around parameterization of continuous time models direct from implied volatility curves, often referred to as 'European volatility surfaces' derived from the Black—Scholes–type models. European volatility surfaces are implied volatility curves, which effectively perform the role of normalized prices, being priced relative to a strike recovered from a Black–Scholes delta and the quoted volatility relative to that delta. As such, the FX option implied volatility curves are representations of parametric and non-parametric models such as the Heston model and its many derivatives. This leads to the question of which comes first: the option price itself or the European volatility surface used to quote the option? This chapter seeks to answer this question for a group of major countries versus the US dollar. A second question naturally follows: with such a well- established paradigm (volatility surface $\rightarrow$ continuous time parametric model $\rightarrow$ volatility surface update), why have a model that can be estimated from spot exchange rates when all that is really needed is to model the volatility surface dynamics itself?

The answer to the second problem is relatively easy. There are only about 70 currency pairs that have some activity in their markets. Whilst one can use

techniques such as the popular Vanna–Volga method (see Castagna and Mercurio [2007] Chater 4 and Chapter 9 for the introduction to the Vanna–Volga technique and review of it's use in constructing untraded volatility surfaces respectively) or the transitive method of Doust [2012] to determine bounds on an untraded implied volatility surface using triangular arrangements in traded legs, certain correlations still need to estimated or imposed and this presents a challenge when one seeks to expand coverage of FX option pricing to less liquid currencies. Therefore a structural model of the European surface estimated from spot data has a high level of value to currency traders, in particular one for which the relative biases versus liquid currency pairs can be well understood.

The remainder of this chapter is organised as follows. Section 3.2 describes the proposed affine stochastic term structure volatility model and also a simplified derivative of this model restricting the interest rates to be constant. Section 3.3 outlines the procedures for estimating the model parameters. With the knowledge above, Section 2.4 illustrates how to construct the volatility given only FX spot price data. And to overcome the term structure mismatch, we also propose an out-of-model calibration adjustment. Section 3.6 reports the performance of the proposed models from empirical analysis, while Section 3.9 concludes.

3.2 Discrete-time affine FX option pricing models

I will introduce three model specifications. Two are FX variants based on existing models, the Heston and Nandi [2000] GARCH type model and its derivative

Christoffersen et al. [2014], which is estimated via high frequency data. My main specification has a stochastic short rate structure, similar to Amin and Jarrow [1991], but operationalised in discrete-time by combining a form of the Heston and Nandi [1999] and Heston and Nandi [2000] models. We can view the non-stochastic interest rate models as restricted versions of the latter model, hence I start with the general form. Evidence from prior studies by Christoffersen et al. [2006]; Christoffersen and Jacobs [2004b]; Christoffersen et al. [2010], provide a series of useful results on spot price derived option models. The performance of a single factor Heston and Nandi [2000] is found to be quite competitive with alternative specifications (whilst not always providing the smallest average pricing error). Further useful evidence in Christoffersen and Jacobs [2004a] indicates that when judging option pricing effectiveness results can be sensitive to the choice of loss function. For FX options the importance of closed form solutions cannot be understated, given the need to convert rapidly between the underlying option pricing model and the resulting volatility surface; as such, option models such as Duan [1995, 1997] are excluded on the grounds of requiring simulations to generate prices.

3.2.1 An affine stochastic term structure with GARCH volatility model, ASTSV

My baseline model presumes three independent disturbance terms and three variance processes. This represents stochasticity in the 'domestic' and 'foreign' deposit rates and the spot exchange rate. This representation is useful as it allows us to formulate various restricted FX pricing models. For instance one could

choose to restrict the dynamics on either the domestic or foreign numéraires as constant or allow only homoskedastic innovations.

Atomically, Heston and Nandi [1999] refer to each pair of first and second moment models of the short rate dynamics as 'two' factor affine volatility models. I can think of the combined model as a six factor affine model. However, at the continuous limit the absolute correlation between disturbance in the variance process and the mean equation approaches unity, hence the model is really three factors with six equations describing the evolution of the first two moments. For tractability of the options prices I presume that the structural disturbance terms are uncorrelated across the short-rate and spot exchange rate processes. However, as the stochastic process driving the rates is lagged to the exchange rate there is a higher order dependence structure intrinsic to the model.[1]

Assumption 1. *I presume a discretely updated two country (indexed by* $k \in \{d, f\}$*) global economy with time indexed by* t*. Consider a forward tenor for a contract* τ*, which spans the time interval* t, T*, where* T *is the maturity date, by definition* $\tau = T - t$*. Assets are valued at nominal prices. For a given discrete time-step denoted* η*,* [2] *the money market accounts are presumed to be a timed deposit account paying* $\exp(r_d(t+\eta))$ *and* $\exp(r_f(t+\eta))$ *on a single unit of domestic or foreign currency respectively. Setting* $S(t)$ *be the spot conversion between domestic and foreign currency. I also presume that forward money and exchange*

[1] GARCH models are used extensively across the asset pricing and risk management spectrum. I nest multiple variations on the quadratic specification of Engle and Ng [1993], as my basic time series building block, generalising the work of Heston and Nandi [1999] and Heston and Nandi [2000]. Previous work on option pricing with GARCH has features in Duan [1997] and Barone-Adesi et al. [2008] whilst Bauwens et al. [2006] reviews some applications to derivatives pricing amongst other applications of correlation dynamics in multivariate settings.

[2] A useful feature of OTC FX options is that they are explicitly tenored, rather than explicitly dated, hence all but eliminating the problem non-integer counts of time steps from t to T.

rate markets are complete.

Given the assumption of complete FX forward markets and complete domestic forward money markets we can set $F(t,T) = \mathbb{E}_{\mathbb{P}}[S(T)] = S(t)\exp(\int_t^T r_d(t) - r_f(t)dt)$, where $\mathbb{P}$ as the physical measure under a filtration $\mathcal{F}_t$. Based on the notational assumption on the time step, we can set $J = \tau\eta^{-1}$ be the integer number of discrete time steps from t to T. I denote $F(t,T) = S(t)\exp(\sum_{j=0}^{J-1} r_d(t+j\eta) - r_f(t+j\eta)dt)$ as the equivalent discrete time forward FX price.

Under my notation the forward FX market is complete if, for a vector of forward FX prices $\mathbf{F}(t,T) = [F(t,t+\eta),\ldots,F(t,t+J\eta)]'$, $\mathbf{F}(t,T) - S(t)\exp(\mathbf{f}(t)) = \mathbf{0}$, where $\mathbf{f}(t) = [\sum_{j=0}^{0} r_d(t+j\eta) - r_f(t+j\eta),\ldots,\sum_{j=0}^{J-1} r_d(t+j\eta) - r_f(t+j\eta)]'$ and $\mathbf{0}$ is a J length null vector.

Assumption 2. *$S(t+\eta)|\mathcal{F}_t$ is conditionally log-normal. Setting $R(t+\eta) = \ln(S(t+\eta)/S(t))$, the first and second moments of $R(t)$ under the measure $\mathbb{P}$ and filtration $\mathcal{F}_t$ are described by the following spot process with GARCH type volatility:*

$$R(t+\eta) = r_d(t) - r_f(t) + \lambda_s h_s(t+\eta) + \sqrt{h_s(t+\eta)}z(t+\eta), \tag{3.1}$$

$$h_s(t+\eta) = \omega_s + \beta_s h_s(t) + \alpha_s(z(t) - \gamma_s\sqrt{h_s(t)})^2, \tag{3.2}$$

where $z(t) \sim^{iid} \mathcal{N}(0,\eta)$. I denote $h_s(t)$ to represent the variance process in the FX spot rate. I presume that $1-\beta_s-\alpha_s\gamma_s^2 > 0$, with $0 \leq \beta_s < 1$ and $0 \leq \alpha_s < 1$.[1]

Of course the conditional variance at $t+n\eta$ from time t is non-stochastic when $n = 1$, therefore the SV monicker is unwarranted in this case. However,

[1] I use $\sqrt{\cdot}$ to denote the principal square root through out this thesis.

in the main, I will always deal with $n > 1$ steps, as one step pricing trivially reduces to the Garman and Kohlhagen [1983] version of the Black-Scholes model under the Rubinstein [1976] condition when continuous rebalancing in the interval is absent. Hence, I classify the forward looking multi-step spot variance as a 'stochastic volatility' model, see Fleming and Kirby [2003] for more discussion on GARCH and stochastic volatility. A simple example is also helpful, a stationary GARCH(1,1) process satisfies the continuous limit: $dX(t) = \sqrt{h(t)}dW^{(1)}(t)$, with $dh(t) = \kappa(\bar{h} - h(t)) + \rho h(t)dW^{(2)}(t)$, where $\kappa > 0$, $\bar{h} > 0$ and $\rho > 0$ are arbitrary parameters. Notice that $W^{(1)}(t)$ and $W^{(2)}(t)$ are independent Weiner processes, see Brockwell et al. [2006] for more discussion on the continuous limits.

It is useful to note that the unconditional expectation $\bar{\mathbb{E}}[h_s(t+\eta)] = (\alpha_s + \omega_s)/(1 - \beta_s - \alpha_s\gamma_s^2)$. Furthermore, whilst β_s determines the persistence in the spot variance, α_s and γ_s are principal parameters that determine the 'kurtosis and skewness' properties in the resulting implied volatility surface. λ_s determines the feedback in spot variance to the mean return. The process driving the term $r_d(t) - r_f(t)$ is now specified parametrically in the next assumption.

Assumption 3. *Let the value at $t+\eta$ of one unit of domestic or foreign currency in a no risk timed deposit account quoted at time t be denoted by $\exp(r_k(t))$ for $k \in \{d, f\}$. I presume that the dynamics of $r_d(t)$ and $r_f(t)$ are driven by a first autoregressive process with potentially GARCH disturbances:*

$$r_k(t+\eta) = \mu_{0k} + \mu_{1k}r_k(t) + \lambda_k h_k(t+\eta) + \sqrt{h_k(t+\eta)}u_k(t+\eta), \tag{3.3}$$

$$h_k(t+\eta) = \omega_k + \beta_k h_k(t) + \alpha_k(u_k(t) - \gamma_k\sqrt{h_k(t)})^2. \tag{3.4}$$

for $k \in \{d, f\}$. Here $u_d(t)$ and $u_f(t)$ are independent standard normal structural

disturbances such that $u_d(t) \sim^{iid} \mathcal{N}(0,\eta)$ *and* $u_f(t) \sim^{iid} \mathcal{N}(0,\eta)$. *I presume in all cases that* $0 \leq \mu_{1k} < 1$ *and* $1 - \beta_k - \alpha_k\gamma_k^2 > 0$, *with* $0 \leq \beta_k < 1$ *and* $0 \leq \alpha_k < 1$.

The structural parameters of the model are collected in the vector $\theta = (\theta_s, \theta_d, \theta_f)'$ where $\theta_s = (\lambda_s, \omega_s, \beta_s, \alpha_s, \gamma_s)$ and $\theta_k = (\mu_{0k}, \mu_{1k}, \lambda_k, \omega_k, \beta_k, \alpha_k, \gamma_k)$, for $k \in \{d, f\}$. The variance equation parameters have the same interpretation as the spot dynamics. When $h_k(t+\eta)$ is time inhomogeneous λ_k is redundant and the AR(1) model parameters μ_{0k} and μ_{1k} describe a discrete time Vasicek model, with rate persistence determined by μ_{1k} and unconditional expectation of $r_k(t+\eta)$ is $\bar{\mathbb{E}}[r_k(t+\eta)] = \mu_{0k}/(1-\mu_{1k})$.[1]

Notice that whilst $z(t)$, $u_d(t)$ and $u_f(t)$ are restricted to being independent structural innovations, $R(t+\eta)$ will have a non-zero conditional correlation with $r_d(t)$ and $r_f(t)$. Setting $\ell = 1|k = d$ and $\ell = -1|k = f$ the uncentered and centred second co-moments are given by:

$$\begin{aligned}
\mathbb{E}_t[R(t+\eta)r_k(t)] =& \ell\lambda_k^2 h_k(t+\eta)^2 + (\mu_{0,k} + \mu_{1,k}r_k(t))\tilde{r} + h_k(t+\eta)\tilde{h} \\
\mathrm{Cov}_t[R(t+\eta), r_k(t)] =& \ell(\mathscr{U}_k(t+\eta)z(t+\eta)\sqrt{h_k(t+\eta)}\sqrt{h_s(t+\eta)} + \\
& - \mathscr{U}_k(t+\eta)\mathscr{U}_j(t+\eta)\sqrt{h_d(t+\eta)}\sqrt{h_f(t+\eta)} + \\
& + \mathscr{U}_k(t+\eta)^2 h_k(t+\eta)) \\
=& \ell h_k(t+\eta),
\end{aligned}$$

where $j, k \in \{d, f\}$ and $j \neq k$, $\mathscr{U}_{j/k}(t+\eta) = u(t+\eta)|j/k = d$ and $\mathscr{U}_{j/k}(t+\eta) = v(t+\eta)|j/k = f$, $\tilde{r} = \ell h_k(t+\eta) + h_s(t+\eta)\lambda_s + \mu_{0,d} - \mu_{0,f} + \mu_{1,d}r_d(t) - \mu_{1,f}r_f(t)$ and $\tilde{h} = \ell - \ell\lambda_k(h_k(t+\eta)\lambda_d + h_s(t+\eta)\lambda_s + \mathscr{R}_k)$ with $\mathscr{R}_k = \mu_{0,k} - 2\mu_{0,j} +$

[1] Under the constant volatility assumption $\beta_k = \alpha_k = 0$ as $\eta \to 0$ the time deposit account converges to the theoretical short rate.

$r_k(t)\mu_{1,k} - 2r_j(t)\mu_{1,j}$. Collectively, I refer to the model described in Assumption 2 and Assumption 3 as the 'Affine Stochastic Term Structure with Stochastic Volatility' model (henceforth ASTSV) when the number of time steps from t to T is greater than one.

Since the FX spot or derivative market involves investors holding bonds denominated in different currencies and holding different measurements of the probability of the asset price movements, we need to make sure we derive the risk-neutral formula for FX markets to avoid arbitrage for either domestic or foreign investors.

Remark 1. *From a domestic investor's point of view, the risk-neutral FX process, under the domestic risk neutral $\mathbb{Q}^{\{d\}}$ measure, for the ASTSV model, is given by the following pair of expressions:*

$$R(t+\eta) = r_d(t) - r_f(t) - 1/2h_s(t+\eta) + \sqrt{h_s(t+\eta)}z^*(t+\eta), \tag{3.5}$$

$$h_s(t+\eta) = \omega_s + \beta_s h_s(t) + \alpha_s(z^*(t) - \gamma_s^*\sqrt{h_s(t)})^2, \tag{3.6}$$

with risk neutral innovations and parameter

$$\begin{aligned} z^*(t) =& z(t) + (\lambda_s + 1/2)\sqrt{h_s(t)}, \\ \gamma_s^* =& \gamma_s + \lambda_s + 1/2. \end{aligned}$$

For brevity, I mark a risk neutral process and expectations under the domestic risk neutral measure, $\mathbb{Q}^{\{d\}}$, with a superscript * henceforth.

Proof. Recall that $M_k(t_1, t_2)$ is the holding of a deposit account from t_1 to t_2, for any $t_2 > t_1$, for $k \in \{d, f\}$. Consider the holding of a single unit of foreign

money in a timed deposit account for the period $t, t+\eta$; this money market account itself would then follow $M_f(t, t+\eta) = \exp(\int_t^{t+\eta} r_f(s)ds)$. Alternatively, holding one unit of a domestic currency in a timed deposit account would yield a quantity $M_d(t, t+\eta) = \exp(\int_t^{t+\eta} r_d(s)ds)$ over the same time frame t to $t+\eta$. As these are time deposit accounts (one night, one month), we can assume that the risk-free rates are constant in each time step, so these quantities simplify to $M_d(t, t+\eta) = \exp(r_d(t+\eta))$ and $M_f(t, t+\eta) = \exp(r_f(t+\eta))$. A domestic investor would expect an asset value to grow at a domestic risk-free rate. Hence, each time step is a single period Garman and Kohlhagen [1983] type model.

Following my assumption of the compounded return process Assumption 2, the conditional expectation of the ratio between the yields on the two timed deposit accounts of a single unit of domestic currency denoted by

$$\begin{aligned}\mathbb{E}\left[\frac{S(t+\eta)M_f(t,t+\eta)}{M_d(t,t+\eta)}\middle|\mathcal{F}_t\right] =& \mathbb{E}\left[S(t)\exp\left((r_d(t)-r_f(t)+\lambda h(t+\eta)+\right.\right.\\ &\left.\left.+\sqrt{h(t+\eta)}z(t+\eta)+(r_f(t)-r_d(t))\right)\middle|\mathcal{F}_t\right]\\ =& \mathbb{E}\left[S(t)e^{\left(\lambda h(t+\eta)+\sqrt{h(t+\eta)}z(t+\eta)\right)}\middle|\mathcal{F}_t\right]\end{aligned}$$

should be a martingale under the risk neutral measure $\mathbb{Q}^*$, such that

$$\mathbb{E}^*\left[\frac{S(t+\eta)M_f(t,t+\eta)}{M_d(t,t+\eta)}\middle|\mathcal{F}_t\right] = S(t),$$

for some filtration $\mathcal{F}_t$ determined by the model characteristics conditioned on the initial spot price $S(t)$, interest rates $r_k(t)$ and spot variance $h_s(t+\eta)$, and the space $\Omega \in \mathbb{R}$. Therefore the random innovation over $t, t+\eta$ has a measurable

σ-algebra. I write the ratio under risk neutral measure $\mathbb{Q}^*$ as

$$S(t)e^{\left(v(t+\eta)+\sqrt{h(t+\eta)}z^*(t+\eta)\right)},$$

where $v(t+\eta)$ is the conditional mean and $z^*(t+\eta)$ is a normal random variable under risk neutral measure. Then the expectation is

$$\mathbb{E}^*\left[S(t)e^{\left(v(t+\eta)+\sqrt{h(t+\eta)}z^*(t+\eta)\right)}\middle|\mathcal{F}_t\right] = S(t)e^{\left(v(t+\eta)+\frac{1}{2}h(t+\eta)\right)} = S(t).$$

This implies that $v(t+\eta) = -0.5h(t+\eta)$ and $v(t+\eta)+\sqrt{h(t+\eta)}z^*(t+\eta) = \lambda h(t+\eta)+\sqrt{h(t+\eta)}z(t+\eta)$. I then recover $z^*(t+\eta) = z(t+\eta)+\sqrt{h(t+\eta)}(\lambda+1/2)$. Then following the Girsanov Theorem, the Radon-Nikodym derivative is

$$\frac{d\mathbb{Q}^*}{d\mathbb{P}} = e^{\left(-\sqrt{h(t+\eta)}(\lambda+\frac{1}{2})z(t+\eta)-\frac{1}{2}h(t+\eta)\left(\lambda+\frac{1}{2}\right)^2\right)}$$

and $\mathbb{E}[d\mathbb{Q}^*/d\mathbb{P}] = 1$, under the risk neutral probability measure $\mathbb{Q}^*$, we still obtain $z^*(t+\eta) \sim^{iid} \mathcal{N}(0,\eta)$. Risk neutralization also requires the variance to be unchanged between both measures, as such:

$$Var^*\left[\frac{S(t+\eta)M_f(t,t+\eta)}{M_d(t,t+\eta)}\right] = Var\left[\frac{S(t+\eta)M_f(t,t+\eta)}{M_d(t,t+\eta)}\right].$$

This is equal to the following equality

$$h(t+\eta) = \omega+\beta h(t)+\alpha(z^*(t)-\gamma^*\sqrt{h(t)})^2 = \omega+\beta h(t)+\alpha(z(t)-\gamma\sqrt{h(t)})^2,$$

therefore we need to adjust γ^* such that

$$\gamma^* = \frac{z^*(t) - z(t) + \gamma\sqrt{h(t)}}{\sqrt{h(t)}} = \gamma + \lambda + \frac{1}{2}.$$

The difference between the standard treatment in continuous-time and discrete-time models are that for another given time increment in the sequence $t_0 + (n-1)\eta, t_0 + n\eta$, where $n \in \mathbb{N}^+$ and $t_0 + n\eta \leq T$, there is another σ-algebra deterministically constructed from the model characteristics conditioned on the initial spot price $S(t)$, spot variance $h(t+\eta)$ and interest rates $r_k(t)$. The σ-algebra of $\mathcal{F}_{t_0+n\eta}$ contains the set of possible updates of the stochastic variables from $\mathcal{F}_{t_0+(n-1)\eta}$ and hence there are all sub-σ-algebras of $\mathcal{F}_T$. Notice that the sequence of σ-algebras $\mathcal{F} = \{\mathcal{F}_{t_0}, \mathcal{F}_{t_0+\eta}, \ldots, \mathcal{F}_T\}$ is finite and the space of outcomes is fixed, hence $\{\mathcal{F}_{t_0} \subseteq \mathcal{F}_{t_0+\eta}, \ldots, \subseteq \mathcal{F}_T\}$. Therefore, $\mathcal{F}_t$ is a filtration. Then from t_0 to T under the probability space $(\Omega, \mathcal{F}, \mathcal{F}_t, \mathbb{P})$,

$$\begin{aligned}\mathbb{E}^*\left[\frac{S(T)M_f(t_0,T)}{M_d(t,T)}\middle|\mathcal{F}_{t_0}\right] =& \mathbb{E}^*\left[\mathbb{E}\left[\frac{S(T)M_f(t-\eta,T)}{M_d(t-\eta,T)}\middle|\mathcal{F}_{T-\eta}\right]\middle|\mathcal{F}_{t_0}\right] \\ =& \mathbb{E}^*\left[\frac{S(T-\eta)M_f(t_0,T-\eta)}{M_d(t_0,T-\eta)}\middle|\mathcal{F}_{t_0}\right].\end{aligned}$$

Continuing the process above, we obtain that

$$\mathbb{E}^*\left[\frac{S(T)M_f(t_0,T)}{M_d(t,T)}\middle|\mathcal{F}_{t_0}\right] = \mathbb{E}^*\left[\frac{S(t+\eta)M_f(t_0,t_0+\eta)}{M_d(t_0,t_0+\eta)}\middle|\mathcal{F}_{t_0}\right] = S(t_0),$$

which affirms that under the risk-neutral probability measure $\mathbb{P}^*$ is consistent not only from t to $t+\eta$ but also t_0 to T and the filtration $\mathcal{F}$ is still a martingale from t_0 to T.

End of proof. □

Based on the assumptions above, we can then apply in discrete time Amin and Jarrow [1991]'s intuition for determining the risk neutral process, given that in each step the interest rate dynamics are describing timed deposits. I provide the exact replication and hedging arguments over a single time step as follow,

Proof. This proof illustrates the no-arbitrage principle across the two numéraires within each time step, when the deposit account is timed. I use $V(t+\eta')$ to denote the price of a contingent claim, the value of which depends on $S(t+\eta')$ at time $t+\eta'$ and within a time step $t < t+\eta' < t+\eta$. From the standard treatment of Itô's Lemma, we can write down:

$$dV(t+\eta') = \frac{\partial V}{\partial \eta'} d\eta' + \frac{\partial V}{\partial S} dS(t+\eta') + \frac{1}{2}\frac{\partial^2 V}{\partial S^2} dS(t+\eta')^2,$$

where the spot price is described by a geometric Brownian motion

$$dS(t+\eta') = (r_d(t) - r_f(t))S(t+\eta')d\eta' + \sqrt{h(t+\eta)}S(t+\eta')dW(\eta').$$

Here $r_{d/f}(t)$ and $h(t+\eta)$ are constant within the time step and can be determined at the beginning t. This implies that $dS(t+\eta')^2 = h(t+\eta)S(t+\eta')d\eta'$ and then we have:

$$dV(t+\eta') = \left[\frac{\partial V}{\partial \eta'} + \frac{1}{2}h(t+\eta)S(t+\eta')^2\frac{\partial^2 V}{\partial S^2}\right] d\eta' + \frac{\partial V}{\partial S} dS(t+\eta').$$

Now I construct a portfolio $\Pi(t+\eta')$, which longs one unit of the contingent claim and shorts $\Theta(t+\eta')$ units of the foreign money market account, which has the

price $\Theta(t+\eta')S(t+\eta')M_f(t,t+\eta')$:

$$\Pi(t+\eta') = V(t+\eta') - \Theta(t+\eta')S(t+\eta')M_f(t,t+\eta'),$$

which should be riskless. From this I derive the portfolio value as:

$$\begin{aligned}
d\Pi(t+\eta') =& dV(t+\eta') - \Theta(t+\eta')d(S(t+\eta')M_f(t,t+\eta')) \\
=& dV(t+\eta') - \Theta(t+\eta')M_f(t,t+\eta')dS(t+\eta') - \Theta(t+\eta')S(t+\eta')dM_f(t,t+\eta') \\
=& dV(t+\eta') - \Theta(t+\eta')M_f(t,t+\eta')dS(t+\eta') + \\
& - \Theta(t+\eta')S(t+\eta')r_f(t+\eta')M_f(t,t+\eta')d\eta' \\
=& dV(t+\eta') - \Theta(t+\eta')M_f(t,t+\eta')\Big[(r_d(t)-r_f(t))S(t+\eta')d\eta' + \\
& + \sqrt{h(t+\eta)}S(t+\eta')dW(\eta')\Big] - \Theta(t+\eta')S(t+\eta')r_f(t)M_f(t,t+\eta')d\eta' \\
=& dV(t+\eta') - \Theta(t+\eta')M_f(t,t+\eta')\Big[r_d(t)S(t+\eta')d\eta' \\
& + \sqrt{h(t+\eta)}S(t+\eta'), dW(\eta')\Big]
\end{aligned}$$

which is equivalent to:

$$\begin{aligned}
d\Pi(t+\eta') =& \frac{\partial V}{\partial \eta'}d\eta' + \frac{1}{2}h(t+\eta)S(t+\eta')^2\frac{\partial^2 V}{\partial S^2}d\eta' + \frac{\partial V}{\partial S}dS(t+\eta') + \\
& - \Theta(t+\eta')M_f(t,t+\eta')\left[r_d(t)S(t+\eta')d\eta' + \sqrt{h(t+\eta)}S(t+\eta')dW(\eta')\right] \\
=& \left[\frac{\partial V}{\partial \eta'} + \frac{1}{2}h(t+\eta)S(t+\eta')^2\frac{\partial^2 V}{\partial S^2} - \Theta(t+\eta')M_f(t,t+\eta')r_d(t)S(t+\eta')\right]d\eta' + \\
& + \frac{\partial V}{\partial S}dS(t+\eta') - \Theta(t+\eta')M_f(t,t+\eta')\sqrt{h(t+\eta)}S(t+\eta')dW(t+\eta')
\end{aligned}$$

Substituting the parameters of the presumed process I recover:

$$\begin{aligned}\Pi(t+\eta') = &\left[\frac{\partial V}{\partial \eta'} + \frac{1}{2}h(t+\eta)S(t+\eta')^2\frac{\partial^2 V}{\partial S^2} - \Theta(t+\eta')M_f(t,t+\eta')r_d(t)S(t+\eta')\right]d\eta' + \\ &+ \frac{\partial V}{\partial S}\left[(r_d(t)-r_f(t))S(t+\eta')d\eta' + \sqrt{h(t+\eta)}S(t+\eta')dW(t+\eta')\right] + \\ &- \Theta(t+\eta')M_f(t,t+\eta')\sqrt{h(t+\eta)}S(t+\eta')dW(t+\eta') \\ = &\left[\frac{\partial V}{\partial \eta'} + \frac{1}{2}h(t+\eta)S(t+\eta')^2\frac{\partial^2 V}{\partial S^2} - \Theta(t+\eta')M_f(t,t+\eta')r_d(t)S(t+\eta') + \right. \\ &\left. + \frac{\partial V}{\partial S}(r_d(t)-r_f(t))S(t+\eta')\right]d\eta' + \\ &+ \left[\frac{\partial V}{\partial S} - \Theta(t+\eta')M_f(t,t+\eta')\right]\sqrt{h(t+\eta)}S(t+\eta')dW(t+\eta').\end{aligned} \tag{3.7}$$

To eliminate the random term containing $W(t+\eta')$, $\Theta(t+\eta')$ needs to satisfy $\Theta(t+\eta')M_f(t,t+\eta') = \partial V/\partial S$, then

$$\Theta(t+\eta') = \frac{1}{M_f(t,t+\eta')}\frac{\partial V}{\partial S}. \tag{3.8}$$

Substituting Eq. (3.8) into Eq. (3.7) yields

$$\begin{aligned}d\Pi(t+\eta') = &\left[\frac{\partial V}{\partial \eta'} + \frac{1}{2}h(t+\eta)S(t+\eta')^2\frac{\partial^2 V}{\partial S^2} - r_d(t)S(t+\eta')\frac{\partial V}{\partial S} + \right. \\ &\left. + \frac{\partial V}{\partial S}(r_d(t)-r_f(t))S(t+\eta')\right]d\eta'.\end{aligned}$$

Since we expect this portfolio to be risk-neutral, the growth of $\Pi(t+\eta')$ should then be equal to that of the domestic riskless money market account, therefore

$d\Pi(t+\eta') = r_d(t)\Pi(t+\eta')d\eta'$, which is

$$\left[\frac{\partial V}{\partial \eta'} + \frac{1}{2}h(t+\eta)S(t+\eta')^2\frac{\partial^2 V}{\partial S^2} - r_d(t)S(t+\eta')\frac{\partial V}{\partial S} + \frac{\partial V}{\partial S}(r_d(t) - r_f(t))S(t+\eta')\right]d\eta'$$
$$= r_d(t)\Pi(t+\eta')d\eta' = r_d(t)\left[V(t+\eta') - \frac{\partial V}{\partial S}S(t+\eta')\right]d\eta',$$

and then we have

$$\frac{\partial V}{\partial \eta'} + \frac{1}{2}h(t+\eta)S(t+\eta')^2\frac{\partial^2 V}{\partial S^2} + (r_d(t) - r_f(t))S(t+\eta')\frac{\partial V}{\partial S} - r_d(t)V(t+\eta') = 0.$$

End of proof. □

Denoting $x(t) = \ln S(t)$ as the natural logarithm of the spot FX price at time t. Let $f^*(\phi)$ denote the conditional characteristic function of the logarithm price under domestic risk neutral measure, with $\phi \in \mathbb{C}$, then we have the following theorem.

Theorem 1. *The characteristic function for the ASTSV model is affine and of the following form*

$$\begin{aligned} f(\phi) =& \mathbb{E}^*[e^{\phi x(T)}] = \exp(\phi x(t) + A(t;T,\phi) + B_d(t;T,\phi)r_d(t) - B_f(t;T,\phi)r_f(t) + \\ &+ C_d(t;T,\phi)h_d(t+\eta) - C_f(t;T,\phi)h_f(t+\eta) + C_s(t;T,\phi)h_s(t+\eta)). \end{aligned} \tag{3.9}$$

where d, f and s denotes the parameters for domestic risk-free rate, foreign risk-free rate and spot FX price respectively. The recursive coefficient terms to be

evaluated from the terminal boundary conditions are as follows:

$$\begin{aligned}
A(t;T,\phi) =& A(t+\eta;T,\phi) + B_d(t+\eta;T,\phi)\mu_{0d} - B_f(t+\eta;T,\phi)\mu_{0f} + \\
&+ C_d(t+\eta;T,\phi)\omega_d - C_f(t+\eta;T,\phi)\omega_f + C_s(t+\eta;T,\phi)\omega_s + \\
&- \frac{1}{2}\ln(1-2C_s(t+\eta;T,\phi)\alpha_s) - \frac{1}{2}\ln(1-2C_d(t+\eta;T,\phi)\alpha_d) + \\
&+ \frac{1}{2}\ln(1-2C_f(t+\eta;T,\phi)\alpha_f), \qquad (3.10a)\\
B_k(t;T,\phi) =& B_k(t+\eta;T,\phi)\mu_{1k} + \phi, \quad k \in \{f,d\}, \qquad (3.10b)\\
C_k(t;T,\phi) =& C_k(t+\eta;T,\phi)\beta_k + B_k(t+\eta;T,\phi)\lambda_k + \gamma_k B_k(t+\eta;T,\phi) + \\
&- \frac{1}{2}\gamma_k^2 + \frac{(B_k(t+\eta;T,\phi)-\gamma_k)^2}{2(1-2C_k(t+\eta;T,\phi)\alpha_k)}, \quad k \in \{f,d\}, \qquad (3.10c)\\
C_s(t;T,\phi) =& C_s(t+\eta;T,\phi)\beta_s - \frac{1}{2}\phi + \gamma_s^*\phi - \frac{1}{2}\gamma_s^{*2} + \frac{(\phi-\gamma_s^*)^2}{2(1-2C_s(t+\eta;T,\phi)\alpha_s)}. \qquad (3.10d)
\end{aligned}$$

The boundary conditions at T are the following:

$$A(T;T,\phi) = B_k(T;T,\phi) = C_s(T;T,\phi) = 0, C_k(T-\eta;T,\phi) = 0, \quad k \in \{f,d\}.$$

Proof. The closed form GARCH pricing framework first suggested in Heston and Nandi [2000] has been modified previously, see for instance Christoffersen et al. [2014]. However, I introduce three new general building blocks in this proof. First, that the change in numéraire for options is admissible using a simple adjustment. Second, affine combinations of vector iid normal increments are easily additive (hence more than one stochastic factor can be included). Finally and more importantly, I provide the exact characteristic function for stationary AR(1) increments, alluded to, but not explicitly defined, in Heston and Nandi [1999].

The general derivation contained herein serves as a useful foundation for combining an arbitrary number of GARCH and AR GARCH factors in an option-pricing model.

The first step is to write down concretely the characteristic function Eq. (3.9). Denoting $x_t = \ln S(t)$, then the characteristic function is presumed to be of the following exponential affine form:

$$\begin{aligned} f^*(t;T,\phi) =& \mathbb{E}^*[e^{\phi x(T)}] \\ =& \exp(\phi x(t) + A(t;T,\phi) + B_d(t;T,\phi)r_d(t) - B_f(t;T,\phi)r_f(t) + \\ &+ C_d(t;T,\phi)h_d(t+\eta) - C_f(t;T,\phi)h_f(t+\eta) + C_s(t;T,\phi)h_s(t+\eta)). \end{aligned}$$

Next I demonstrate the coefficients $A, B_{d/f}$ and $C_{d/f/s}$ under the risk-neutral measure can be recovered from the backward recursion. At time T the log price $x(T)$ is known with certainty, however, the relevant timed deposit rates are actually determined at $r_{d/f}(T-\eta)$ hence the terminal conditions are:

$$A(T;T,\phi) = B_k(T;T,\phi) = C_s(T;T,\phi) = 0, C_k(T-\eta;T,\phi) = 0, \quad k \in \{f,d\}.$$

Then can now apply the law of iterated expectations to $f^*(t;T,\phi)$ and hence I recover:

$$\begin{aligned} f^*(t;T,\phi) =& \mathbb{E}^*[f^*(t+\eta;T,\phi)] \\ =& \mathbb{E}\Big[\exp(\phi x(t+\eta) + A(t+\eta;T,\phi) + B_d(t+\eta;T,\phi)r_d(t+\eta) + \\ &- B_f(t+\eta;T,\phi)r_f(t+\eta) + C_d(t+\eta;T,\phi)h_d(t+2\eta) + \\ &- C_f(t+\eta;T,\phi)h_f(t+2\eta) + C_s(t+\eta;T,\phi)h_s(t+2\eta))\Big]. \end{aligned} \tag{3.11}$$

I denote $A(t), B_{d/f}(t), C_{d/f/s}(t)$ for convenience, and substituting the processes into Eq. (3.11) yields

$$
\begin{aligned}
f^*(t;T,\phi) =& \mathbb{E}\Big[\exp\Big(\phi x(t) + \phi r_d(t) - \phi r_f(t) - \frac{1}{2}\phi h_s(t+\eta) + \\
&+ \phi\sqrt{h_s(t+\eta)} z^*(t+\eta) + A(t+\eta) + \\
&+ B_d(t+\eta)(\mu_{0d} + \mu_{1d} r_d(t) + \lambda_d h_d(t+\eta) + \sqrt{h_d(t+\eta)} u_d(t+\eta)) + \\
&- B_f(t+\eta)(\mu_{0f} + \mu_{1f} r_f(t) + \lambda_f h_f(t+\eta) + \sqrt{h_f(t+\eta)} u_f(t+\eta)) + \\
&+ C_d(t+\eta)(\omega_d + \beta_d h_d(t+\eta) + \alpha_d(u_d(t+\eta) - \gamma_d\sqrt{h_d(t+\eta)})^2) + \\
&- C_f(t+\eta)(\omega_f + \beta_f h_f(t+\eta) + \alpha_f(u_f(t+\eta) - \gamma_f\sqrt{h_f(t+\eta)})^2) + \\
&+ C_s(t+\eta)(\omega_s + \beta_s h_s(t+\eta) + \alpha_s(z^*(t+\eta) - \gamma_s^*\sqrt{h_s(t+\eta)})^2)\Big)\Big]
\end{aligned}
$$

Then we can rearranging the right hand side by gathering the coefficients for

$r_k(t)$, $h_{d/f/s}(t+\tau)$ and the terms having $\sqrt{(h_{d/f/s})}$ respectively,

$$
\begin{aligned}
f^*(t;T,\phi) =& \mathbb{E}\Big[\exp\Big(\phi x(t) + A(t+\eta) + B_d(t+\eta)\mu_{0d} - B_f(t+\eta)\mu_{0f} + \\
&+ C_d(t+\eta)\omega_d - C_f(t+\eta)\omega_f + C_s(t+\eta)\omega_s + \\
&+ (B_d(t+\eta)\mu_{1d} + \phi)r_d(t) - (B_f(t+\eta)\mu_{1f} + \phi)r_f(t) + \\
&- \frac{1}{2}\phi h_s(t+\eta) + \phi\sqrt{h_s(t+\eta)}z^*(t+\eta) + \\
&+ C_s(t+\eta)\beta_s h_s(t+\eta) + C_s(t+\eta)\alpha_s(z^*(t+\eta) - \gamma_s^*\sqrt{h_s(t+\eta)})^2 + \\
&+ B_d(t+\eta)\lambda_d h_d(t+\eta) + B_d(t+\eta)\sqrt{h_d(t+\eta)}u_d(t+\eta) + \\
&+ C_d(t+\eta)\beta_d h_d(t+\eta) + C_d(t+\eta)\alpha_d(u_d(t+\eta) - \gamma_d\sqrt{h_d(t+\eta)})^2 + \\
&- B_f(t+\eta)\lambda_f h_f(t+\eta) - B_f(t+\eta)\sqrt{h_f(t+\eta)}u_f(t+\eta) + \\
&- C_f(t+\eta)\beta_f h_f(t+\eta) - C_f(t+\eta)\alpha_f(u_f(t+\eta) - \gamma_f\sqrt{h_f(t+\eta)})^2\Big)\Big].
\end{aligned}
\tag{3.12}
$$

Notice the terms having $\sqrt{h_{d/f/s}}$, these can now be expressed using the following pattern:

$$H_{d/f/s} = F(\phi)\sqrt{h}w + C(t+\eta)\alpha(w - \gamma\sqrt{h})^2,$$

where $F(\phi)$ is a function of ϕ representing either ϕ or $B_{d/f}(t+\eta)$, and w denotes the three *iid* structural disturbances $z(t), u_d(t)$ and $u_f(t)$, recalling that these are

assumed to have independent moments, we can subsequently derive this part as

$$
\begin{aligned}
H_{d/f/s} =& F(\phi)\sqrt{h}w + C(t+\eta)\alpha(w^2 - 2\gamma w\sqrt{h} + \gamma^2 h) \\
=& C(t+\eta)\alpha\left(w^2 - 2\gamma w\sqrt{h} + \gamma^2 h + \frac{F(\phi)\sqrt{h}w}{C(t+\eta)\alpha}\right) \\
=& C(t+\eta)\alpha\Bigg(w^2 - 2\gamma w\sqrt{h} + \frac{F(\phi)\sqrt{h}w}{C(t+\eta)\alpha} + \gamma^2 h - \frac{\gamma F(\phi)h}{C(t+\eta)\alpha} + \\
&+ \frac{F^2(\phi)h}{4C^2(t+\eta)\alpha^2} + \frac{\gamma F(\phi)h}{C(t+\eta)\alpha} - \frac{F^2(\phi)h}{4C^2(t+\eta)\alpha^2}\Bigg) \\
=& C(t+\eta)\alpha\Bigg(w^2 - 2w\left(\gamma - \frac{F(\phi)}{2C(t+\eta)\alpha}\right)\sqrt{h} + \\
&+ \left(\left(\gamma - \frac{F(\phi)}{2C(t+\eta)\alpha}\right)\sqrt{h}\right)^2 + \frac{\gamma F(\phi)h}{C(t+\eta)\alpha} - \frac{F^2(\phi)h}{4C^2(t+\eta)\alpha^2}\Bigg) \\
=& C(t+\eta)\alpha\left(w - \left(\gamma - \frac{F(\phi)}{2C(t+\eta)\alpha}\right)\sqrt{h}\right)^2 + (\gamma F(\phi) - \frac{F^2(\phi)}{4C(t+\eta)\alpha})h.
\end{aligned}
\tag{3.13}
$$

To solve the expectation of this I follow Heston and Nandi [2000] and use the following device, that for a standard normal random variable w to separate the first and second moments:

$$
\mathbb{E}[\exp(a(w+b)^2)] = \exp\left(-\frac{1}{2}\ln(1-2a) + \frac{ab^2}{1-2a}\right). \tag{3.14}
$$

Applying Eq. (3.14) into Eq. (3.13), we can then calculate the expectation of

$H_{d/f/s}$:

$$\begin{aligned}\mathbb{E}[\exp(H_{d/h/s})] = \exp\Big((\gamma F(\phi) - \frac{F^2(\phi)}{4C(t+\eta)\alpha})h + \\ - \frac{1}{2}\ln(1-2C(t+\eta)\alpha) + \frac{C(t+\eta)\alpha\gamma^2 - \gamma F(\phi) + \frac{F^2(\phi)}{4C(t+\eta)\alpha}}{1-2C(t+\eta)\alpha}h\Big).\end{aligned}$$

Rearranging and simplifying the preceding expression I recover:

$$\begin{aligned}&\mathbb{E}[\exp(H_{d/h/s})] \\ &= \exp\Big(-\frac{1}{2}\ln(1-2C(t+\eta)\alpha) + \Big(\gamma F(\phi) - \frac{1}{2}\gamma^2 + \frac{(F(\phi)-\gamma)^2}{2(1-2C(t+\eta)\alpha)}\Big)h\Big).\end{aligned} \tag{3.15}$$

Applying Eq. (3.15) back into Eq. (3.12), we have:

$$\begin{aligned}f^*(t;T,\phi) = \exp\Big(&\phi x(t) + A(t+\eta) + B_d(t+\eta)\mu_{0d} - B_f(t+\eta)\mu_{0f} + C_d(t+\eta)\omega_d + \\ &- C_f(t+\eta)\omega_f + C_s(t+\eta)\omega_s + -\frac{1}{2}\ln(1-2C_s(t+\eta)\alpha_s) + \\ &- \frac{1}{2}\ln(1-2C_d(t+\eta)\alpha_d) + \frac{1}{2}\ln(1-2C_f(t+\eta)\alpha_f) + \\ &+ (B_d(t+\eta)\mu_{1d} + \phi)r_d(t) - (B_f(t+\eta)\mu_{1f} + \phi)r_f(t) + \\ &+ \Big(C_s(t+\eta)\beta_s - \frac{1}{2}\phi + \gamma_s^*\phi - \frac{1}{2}\gamma_s^{*2} + \frac{(\phi-\gamma_s^*)^2}{2(1-2C_s(t+\eta)\alpha_s)}\Big)h_s(t+\eta) + \\ &+ \Big(C_d(t+\eta)\beta_d + B_d(t+\eta)\lambda_d + \gamma_d B_d(t+\eta) - \frac{1}{2}\gamma_d^2 + \\ &+ \frac{(B_d(t+\eta)-\gamma_d)^2}{2(1-2C_d(t+\eta)\alpha_d)}\Big)h_d(t+\eta) - \Big(C_f(t+\eta)\beta_f + B_f(t+\eta)\lambda_f + \\ &+ \gamma_f B_f(t+\eta) - \frac{1}{2}\gamma_f^2 + \frac{(B_f(t+\eta)-\gamma_f)^2}{2(1-2C_f(t+\eta)\alpha_f)}\Big)h_f(t+\eta)\Big).\end{aligned} \tag{3.16}$$

Finally, comparing Eq. (3.11) with Eq. (3.16), we get the iteration term for $A(t)$,

$B_{d/f}(t)$ and $C_{d/f/s}(t)$:

$$
\begin{aligned}
A(t;T,\phi) =& A(t+\eta;T,\phi) + B_d(t+\eta;T,\phi)\mu_{0d} - B_f(t+\eta;T,\phi)\mu_{0f} + \\
&+ C_d(t+\eta;T,\phi)\omega_d - C_f(t+\eta;T,\phi)\omega_f + C_s(t+\eta;T,\phi)\omega_s + \\
&- \frac{1}{2}\ln(1-2C_s(t+\eta;T,\phi)\alpha_s) - \frac{1}{2}\ln(1-2C_d(t+\eta;T,\phi)\alpha_d) + \\
&+ \frac{1}{2}\ln(1-2C_f(t+\eta;T,\phi)\alpha_f), \\
B_d(t;T,\phi) =& B_d(t+\eta;T,\phi)\mu_{1d} + \phi, \\
B_f(t;T,\phi) =& B_f(t+\eta;T,\phi)\mu_{1f} + \phi, \\
C_d(t;T,\phi) =& C_d(t+\eta;T,\phi)\beta_d + B_d(t+\eta;T,\phi)\lambda_d + \gamma_d B_d(t+\eta;T,\phi) + \\
&- \frac{1}{2}\gamma_d^2 + \frac{(B_d(t+\eta;T,\phi)-\gamma_d)^2}{2(1-2C_d(t+\eta;T,\phi)\alpha_d)} \\
C_f(t;T,\phi) =& C_f(t+\eta;T,\phi)\beta_f + B_f(t+\eta;T,\phi)\lambda_f + \gamma_f B_f(t+\eta;T,\phi) + \\
&- \frac{1}{2}\gamma_f^2 + \frac{(B_f(t+\eta;T,\phi)-\gamma_f)^2}{2(1-2C_f(t+\eta;T,\phi)\alpha_f)}, \\
C_s(t;T,\phi) =& C_s(t+\eta;T,\phi)\beta_s - \frac{1}{2}\phi + \gamma_s^*\phi - \frac{1}{2}\gamma_s^{*2} + \frac{(\phi-\gamma_s^*)^2}{2(1-2C_s(t+\eta;T,\phi)\alpha_s)}.
\end{aligned}
$$

Setting $k \in \{d, f\}$, I recover the expression in the theorem.

End of proof. □

The closed form characteristic function can then be used to price the option. The main idea here is that characteristic function is the Fourier transform of the probability density function of the spot rate at terminal, thus describes the distribution of the future spot rate. Notice the staggered boundary conditions for the domestic and foreign spot timed deposit rates versus spot FX variance equation. This differs from those found in the Ingersoll [1987], Heston and Nandi [1999] and Heston and Nandi [2000] specifications. Recall that at each time step

the timed deposit rate is already set, hence for the last step, the future variation of the rate for $T+\eta$ is not required. Therefore, the adjusted terminal condition. This illustrates my trivial case, when $\tau = J\eta$ for $J = 1$, the model collapses completely to a one period Black-Scholes/Garman and Kohlhagen model and subsequently breaking the implied volatility skew structure needed to properly fit the observed market characteristics.

Remark 2. *To derive the exact price I follow Ingersoll [1987] and use a single characteristic function to combine the timed deposit rate and spot exchange rate dynamics*

$$\begin{aligned}\mathbb{E}_t^*[max(S(T)-K,0)] =& f^*(1)\left(\frac{1}{2}+\frac{1}{\pi}\int_0^\infty \Re\left[\frac{K^{-\phi}f^*(\phi+1)}{\phi f^*(1)}\right]d\phi\right)+ \\ &- K\left(\frac{1}{2}+\frac{1}{\pi}\int_0^\infty \Re\left[\frac{K^{-\phi}f^*(\phi)}{\phi}\right]d\phi\right). \qquad (3.17)\end{aligned}$$

Proof. I use $f^*(\phi)$ to obtain the probability density function via an inverse Fourier transform, which is also referred to as the Inversion Theorem. Following Lévy [1925], who provided a fundamental inversion formula, Gil-Pelaez [1951] provides a useful treatment of the Fourier inversion theorem, which shows the cumulative distribution function $F_X(x) = \int_\infty^x f_X(x)dx$ (given $f_X(x)$ is the probability density function of an random variable x) is

$$F_X(x_T) = \mathbb{P}(x \leqslant x_T) = \frac{1}{2} + \frac{1}{2\pi}\int_0^\infty \frac{e^{\phi x_T}f^*(-\phi) - e^{-\phi x_T}f^*(\phi)}{\phi}d\phi.$$

Consider a complex number $\mathbf{z} \in \mathbb{C}$ with properties such that its real part is $\Re[\mathbf{z}] = (\mathbf{z}+\bar{\mathbf{z}})/2$ and its imaginary part is $\Im[\mathbf{z}] = (\mathbf{z}-\bar{\mathbf{z}})/2$, where $\bar{\mathbf{z}}$ is the

complex conjugate. For the characteristic function

$$\Re[f^*(\phi)] = \frac{f^*(\phi) + f^*(-\phi)}{2}, \Im[f^*(\phi)] = \frac{f^*(\phi) - f^*(-\phi)}{2},$$

which implies that the real part of $f^*(\phi)$ is an even function and the imaginary part is odd. Then I derive that

$$\begin{aligned} F_x(x_T) &= \frac{1}{2} + \frac{1}{2\pi}\int_0^\infty \frac{e^{i\phi x_T} f^*(-i\phi) - e^{-i\phi x_T} f^*(i\phi)}{i\phi} d\phi \\ &= \frac{1}{2} + \frac{1}{2\pi}\int_0^\infty \left[\overline{\left(\frac{e^{-\phi x_T} f^*(\phi)}{-\phi}\right)} - \frac{e^{-\phi x_T} f^*(\phi)}{\phi}\right] d\phi \\ &= \frac{1}{2} - \frac{1}{\pi}\int_0^\infty \Re\left[\frac{e^{-\phi x_T} f^*(\phi)}{\phi}\right] d\phi. \end{aligned}$$

Now we can calculate that the probability $\mathbb{P}(x_T \geqslant \ln K) = \int_{\ln K}^\infty f_X(x)dx$ is simply $1 - \mathbb{P}(x_t \leqslant \ln K)$, which is

$$\mathbb{P}(x_T \geqslant \ln K) = \frac{1}{2} + \frac{1}{\pi}\int_0^\infty \Re\left[\frac{e^{-\phi \ln K} f^*(\phi)}{\phi}\right] d\phi. \tag{3.18}$$

The final thing to demonstrate in the raw affine model is that the expectation of the terminal payoff is

$$\begin{aligned} \mathbb{E}_t^*[\max(S(T) - K, 0)] &= \mathbb{E}_t^*[\max(e^{x_T} - K, 0)] \\ &= \mathbb{E}_t^*[e^{x_T}\mathbf{1}_{S(T)\geqslant K}] - K\mathbb{E}_t^*[1_{S(T)\geqslant K}]. \end{aligned} \tag{3.19}$$

I have shown the derivation of the second summand term, since $\mathbb{E}_t^*[\mathbf{1_{S(T)\geqslant K}}] = \mathbb{P}(x_T \geqslant \ln K)$. The first expectation term $\mathbb{E}_t^*[e^{x_T}\mathbf{1}_{S(T)\geqslant K}]$ needs adjustments. Observing $\mathbb{E}_t^*[e^{x_T}\mathbf{1}_{S(T)\geqslant K}] = \int_{\ln K}^\infty e^{x_T} f_X(x)dx$, we can introduce a change of measure

from $\mathbb{Q}^*$ to $\tilde{\mathbb{Q}}^*$ with Radon-Nikodym derivative

$$\frac{d\tilde{\mathbb{Q}}^*}{d\mathbb{Q}^*} = \frac{e^{x_T}}{\mathbb{E}^{\mathbb{Q}^*}[e^{x_T}]}.$$

This is equivalent to an adjusted probability density function defined by

$$\tilde{f}_X(x) = \frac{e^{x_T} f_X(x)}{\mathbb{E}^{\mathbb{Q}^*}[e^{x_T}]} = \frac{e^{x_T} f_X(x)}{f^{\mathbb{Q}^*}(1)}.$$

Under the new measure $\tilde{\mathbb{Q}}^*$, the characteristic function is

$$f^{\tilde{\mathbb{Q}}^*}(\phi) = \mathbb{E}^{\tilde{\mathbb{Q}}^*}[e^{\phi x_T}] = \frac{\mathbb{E}^{\mathbb{Q}^*}[e^{x_T} e^{\phi x_T}]}{\mathbb{E}^{\mathbb{Q}^*}[e^{x_T}]} = \frac{f^{\mathbb{Q}^*}(\phi+1)}{f^{\mathbb{Q}^*}(1)}.$$

Then we can derive the first term as

$$\begin{aligned}\mathbb{E}_t^*[e^{x_T}\mathbf{1}_{S(T)\geqslant K}] &= \int_{\ln K}^{\infty} e^{x_T} f_X(x)dx = f^{\mathbb{Q}^*}(1)\int_{\ln K}^{\infty} \tilde{f}_X(x)dx \\ &= f^*(1)\left(\frac{1}{2} + \frac{1}{\pi}\int_0^{\infty} \Re\left[\frac{e^{-\phi \ln K} f^*(\phi+1)}{\phi f^*(1)}\right] d\phi\right). \qquad (3.20)\end{aligned}$$

Substituting Eq. (3.20) and Eq. (3.18) into Eq. (3.19), we can get

$$\begin{aligned}&\mathbb{E}_t^*[\max(S(T)-K,0)] \\ =&f^*(1)\left(\frac{1}{2} + \frac{1}{\pi}\int_0^{\infty} \Re\left[\frac{K^{-\phi} f^*(\phi+1)}{\phi f^*(1)}\right] d\phi\right) - K\left(\frac{1}{2} + \frac{1}{\pi}\int_0^{\infty} \Re\left[\frac{K^{-\phi} f^*(\phi)}{\phi}\right] d\phi\right).\end{aligned}$$

Hence the price satisfies the no-arbitrage assumption under the domestic measure.

End of proof. □

Denoting $D_d(\tau)$ as the domestic discounting factor, and from $\tau = T-t$ then we

can write the value of the option as the present value today of this expectation.[1] We now have sufficient components to determine the FX option pricing formula:

Corollary 2. *The call option price for an FX option following the ASTSV dynamics under the risk-neutral measure $\mathbb{Q}^{\{d\}}$ is given by the following expression:*

$$\begin{aligned} P_c =& D_d(\tau)\mathbb{E}_t^*[max(S(T)-K,0)] \\ =& D_d(\tau)f^*(1)\left(\frac{1}{2}+\frac{1}{\pi}\int_0^\infty \Re\left[\frac{K^{-iu}f^*(iu+1)}{uf^*(1)}\right]du\right)+ \\ & - D_d(\tau)K\left(\frac{1}{2}+\frac{1}{\pi}\int_0^\infty \Re\left[\frac{K^{-iu}f^*(iu)}{iu}\right]du\right). \end{aligned} \tag{3.21}$$

The put option price can be then calculated by the put-call parity as

$$P_p = P_c - D_f(\tau)S(t) + D_d(\tau)K. \tag{3.22}$$

3.2.2 Affine stochastic volatility (ASV) and affine realised variance (ARV) models

For FX options with shorter maturities, for instance less than two years, the variance of the deposit rate usually has a vanishing contribution to the overall price. We can simplify short maturity models using the following assumption.

Assumption 4. *Pricing options with constant drift $r_d - r_f$. Let R_d and R_f be the currently quoted timed deposit rates as discrete annual percentage rates for the domestic and foreign numéraires from time t to option maturity date T. Let*

[1] Recall that τ is measured in units of η, hence if η is one day then $T-t$ is the number of trading days from t to T. We suffer less from the problem of time-mismatches between the trading day and one days interest, but this still needs to be included as this is a substantial source of error for long maturities.

$\mathscr{A}(\eta, \tau) = A\tau^{-1}\eta$ *be an annualization conversion factor for a given combination of* η *and* τ*, such that* $r_k = \mathscr{A}(\eta, \tau)\ln(1 + R_k/100)$.

For instance, with spot prices traded for five days a week, a year typically contains 252 business days (Monday to Friday, with US holidays); hence if η is daily, there will be 252/1 increments from t_0 to T for each day's free variation. The factor $\mathscr{A}(\eta, \tau) = 365/(252/1)$ provides the adjustment to the daily risk-free rate to account for the difference in trading time versus calendar time for each increment. Hence $r_k = \mathscr{A}(\eta, \tau)\ln(1 + R_k/100)$, for $k \in \{d, f\}$ for an annually reported percentage rate R_k.

For short maturity options this can yield only a very small deviations from the 'correct' price, but for longer maturity options the incorrect identification of $\mathscr{A}(\eta, \tau)$ can lead to substantial pricing errors.

Assumption 5. *The ASV Model. When foreign and domestic numéraires are constant, the ASTSV model collapses to a Heston and Nandi [2000] model with constant drift* $r_d - r_f$ *(henceforth referred to as the Garman and Kohlhagen [1983] adjustment):*

$$R(t + \eta) = r_d - r_f - \frac{1}{2}h_s(t + \eta) + \sqrt{h_s(t + \eta)}z^*(t + \eta), \tag{3.23}$$

$$h_s(t + \eta) = \omega_s + \beta_s h_s(t) + \alpha_s(z^*(t) - \gamma_s^*\sqrt{h_s(t)})^2. \tag{3.24}$$

The corresponding characteristic function is easily defined as a constrained form of the ASTSV model and is given in the following proposition:

Proposition 1. *The ASV Model Characteristic Function. The characteristic*

function for the ASV model with deterministic deposit rates is given by:

$$f^*(\phi) = \mathbb{E}^*[e^{\phi x(T)}] = e^{\phi x(t)} e^{(A^*(t;T,\phi)+B^*(t;T,\phi)h_s(t+\eta))}, \tag{3.25}$$

where

$$\begin{aligned} A^*(t;T,\phi) =& A^*(t+\eta;T,\phi) + \phi(r_d - r_f) + B^*(t+\eta;T,\phi)\omega_s + \\ & - \frac{1}{2}\ln(1-2\alpha_s B^*(t+\eta;T,\phi)); \end{aligned} \tag{3.26a}$$

$$\begin{aligned} B^*(t;T,\phi) =& \phi(-\frac{1}{2}+\gamma_s^*) - \frac{1}{2}\gamma_s^{*2} + \beta_s B^*(t+\eta;T,\phi) + \\ & + \frac{(\phi-\gamma_s^*)^2}{2(1-2\alpha_s B^*(t+\eta;T,\phi))}. \end{aligned} \tag{3.26b}$$

These coefficients can be can be calculated recursively under the terminal conditions $A^*(T;T,\phi) = B^*(T;T,\phi) = 0$.

Proof. Proposition 1 closely follows the analysis in Heston and Nandi [2000], but it is important to illustrate that the two numéraires do indeed allow for a similar functional form. The proof is actually an simplified version of the ASTSV's characteristic function derivation. So we will just refer to the former proof. End of proof. □

Assumption 6. *The ARV Model. An alternative to the GARCH–type assumption for the ASV model uses realised quadratic variation to construct an exogenous time series of conditional variances* $\hat{h}_s(t+\eta)$ *under the following approximation:*

$$\int_t^{t+\eta} h(t)dt = \hat{h}_s(t+\eta) \to \sum_{m=1}^{M} \epsilon_s^2(t+\frac{m}{M}\eta), \tag{3.27}$$

where M *is the number of intra-day observations and* $h(t)$ *is the instantaneous*

spot variance.

This model can then be fitted in a two stage estimation via non-linear least squares.

3.3 Estimation procedures

I fit the various model specifications via non-linear least squares (NLLS) and maximum likelihood estimation (MLE). Specifically, I fit the timed deposit rate models via NLLS directly to the yield curve, the ARV model is fitted by NLLS to the time series of realised quadratic variance estimated from five-minute data and the GARCH models are fitted via MLE to the filtered spot rate dynamics. I detail these procedures in reverse order, starting with the GARCH models.

3.3.1 Spot FX GARCH volatility model estimation via MLE

Let $\theta_s = (\lambda_s, \omega_s, \beta_s, \alpha_s, \gamma_s)$ represents the model parameters for the spot rate dynamics in Assumption 2. Notice that the term $r_d(t) - r_f(t)$ is lagged in respect to $R(t+\eta)$. Let $n \in \{1, \ldots, N\}$ index a set of historical observations of exchange rate fluctuations and timed deposit accounts denoted $R_n(t)$, $r_{d,n}(t)$ and $r_{f,n}(t)$. The econometric specification can be explicitly stated by

$$R_n(t+\eta) - r_{d,n}(t) + r_{f,n}(t) = \lambda_s h_{s,n}(t+\eta) + \sqrt{h_{s,n}(t+\eta)} z_n(t+\eta) = \epsilon_{s,n}(t+\eta),$$
$$h_{s,n}(t+\eta) = \omega_s + \beta_s h_{s,n}(t) + \alpha_s (z_n(t) - \gamma_s \sqrt{h_{s,n}(t)})^2.$$

The Gaussian log likelihood function for a given parameter vector $\theta_s \in \Theta_s$ is denoted by:

$$\mathfrak{L}(\theta_s) = -\frac{N}{2}\ln(2\pi) - \frac{1}{2}\sum_{n=n_0}^{N}\ln h_{s,n}(t+\eta|\theta_s) - \frac{1}{2}\sum_{n=n_0}^{N}\frac{(\epsilon_{s,n}(t+\eta) - \lambda_s h_{s,n}(t+\eta|\theta_s))^2}{h_{s,n}(t_0+\eta|\theta_s)}.$$

where Θ_s is the set of all admissible parameter vectors. Estimation proceeds via:

$$\begin{aligned}
&\hat{\theta}_s := \arg\max_{\theta_s} \mathfrak{L}(\theta_s), \\
&s.t. \quad 1 > \beta_s + \alpha_s\gamma_s^2 \geq 0, \quad 1 > \beta_s \geq 0, \quad 1 > \alpha_s \geq 0,
\end{aligned}$$

with an initial condition of $h(t_0|\theta_s) = \omega_s/(1-\beta_s-\alpha_s\gamma_s^2)$. The number of initialization observations n_0 is obviously subject to discretion. As $\beta_s + \alpha_s\gamma_s^2 \to 1$, the results will be increasingly sensitive to the initial condition.

Finally, let $\mathbf{H}_s(\theta_s) = (\partial^2/\partial\theta_s\partial\theta_s')\mathfrak{L}(\theta_s)$ be the Hessian matrix of second order partial derivatives of $\mathfrak{L}(\theta_s)$. Notice that dependency structure of this type of GARCH model forces us to approximate the Hessian by finite differencing, a simple and robust approach is for each pair of parameters to randomly sample a small number of points, I use 50, in the interval $(\theta_s - \bar{\iota}, \theta_s + \bar{\iota})$, where $\bar{\iota}$ is the fourth root of the smallest floating point integer difference available (depends on the computer) and then fit the closest bivariate second order polynomial, this modifies a forward and backward differencing approach suggested by Kevin Sheppard in the MFE-GARCH toolbox, see https://www.kevinsheppard.com/MFE_Toolbox, last accessed December 2016. The coefficients of the quadratic terms yield the derivatives of interest.

The asymptotic variance covariance matrix $\hat{\mathbf{Q}} = Asy.Cov.[\hat{\theta}_s|\theta_{0s}] = ((N -$

$n_0)\mathbf{H}_s(\hat{\theta}_s))^{-1}$, where θ_{0s} is the 'true' parameter vector. Notice that we can write down expressions for the derivatives of $\mathfrak{L}(\theta_s)$ using the recursion from the preceding section.

3.3.2 Spot FX realised volatility model estimation via NLLS

Following Assumption 6, I presume that $\hat{h}_s(t+\eta) \to \sum_{m=1}^{M} \epsilon_s^2(t+\frac{m}{M})$ is identified from high frequency data, I will utilise a five minute grid from tick data. Estimation of the structural parameters then proceeds via NLLS estimation of the following pair of equations:

$$\begin{aligned}
\epsilon_{s,n}(t+\eta) =& \lambda_s \hat{h}_{s,n}(t+\eta) + \sqrt{\hat{h}_{s,n}(t+\eta)} z_{RV,n}(t+\eta); \\
\hat{h}_{s,n}(t+\eta) =& \omega_s + \beta_s \hat{h}_{s,n}(t) + \alpha_s \gamma_s^2 \hat{h}_{s,n}(t) + \\
& - 2\alpha_s \gamma_s \sqrt{\hat{h}_{s,n}(t)} z_{RV,n}(t) + \alpha_s z_{RV,n}^2(t) + \xi_n(t+\eta).
\end{aligned}$$

First I compute:

$$\begin{aligned}
\hat{\lambda}_s :=& \arg\min_{\lambda_s} \sum_{n=1}^{N} (\lambda_s \hat{h}_{s,n}(t+\eta) + \sqrt{\hat{h}_{s,n}(t+n\eta)} z_{RV,n}(t+\eta) - \epsilon_{s,n}^2(t+\eta))^2 \\
& s.t. \quad \sum\nolimits_n^N z_{RV,n}(t+\eta) = 0, \quad \sum\nolimits_n^N z_n^2(t+\eta) = 1.
\end{aligned}$$

Notice that there is more than sufficient slackness in the identification $\tilde{z}(t)$ to satisfy the restrictions. Next I input the recovered disturbances $z_{RV,n}(t+\eta)$ in

the variance equation, given the estimated $\hat{\lambda}$ and observed $\hat{h}_{s,n}(t)$. Setting

$$\begin{aligned} g_{n+1}(\theta_{RV}|t+\eta) =& \omega_s + \beta_s \hat{h}_{s,n}(t+\eta) + \alpha_s \gamma_s^2 \hat{h}_{s,n}(t+\eta) + \\ & - 2\alpha_s \gamma_s \sqrt{\hat{h}_{s,n}(t+\eta)} z_{RV}(t+\eta) + \alpha_s z_{RV}^2(t+\eta) \end{aligned}$$

to be the one step ahead, in data, forecasts of the conditional variance.

$$\begin{aligned} \{\hat{\omega}_s, \hat{\beta}_s, \hat{\alpha}_s, \hat{\gamma}_a\} &:= \underset{\{\omega_s, \beta_s, \alpha_s, \gamma_a\}}{\arg\min} \ \mathfrak{L}_{RV}(\omega_s, \beta_s, \alpha_s, \gamma_a), \quad \text{where} \\ \mathfrak{L}_{RV}(\omega_s, \beta_s, \alpha_s, \gamma_a) &= \sum_{n=1}^{N} (\hat{h}_{s,n}(t+\eta) - g_n(\theta_{RV}|t+\eta))^2, \end{aligned}$$

As $\hat{\lambda}_s$ is uniquely identified I set $\theta_{RV} = (\omega_s, \beta_s, \alpha_s, \gamma_a)'$.

3.3.3 Asymptotic error of the call option price

Let $P_c(\theta_s)$ be the call option price as a function of the spot exchange rate model parameters. The ASV derivatives of the call price with respect to the underlying parameters are given by

$$\hat{\mathbf{\Delta}}_{\mathbf{s}}(\theta_{\mathbf{s}}) := \frac{\partial P_c(\theta_s)}{\partial \theta_s} \to \frac{1}{2}\left[\frac{P_c(\theta_{i,s}+\zeta) - P_c(\theta_{i,s})}{\zeta}\right] + \frac{1}{2}\left[\frac{P_c(\theta_{i,s}-\zeta) - P_c(\theta_{i,s})}{-\zeta}\right]. \tag{3.28}$$

Unfortunately the elements of, $\hat{\mathbf{\Delta}}_{\mathbf{s}}(\theta_{\mathbf{s}})$ do not have convenient closed form solutions and hence have to be determined by numerical approximation, via a finite difference ζ. Using the 'delta' method we can approximate the distribution of $P_c(\theta_s)$ in the following way. I denote $\sqrt{N}(\hat{\theta}_s - \theta_{0,s}) \to^d \mathcal{N}(0, N\hat{\mathbf{Q}})$; this implies that $\sqrt{N}(P_c(\hat{\theta}_s) - P_c(\theta_{0,s})) \to^d \mathcal{N}(0, \hat{\mathbf{\Delta}}'_{\mathbf{s}}(\theta_{\mathbf{s}}) N \hat{\mathbf{Q}} \hat{\mathbf{\Delta}}_{\mathbf{s}}(\theta_{\mathbf{s}}))$ and yields an obvious,

but very useful new result combining the 'GARCH parameter derivatives' and the asymptotic covariance matrix from the estimation phase:

Corollary 3. *Asymptotic Variance of the Estimated Call Price*

$$Asy.Var.[P_c(\hat{\theta}_s)] = \hat{\mathbf{\Delta}}'_{\mathbf{s}}(\theta_{\mathbf{s}})\hat{\mathbf{Q}}\hat{\mathbf{\Delta}}_{\mathbf{s}}(\theta_{\mathbf{s}}). \tag{3.29}$$

I provide a sketch of the proof of continuity of Eq. (3.28) as the following

Proof. The majority of Corollary 3 is easily verifiable from the standard properties of the delta method, see Casella and Berger [2002]. The problem reduces to ascertaining that $P_c(\theta_s)$ for $\theta_s \in \Theta_s$ is at least $\mathcal{C}^2$ and hence the numerical approximation in Eq. (3.28) is valid, using the Bolzano-Weierstrass theorem, when $\hat{\theta}_s$ is from the feasible parameter set Θ_s. First, notice that we can reduce this problem to simply ascertaining that

$$\begin{aligned}&\mathbb{E}[\exp(H_{d/h/s})] \\ =&\exp\Big(-\frac{1}{2}\ln(1-2C(t+\eta)\alpha) + \Big(\gamma F(\phi) - \frac{1}{2}\gamma^2 + \frac{(F(\phi)-\gamma)^2}{2(1-2C(t+\eta)\alpha)}\Big)h\Big),\end{aligned}$$

is continuous with respect to $\theta = \{\omega, \beta, \alpha, \gamma\}$, for $0 \leq \beta < 1$, $0 \leq \alpha < 1$ and $1 - \beta - \alpha\gamma^2 > 0$. This is dues to the call price, Eq. (3.21) as an integral of the characteristic function, which must itself obey the fundamental theorem of Lebesgue integral calculus. If this is the case then the pattern for the three processes is additive hence preserving continuity. It is straightforward to note that via the chain rule the polynomial property of $C(t+\eta)$ with respect to θ results in always continuous derivative for $\mathbb{E}[\exp(H_{d/h/s})]$. Therefore, with at least one time step $\mathbb{E}[\exp(H_{d/h/s})]$ is at least $\mathcal{C}^2$.

End of proof. □

3.3.4 Capturing the term structure dynamics

Given the dynamic of the interest rate in Assumption 3, we can derive the bond price accordingly. For a money account $M(t)$ associated with interest rate $r_k(t)$, assume it has an initial value at t being $M(t) = 1$. Then here we use the moment generating function for the future logarithm money account value $m(T) = \ln M(T)$, which is affine and of the following form

$$f(u) = \mathbb{E}^*[e^{um(T)}] = \exp(A(t;T,u) + B_d(t;T,u)r_k(t) + C_k(t;T,u)h_k(t+\eta)).$$

where $k \in d, f$ denotes the parameters for domestic or foreign interest rates respectively. The recursive coefficient terms to be evaluated from the terminal boundary conditions are as follows:

$$\begin{aligned}
A(t;T,u) =& A(t+\eta;T,u) + B_k(t+\eta;T,u)\mu_{0k} + C_k(t+\eta;T,u)\omega_k + \\
&- \frac{1}{2}\ln(1 - 2C_k(t+\eta;T,u)\alpha_k) \\
B_k(t;T,u) =& B_k(t+\eta;T,u)\mu_{1k} + u, \\
C_k(t;T,u) =& C_k(t+\eta;T,u)\beta_k + B_k(t+\eta;T,u)\lambda_k + \gamma_k B_k(t+\eta;T,u) + \\
&- \frac{1}{2}\gamma_k^2 + \frac{(B_k(t+\eta;T,u) - \gamma_k)^2}{2(1 - 2C_k(t+\eta;T,u)\alpha_k)}.
\end{aligned}$$

The boundary conditions at T are the following:

$$A(T;T,u) = B_k(T;T,u) = C_k(T;T,u) = 0, C_k(T-\eta;T,u) = 0, \quad k \in \{f,d\}.$$

We can then notice that the moment generating function becomes bond price when moment $u = -1$.

Let $\bar{B}(s\eta)$ be the quoted bond price on a time deposit account with maturity $s\eta$ at time t_0. If we consider the collection of bond prices $\{B(s\eta)|s \in \{0, \ldots, \tau\eta^{-1}\}\}$ describing the yield curve for available timed deposit accounts. Recalling that $\theta_k = (\lambda_k, \omega_k, \beta_k, \alpha_k, \gamma_k)'$, the calibrated yield curve models can be obtained from the following non-linear least squares fitting:

$$\hat{\theta}_k := \arg\min_{\theta_k} \sum_{s=1}^{\tau\eta^{-1}} (f(t_0 + s\eta; T, u = -1) - B(t_0 + s\eta)])^2.$$

We can make use of the standard asymptotic normality assumption for the non-linear least squares estimator to obtain $\sqrt{\tau\eta^{-1}}(\hat{\theta}_k - \theta_0) = \mathbf{H}^{-1}[\hat{\theta}_k]$, where $\mathbf{H}[\theta_k]$ is the Hessian matrix such that:

$$\mathbf{H}[\theta_k] = \frac{\partial^2}{\partial\theta_k \partial\theta_k'} \sum_{s=1}^{\tau\eta^{-1}} (f(t_0 + s\eta; T, u = -1) - B(t_0 + s\eta)])^2.$$

If we restrict the functional form of the model by setting $\beta_k = \alpha_k = \gamma_k = 0$ and hence implying that $\lambda_k = 0$, we can determine a simple formulation for the long term rate, $\tau \to \infty$, denoted by $\bar{r}_k$, under the assumption that $|\mu_{1k}| < 1$: $\bar{r}_k = \mu_{0k}/(1 - \mu_{1k})$ we can determine the expectation of any forward rate $\bar{r}_{k,t+s}$ in the standard way for any discrete-time Vasicek-type model whereby $\bar{r}_k(t + s\eta) = \sum_{i=0}^{s-1} \mu_{0k}\mu_{1k}^i + \mu_{1k}^s r_{k,t}$. The proposed interest dynamic with tenor equals time-step size can also be estimated by MLE based on its time series.

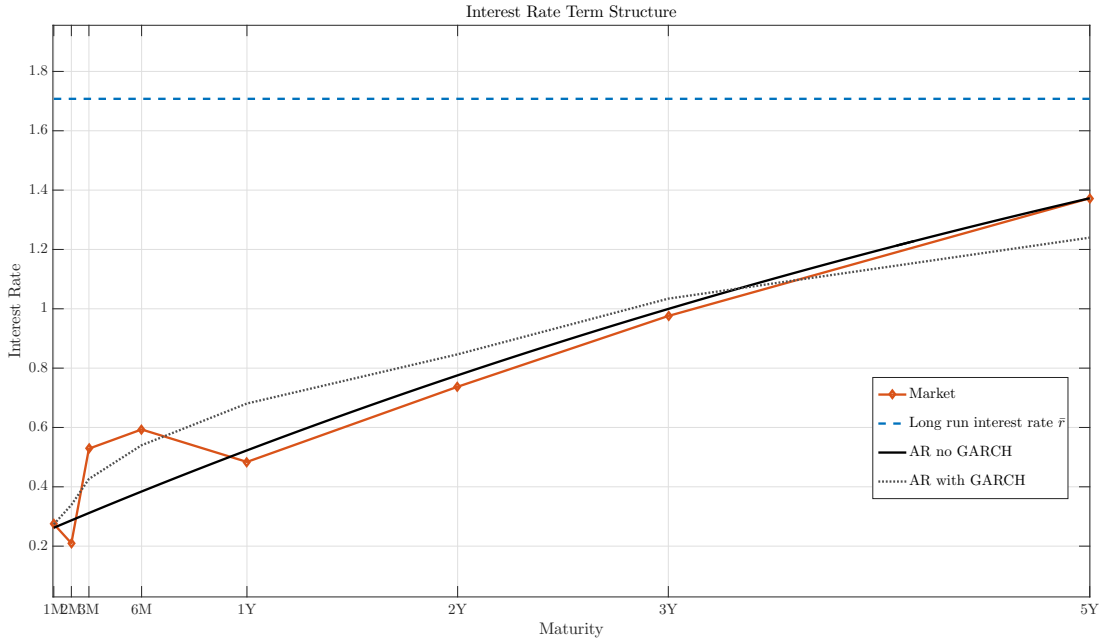

Figure 3.1: Term structure of the short rate models, with and without GARCH terms. First five years of the US dollar term structure (red line), with the predicted model fit from a calibrated discrete-time Vasicek model. The dashed line is the yield on a 20-year treasury bond. The yellow line presents the calibrated model with a dynamic variance equation, whilst the blue line presents a standard Vasicek-type fit, in discrete-time with constant variance.

3.3.5 Empirical illustration of term structure calibration with and without GARCH dynamics

Fig. 3.1 illustrates this calibration procedure for a US yield curve for a single day. We can see the relative advantages and disadvantages of the two approaches. The markers on the red line represent market quotes. They generate enough comparative rates for calibration of the seven parameters in the unrestricted specification; I have used linear interpolation to generate a larger number of market rates.

The unrestricted model has more flexibility in matching the kinks in the quoted deposit rates during the early part of the term structure, but this comes

at a cost in terms of accuracy for the longer part of the curve. The restricted model (standard discrete-time Vasicek) matches the long rates very well.

3.4 Computing quoted FX surface error bounds

I have showed the volatlity surface construction process in Section 2.4 of Chapter 2. However, 'bottom-up' computation of the surface and identification of the error bounds is completely absent in the literature and not entirely straightforward. We also need to make use of the delta method once more to determine the actual error bounds on the quotes given the noisy preceding estimation.

To generate confidence bounds in the resulting structurally derived quotes, I use the delta method to translate the estimation error into a pricing error. Here I follow the process in Section 2.4 and keep alignment of the notations.

Let $\mathscr{Q}(\hat{\theta}) = [\widetilde{BF}_{10}, \widetilde{BF}_{25}, \widetilde{AT}, \widetilde{RR}_{25}, \widetilde{RR}_{10}]'$ be the vector of estimated quotes as a function of the model parameter point estimates $\hat{\theta}$. Next I set $\hat{\mathbf{D}} = [\hat{\mathbf{\Delta}}'_{\mathbf{s},\varphi}(\hat{\theta}_{\mathbf{s}})]$ to be a matrix with columns formed by the vectors of partial derivatives of the following pivotal options prices $\hat{\mathbf{P}}(\hat{\theta}_s) = [\hat{P}_{10c}, \hat{P}_{25c}, \hat{P}_{50c}, \hat{P}_{50p}, \hat{P}_{25p}, \hat{P}_{10p}]'$ where I extend my previous notation such that for a put or call option satisfying $\partial P_{\varpi\in\{p,c\}}(\hat{\theta}_s)/\partial S(t) = \varphi$ is denoted $\hat{P}_{\varpi}$. Subsequently, we can collect all of the pivot prices at the critical market deltas $\varphi \in \{10c, 25c, 50c, 50p, 25p, 10p\}$ and collect the partial derivatives with respect to the underlying model parameters at the optimum. It is evident that the sequence of transformations in Eq. (2.1) is smooth hence from from the inverse function theorem the derivative $\partial\mathscr{Q}(\hat{\theta})/\partial\hat{\mathbf{P}} = \hat{\mathbf{\Gamma}}$ exists and is smooth, hence using the result in Corollary 3 we can extend the delta

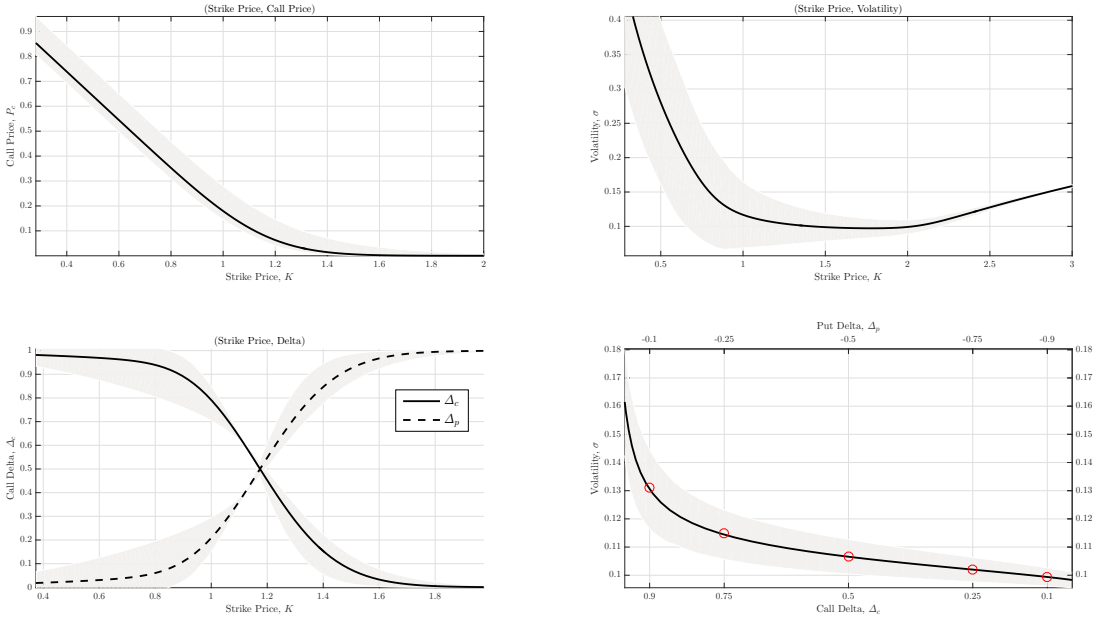

Figure 3.2: Recovering the market quotes from the model option price curve. The upper left quadrant depicts the call price curve with its 95% error bound in grey over a range of strikes. Using the Garmen-Kohlhagen adjustment to the Black-Scholes-Merton model for FX options, I then back out the Black-Scholes-Merton implied volatilities the preceding range of strikes; this is plotted in the top right corner. Combining the implied volatilities and the strike price, we can compute the spot or forward delta for put and call prices. The lower left quadrant depicts the absolute spot delta (recalling that the put delta is negative) as a function of the strike price. Combining the upper right quadrant and the lower left quadrant, we can then identify the European surface as a function of the spot delta. In each case the 95% error bound is computed via the delta method carried over from the previous calculation. Note that $|\Delta_{p/c}| = 0.5$, is for plotting purposes.The at the money volatility occurs at the point at which $\Delta_p + \Delta_c = 0$.

method to further derive the asymptotic covariance matrix of the quotes

$$\sqrt{N}(\mathscr{Q}(\hat{\theta}) - \mathscr{Q}(\theta_0)) \sim^d \mathcal{N}(\mathbf{0}, N\hat{\mathbf{\Gamma}}'\hat{\mathbf{D}}'\hat{\mathbf{Q}}\hat{\mathbf{D}}\hat{\mathbf{\Gamma}})$$

which gives an asymptotic variance for the quotes as

$$Asy.Var.[\mathscr{Q}(\hat{\theta})] = \text{diag}[\hat{\mathbf{\Gamma}}'\hat{\mathbf{D}}'\hat{\mathbf{Q}}\hat{\mathbf{D}}\hat{\mathbf{\Gamma}}]$$

and deriving the desired error bound on the market quote. In Fig. 3.2 I illustrate the 'passing-through' of the error structure from the estimation stage to the volatility surface to assist in visualising the preceding steps. The grey area presents the error bounds at each step, the lower right plot then illustrates the volatility surface and the error bounds at the pivot points (the red circles) used to recover the quotes.

3.5 Joint calibration to the observed European volatility surface

Prior to comparing the fit of any structural models estimated from spot data to option market quotes, it is important to check if it is actually possible to accurately model the volatility surface, given the 'optimal' parameter configurations. It makes very little sense to compare models that cannot effectively fit the observed European surface under any circumstances. It is also useful to understand, if some historical option pricing data is available, how much of an improvement can be made by jointly estimating and calibrating to the surface.

As an example, I consider the close-of-day Euro US dollar volatility surface for September 30, 2015 and fit the closest approximating volatility surfaces for the six-month (6M), one-year (1Y) and two-year (2Y) tenors. I employ the ASV and ASTSV models for this purpose and I utilise the '–C' to represent calibration from an observed European surface.

The Fig. 3.3 outlines the fit characteristics for the ASV-C and ASTSV-C models for EURUSD from 6M to 2Y maturity. Notice that the best fitting surface

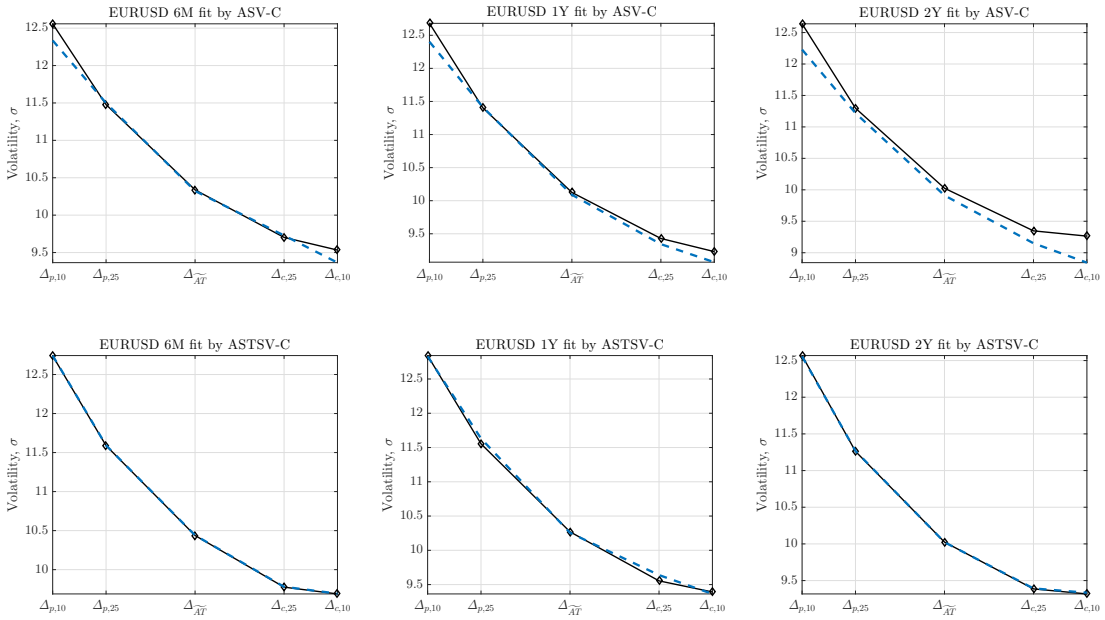

Figure 3.3: Comparison of the ASV-C, ASTSV-C estimated volatility surfaces EURUSD from 6M to 2Y maturity on September 30, 2015.
This figure illustrates some examples of the ASV model and ASTSV model fit surface after direct calibration, to the market volatility surface of the EURUSD call option (black line) on September 30, 2015 for a variety of tenors.

for the optimal ASV-C model is for near maturities, whereas the ASTSV-C model fits the 2Y European surface with the same level of precision as it does for the 6M European surface.

For a general comparison, observe the level of agreement in the European surfaces in Fig. 3.3 with those in Fig. 3.4, which are taken from the closest fitting model estimated exclusively from spot data, the ASTSV model. We can see from these two figures about the improvement by calibration.

For the ASTSV model I set η to be in monthly time increments and for the ASV model I set η to be daily time increments to model the short maturities. This also reduces the computational burden substantially. For instance, for a 2Y volatility surface, a daily update requires over 500 iterations to compute the

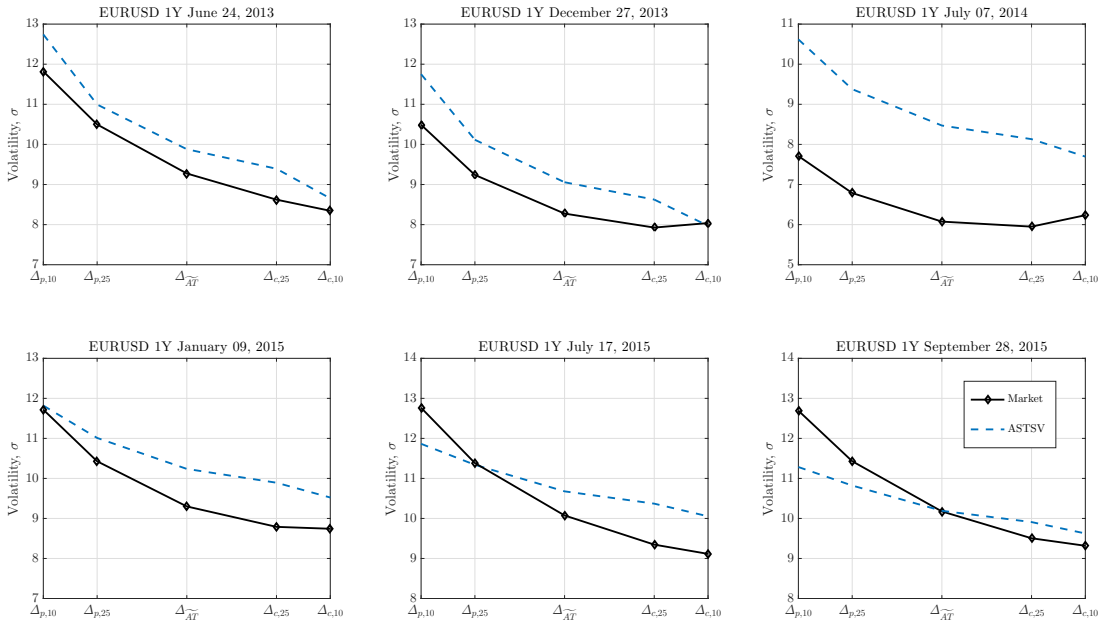

Figure 3.4: Raw ASTSV estimated volatility surfaces for six days for EURUSD 1Y contract.
Compared with Fig. 3.3, this figure shows the raw ASTSV model implied volatility surfaces for six random selected days for EURUSD 1Y contract (dash line) against market quotations (black line).

characteristic function for each moment. Typically, the numerical evaluation of the integral in Eq. (3.21) requires more than 100 evaluations of the characteristic function, to ensure that the resulting call prices form a smooth function with respect to the input parameters and initial variance, interest rate and spot exchange rate conditions. Switching to a monthly frequency for longer tenors reduces this computational complexity markedly.

The $\widetilde{AT}$ volatilities by tenor provide the benchmark for the volatility surface, and I will now focus on adjustments to the spot variance $\hat{h}_s(t)$ and parameter vector θ to correct the $\widetilde{AT}$ term structure and the observed term structure bias.

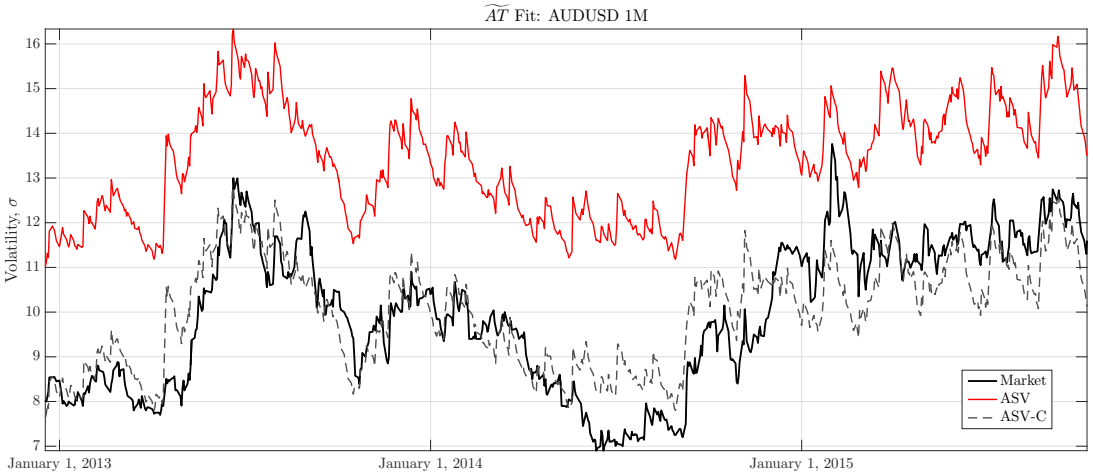

Figure 3.5: The $\widetilde{AT}$ quote for the Australian dollar to US dollar one month FX options from December 17, 2012 to October 8, 2015
The blue line shows the market quotes, the red line is the model quote from the ASV model without calibration and the yellow line is the estimated quote for the ASV model with calibration from an initial 10 days of market quotes.

3.5.1 Calibration of volatility term structures

Evidence from the time series of market quotes suggests that for given tenors the bias in the point estimate is very consistent, and with a subtle adjustment to the spot variance we can correct it without having to re-estimate the parameters on a daily basis. Fig. 3.5 illustrates this effect by plotting the time series of the $\widetilde{AT}$ market quote versus the raw estimates from the spot data for the ASV model for Australian Dollar to US Dollar 1M FX options. The out-of-sample point estimates from the ASV model for the $\widetilde{AT}$ are shown in the red line, labeled simply ASV, to denote an uncalibrated model from spot data only. It is relatively easy to see that the point estimate is systematically biased upward by an almost constant factor.

The simplest way of adjusting the model, whilst maintaining the structural assumptions, is to adjust the point estimates of the spot variance $\hat{h}_s(t)$ and a

subset of the parameter vector θ. I find that for the $\widetilde{AT}$ quotes only α needs to be calibrated. However, for the $\widetilde{BF}$ and $\widetilde{RR}$ quotes calibration of γ is desirable to ensure that correct skew/kurtosis effect is captured by the models implied volatility smile. I detail my approach in the following assumption:

Assumption 7. *Joint calibration with observed prices. The spot variance $h_s(t)$ for the ASV model for can be adjusted by α and a tenor dependent parameter ζ, to yield the following affine term structure adjustment:*

$$\tilde{h_s}(t) = \begin{cases} \zeta(\hat{h}_s(t) - \bar{h_s}) + \bar{h_s} & \min \zeta(\hat{h}_s(t) - \bar{h_s}) + \bar{h_s} \geqslant 0 \\ \zeta(\hat{h}_s(t) - \bar{h_s}) + \bar{h_s} - \min \zeta(\hat{h}_s(t) - \bar{h_s}) & \min \zeta(\tau)(\hat{h}_s(t) - \bar{h_s}) + \bar{h_s} < 0, \end{cases}$$

where $\bar{h}_s = \sum_{t_0}^{T} \hat{h}_s(t)/N$ is the average level of the estimated spot variance process. Let $\widetilde{AT}_{0,d}(\tau)$ be the market quote for an estimation period $d \in \{1, \ldots, D\}$ for tenor τ. Let $\widetilde{AT}_{0,d}(\alpha, \zeta|\theta)$ be the model estimate with other parameters fixed and conditioned on the model estimate $\{\hat{h}_s(t)\}_d$:

$$\{\hat{\alpha}, \hat{\zeta}\} := \underset{\{\hat{\alpha},\zeta\}}{\arg\min} \sum_{d=1}^{D} (\widetilde{AT}_{0,d}(\tau) - \widetilde{AT}_{0,d}(\alpha, \zeta|\theta))^2. \tag{3.30}$$

For butterflies $\widetilde{BF}_{0,d}(\tau)$ and risk reversals $\widetilde{RR}_{0,d}(\tau)$, γ is also calibrated to fit the out of the money delta surface:

$$\{\hat{\alpha}, \hat{\gamma}, \hat{\zeta}\} := \underset{\{\hat{\alpha},\hat{\gamma},\zeta\}}{\arg\min} \sum_{d=1}^{D} (\widetilde{BF}/\widetilde{RR}_{0,d}(\tau) - \widetilde{BF}/\widetilde{RR}_{0,d}(\alpha, \gamma, \zeta|\theta))^2.$$

The dashed plot in Fig. 3.5 illustrates the adjustment for the optimal ζ and α, computed by calibration to the initial $D = 10$ days of data; the parameters are

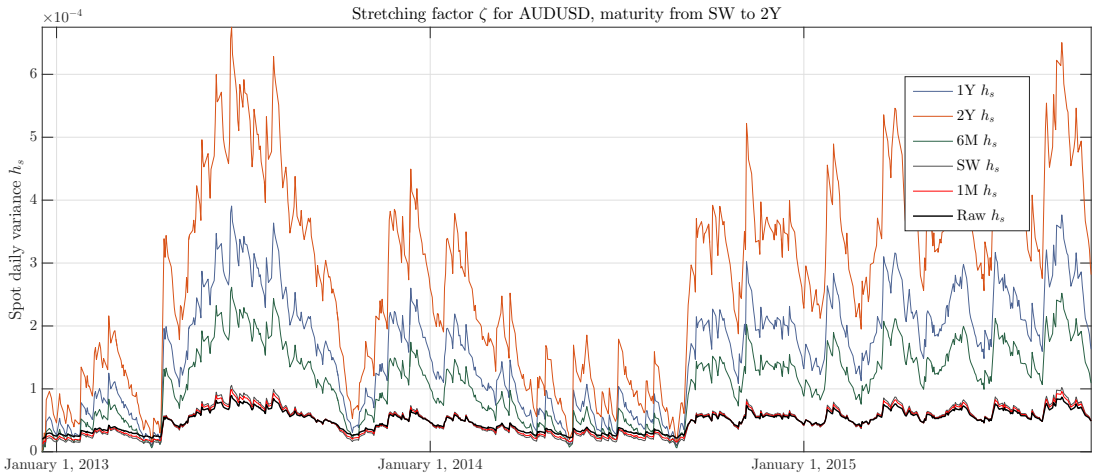

Figure 3.6: The stretching parameter adjusts $h(t)$ across different maturities. This figure shows how the stretching parameter adjusts $h(t)$ across different maturities. Generally the 1M option would share similar information about the implied volatility process compared with the spot price market, thus $\zeta(\tau = 1M)$ is close to 1. Maturities longer or shorter than 1M would anticipate more volatilities in the spot variance process, $h(t)$. ζ will be larger if time to maturity becomes either longer or shorter.

then left constant for the remainder of the sample period (pictured in the plot). A key point here is that for the sample period in the plot (708 days of data) all of the coefficients ζ and θ are fixed, hence the estimates for the dashed line are still out of sample. Because ζ effectively 'stretches' the shape of the spot variance process $h(t)$, we can refer to ζ as a stretching parameter.

In Fig. 3.6 I plot the optimally adjusted spot variances for the Australian Dollar to US Dollar FX options for tenors out to two years (2Y). The thick blue line is the unadjusted spot variance from the point estimates of the model. Each adjustment is computed from the initial ten days of data. I label the re-calibrated ASV model ASV-C to indicate that the model estimates for the market quotes have been calibrated to a sample of market data.

3.6 Empirical demonstration with five currency pairs versus the dollar

I will now compare the performance, out-of-sample, of the various model specifications for five currencies: Australian dollar (AUD), Euro (EUR), Sterling (GBP), Canadian dollar (CAD) and Japanese Yen (JPY) versus the dollar, the FX rates are denoted AUDUSD, EURUSD, GBPUSD, USDCAD and USDJPY respectively. I will forecast out-of-sample FX option quotes for tenors out to five years across the five pivotal quote types ($\widetilde{RR}_{10}$, $\widetilde{RR}_{25}$, $\widetilde{AT}$, $\widetilde{BF}_{25}$ and $\widetilde{BF}_{10}$). The ASV, ARV and ASV-C models are specified over daily data for a 252-business day year for the same-week (SW) to two-year tenor (2Y) (Monday to Friday); I exclude weekends as the quote updates for spot and FX option data are substantially lower. For maturities beyond two years it is impractical to estimate daily models. Hence I will use $\eta = 1month$ for tenors beyond two years. Hence, for three-year (3Y) and five-year (5Y) tenors, the time step is presumed to be monthly. I have an overlap that allows us to compare the time step sizes for tenors from 6M to 2Y. The realized variances for the ARV model use five-minute data on a grid from midnight to midnight GMT. Daily FX spot rates are taken at midnight GMT.

There are a large number of comparative out-of-sample empirical tests that could be undertaken with the preceding specifications. In this section, I focus on comparing the models in terms of increasing complexity by comparison of the simplest ASV specification to the ASTSV specification with stochastic interest rates. I illustrate the value of modest calibration of the ASV-C model to historical options data and the effectiveness of using the ASTSV on monthly increments rather than daily for longer maturity options.

To compare model forecasts I employ a modification of the Hansen and Lunde [2005] approach. This entails fitting the models over a fixed estimation window and then rolling the forecasts forward in a forecasting window for each day, updating only the spot FX data (and hence the next day estimated spot variance). I then compute the point estimates for the FX option quotes and compare them to the actual market quotes. For comparison, I use the standard root mean squared error, RMSE, but supplement this with the absolute of the mean of the error, (ME). The second comparison is useful, as if the two average losses converge then this indicates that the error is systematic (equivalent to the intercept in Mincer-Zarnowitz type regressions) and can be adjusted by an affine transformation of the forecast. In the later section, I provide a recursive comparative loss analysis (again using quadratic loss functions), following Diebold and Mariano [1995], Giacomini and White [2006] and Giacomini and Rossi [2016].

The out-of-sample evaluation window for the option quotes is from Monday December 17, 2012 to October 15, 2015, a total of 708 business days. The ASV-C requires a short number of days to calibrate the term structure adjustment. I use the first ten business days of the available option quotes (from December 17, 2012) for this calibration exercise and exclude them from the evaluation window.

3.6.1 Summary of data

The data I use is sourced from the Thomson–Reuters FX feed and warehoused by SIRCA; Table 3.1 provides the sample characteristic for the data. I collect all updated quotes for spot and FX options, both bid and ask, and compute the mid-price for use in the models. I am led to believe by the vendor that the quote

Table 3.1: Sample characteristics

	Number of quotes								
	AUDUSD			EURUSD			GBPUSD		
Data Type	Days	Ticks	Ticks/Day	Days	Ticks	Ticks/Day	Days	Ticks	Ticks/Day
Spot	7,057	150,773,633	21,365	6,218	250,750,845	40,327	7,057	205,025,549	29,053
r_f-SW	7,224	186,972	26	6,439	912,030	142	7,224	853,584	118
r_f-1M	7,224	220,221	30	6,439	1,571,198	244	7,224	1,155,670	160
r_f-6M	7,224	604,931	84	6,439	2,241,700	348	7,224	2,672,198	370
r_f-1Y	6,979	1,533,812	220	6,161	9,215,498	1,496	4,440	4,068,958	916
r_f-2Y	6,979	2,030,450	291	6,161	22,026,599	3,575	7,220	9,503,409	1,316
r_f-3Y	6,979	1,981,043	284	6,161	32,168,789	5,221	7,220	12,460,839	1,726
r_f-5Y	6,979	1,563,020	224	6,161	28,617,837	4,645	7,220	13,948,876	1,932
r_d-SW	7,228	1,293,587	179	7,228	1,293,587	179	7,228	1,293,587	179
r_d-1M	7,228	1,479,839	205	7,228	1,479,839	205	7,228	1,479,839	205
r_d-6M	7,228	2,185,738	302	7,228	2,185,738	302	7,228	2,185,738	302
r_d-1Y	7,224	10,895,576	1,508	7,224	10,895,576	1,508	7,224	10,895,576	1,508
r_d-2Y	7,224	18,198,204	2,519	7,224	18,198,204	2,519	7,224	18,198,204	2,519
r_d-3Y	7,224	23,285,073	3,223	7,224	23,285,073	3,223	7,224	23,285,073	3,223
r_d-5Y	7,224	27,108,230	3,753	7,224	27,108,230	3,753	7,224	27,108,230	3,753
Vol-SW	704	69,340	98	708	76,515	108	708	50,123	71
Vol-1M	704	63,731	91	708	93,740	132	708	64,625	91
Vol-6M	704	40,653	58	708	64,187	91	708	46,378	66
Vol-1Y	704	38,578	55	708	58,185	82	708	42,776	60
Vol-2Y	704	27,830	40	708	30,117	43	708	24,332	34
Vol-3Y	704	10,611	15	708	15,478	22	708	9,144	13
Vol-5Y	704	10,353	15	708	14,310	20	708	9,030	13

	USDCAD			USDJPY		
Data Type	Days	Ticks	Ticks/Day	Days	Ticks	Ticks/Day
Spot	7,066	120,846,026	17,102	7,057	204,418,497	28,967
r_f-SW	7,228	1,293,587	179	7,228	1,293,587	179
r_f-1M	7,228	1,479,839	205	7,228	1,479,839	205
r_f-6M	7,228	2,185,738	302	7,228	2,185,738	302
r_f-1Y	7,224	10,895,576	1,508	7,224	10,895,576	1,508
r_f-2Y	7,224	18,198,204	2,519	7,224	18,198,204	2,519
r_f-3Y	7,224	23,285,073	3,223	7,224	23,285,073	3,223
r_f-5Y	7,224	27,108,230	3,753	7,224	27,108,230	3,753
r_d-SW	7,224	180,098	25	7,224	684,751	95
r_d-1M	7,224	217,847	30	7,224	1,066,954	148
r_d-6M	7,224	984,930	136	7,224	5,294,711	733
r_d-1Y	7,224	1,484,733	206	7,220	1,234,515	171
r_d-2Y	4,337	1,907,668	440	7,220	2,737,514	379
r_d-3Y	3,796	3,172,322	836	7,220	3,478,831	482
r_d-5Y	4,337	2,392,454	552	7,220	3,582,771	496
Vol-SW	707	42,580	60	725	73,913	102
Vol-1M	707	48,523	69	725	82,360	114
Vol-6M	707	37,798	53	725	54,479	75
Vol-1Y	707	33,745	48	725	47,715	66
Vol-2Y	707	21,056	30	725	28,048	39
Vol-3Y	707	9,250	13	725	12,555	17
Vol-5Y	707	8,256	12	725	11,581	16

Notes: We spline the spot exchange rate tick data to a five minute grid from 1 millisecond past midnight to 1 millisecond to midnight GMT. Notice that the frequency of updates for quotes in the OTC-FXO market is roughly two orders of magnitude lower than the updates in quotes for the spot exchange rate. The OTC-FXO market releases most quotes in pairs (as the updates are usually from a single source, or are the result of an aggregator releasing an updated average). Deposit (SW to 1Y) and swap rates (2Y to 5Y) also have a great deal of variation in the update frequency. To assist in the calibration of the ASTSV model, we also collect long rates for sovereigns, but we exclude these from the table as they are not strictly required in the estimation.

history for the FX options is complete, in the sense that all of the active broker dealers are included in the survey. For the spot and deposit data the picture is

less clear. Certain FX feeds have tighter bid-ask spreads than the quotes from the banks surveyed by Reuters. For each day, the irregularly updated quotes are matched to a five-minute grid to compute the realised variance. Spot and yield curve data for AUDUSD, GBPUSD, USDCAD and USDJPY exchange rates is taken from January 1, 1996 to October 12, 2015, while for EURUSD the spot and yield curve data starts from February 28, 1998. For the yield curves I use quoted timed deposits for each currency out to one year and quoted swap rates for tenors up to 5Y. For short rate calibration purposes, I collect long swap rates (> 10Y) for each currency. Whilst Bloomberg and other data vendors provide some end-of-day benchmarks for FX options, the source for the data is unclear. Hence I construct from the intraday quote record.

For the ASTSV, I fit the model for six-month (6M) to 5Y tenors only using monthly time steps (hence I exclude SW and 1M tenors from the comparison). However, the spot variance is estimated at a daily frequency and rescaled to monthly increments by a factor of $252/12$, allowing us to estimate closing market quotes for each day whilst using a monthly time step.

Table 3.2 and Table 3.3 provide a comparison of the MLE estimates for the exchange rate variance process parameters with those recovered from the non-linear least squares fitting for the ARV model. The models are fitted over the estimation window from January 1, 1996 to December 14, 2012. The most interesting variation is in the estimated skew parameter γ_s versus $\gamma_{RV,s}$. The MLE estimates indicate values between -61 (USDCAD) and 121 (GBPUSD), noting the difference in the direction of quotation for USDCAD versus the other currency pairs.

The ARV model's highly variable estimates for the skew parameter will pos-

Table 3.2: ASV parameter estimation.

Currency	λ_s	ω_s	β_s	α_s	γ_s	$\mathfrak{L}(\hat{\theta}_s)$
AUDUSD	-0.0647	1.6396e-11	0.9447	2.2714e-06	79.7246	1.7513e+04
	(0.0054)	(0.5557)	(0.0017)	(0.0018)	(8.4751e-4)	
EURUSD	0.0993	3.1848e-18	0.9740	9.4560e-7	58.2033	1.6020e+04
	(0.0071)	(24.6432)	(0.0022)	(0.0023)	(0.0014)	
GBPUSD	-0.0602	3.0357e-12	0.9664	6.8812e-7	121.5577	1.9038e+04
	(0.0075)	(0.8251)	(0.0021)	(0.0021)	(0.0017)	
USDCAD	-0.3351	2.0742e-15	0.9582	9.2704e-7	-61.0273	1.9606e+04
	(0.0082)	(11.6105)	(0.0018)	(0.0017)	(0.0013)	
USDJPY	0.6133	2.1390e-12	0.9261	2.7293e-6	70.3874	1.8021e+04
	(0.0060)	(3.7675)	(0.0018)	(0.0017)	(7.1371e-4)	

Table 3.3: ARV parameter estimation.

Currency	$\lambda_{RV,s}$	$\omega_{RV,s}$	$\beta_{RV,s}$	$\alpha_{RV,s}$	$\gamma_{RV,s}$	Sq. Error
AUDUSD	-0.1102	1.2369E-11	0.9090	1.2842E-06	227.4733	1.5022e-06
EURUSD	0.0054	2.8207E-18	0.7621	4.8472E-06	-137.9202	2.1132e-06
GBPUSD	0.012	-1.638E-11	0.8669	3.5318E-06	11.7053	5.5689e-06
USDCAD	-0.3785	3.5583E-14	0.9597	1.1182E-07	-584.3087	7.1528e-06
USDJPY	0.5966	1.0266E-12	0.8726	3.2265E-06	150.0708	2.7178e-06

Notes: Parameter estimates for the spot exchange rate process: $R(t+\eta) = r_d(t) - r_f(t) - \frac{1}{2}h_s(t+\eta) + \sqrt{h_s(t+\eta)}z^*(t+\eta)$ with spot variance $h_s(t+\eta) = \omega_s + \beta_s h_s(t) + \alpha_s(z^*(t) - \gamma_s^*\sqrt{h_s(t)})^2$. Table 3.2 reports the parameter estimates as a standard GARCH in mean via maximum likelihood estimation for each currency pair; the final column reports the estimated log-likelihood at the optimum. Table 3.3 reports the estimates for the equivalent parameters with the spot variance $\hat{h}_s t$ approximated by $\sum_{m=1}^{M} \epsilon_s^2(t + \frac{m}{M}\eta) \approx \hat{h}_s(t+\eta)$, from high frequency data. The parameters are then estimated via non-linear least squares. The sum of squared errors (Sq. Error) of the regression are reported in the final column.

sibly go some way to explaining the highly variable performance in the out-of-sample tests, which I will now look at in detail.

Table 3.4 presents the parameter estimates for ASTSV model. The domestic and foreign stochastic short-rate models are fitted via calibration to the yield

Table 3.4: ASTSV parameter estimation.

	GBPUSD				
	6M	1Y	2Y	3Y	5Y
μ_{0f}	-6.55E-06	-1.07E-05	-8.93E-06	-6.99E-06	-2.81E-06
μ_{1f}	1.00	1.00	1.00	1.00	1.00
λ_f	-10.00	-9.99	-9.98	-9.67	-9.99
ω_f	9.47E-233	3.27E-25	6.97E-47	6.75E-37	1.30E-08
β_f	0.78	0.76	0.85	0.86	0.39
α_f	8.02E-09	8.46E-09	4.01E-09	3.99E-09	5.02E-09
γ_f	-500.00	-500.00	499.93	500.00	-500.00
$\mathfrak{L}(\hat{\theta}_d)$	1.72E+03	1.07E+03	1.72E+03	1.71E+03	1.71E+03
μ_{0d}	-1.64E-06	1.48E-06	-2.40E-06	3.67E-06	1.03E-05
μ_{1d}	0.99	1.00	1.00	0.99	0.99
λ_d	10.00	10.00	9.95	9.97	10.00
ω_d	2.81E-09	1.64E-289	8.07E-203	2.78E-290	4.80E-32
β_d	0.70	0.83	0.89	0.89	0.92
α_d	8.98E-09	4.12E-09	3.89E-09	4.99E-09	3.84E-09
γ_d	500.00	500.00	500.00	500.00	500.00
$\mathfrak{L}(\hat{\theta}_k)$	1.70E+03	1.09E+03	1.70E+03	1.67E+03	1.65E+03
λ_s	1.19	-0.26	1.07	0.90	0.57
ω_s	6.10E-05	7.12E-05	6.11E-05	6.10E-05	6.05E-05
β_s	0.82	0.83	0.82	0.82	0.82
α_s	2.39E-05	1.02E-05	2.39E-05	2.36E-05	2.32E-05
γ_s	37.66	291.44	38.75	39.99	41.16
$\mathfrak{L}(\hat{\theta}_s)$	546.49	331.85	546.22	546.25	546.42

Notes: The short rate dynamics $r_k(t+\eta) = \mu_{0k} + \mu_{1k} r_k(t) + \lambda_k h_k(t+\eta) + \sqrt{h_k(t+\eta)} u_k(t+\eta)$ and $h_k(t+\eta) = \omega_k + \beta_k h_k(t) + \alpha_k (u_k(t) - \gamma_k \sqrt{h_k(t)})^2$ are calibrated to the historical yield curve data. We apply the short rate estimated dynamics to the one-month quoted timed deposit rate and return the observed log-likelihoods $\mathfrak{L}(\hat{\theta}_k)$ for comparison with $\mathfrak{L}(\hat{\theta}_s)$ the log-likelihoods of the spot exchange rate returns at the monthly frequency. The parameters for the other 4 currency pairs can be found in the Appendix Table 1.

curve data prior to the evaluation window. As this model is set up for a monthly frequency, the spot exchange rate parameters θ_s need to be re-estimated at this frequency. To generate daily estimates for the quoted currencies, the daily spot variance from the ASV models is used and rescaled to the monthly frequency. I also compute the results using the ARV model daily spot-realised variance for this purpose, but the results are not materially different to the ASV model estimates.

Table 3.5: Root mean squared error (RMSE) and mean error (ME) for at-the-money Straddle

Currency	Maturity	$\widetilde{AT}$							
		ASV		ARV		ASTSV		ASV-C	
		RMSE	ME	RMSE	ME	RMSE	ME	RMSE	ME
AUDUSD	SW	3.1273	2.5096	2.7537	0.4209	-	-	2.1497	1.1533
	1M	3.9170	3.6283	2.6527	1.3171	-	-	1.2143	0.0470
	6M	4.3218	4.0928	5.6920	5.4739	**2.8048**	**2.5513**	0.8813	0.0617
	1Y	4.0491	3.8895	5.4009	5.2638	**2.6231**	**2.4378**	0.7357	0.0512
	2Y	3.7084	3.5501	5.0454	4.9211	**2.0184**	**1.7491**	0.6966	0.0446
	3Y	**1.5335**	**1.1749**	**3.4440**	**2.9034**	**1.8911**	**1.5061**	-	-
	5Y	**1.2607**	**0.6620**	**1.7369**	**1.1109**	**1.2073**	**0.1567**	-	-
EURUSD	SW	2.6408	1.9056	2.3370	0.8031	-	-	2.2348	1.4308
	1M	3.1452	2.9188	2.6407	2.0353	-	-	1.1984	0.0736
	6M	3.8133	3.6159	2.7113	2.2754	**1.6492**	**1.3473**	0.6719	0.2175
	1Y	3.6470	3.4903	2.3497	2.0269	**1.1641**	**0.8332**	0.6110	0.2172
	2Y	3.3831	3.2540	2.8998	2.7196	**1.7662**	**1.5780**	0.5990	0.1704
	3Y	**1.0093**	**0.7621**	**2.8493**	**0.4445**	**0.9799**	**0.7482**	-	-
	5Y	**0.6764**	**0.4050**	**2.9641**	**0.5560**	**0.6385**	**0.4162**	-	-
GBPUSD	SW	2.3232	1.8167	1.8319	0.7198	-	-	1.5387	0.5271
	1M	2.5832	2.3696	1.9300	1.3923	-	-	1.0134	0.2440
	6M	2.6787	2.4864	1.6507	1.1837	**1.1119**	**0.5632**	0.7662	0.0443
	1Y	2.4353	2.2912	1.2775	0.8997	**0.8775**	**0.5122**	0.6082	0.0341
	2Y	2.0943	1.9605	1.3898	1.1439	**0.6957**	**0.0058**	0.5242	0.0075
	3Y	**0.7814**	**0.5136**	**3.1472**	**2.7531**	**0.5958**	**0.0504**	-	-
	5Y	**1.3121**	**1.1817**	**4.2683**	**4.0501**	**0.5818**	**0.0893**	-	-
USDCAD	SW	1.6705	0.9669	2.6351	1.6040	-	-	1.3422	0.5784
	1M	2.0073	1.6831	3.0697	2.2900	-	-	0.8467	0.1195
	6M	2.1439	1.8414	3.4183	2.9387	**0.5734**	**0.0244**	0.6409	0.0172
	1Y	1.8894	1.6294	3.6160	3.3128	**1.3368**	**1.2160**	0.5763	0.0255
	2Y	1.5831	1.2410	3.8026	3.6636	**0.9079**	**0.2270**	0.5697	0.0260
	3Y	**0.8509**	**0.4827**	**2.1091**	**0.9257**	**0.7715**	**0.1112**	-	-
	5Y	**0.9561**	**0.6187**	**3.9722**	**3.7960**	**0.9543**	**0.2078**	-	-
USDJPY	SW	2.3137	1.4267	2.9662	0.9300	-	-	1.8539	0.4005
	1M	3.0812	2.5797	2.6632	1.8034	-	-	1.6400	0.9012
	6M	3.3258	2.9002	2.5595	1.9453	**1.3873**	**0.2713**	1.2985	0.6182
	1Y	3.0143	2.6626	2.2002	1.6748	**1.6248**	**1.1968**	1.1860	0.5173
	2Y	2.4668	2.1265	5.0226	4.8391	**1.1393**	**0.2647**	1.0530	0.4272
	3Y	**1.4322**	**1.0284**	**4.6950**	**1.2599**	**1.3500**	**0.6813**	-	-
	5Y	**2.4027**	**2.9062**	**6.4343**	**6.1912**	**2.0731**	**1.3613**	-	-

Notes: The Root Mean Squared Error, RMSE, is given by $\sqrt{\sum_{n=1}^{N}(\hat{y}_n - y_n)^2/N}$, where y_n stands for the market quotation for the strategies of $\{\widetilde{AT}, \widetilde{BF}_{\Delta}, \widetilde{RR}_{\Delta}\}$ and $\hat{y}_n$ is the calculated quotations from the model selected. The Mean Error, ME, is calculated by $|\sum_{n=1}^{N}(\hat{y}_n - y_n)/N|$.

Table 3.6: RMSE and ME for 10-delta butterfly

		$\widetilde{BF}_{10}$							
		ASV		ARV		ASTSV		ASV-C	
		RMSE	ME	RMSE	ME	RMSE	ME	RMSE	ME
AUDUSD	SW	0.305	0.2855	0.3292	0.3093	-	-	0.089	0.0023
	1M	0.3999	0.377	0.2009	0.1562	-	-	0.1613	0.033
	6M	1.3705	1.3469	1.3123	1.2877	**1.1416**	**1.1189**	0.3529	0.0718
	1Y	1.8471	1.8219	1.8228	1.7973	**0.3854**	**0.1419**	1.713	1.6858
	2Y	2.06	2.0482	2.0475	2.0359	**1.6994**	**1.6833**	1.4827	1.4656
	3Y	**2.1143**	**2.1092**	**2.4235**	**2.0333**	**1.7458**	**1.7095**	-	-
	5Y	**2.2501**	**2.2448**	**0.9545**	**0.7981**	**0.9616**	**0.3592**	-	-
EURUSD	SW	0.2969	0.2822	0.1638	0.0586	-	-	0.0573	0.0113
	1M	0.3818	0.3631	0.1368	0.0692	-	-	0.0843	0.0128
	6M	0.8392	0.8273	0.7928	0.7805	**0.6704**	**0.6541**	0.1752	0.0138
	1Y	1.046	1.038	1.0498	1.0419	**0.4937**	**0.3278**	0.2664	0.0482
	2Y	1.0897	1.0846	1.09	1.0849	**0.3455**	**0.3218**	1.0102	1.0045
	3Y	**0.9233**	**0.9212**	**1.1133**	**1.1118**	**0.2956**	**0.2289**	-	-
	5Y	**0.9202**	**0.9159**	**0.8151**	**0.7405**	**0.8635**	**0.4294**	-	
GBPUSD	SW	0.3411	0.3324	0.864	0.8526	-	-	0.0861	0.0111
	1M	0.4291	0.4168	0.2737	0.2517			0.0956	0.0067
	6M	0.8978	0.8894	0.9005	0.8922	**0.8662**	**0.8564**	0.1783	0.0367
	1Y	1.1279	1.1224	1.1352	1.1299	**2.0662**	**0.3393**	0.2262	0.0403
	2Y	1.157	1.1548	1.1602	1.158	**0.9007**	**0.8960**	1.0062	0.0018
	3Y	**1.2087**	**1.2063**	**1.2158**	**0.7012**	**0.5408**	**0.5281**	-	-
	5Y	**1.1654**	**1.1639**	**1.1928**	**1.1912**	**0.7111**	**0.6562**	-	-
USDCAD	SW	0.3369	0.2187	1.618	0.0498	-	-	0.0466	0.0023
	1M	0.3519	0.3433	0.4609	0.4554	-	-	0.0765	0.0454
	6M	0.8379	0.8287	0.8358	0.827	**0.9071**	**0.9000**	0.1238	0.0062
	1Y	1.0887	1.0784	1.0129	1.0024	**2.1852**	**2.1780**	0.1579	0.0107
	2Y	1.203	1.1957	1.0181	1.0101	**1.1059**	**1.0994**	0.1318	0.0115
	3Y	**1.6946**	**1.3303**	**1.6361**	**1.3453**	**0.9396**	**0.9147**	-	-
	5Y	**1.4314**	**1.4237**	**1.4247**	**1.4172**	**0.9274**	**0.7972**	-	-
USDJPY	SW	0.4329	0.3964	5.0639	2.1118	-	-	0.195	0.0529
	1M	0.4647	0.4317	0.3934	0.3517	-	-	0.1652	0.0919
	6M	1.2298	1.2023	1.2157	1.1879	**1.0106**	**0.9868**	0.2429	0.0324
	1Y	1.7793	1.7573	1.7604	1.7382	**1.4577**	**1.4278**	0.2603	0.0571
	2Y	2.1024	2.0816	2.0804	2.0593	**1.4369**	**1.4127**	0.2947	0.0582
	3Y	**2.0081**	**1.9845**	**2.5914**	**2.4603**	**1.4860**	**1.4625**	-	-
	5Y	**2.1674**	**2.1436**	**2.2594**	**2.2358**	**1.4577**	**1.4278**	-	-

3.6.2 Out-of-sample results

Table 3.5 to Table 3.9 report the root mean squared error (RMSE) and mean absolute error (ME) for each of my models, out-of-sample for each quotation type. The RMSE provides the overview of the comparative adequacy of the model fit, whilst the ME illustrates the degree of average bias. If the RMSE and the ME

Table 3.7: RMSE and ME for 25-delta butterfly

		$\widetilde{BF}_{25}$							
		ASV		ARV		ASTSV		ASV-C	
		RMSE	ME	RMSE	ME	RMSE	ME	RMSE	ME
AUDUSD	SW	0.1061	0.1021	0.2133	0.1079	-	-	0.0331	0.0044
	1M	0.2448	0.1488	0.0802	0.0717	-	-	0.0321	0.0025
	6M	0.38	0.3742	0.3798	0.3741	**0.3124**	**0.3048**	0.0843	0.0069
	1Y	0.4948	0.4892	0.4958	0.4902	**0.1866**	**0.1656**	0.1074	0.0274
	2Y	0.5207	0.5172	0.5213	0.5178	**0.4479**	**0.4428**	0.0916	0.0123
	3Y	**0.5101**	**0.5049**	**0.5362**	**0.5311**	**0.4150**	**0.4097**	-	-
	5Y	**0.5646**	**0.5557**	**0.7254**	**0.7184**	**0.3880**	**0.3619**	-	-
EURUSD	SW	0.0888	0.0855	0.1058	0.0172	-	-	0.0237	0.0091
	1M	0.1373	0.1335	0.0857	0.0778	-	-	0.0244	0.0055
	6M	0.2589	0.2566	0.2517	0.2493	**0.2130**	**0.2107**	0.0497	0.0043
	1Y	0.3192	0.3155	0.3193	0.3156	**0.1886**	**0.1757**	0.0574	0.0013
	2Y	0.3198	0.3179	0.3198	0.3179	**0.1780**	**0.1429**	0.045	0.0175
	3Y	**0.2773**	**0.2743**	**0.3410**	**0.2290**	**0.1705**	**0.1629**	-	-
	5Y	**0.2729**	**0.2714**	**0.3866**	**0.3854**	**0.1657**	**0.1437**	-	-
GBPUSD	SW	0.1118	0.1093	0.3864	0.353	-	-	0.0222	0.0055
	1M	0.1511	0.1477	0.1021	0.0966	-	-	0.0486	0.0373
	6M	0.2752	0.2733	0.272	0.2701	**0.2636**	**0.2617**	0.0615	0.0256
	1Y	0.3266	0.3178	0.326	0.3244	**0.3403**	**0.3386**	0.0869	0.0527
	2Y	0.3238	0.3231	0.3236	0.3229	**0.2763**	**0.2754**	0.0233	0.0043
	3Y	**0.3658**	**0.3634**	**0.9157**	**0.0095**	**0.2191**	**0.2161**	-	-
	5Y	**0.3613**	**0.3588**	**0.3681**	**0.3656**	**0.0674**	**0.0554**	-	-
USDCAD	SW	0.0878	0.0757	0.1088	0.1034	-	-	0.0165	0.0053
	1M	0.1272	0.1248	0.1579	0.1564	-	-	0.0213	0.0066
	6M	0.2506	0.2487	0.2451	0.2435	**0.2754**	**0.2735**	0.0349	0.0069
	1Y	0.3142	0.3123	0.277	0.2753	**0.3889**	**0.5404**	0.0447	0.0016
	2Y	0.3405	0.3384	0.2497	0.2474	**0.2862**	**0.2845**	0.0385	0.006
	3Y	**0.4499**	**0.4456**	**2.4416**	**0.1827**	**0.2826**	**0.2784**	-	-
	5Y	**0.4554**	**0.4523**	**0.4542**	**0.4509**	**0.2776**	**0.2715**	-	-
USDJPY	SW	0.1624	0.1517	0.8659	0.2703	-	-	0.0443	0.0178
	1M	0.1976	0.1882	0.1683	0.1566	-	-	0.052	0.0181
	6M	0.3993	0.3929	0.3845	0.3779	**0.3255**	**0.3187**	0.0566	0.0089
	1Y	0.5212	0.5153	0.5056	0.4996	**0.3849**	**0.3565**	0.0715	0.011
	2Y	0.572	0.5618	0.5559	0.5454	**0.4170**	**0.4061**	0.1039	0.0171
	3Y	**0.4993**	**0.4844**	**1.0206**	**1.0011**	**0.4205**	**0.4040**	-	-
	5Y	**0.4615**	**0.4384**	**0.4973**	**0.4740**	**0.3840**	**0.3565**	-	-

are very similar, this indicates that the majority of the forecast error is from a systematic inaccuracy in the model, which could be eliminated by adjusting the forecast via the ME (this would then be in sample, of course).

Table 3.10 illustrates the additional 'ad-hoc' calibration of the spot variance for the ASV-C model versus the ASV model. Recall that the ASV-C model adjusts the spot variance via stretching factors ζ, α and γ from the first ten

Table 3.8: RMSE and ME for 10-delta risk reversal

		$\widetilde{RR}_{10}$							
		ASV		ARV		ASTSV		ASV-C	
		RMSE	ME	RMSE	ME	RMSE	ME	RMSE	ME
AUDUSD	SW	0.8316	0.5998	1.3471	1.215	-	-	0.5583	0.005
	1M	0.9719	0.6609	1.42	1.2058	-	-	0.6729	0.1686
	6M	3.293	3.1595	1.981	1.7475	**3.4444**	**3.3140**	0.8585	0.0959
	1Y	4.5447	4.4345	3.6223	3.4831	**2.4513**	**2.1626**	0.988	0.0742
	2Y	5.1334	5.0446	4.4817	4.3795	**3.6467**	**3.4979**	0.9501	0.076
	3Y	**4.2536**	**4.1699**	**5.1394**	**5.0722**	**3.3192**	**3.0981**	-	-
	5Y	**4.8657**	**4.8047**	**2.5694**	**2.4371**	**2.5026**	**0.3918**	-	-
EURUSD	SW	0.6665	0.4528	0.6582	0.441	-	-	0.4915	0.0271
	1M	0.9612	0.7026	1.0484	0.8132	-	-	0.5968	0.0459
	6M	2.0973	1.8378	1.4045	0.9658	**1.7702**	**1.5080**	0.7853	0.0979
	1Y	2.5427	2.3387	2.8982	2.7203	**1.5200**	**0.3318**	0.9501	0.0319
	2Y	2.5969	2.4422	2.614	2.4604	**2.5841**	**1.2766**	0.8078	0.0182
	3Y	**1.3574**	**1.1612**	**2.7296**	**2.6316**	**0.9769**	**0.7087**	-	-
	5Y	**1.3945**	**1.1766**	**2.0929**	**1.9107**	**1.6788**	**1.4665**	-	-
GBPUSD	SW	0.7177	0.2055	1.2512	1.0469	-	-	0.4081	0.1438
	1M	0.8491	0.212	1.2449	0.922	-	-	0.582	0.0036
	6M	1.6038	1.136	2.3322	2.0334	**1.8259**	**1.4188**	1.0453	0.0506
	1Y	1.981	1.63	2.625	2.3701	**1.0766**	**0.3188**	1.0112	0.0179
	2Y	2.0551	1.8265	2.3174	2.1172	**1.2977**	**0.8681**	0.9359	0.047
	3Y	**1.5122**	**1.2807**	**2.4525**	**2.2920**	**1.2001**	**0.7939**	-	-
	5Y	**1.5492**	**1.3508**	**1.9496**	**1.7961**	**1.5461**	**1.1816**	-	-
USDCAD	SW	0.5809	0.4445	0.7788	0.6824	-	-	0.3744	0.0482
	1M	0.8539	0.6934	0.6839	0.4647	-	-	0.4809	0.1053
	6M	1.8757	1.7942	0.8172	0.6232	**2.4152**	**2.3553**	0.559	0.097
	1Y	2.2612	2.2007	0.7226	0.5272	**0.5149**	**0.0552**	0.5249	0.0802
	2Y	2.4076	2.3612	4.9047	2.0483	**0.8764**	**0.7199**	0.4713	0.0396
	3Y	**2.7767**	**2.7284**	**2.7218**	**2.6718**	**1.3349**	**1.0166**	-	-
	5Y	**2.8628**	**2.8143**	**2.7912**	**2.7413**	**2.3295**	**1.5771**	-	-
USDJPY	SW	0.9282	0.0472	4.4812	4.3518	-	-	0.9149	0.1474
	1M	1.34	0.9791	1.0251	0.4536	-	-	0.9253	0.1253
	6M	1.4059	0.6378	1.2586	0.1196	**1.2441**	**0.2328**	1.2573	0.0869
	1Y	1.562	0.2525	1.5483	0.1442	**1.5558**	**0.0160**	1.5415	0.0019
	2Y	2.2229	0.6807	2.1162	0.0215	**2.1825**	**0.0254**	2.1167	0.0527
	3Y	**2.7986**	**1.4543**	**4.7480**	**4.0610**	**2.6200**	**0.1983**	-	-
	5Y	**3.8490**	**2.3051**	**3.6493**	**1.8997**	**3.2647**	**0.1117**	-	-

or so days of the FX option data. I make this adjustment, both by tenor and quotation type. The estimates of ζ, α and γ are then carried through the entire evaluation window out-of-sample. Hence the ASV-C model for the out-of-sample period is only updated by adjustments in the spot exchange rate. We see clearly that the majority of adjustments are systematic by tenor and across quotation type. However, the useful aspect of this adjustment is the degree of stability in

Table 3.9: RMSE and ME for 25-delta risk reversal

		$\widetilde{RR}_{25}$							
		ASV		ARV		ASTSV		ASV-C	
		RMSE	ME	RMSE	ME	RMSE	ME	RMSE	ME
AUDUSD	SW	0.4863	0.3671	0.7637	0.6923	-	-	0.2776	0.0027
	1M	0.5574	0.4049	0.801	0.6925	-	-	0.3622	0.0982
	6M	1.7198	1.6561	1.03	0.9187	**1.8019**	**1.7374**	0.4247	0.063
	1Y	2.331	2.2856	1.8509	1.7935	**0.6071**	**0.3640**	0.4533	0.0259
	2Y	2.5286	2.4918	2.1844	2.1416	**1.8601**	**1.8082**	0.3902	0.0483
	3Y	**2.1168**	**2.0749**	**2.5758**	**2.5430**	**1.8445**	**1.7822**	-	-
	5Y	**2.4111**	**2.3809**	**1.5919**	**1.5363**	**0.9712**	**0.4782**	-	-
EURUSD	SW	0.398	0.2804	0.379	0.2528	-	-	0.2875	0.0518
	1M	0.5834	0.444	0.5297	0.3674	-	-	0.3458	0.0628
	6M	1.2091	1.0712	0.8325	0.6114	**1.0287**	**0.8864**	0.4111	0.0575
	1Y	1.4235	1.3103	1.6107	1.511	**0.7121**	**0.2391**	0.4782	0.0072
	2Y	1.3985	1.3224	1.4076	1.3319	**0.7112**	**0.0803**	0.3931	0.0109
	3Y	**0.7396**	**0.6421**	**1.4582**	**1.4091**	**0.3500**	**0.1348**	-	-
	5Y	**0.7382**	**0.6333**	**1.1065**	**1.0264**	**0.4506**	**0.2675**	-	-
GBPUSD	SW	0.4007	0.1325	0.8632	0.7818	-	-	0.2023	0.0077
	1M	0.5096	0.16	0.7266	0.5356	-	-	0.4019	0.1616
	6M	0.8992	0.6471	1.2841	1.1192	**1.0099**	**0.7911**	0.4713	0.0217
	1Y	1.0768	0.8901	1.4151	1.2782	**0.5711**	**0.1252**	0.545	0.0042
	2Y	1.1026	0.9782	1.2405	1.1311	**0.8121**	**0.6246**	0.4496	0.0031
	3Y	**0.9492**	**0.8612**	**1.4778**	**1.4074**	**0.4702**	**0.2363**	-	-
	5Y	**0.9537**	**0.8873**	**1.1865**	**1.1298**	**0.6343**	**0.8350**	-	-
USDCAD	SW	0.3683	0.2818	0.4775	0.4148	-	-	0.2438	0.0266
	1M	0.5492	0.459	0.4555	0.3398	-	-	0.2907	0.0707
	6M	1.1024	1.0527	0.5405	0.4376	**1.3656**	**1.3319**	0.3346	0.0575
	1Y	1.2925	1.2585	0.6195	0.3823	**0.4079**	**0.2824**	0.2717	0.0251
	2Y	1.3567	1.3303	3.0579	1.0748	**0.5687**	**0.5003**	0.2672	0.0216
	3Y	**1.7004**	**1.6591**	**4.1879**	**4.1706**	**0.7744**	**0.6258**	-	-
	5Y	**1.6059**	**1.5830**	**1.5687**	**1.5435**	**1.0505**	**0.8297**	-	-
USDJPY	SW	0.5397	0.0083	2.4686	2.411	-	-	0.5309	0.1519
	1M	0.732	0.5267	0.5676	0.2477	-	-	0.5146	0.0727
	6M	0.755	0.3696	0.6653	0.0963	**0.6541**	**0.1309**	0.6597	0.0415
	1Y	0.8153	0.1915	0.7927	0.0172	**0.7774**	**0.0597**	0.7925	0.0008
	2Y	1.0869	0.2441	1.0666	0.1259	**1.0987**	**0.1330**	1.0595	0.0211
	3Y	**1.5148**	**0.7973**	**2.5363**	**2.1702**	**1.3788**	**0.2667**	-	-
	5Y	**2.0892**	**1.2629**	**1.9543**	**1.0326**	**1.7620**	**0.3698**	-	-

the model fit, given these parameters, over the evaluation window, and we will see this in the results from the out-of-sample analysis.

The four models are arranged as follows. The first three are termed 'purely-spot-only', as they are estimated in the sample window without reference to the market quoted European surface. I progress from the simplest model (the ASV fitted by MLE) through to the ARV model, which uses high frequency

Table 3.10: ASV calibration adjustments

Currency	Strategy	SW			1M			6M		
		α	γ	ζ	α	γ	ζ	α	γ	ζ
AUDUSD	$\widetilde{BF}_{10}$	6.35E-06	85.1217	-0.1578	7.82E-06	79.1728	-0.4516	2.80E-06	112.9296	1.1078
	$\widetilde{BF}_{25}$	3.07E-06	112.3086	1.0835	1.65E-05	55.3784	-0.3304	2.90E-05	43.0187	1.6131
	$\widetilde{AT}$	5.35E-14		1.458	3.06E-07		1.2351	8.97E-07		3.7733
	$\widetilde{RR}_{25}$	4.27E-06	142.005	1.6026	1.52E-06	162.4441	1.7208	2.22E-06	134.2332	7.5721
	$\widetilde{RR}_{10}$	3.06E-06	132.1231	1.6966	1.55E-06	154.3426	1.7221	1.91E-06	148.6812	4.2606
EURUSD	$\widetilde{BF}_{10}$	3.91E-06	75.8195	-0.8181	5.31E-06	50.343	-0.9797	3.00E-06	48.9779	-1.0535
	$\widetilde{BF}_{25}$	1.33E-06	91.0748	-0.576	8.05E-06	37.9779	-0.8244	1.28E-06	83.4702	0.6732
	$\widetilde{AT}$	1.85E-14		1.3756	1.55E-12		1.2054	3.38E-07		2.3123
	$\widetilde{RR}_{25}$	1.47E-06	109.9382	-0.9358	2.65E-06	54.5884	2.0113	2.24E-06	76.0455	6.276
	$\widetilde{RR}_{10}$	1.45E-06	104.768	-16.6797	2.39E-06	54.5197	1.9313	9.33E-01	141.4175	2.137
GBPUSD	$\widetilde{BF}_{10}$	1.29E-06	151.7499	1.2576	5.17E-06	76.0272	-0.033	9.08E-07	165.1314	1.1026
	$\widetilde{BF}_{25}$	9.02E-07	145.0068	0.1777	1.39E-05	0.4716	-18.4367	3.39E-05	25.6752	-25.7204
	$\widetilde{AT}$	2.22E-14		1.2952	3.57E-14		1.0845	3.56E-07		2.3791
	$\widetilde{RR}_{25}$	2.16E-06	76.9678	0.18	3.20E-06	70	4.1	2.09E-06	67.6894	13.4849
	$\widetilde{RR}_{10}$	3.13E-06	55.5853	1.5613	8.68E-06	20.9142	8.2328	1.56E-07	463.7046	2.0531
USDCAD	$\widetilde{BF}_{10}$	4.16E-06	-39.8127	-0.2497	3.85E-06	-84.8983	-1.6899	3.55E-06	-100.982	0.12
	$\widetilde{BF}_{25}$	3.14E-06	-22.205	-0.4146	4.80E-06	-90.746	-0.7279	3.64E-06	-88.7209	-1.9035
	$\widetilde{AT}$	2.66E-14		1.2252	1.91E-07		1.2945	4.12E-07		3.7794
	$\widetilde{RR}_{25}$	1.56E-06	-105.653	0.0415	1.01E-06	-127.909	2.3183	1.79E-06	-108.216	-0.3266
	$\widetilde{RR}_{10}$	1.04E-05	-15.8349	1.8341	9.63E-07	-105.269	2.3489	1.73E-06	-106.121	-0.2274
USDJPY	$\widetilde{BF}_{10}$	8.36E-06	-23.277	-0.58	1.80E-04	-6.3584	-6.161	5.01E-06	-113.932	1.7877
	$\widetilde{BF}_{25}$	1.16E-05	-79.6234	-0.436	8.88E-06	-54.0836	57.0237	2.82E-06	-152.589	3.2173
	$\widetilde{AT}$	4.12E-14		1.2845	9.99E-07		1.9933	1.13E-06		6.8383
	$\widetilde{RR}_{25}$	2.54E-05	14.1881	1.6386	2.08E-06	37.8976	1.7695	2.30E-06	38.3404	1.7278
	$\widetilde{RR}_{25}$	3.23E-05	12.5069	1.9381	2.15E-06	36.4698	1.7111	1.26E-05	8.2827	-11.0466

Notes: To fit the market quotation of $\widetilde{AT}$, α and ζ are calibrated though $\{\hat{\alpha}, \hat{\zeta}\} := \arg\min_{\{\hat{\alpha},\zeta\}} \sum_{d=1}^{D} (\widetilde{AT}_{0,d}(\tau) - \widetilde{AT}_{0,d}(\alpha, \zeta|\theta))^2$ while γ is also adjusted to model the quotations of $\widetilde{BF}_{\Delta}$ and $\widetilde{RR}_{\Delta}$. Then we fix the parameters $\hat{\theta}$ and carried through the entire evaluation window out-of-sample. The useful aspect of this adjustment is the degree of stability in the model fit given these parameters over the evaluation window, which is useful for the application on sparsely quoted FXOs. For more maturity, see Appendix Table 2.

observations to construct the spot variance process, to the ASTSV model, which includes stochastic short rates. The final model, ASV-C, uses the first ten days of the European volatility surface for calibration. Note that whilst the ASV-C model uses a snippet of initial options data, from the estimation window; in the

out-of-sample evaluation window the estimated surfaces are generated entirely by the variation in the spot price providing the innovations to the model.

I order the tables in the following order: first, the $\widetilde{AT}$ (Table 3.5); second, the $\widetilde{BF}_{10-1vol}$ and $\widetilde{BF}_{25-1vol}$ (Table 3.6, Table 3.7); third, the $\widetilde{RR}_{10}$ and $\widetilde{RR}_{25}$ (Table 3.8, Table 3.9). Note that the "−" is for models that cannot be fitted for that tenor/model specification.

The numbers in bold refer to models estimated using a monthly time-step, whilst the reminder are computed using a daily time step. For brevity I exclude numerous redundant combinations (such as the ASTSV model at daily frequency, which performs almost identically to the ASV model).

Overall, I observe the more-or-less anticipated results. The ASV and ARV models estimated directly from spot data and in the absence of a stochastic short-rate model generally perform poorly compared to the ASTSV model estimated at a monthly frequency for 6M to 2Y tenors. Indeed, for a spot-only-estimated model, the ASTSV model for these tenors is exceptional. For instance, for several currency pairs, (see EURUSD and GBPUSD for $\widetilde{BF}_{10-1vol}$), the ASTSV model actually out-performs the ASV-C model, which uses daily increments, but is calibrated in the estimation window to the European surface.

For short maturity tenors (SW and 1M), having some knowledge of past quotes improves the out-of-sample fit considerably. However, the realised volatility information from the ARV model can provide some competition, albeit with a high degree of variability. Indeed, the ARV model for short tenors can be both the best performing spot only model (EURUSD) and the worst performing model (USD-JPY). Hence, the evidence for the value of realised volatility over traditional spot only estimates such as GARCH is quite mixed.

Unsurprisingly, the spot only models (ASV, ARV and ASTSV) normally perform far better for the 25-delta quotes ($\widetilde{BF}_{25-1vol}$ and $\widetilde{RR}_{25}$) than the 'wings' quotes ($\widetilde{BF}_{10-1vol}$ and $\widetilde{RR}_{10}$), with the best fits being for the at-the-money ($\widetilde{AT}$) volatility quotes. The AUSUSD $\widetilde{RR}_{10}$ provides considerable problems for all the spot only models; indeed, the estimates of $\widetilde{RR}_{10}$ for a 6M tenor from the ASTSV model are amongst the poorest across all the model, currency, tenor and quotation combinations. The only estimates to perform worse are the ARV estimates of USDJPY, for the very hard to predict combination of SW tenor and $\widetilde{RR}_{10}$, and the highly volatile ARV estimates of the USDJPY $\widetilde{AT}$ for long tenors.

A more interesting comparison occurs between the ASTSV and the ASV-C models. As noted previously, there is a trade-off tenor between which using a stochastic short rate model (with term structure calibrations) appears to be a better choice than the static model calibrated to the European surface. Looking at Table 3.5 we clearly see this transition occurring at about 1Y. Whilst the ASV-C model certainly out-performs the ASTSV model in most cases, the comparative performance from 6M to 2Y is relatively similar. For instance USDJPY, RMSE for 1Y is 1.6248 (ASTSV) versus 1.1860 (ASV-C); however, up to 2Y the difference is 1.1393 (ASTSV) versus 1.0530 (ASV-C), with a lower ME for the ASTSV.

This lends credence to practitioner anecdotes that comparative term structure dynamics (in particular rate skews) dominate the valuation of long maturity options. Indeed, several currencies versus JPY do occasionally have options quoted at tenors longer than 15 years, to cater for carry trade investors looking to hedge systematic changes in monetary policy. At this point the potential stochastic variation in yield curve dynamics in response to macro-economic (and even demographic) variation would be the only factor in determining the current period

Table 3.11: Example of a market volatility surface for AUDUSD on 08 October 2015.

AUDUSD (spot reference 0.7229)					
Tenor	$\widetilde{AT}$	$\widetilde{BF}_{25}$	$\widetilde{BF}_{10}$	$\widetilde{RR}_{25}$	$\widetilde{RR}_{10}$
ON	13.7130%	0.1750%	0.8130%	-0.5250%	-0.9750%
SW	11.3250%	0.1625%	0.5000%	-0.8000%	-1.3500%
1M	11.5000%	0.2125%	0.6630%	-1.1750%	-2.1000%
6M	11.6000%	0.4190%	1.6125%	-2.3000%	-4.1750%
1Y	11.7000%	0.5250%	2.0750%	-2.7750%	-5.1250%
2Y	12.1500%	0.5560%	2.2625%	-2.9500%	-5.6750%

Notes: The quotes in this table allow a market participant to price an option for any delta by first constructing the European surface at 10, 25 put and call deltas and at-the-money.

expectation of the 15-year risk neutral density.

3.7 Forecast breakdown test

This section provides additional model forecast breakdown analyses and some helpful information for replication. Table 3.11 provides an example volatility surface data for the AUDUSD. These strategies, at-the-money ($\widetilde{AT}$), butterfly ($\widetilde{BF}$), and risk reversal ($\widetilde{RR}$), mainly at 25-delta and 10-delta, give different measurements of the volatility surface as discussed in previous sections.

Following Diebold and Mariano [1995], Giacomini and White [2006] and Giacomini and Rossi [2016], I test the forecast performance between model pairs ASV-C vs. ASV; ASV-C vs. ARV; ASTSV vs. ASV and ASTSV vs. ARV. The test statistic is computed by a rolling sum of the difference of two loss functions and divided by the heteroskedasticity and autocorrelation robust rolling standard deviation. Asymptotic inference is given in Giacomini and Rossi [2016].

Assume the real market value within the forecasting period is y_t, where $t = 1, ..., T$, and the forecast value calculated from two models for this period are $\hat{y}_{1,t}$ and $\hat{y}_{2,t}$. The information available at time t is $\mathcal{F}_t$, a filtration defined on the probability space $(\Omega, \mathcal{F}, \mathbb{P})$. Then define the loss function as $L_{i,t}(\hat{y}_{i,t}, y_t|\mathcal{F}_t)$, $i = 1, 2$, which can be described as squared error loss function $(\hat{y}_{i,t} - y_t)^2$, absolute error loss function $|\hat{y}_{i,t} - y_t|$, linear exponential loss function $\exp(\phi(\hat{y}_{i,t} - y_t)) - \phi(\hat{y}_{i,t} - y_t) - 1, \phi \in \mathbb{R}$ or other appropriate loss function. For the chosen loss function, in this section I choose the squared error loss function; The null hypothesis for equally performed forecast $\hat{y}_{1,t}$ and $\hat{y}_{2,t}$ is

$$H_0 \quad : \mathbb{E}[L(\hat{y}_{1,t}, y_t|\mathcal{F}_t) - L(\hat{y}_{2,t}, y_t|\mathcal{F}_t)] = 0 \quad \text{almost surely.}$$

The term in the expectation, $L(\hat{y}_{1,t}, y_t|\mathcal{F}_t) - L(\hat{y}_{2,t}, y_t|\mathcal{F}_t)$, is called the differential loss function and denoted by the following comparative prediction error: $d_t(\hat{y}_{1,t}, \hat{y}_{2,t}, y_t|\mathcal{F}_t)$. The forecast breakdown test statistic is then defined as

$$l_t(\hat{y}_{1,t}, \hat{y}_{2,t}, y_t|\mathcal{F}_t) = \frac{\sum_{s=1}^{t} d_s(\hat{y}_{1,s}, \hat{y}_{2,s}, y_s|\mathcal{F}_s)}{\sqrt{\sum_{s=1}^{t} \frac{d_s(\hat{y}_{1,s}, \hat{y}_{2,s}, y_s|\mathcal{F}_s)' d_s(\hat{y}_{1,s}, \hat{y}_{2,s}, y_s|\mathcal{F}_s)}{s}}}.$$

If the null hypothesis is true and the forecast under two candidate models perform equally, the test statistic $l_t(\hat{y}_{1,t}, \hat{y}_{2,t}, y_t|\mathcal{F}_t) \sim \mathcal{N}(0, 1)$. I use the approach above to test the forecast performances on $\widetilde{AT}$ with 1-year and 2-year maturities of five currency pairs between four model pairs and illustrates the result by the following figures.

The left panels of Fig. 3.7 (for 1Y tenor) and Fig. 3.8 (for 2Y tenor) demonstrate the time serieses of the models quoted and market $\widetilde{AT}$. The ASV and ARV

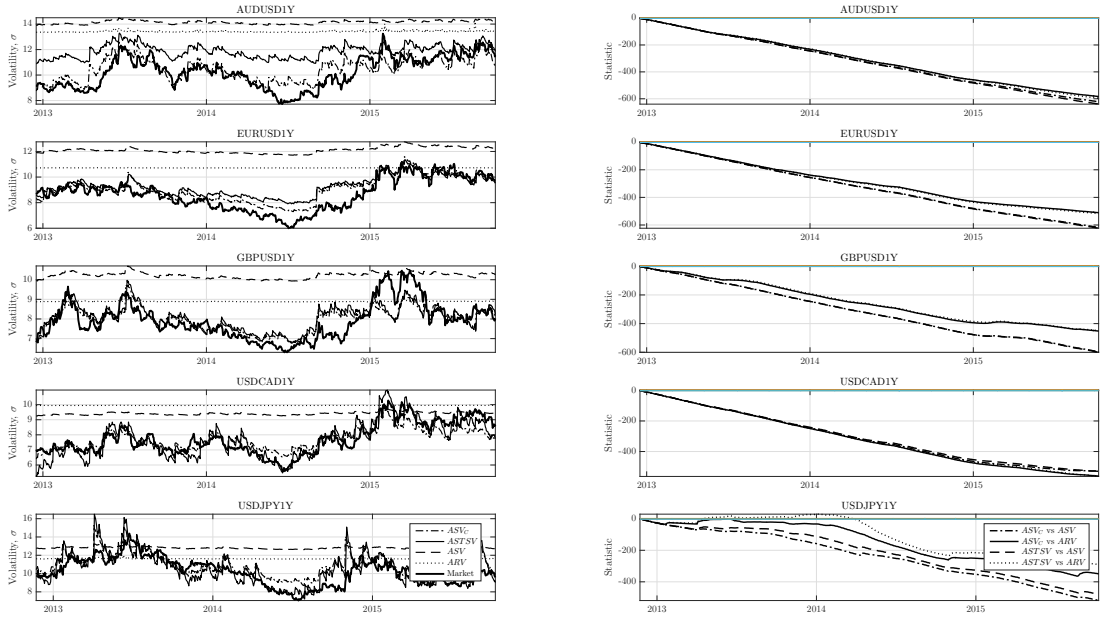

Figure 3.7: Forecast breakdown test among different models applied on 1Y tenor FX options.
The left panel presents the $\widetilde{AT}$ quotes with 1-year maturity of five currency pairs fitted by the four models, and the right panel shows the corresponding forecast breakdown test statistics. The statistics time series indicates that the null hypothesis is rejected almost surely, which means that ASTSV and ASV-C generally out-perform ARV and ASV.

models' quotations loss most of the fluctuation and become much more flat compared with other quotes. The ASTSV and ASV-C model tracks the movement of the market $\widetilde{AT}$ through out the data period. As the tenor increases to 2Y, ATSTV and ASV-C's $\widetilde{AT}$ also tends to loss track of the market dynamic.

The null hypothesis indicates that the forecast breakdown test statistic for two equally performing models should lie within $[-2.3263, 2.3263]$ with 99% confidence. However in the right panels of both of the two figures, the test statistics are far beyond this area even at the beginning of the data period. The breakdown statistic for ASTSV vs. ASV is similar to ASV-C vs. ASV, indicating both of the proposed models have good performance in pricing longer tenor FX options,

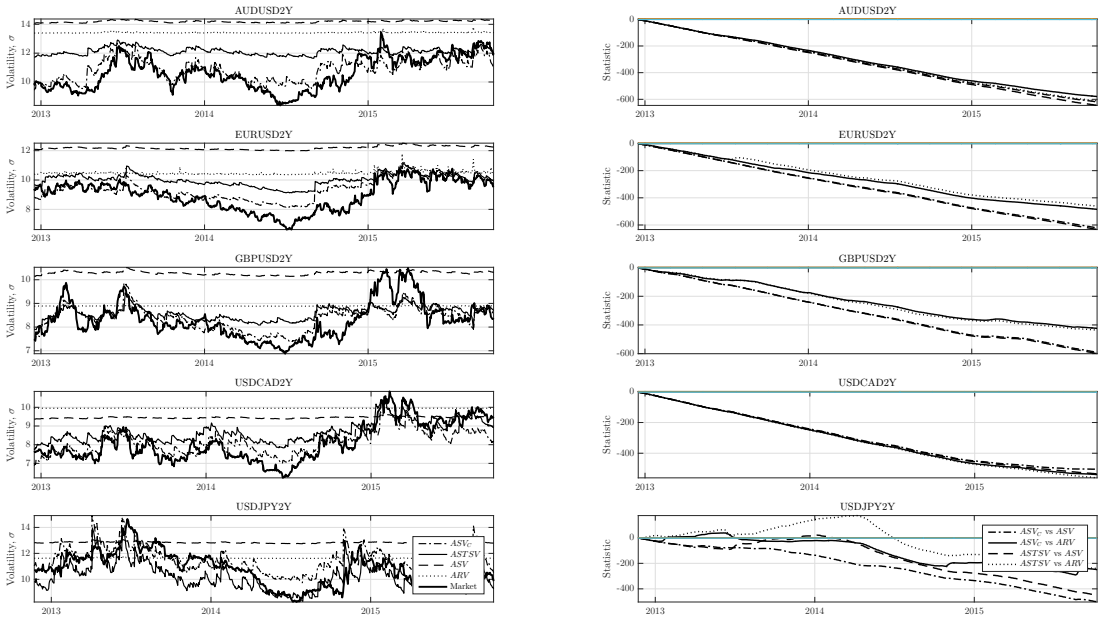

Figure 3.8: Forecast breakdown test among different models applied on 2Y tenor FX options.
This figure shows the fitted quotes and forecast breakdown test statistics for $\widetilde{AT}$ with 2-year maturity of 5 currency pairs.

especially in tracking the movement of the implied volatility level.

For ASV-C model, the improvement of performance comes from the calibration of the state variable dynamic. The adjustments for α and ζ change the mean reverting property of the variance process, thus avoid the variance converging to the long-term level when iteration number is large and lost the implied volatility dynamic. On the other hand for ASTSV, the model benifits from the stochastic interest rate and more suitable time-step size. The change of time-step size also improves the computational speed.

3.8 Comparison between closed form and simulated characteristic function

For many option pricing models, a closed form solution is not possible and therefore many models rely on Monte Carlo simulation to generate option prices. In this section, I provide one benefit from a closed form solution compared with simulated solution.

In this experiment, I choose to simulate the ASTSV model based on the GBPUSD point estimate parameters. I generate $n \times T/\eta, n = 100,000$ standard normal distributed random variables for each of the shocks in the risk neutral dynamic as in Remark 1. Recall that here T/η represents the number of time-steps needed from spot to maturity. Then I recover the empirical characteristic function of the terminal cross section of log spot exchange rates, at $T \in \{6, 12, 18, 24\}$ months:

$$f(\phi) = \mathbb{E}[e^{\phi x(T)}] = \sum_{i=1}^{n} \frac{e^{\phi x_i(T)}}{n},$$

where $\phi \in \mathbb{C}$, and $x_i(T)$ is the ith simulated log spot rates at T.

Fig. 3.9 presents the initial evaluation of the characteristic function $f(\phi)$, with $\Re f(\phi)$ plotted on the abscissa axis and $\Im f(\phi)$ on the ordinate axis. We can see that for longer time frames there is a small bias in the characteristic function for longer iterations (measured in integer months). Fig. 3.10 presents the "tail" of the characteristic function, where we can see where the bias emerges from. The tail of the characteristic function determines the smoothness of the density function, which means how many times the density function can be differentiated. Hence, as the number of steps in the simulation increases the increased perturbation of

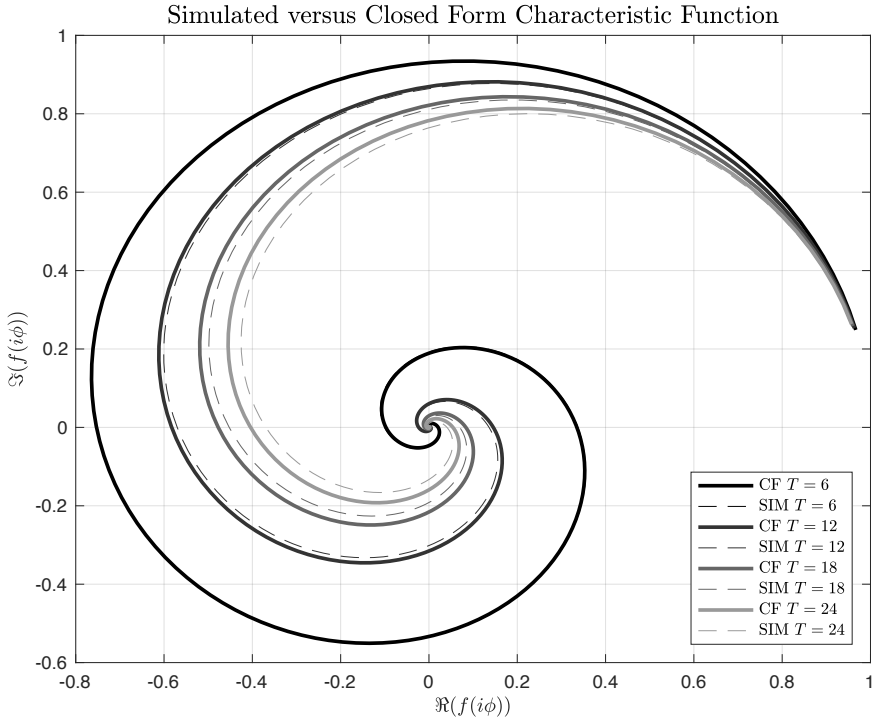

Figure 3.9: Characteristic function For GBPUSD
This figure illustrates the characteristic functions based on closed-form solution and simulation. Simulated CF is represented by the dot lines and closed-form CF is the solid lines. Darker colour represents for longer tenor.

tail of the characteristic function results in a slightly increasing error between the closed form and the simulated CF. The bias in CF indicates the mis-specification of the simulated probability density function and causing errors in the variance, skewness and other moments of the distribution. And then these errors are transferred into the final synthetic implied volatility surface quotes as shown in our delta method. Indeed, this provides an illustration of the accuracy benefits of a closed form model over a simulation, for very long tenors, the simulation can have a sizeable error even with a very large number of draws.

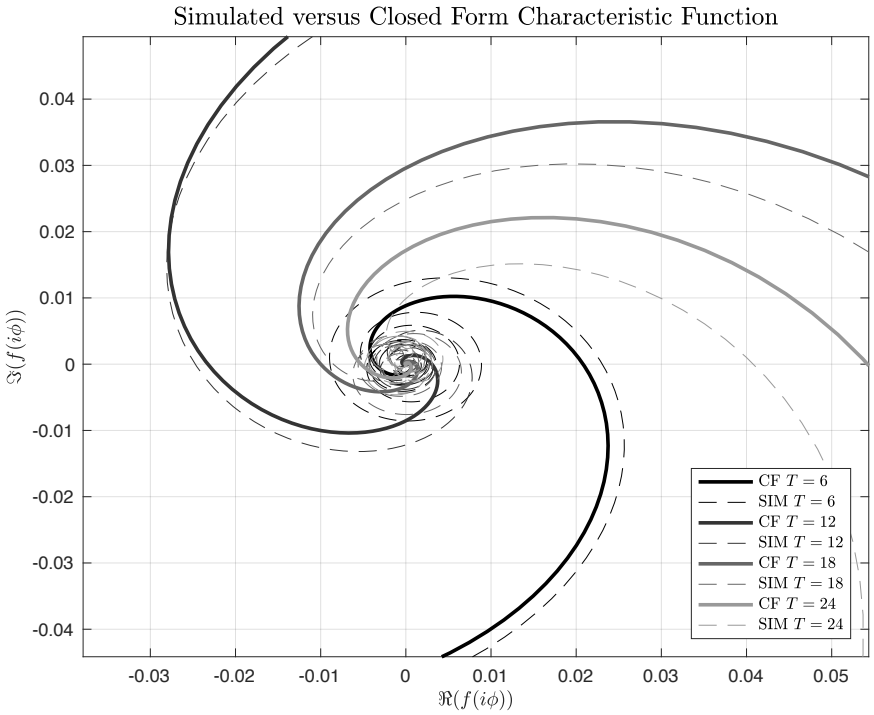

Figure 3.10: Higher moments of the characteristic function
Similar to Fig. 3.9, this figure emphasises on the "tail" part of the CF, which determines the smoothness of the density function.

3.9 Chapter conclusions

I have specified in generality a discrete-time model for pricing over-the-counter foreign exchange options with stochastic short rates for domestic and overseas numéraires. Restricting the yield curve dynamics yields an FX option version of the classic Heston and Nandi [2000] GARCH-type affine model in discrete-time. Building FX option models from scratch presents a number of problems, not least of which is the quotation style for FX options, which is by delta and quoted in the Garmen-Kohlhagen-style adjustment to the Black-Scholes implied volatility. To generate the market quotes from the spot-estimated models, I introduce a new procedure for computing the implied volatility by delta surface and illustrate how

to carry the inherent asymptotic error in the model estimation phase to the actual quotes.

I further test the various model specifications and estimation strategies out-of-sample on quoted data for five actively traded currencies over six distinct tenors. By fitting against the five common quotation types in the OTC-FX market, my results permit us to analyse the effectiveness of spot-based models in capturing the entire European volatility surface as opposed to just the at-the-money traded volatilities.

My baseline suggested strategy for implementation is that for short tenors, dropping the stochastic short rate model and calibrating to a snippet of options data is very effective. For longer tenors (most notably $\geq$3Y), the calibrated stochastic short-rate model performs very well compared to its alternatives. Arguably the most useful aspect of the exercise is in illustrating that an affine structural model with time-inhomogeneous spot variance estimated from spot FX and spot yield curve data can provide a relatively good fit, without having any recourse to the quoted European surface. Hence, for less liquid options on free-floating currency pairs, which constitute the vast majority of currency pairs traded, my approach provides a good first pass for generating quotes when options data is absent.

The two obvious areas to extend my approach are a) the inclusion of time-homogenous and time-inhomogeneous jumps in the model; and b) re-specification of the variance process to permit multi-currency pricing. For instance, in the latter case the addition of a triangular arbitrage correction factor would ensure that the stochastic processes driving all three legs of the triangle is off the same form. Doust [2012] undertakes this exercise for the popular SABR model (with

the beta parameter set to 1).

Chapter 4

Implied Hidden Factors Within The Term Structure of Interest Rate

4.1 FX Option implied latent factor structures

Yield curves for most countries have a more complex structure than can be determined by a single factor model. Indeed, many cases need more than two factors, hence a general specification for the structure of the parity condition is desirable. Furthermore, there is a great deal of evidence from the lack of fit for standard volatility models and the variation between the term structure of option implied volatility and that from a single factor GARCH model implies more than a single factor for the spot variance structure of exchange rates. As such there is a need for an affine model with multiple factors in the determination of the parity and the volatility structure to provide a closed form solution under a more general

structure. In this chapter I derive a general factor model with an arbitrary factor structure for the three components and provide a closed form solution for the volatility surface. I then illustrate the benefits of this model over the single factor volatility model.

The proposed new discrete option pricing model contains multiple factors driving the return and autoregressive conditional Poisson (ACP) jump components that can be filtered from high frequency spot data. This model can be adjusted and calibrated from observed option data. The attractive feature of this approach is that an arbitrary number of observable or latent interest factors can be added. Thus this framework effectively generalises the approach suggested in Christoffersen et al. [2015] and Ornthanalai [2014].

Most of the existing models for FX options pricing are based on continuous time models such as the Heston [1993] stochastic volatility model, the Pan [2002] double jump model, the Hagan et al. [2002] SABR model and the local stochastic volatility models, such as Pagliarani and Pascucci [2012]; Reghai et al. [2012]; Shiraya and Takahashi [2013]. These models rely on actively updated market option data to calibrate against, and therefore have limitations in finding out the property of the option implied latent interest factor, because it is difficult to distinguish the hidden interest factor estimation from spot rate parameter estimation. Thus an ideal model should have spot rate process that can be directly estimated from the underlying spot data.

Discrete models based on GARCH can overcome such disadvantage of continuous models. This type of model is used extensively across the asset pricing and risk management spectrum. I nest multiple variations on the quadratic specification of Engle and Ng [1993], as my basic time series building block, gener-

alising the work in Chapter 3. Previous works on option pricing with GARCH have features in Duan [1997], Barone-Adesi et al. [2008] and Christoffersen et al. [2013] whilst Bauwens et al. [2006] review some applications to derivatives pricing amongst other applications of correlation dynamic in multivariate settings. The most similar specification to one in this chapter can be found in Christoffersen et al. [2015] and Ornthanalai [2014]. In both cases, there is a jump in risk premium embedded into the GARCH process. The model I proposed distinguishes from these two models that my model focuses on the multi-factor structure which can be applied to identify the latent drift terms in option pricing, and the jump process can be estimated based on more general jump detection methods.

Utilising multi-factor volatility and jump components has been the subject of considerable research in option pricing. Firstly, as Ait-Sahalia et al. [2008] point out, it is more common to include multiple state variables into the models in finance. Sundaresan [2000] lists examples of this trend, such as asset pricing models with multiple explanatory factors, term structure models with multiple yields or factors and stochastic volatility or stochastic mean reversion models. These multiple factors provide more freedom to the models. Secondly, the importance of jump in option pricing can be found in literature including Eraker et al. [2003], Eraker [2004], Andersen et al. [2015]. Using the jump framework, these studies find that for equity market, priced jump risks affect risk premium pricing, contribute to the micro-structure, and have strong and persistent impacts to the economic negative shocks compared with just asset volatility. Pan [2002] shows that jumps in equity variance dynamic also have influence on the risk premium. Lin et al. [2015] study specifically the effects of jump in FX option pricing and currency price circle.

FX options regularly quotes volatility surfaces from very short tenors such as overnight (ON) or spot next (SN) all the way out to 7+ years. This makes option pricing using discrete-time models computationally intensive and time consuming, even when a closed form solution exists. Hence I outline a varying time-step version of the model to cater short and long tenor option pricing. These model specifications are then fitted to spot data for six actively traded currencies against US dollar (USD): Australian dollar (AUD), Canadian dollar (CAD), Swiss franc (CHF), Euro (EUR), UK pound (GBP) and Japanese yen (JPY). I find that adjusting the time-step size corresponding to the tenor will improve the pricing performance of the model.

With the GARCH based return processes, jump components and the adjusted time-step size, the proposed model can capture most of the FX spot rate dynamic and can be estimated from spot rate data only. This helps separating the impact of the hidden factors within the interest rate on OTC FX option prices. Then I identify the hidden factor's dynamic by calibrating the proposed model against the real market option quotes, and show that hidden factors extracted from the FX option quotes have strong persistence property.

The remainder of this chapter is organised as follows. Section 4.2 describes the proposed affine stochastic volatility with jump component model and also a simplified specification of this model restricting the interest rates to be constants. Section 4.3 outlines the procedures for estimating the model parameters. With the these settings, Section 4.4 illustrates the time-step size adjustment method, and more importantly, recover the hidden factors within the interest rates. Section 4.5 reports the performance of the proposed models from empirical analysis, and Section 4.6 concludes.

4.2 Discrete-time affine FX option pricing models

The basic specification considered in this chapter has a multi-factor GARCH structure and includes an ACP jump type specification in the spot exchange rate processes. This generalises the work of Christoffersen et al. [2015] and Ornthanalai [2014] in two ways. Firstly the introduction of multi-factor drift terms allow the model to handle both observable and unobservable factors that drive the interest rate return. The proposed model can also categorise factors into domestic or foreign environments. Secondly the jump component I apply in the model can be detected based on various existing non-parametric jump detection techniques. When the observed interest rates is believed to dominate the drift of the spot rate return, the proposed model can be restricted to a non-stochastic interest rate model as a simplified version. Here I will start with the general form.

4.2.1 Multi-factor conditional jump models

The baseline model presumes multiple factors and ACP jump in the return process with random jump size, and I will refer the model as MFJ. Multi-factors represent stochasticity in the 'domestic' and 'foreign' economy factors. This representation is useful as it allows us to formulate various restricted FX pricing models given covered interest parity is violated or not. The factors describing the economy return share a common disturbance and also have their unique shocks, which provides certain dependence structure intrinsic to the model.

Assumption 8. *I presume a discretely updated two country (indexed by* $k \in$

$\{d, f\}$) *global economy. Consider a forward tenor* T *for a contract, which spans the time interval* $0, T$*. At any time* t *before maturity, assets are valued at nominal prices relative to potentially stochastic theoretical instant short rates* $r_d(t)$ *and* $r_f(t)$*. They can be used to model the risk-free rates or implied interest return processes. For a given discrete time-step denoted* η,[1] *the money market accounts are presumed to be timed deposit accounts paying* $\exp(r_d(t+\eta))$ *and* $\exp(r_f(t+\eta))$ *on a single unit of domestic or foreign currency respectively. Setting* $S(t)$ *be the spot conversion between domestic and foreign currency.*

I denote $\mathbb{P}$ as the physical measure (from the domestic investor's point of view) under a filtration $\mathcal{F}_t$, and the probability space $(\Omega, \mathcal{F}, \mathcal{F}_t, \mathbb{P})$ follows normal condition as in Protter [2004]. Given the notational assumption on the time step, I set $\tau = T\eta^{-1}$ be the integer number of discrete time steps to T.

Assumption 9. *$S(t+\eta)|\mathcal{F}_t$ is conditionally log-normal. Setting the logarithm return $R(t+\eta) = \ln(S(t+\eta)/S(t))$, then the state variable processes, $(R(t), f_{k,i}(t), h(t), \lambda(t))'$ under the probability space $(\Omega, \mathcal{F}, \mathcal{F}_t, \mathbb{P})$ are described by*

[1] A useful feature of OTC FX options is that they are explicitly tenored, rather than explicitly dated, hence all but eliminating the problem non-integer counts of time steps from t to T.

the following spot process with GARCH type volatility:

$$R(t+\eta) = \sum_{i=1}^{n} f_{d,i}(t) - \sum_{i=1}^{m} f_{f,i}(t) + \zeta_s h(t+\eta) - \zeta_J \lambda(t+\eta) + \\ + \sqrt{h(t+\eta)} z(t+\eta) + \sum_{j=0}^{N(t+\eta;\lambda(t+\eta))} u_j(t+\eta) \tag{4.1}$$

$$f_{k,i}(t+\eta) = \omega_{k,i} + \beta_{k,i} f_{k,i}(t) + \alpha_{k,i}(z(t+\eta) - \gamma_s \sqrt{h(t+\eta)})^2 + \sigma_{k,i} v_{k,i}(t) \tag{4.2}$$

$$h(t+\eta) = \omega_s + \beta_s h(t) + \alpha_s (z(t) - \gamma_s \sqrt{h(t)})^2 \tag{4.3}$$

$$\lambda(t+\eta) = \omega_J + \beta_J \lambda(t) + \alpha_J N(t), \tag{4.4}$$

where each disturbance term $(z(t), v_{d,1}, \ldots, v_{d,n}(t), v_{f,1}(t), \ldots, v_{f,n}(t))'$ *independent and identically follows standard normal distribution and jump size* $u_j(t) \sim^{iid} \mathcal{N}(\mu_J, \sigma_J)$. *In total there will be* n *and* m *factors describing the domestic and foreign economies respectively.*

Each interest rate factor $f_{k,i}(t+\eta)$ contains a common disturbance with return process, $z(t+\eta)$. This shared shock also drives the Cox-Ingersoll-Ross (CIR) variance process denoted by $h(t+\eta)$. The unique shock $v_{k,i}(t)$ provides freedom in the factor dynamic. For the variance process $h(t)$, it is useful to note that whilst β_s determines the persistence in the spot variance, α_s and γ_s are principal parameters that determine the 'kurtosis and skewness' properties in the resulting implied volatility surface. The factor equation parameters have the same interpretation as the variance dynamic. $f_{k,i}(t+\eta)$ is time inhomogeneous and AR(1), with factor persistence determined by $\beta_{k,i}$. ζ_s reflects the risk premium in the return dynamic and ζ_J is compensator for jump. The structural parameters of the model are collected in the vector $\theta = (\theta_s, \theta_k, \theta_J)'$, where $\theta_s = (\zeta_s, \omega_s, \beta_s, \alpha_s, \gamma_s)'$ is for

return and variance, $\theta_J = (\zeta_J, \omega_J, \beta_J, \alpha_J, \mu_J, \sigma_J)'$ is for the jump process and $\theta_{k,i} = (\omega_{k,i}, \beta_{k,i}, \alpha_{k,i}, \gamma_{k,i}, \sigma_{k,i})'$ is for the ith factor.

Define the de-trend return $\bar{R}(t+\eta) = R(t+\eta) - \sum_{i=1}^{n} f_{d,i}(t+\eta) + \sum_{i=1}^{m} f_{f,i}(t+\eta)$. Because of the existence of the shared shock among factors and return process, $\bar{R}(t)$ will have a non-zero conditional correlation with the factors.

$$
\begin{aligned}
& Cov_{t+\eta}[\bar{R}(t+\eta), f_{k,i}(t+\eta)] \\
=& \mathbb{E}_t[\bar{R}(t+\eta) f_{k,i}(t+\eta)] - \mathbb{E}_t[\bar{R}(t+\eta)]\mathbb{E}_t[f_{k,i}(t+\eta)] \\
=& -2\alpha_{k,i}\gamma_s h(t+\eta).
\end{aligned}
$$

Then similar to HN, the de-trend return and one time step further variance process have the covariance of

$$Cov_{t+\eta}[\bar{R}(t+\eta), h(t+2\eta)] = -2\alpha_s\gamma_s h(t+\eta).$$

The arbitrage free price of the option can be derived by replication. Whereby a representative domestic or foreign investor can construct a self-financing position by being short or long in the bond market of either currency and financing a payoff in the opposite currency at some fixed date. This is then replicated by holding a cash and option delivering an identical payoff. From this replication setting I can derive the risk neutral formula for FX markets no-arbitrage from the viewpoint of either a domestic or foreign investor. Based on the assumptions above, I can then apply in discrete time Amin and Jarrow [1991]'s intuition for determining the risk neutral process, given that in each step the interest rate dynamic is describing timed deposits. In this chapter, I will only focus on the

domestic measure, since it is an analogue for foreign measure.

Remark 3. *From a domestic investor's point of view, the risk neutral FX process of the MFJ model, under the domestic risk neutral $\mathbb{Q}$ measure, is given by the following pair of expressions:*

$$\begin{aligned}
R(t+\eta) =& r_d(t) - r_f(t) - \frac{1}{2}h(t+\eta) - (e^{\mu_J+\frac{1}{2}\sigma_J^2} - 1)\lambda^*(t+\eta) + \\
&+ \sqrt{h(t+\eta)}z^*(t+\eta) + \sum_{j=0}^{N^*(t+\eta)} u_j(t+\eta), \\
r_k(t) =& \sum_{i=1}^{n,m} f_{k,i}(t), \\
f_{k,i}(t+\eta) =& \omega_{k,i} + \beta_{k,i} f_{k,i}(t) + \alpha_{k,i}(z^*(t+\eta) - \gamma_s^*\sqrt{h(t+\eta)})^2 + \sigma_{k,i} v_{k,i}(t), \\
h(t+\eta) =& \omega_s + \beta_s h(t) + \alpha_s(z^*(t) - \gamma_s^*\sqrt{h(t)})^2, \\
\lambda^*(t+\eta) =& \omega_J^* + \beta_J \lambda^*(t) + \alpha_J N^*(t),
\end{aligned}$$

where

$$z^*(t) = z(t) + (\frac{1}{2} + \zeta_s)\sqrt{h_s(t)}, \tag{4.5a}$$

$$\gamma_s^* = \gamma_s + \frac{1}{2} + \zeta_s, \tag{4.5b}$$

$$\lambda^*(t) = \frac{\zeta_J}{e^{\mu_J+\frac{1}{2}\sigma_J^2} - 1}\lambda(t) \tag{4.5c}$$

$$\omega_J^* = \frac{\zeta_J}{e^{\mu_J+\frac{1}{2}\sigma_J^2} - 1}\omega_J. \tag{4.5d}$$

Under the risk neutral measure, the interest rate factors are categorised into domestic factors and foreign factors, together acting as risk neutral drift terms.

Here I follow the steps as in the Chapter 3 for ASTSV model to guarantee

$$\mathbb{E}^* \left[\frac{S(t+\eta) M_f(t, t+\eta)}{M_d(t, t+\eta)} \middle| \mathcal{F}_t \right] = S(t),$$

where $M_k(t, t+\eta), k \in \{d, f\}$, is the money account for one of the currency of the currency pair. The left side of the equation, discounted spot FX rate, is a martingale after adjustment Eq. (4.5). Specifically, the last two adjustments, for jump intensity process $\lambda^*(t)$ and jump parameter ω_J^*, are associated with the jump process risk neutralisation by a fraction $\zeta_J/(e^{\mu_J + \frac{1}{2}\sigma_J^2} - 1)$, where $e^{\mu_J + \frac{1}{2}\sigma_J^2} - 1$ is the expected jump size from the jump measure. For brevity, I mark a risk neutral process and expectations under the domestic risk neutral measure $\mathbb{Q}$ with a superscript * henceforth.

Denoting $x(t) = \ln S(t)$ as the natural logarithm of the spot FX price at time t. I follow Duffie et al. [2000] where instead of using the normal conditional characteristic function as $\mathbb{E}_t[\exp(\phi x(T))], \phi \in \mathbb{C}$, they use the discounted conditional characteristic function $\Psi(t; T, \phi) = \mathbb{E}_t[\exp(-\sum_{j=0}^{J} r_d(t + j\eta)) \exp(\phi x(T))]$ for the logarithm price under domestic risk neutral measure. The advantage using the discounted version of the CF is that it can then track the discount factors simultaneously with each backward iteration. Thus I do not need to separate the interest rate dynamic from the calculation. Further more I assume the discounted characteristic function takes the log-linear form, then we have the following theorem.

Theorem 4. *The discounted conditional characteristic function for the MFJ*

model is affine and of the following form

$$
\begin{aligned}
&\Psi(t;T,\phi)\\
=&\mathbb{E}_t^*[e^{-\sum_{j=0}^{J} r_d(t+j\eta)} e^{\phi x(T)}]\\
=&\exp(\phi x(t) + A(t;T,\phi) + \sum_{i=1}^{n} B_{d,i}(t;T,\phi) f_{d,i}(t) - \sum_{i=1}^{m} B_{f,i}(t;T,\phi) f_{f,i}(t) +\\
&+ C(t;T,\phi)h(t+\eta)) + D(t;T,\phi)\lambda^*(t+\eta). \qquad (4.6)
\end{aligned}
$$

where d, f denote the parameters for domestic and foreign interest rate, respectively. The recursive coefficients to be evaluated from the terminal boundary conditions are as follows:

$$
\begin{aligned}
A(t) &= A(t+\eta) + \sum_{d,i}^{n} B_{d,i}(t+\eta)\omega_{d,i} - \sum_{f,i}^{m} B_{f,i}(t+\eta)\omega_{f,i} + C(t+\eta)\omega_s +\\
&\quad + D(t+\eta)\omega_J^* - \frac{1}{2}\ln(1-2G(t+\eta)) + \frac{1}{2}\sum_{i=1}^{n} B_{d,i}^2(t+\eta)\sigma_{d,i}^2 +\\
&\quad - \frac{1}{2}\sum_{i=1}^{m} B_{f,i}^2(t+\eta)\sigma_{f,i}^2 \qquad (4.7a)\\
B_{d,i}(t) &= \phi - 1 + B_{d,i}(t+\eta)\beta_{d,i} \qquad (4.7b)\\
B_{f,i}(t) &= \phi + B_{f,i}(t+\eta)\beta_{f,i} \qquad (4.7c)\\
C(t) &= C(t+\eta)\beta_s - \frac{\phi}{2} + \sum_{i=1}^{n} B_{d,i}(t+\eta)\sigma_{d,i}\gamma_s^{*2} - \sum_{i=1}^{m} B_{f,i}(t+\eta)\sigma_{f,i}\gamma_s^{*2} +\\
&\quad + C(t+\eta)\alpha_s\gamma_s^{*2} + \frac{(\phi - 2\gamma_s^* G(t+\eta))^2}{2(1-2G(t+\eta))} \qquad (4.7d)\\
D(t) &= D(t+\eta)\beta_J - \phi(e^{\mu_J + \frac{1}{2}\sigma_J^2} - 1) + e^{D(t+\eta)\alpha_J + \phi\mu_J + \frac{1}{2}\phi^2\sigma_J^2} - 1 \qquad (4.7e)
\end{aligned}
$$

where

$$G(t+\eta) = \sum_{i=1}^{n} B_{d,i}(t+\eta)\alpha_{d,i} - \sum_{i=1}^{m} B_{f,i}(t+\eta)\alpha_{f,i} + C(t+\eta)\alpha_s,$$

These coefficients can be calculated recursively from the following boundary conditions at T:

$$A(T;T,\phi) = B_{k,i}(T;T,\phi) = C_s(T;T,\phi) = D(T;T,\phi) = 0, \quad k \in \{f,d\}. \quad (4.8)$$

The Proof of Theorem 4 relies on the affine structure of the volatility and jump terms and is given as follows:

Proof. Given the assumption of the discounted characteristic function, I expand the expectation at $t+\eta$ as:

$$\begin{aligned}
&\Psi(t+\eta;T,\phi) \\
=&\exp(\phi x(t+\eta) + A(t+\eta) + \sum_{i=1}^{n} B_{d,i}(t+\eta) f_{d,i}(t+\eta) + \\
&- \sum_{i=1}^{m} B_{f,i}(t+\eta) f_{f,i}(t+\eta) + C(t+\eta) h_s(t+2\eta) + D(t+\eta)\lambda^*(t+2\eta))
\end{aligned}$$

Expanding this equation with the model processes, I have

$$
\begin{aligned}
&\Psi(t+\eta;T,\phi)\\
&=\exp(\phi(x(t)+\sum_{i=1}^{n} f_{d,i}(t)-\sum_{i=1}^{m} f_{f,i}(t)-\frac{1}{2}h_s(t+\eta)-(e^{\mu_J+\frac{1}{2}\sigma_J^2}-1)\lambda^*(t+\eta)+\\
&+\sqrt{h_s(t+\eta)}z^*(t+\eta)+\sum_{j=0}^{N^*(t+\eta)} u_j(t+\eta))+A(t+\eta)+\sum_{i=1}^{n} B_{d,i}(t+\eta)(\omega_{d,i}+\\
&+\beta_{d,i}f_{d,i}(t)+\alpha_{d,i}(z^*(t+\eta)-\gamma_s^*\sqrt{h_s(t+\eta)})^2+\sigma_{d,i}v_{d,i}(t))-\sum_{i=1}^{m} B_{f,i}(t+\eta)(\omega_{f,i}+\\
&+\beta_{f,i}f_{f,i}(t)\alpha_{f,i}(z^*(t+\eta)-\gamma_s^*\sqrt{h_s(t+\eta)})^2+\sigma_{f,i}v_{f,i}(t))+C(t+\eta)(\omega_s+\\
&+\beta_s h_s(t+\eta)+\alpha_s(z^*(t+\eta)-\gamma_s^*\sqrt{h_s(t+\eta)})^2)+D(t+\eta)(\omega_J^*+\beta_J\lambda^*(t+\eta)+\\
&+\alpha_J N^*(t+\eta).
\end{aligned}
$$

Rearranging the terms, I have

$$
\begin{aligned}
&\Psi(t+\eta;T,\phi)\\
&=\exp(\phi x(t)+A(t+\eta)+\sum_{i=1}^{n}B_{d,i}(t+\eta)\omega_{d,i}-\sum_{i=1}^{m}B_{f,i}(t+\eta)\omega_{f,i}+\\
&+C(t+\eta)\omega_s+D(t+\eta)\omega_J^*+\sum_{i=1}^{n}(\phi+B_{d,i}(t+\eta)\beta_{d,i})f_{d,i}(t)-\sum_{f,i}^{m}(\phi+\\
&+B_{f,i}(t+\eta)\beta_{f,i})f_{f,i}(t)+(D(t+\eta)\beta_J-\phi(e^{\mu_J+\frac{1}{2}\sigma_J^2}-1))\lambda^*(t+\eta)+\\
&+\sum_{i=1}^{n}B_{d,i}(t+\eta)\sigma_{d,i}v_{d,i}(t)-\sum_{i=1}^{m}B_{f,i}(t+\eta)\sigma_{f,i}v_{f,i}(t)+D(t+\eta)\alpha_J N^*(t+\eta)+\\
&+\sum_{j=0}^{N^*(t+\eta)}\phi u_j(t+\eta)+(\sum_{i=1}^{n}B_{d,i}(t+\eta)\alpha_{d,i}-\sum_{i=1}^{m}B_{f,i}(t+\eta)\alpha_{f,i}+\\
&+C(t+\eta)\alpha_s)z^{*2}(t+\eta)+(\phi-2\gamma_s^*(\sum_{i=1}^{n}B_{d,i}(t+\eta)\alpha_{d,i}-\sum_{i=1}^{m}B_{f,i}(t+\eta)\alpha_{f,i}+\\
&+C(t+\eta)\alpha_s))\sqrt{h_s(t+\eta)}z^*(t+\eta)+(C(t+\eta)\beta_s-\frac{\phi}{2}+\sum_{i=1}^{n}B_{d,i}(t+\eta)\alpha_{d,i}\gamma_s^{*2}+\\
&-\sum_{i=1}^{m}B_{f,i}(t+\eta)\alpha_{f,i}\gamma_s^{*2}+C(t+\eta)\alpha_s\gamma_s^{*2})h_s(t+\eta).
\end{aligned}
$$

Separating the independent shocks, I have the expectation at t to be

$$
\begin{aligned}
&\mathbb{E}_t^*[e^{-r_d(t)}\Psi(t+\eta;T,\phi)]] \\
&= \exp(\phi x(t) + A(t+\eta) + \sum_{i=1}^{n} B_{d,i}(t+\eta)\omega_{d,i} - \sum_{i=1}^{m} B_{f,i}(t+\eta)\omega_{f,i} + C(t+\eta)\omega_s + \\
&+ D(t+\eta)\omega_J^* + \sum_{i=1}^{n}(\phi - 1 + B_{d,i}(t+\eta)\beta_{d,i})f_{d,i}(t) - \sum_{f,i}^{m}(\phi + B_{f,i}(t+\eta)\beta_{f,i})f_{f,i}(t) + \\
&+ (C(t+\eta)\beta_s - \frac{\phi}{2} + \sum_{i=1}^{n} B_{d,i}(t+\eta)\alpha_{d,i}\gamma_s^{*2} - \sum_{i=1}^{m} B_{f,i}(t+\eta)\alpha_{f,i}\gamma_s^{*2} + \\
&+ C(t+\eta)\alpha_s\gamma_s^{*2})h_s(t+\eta) + (D(t+\eta)\beta_J - \phi(e^{\mu_J + \frac{1}{2}\sigma_J^2} + \\
&- 1))\lambda^*(t+\eta))\mathbb{E}_t^*[\exp(D(t+\eta)\alpha_J N^*(t+\eta) + \sum_{j=0}^{N^*(t+\eta)} \phi u_j(t+\eta))] \times \\
&\times \mathbb{E}_t^*[\exp(\sum_{i=1}^{n} B_{d,i}(t+\eta)\sigma_{d,i}v_{d,i}(t))]\mathbb{E}_t^*[\exp((\sum_{i=1}^{n} B_{d,i}(t+\eta)\alpha_{d,i} - \sum_{i=1}^{m} B_{f,i}(t+\eta)\alpha_{f,i} + \\
&+ C(t+\eta)\alpha_s)z^{*2}(t+\eta) + (\phi - 2\gamma_s^*(\sum_{i=1}^{n} B_{d,i}(t+\eta)\alpha_{d,i} - \sum_{i=1}^{m} B_{f,i}(t+\eta)\alpha_{f,i} + \\
&+ C(t+\eta)\alpha_s))\sqrt{h_s(t+\eta)}z^*(t+\eta)]/\mathbb{E}_t^*[\exp[\sum_{i=1}^{m} B_{f,i}(t+\eta)\sigma_{f,i}v_{f,i}(t)]
\end{aligned}
$$

Notice that for a standard normal random variable

$$\mathbb{E}[\exp(a(z+b)^2)] = \exp\left(-\frac{1}{2}\ln(1-2a\sigma_z^2) + \frac{a(b+\mu_z)^2}{1-2a\sigma_z^2}\right),$$

For the $z^*(t+\eta)$ terms, denote

$$G(t+\eta) = \sum_{i=1}^{n} B_{d,i}(t+\eta)\alpha_{d,i} - \sum_{i=1}^{m} B_{f,i}(t+\eta)\alpha_{f,i} + C(t+\eta)\alpha_s,$$

I have

$$\begin{aligned}
&\mathbb{E}_t^*[\exp(G(t+\eta)z^{*2}(t+\eta)+(\phi-2\gamma_s^*G(t+\eta))\sqrt{h_s(t+\eta)}z^*(t+\eta))]\\
=&\mathbb{E}_t^*[\exp(G(t+\eta)(z^{*2}(t+\eta)+2\frac{\phi-2\gamma_s^*G(t+\eta)}{2G(t+\eta)}\sqrt{h_s(t+\eta)}z^*(t+\eta)))]\\
=&\mathbb{E}_t^*[\exp(G(t+\eta)(z^*(t+\eta)+\frac{\phi-2\gamma_s^*G(t+\eta)}{2G(t+\eta)}\sqrt{h_s(t+\eta)})^2+\\
&-\frac{(\phi-2\gamma_s^*G(t+\eta))^2}{4G(t+\eta)}h_s(t+\eta))]\\
=&\exp(-\frac{1}{2}\ln(1-2G(t+\eta))+\frac{(\phi-2\gamma_s^*G(t+\eta))^2}{2(1-2G(t+\eta))}h_s(t+\eta))
\end{aligned}$$

And

$$\mathbb{E}_t^*[\exp[\sum_{i=1}^{n}B_{k,i}(t+\eta)\sigma_{k,i}v_{k,i}(t)]=\exp(\frac{1}{2}\sum_{i=1}^{n}B_{d,i}^2(t+\eta)\sigma_{d,i}^2)$$

Also for the jump term

$$\begin{aligned}
&\mathbb{E}_t^*[\exp(D(t+\eta)\alpha_J N^*(t+\eta)+\sum_{j=0}^{N^*(t+\eta)}\phi u_j(t+\eta)))]\\
&=\mathbb{E}_t^*[\exp(\sum_{j=0}^{N^*(t+\eta)}D(t+\eta)\alpha_J+\phi u_j(t+\eta))]\\
&=\exp(\lambda^*(t+\eta)(e^{D(t+\eta)\alpha_J+\phi\mu_J+\frac{1}{2}\phi^2\sigma_J^2}-1)),
\end{aligned}$$

Then the expectation becomes

$$
\begin{aligned}
&\mathbb{E}_t^*[\mathbb{E}_{t+\eta}^*[e^{\phi x(T)}]] \\
&= \exp(\phi x(t) + A(t+\eta) + \sum_{i=1}^{n} B_{d,i}(t+\eta)\omega_{d,i} - \sum_{f,i}^{m} B_{f,i}(t+\eta)\omega_{f,i} + C(t+\eta)\omega_s + \\
&+ D(t+\eta)\omega_J^* - \frac{1}{2}\ln(1-2G(t+\eta)) + \frac{1}{2}\sum_{i=1}^{n} B_{d,i}^2(t+\eta)\sigma_{d,i}^2 - \frac{1}{2}\sum_{i=1}^{m} B_{f,i}^2(t+\eta)\sigma_{f,i}^2 + \\
&+ \sum_{i=1}^{n}(\phi - 1 + B_{d,i}(t+\eta)\beta_{d,i})f_{d,i}(t+\eta) - \sum_{f,i}^{m}(\phi + B_{f,i}(t+\eta)\beta_{f,i})f_{f,i}(t+\eta) + \\
&+ (C(t+\eta)\beta_s - \frac{\phi}{2} + \sum_{i=1}^{n} B_{d,i}(t+\eta)\alpha_{d,i}\gamma_s^{*2} - \sum_{i=1}^{m} B_{f,i}(t+\eta)\alpha_{f,i}\gamma_s^{*2} + C(t+\eta)\alpha_s\gamma_s^{*2} + \\
&+ \frac{(\phi - 2\gamma_s^* G(t+\eta))^2}{2(1-2G(t+\eta))})h_s(t+\eta) + (D(t+\eta)\beta_J - \phi(e^{\mu_J + \frac{1}{2}\sigma_J^2} - 1) + \\
&+ e^{D(t+\eta)\alpha_J + \phi\mu_J + \frac{1}{2}\phi^2\sigma_J^2} - 1)\lambda^*(t+\eta)).
\end{aligned}
$$

Compared with the original affine form, I have the coefficients as in the theorem.

End of proof. □

Corollary 5. *Given the discounted characteristic function the call option price for an FX option following the MSJ dynamic under the risk-neutral measure $\mathbb{Q}$ is given by the following expression:*

$$
\begin{aligned}
P_c =& \Psi(1)\left(\frac{1}{2} + \frac{1}{\pi}\int_0^\infty \Re\left[\frac{K^{-iu}\Psi(iu+1)}{iu\Psi(1)}\right]du\right) + \\
&- K\left(\frac{\Psi(0)}{2} + \frac{1}{\pi}\int_0^\infty \Re\left[\frac{K^{-iu}\Psi(iu)}{iu}\right]du\right).
\end{aligned} \tag{4.9}
$$

The put option price can be calculated by the put-call parity as

$$P_p = P_c + D_d(\tau)K - D_f(\tau)S(t). \tag{4.10}$$

4.2.2 A simplified version of the model

For FX options with not long maturities, for instance less than two years, the variance of the deposit rate usually has a vanishing contribution to the overall price. I simplify short maturity models using the following assumption.

Assumption 10. *The Simplified Model. When foreign and domestic numéraires are constant, the MFJ model collapses to a model with constant drift $r_d - r_f$ and extra ACP jump process:*

$$\begin{aligned} R(t+\eta) =& r_d - r_f - \frac{1}{2}h_s(t+\eta) - (e^{\mu_J + \frac{1}{2}\sigma_J^2} - 1)\lambda^*(t+\eta) + \\ &+ \sqrt{h(t+\eta)}z^*(t+\eta) + \sum_{j=0}^{N^*(t+\eta)} u_j(t+\eta), \end{aligned} \tag{4.11}$$

$$h(t+\eta) = \omega_s + \beta_s h(t) + \alpha_s(z^*(t) - \gamma_s^*\sqrt{h(t)})^2, \tag{4.12}$$

$$\lambda^*(t+\eta) = \omega_J^* + \beta_J\lambda^*(t) + \alpha_J N^*(t), \tag{4.13}$$

The corresponding discounted characteristic function is easily defined as a constrained form of the MFJ model and is given in the following proposition:

Proposition 2. *The Simplified Model Characteristic Function. The characteristic function for the simplified model with deterministic deposit rates is given*

by:

$$\begin{aligned}\Psi(t;T,\phi) =& \mathbb{E}_t^*[e^{-Jr_d}e^{\phi x(T)}] \\ =& \exp(\phi x(t) + A(t;T,\phi) + C(t;T,\phi)h(t+\eta) + D(t;T,\phi)\lambda^*(t+\eta)),\end{aligned} \tag{4.14}$$

where

$$\begin{aligned}A(t) =& A(t+\eta) + \phi(r_d - r_f) - r_d + C(t+\eta)\omega_s + D(t+\eta)\omega_J^* + \\ & - \frac{1}{2}\ln(1-2C(t+\eta)\alpha_s) \\ C(t) =& C(t+\eta)\beta_s - \frac{\phi}{2} + C(t+\eta)\alpha_s\gamma_s^{*2} + \frac{(\phi - 2\gamma_s^* C(t+\eta)\alpha_s)^2}{2(1-2C(t+\eta)\alpha_s)} \\ D(t) =& D(t+\eta)\beta_J - \phi(e^{\mu_J + \frac{1}{2}\sigma_J^2} - 1) + e^{D(t+\eta)\alpha_J + \phi\mu_J + \frac{1}{2}\phi^2\sigma_J^2} - 1,\end{aligned}$$

These coefficients can be calculated recursively under the terminal conditions

$$A(T;T,\phi) = C(T;T,\phi) = D(T;T,\phi) = 0.$$

4.3 Estimation procedures

In this section, I will firstly provide the jump detection tool selected for the empirical section. Then in the rest part of this section, I will show how to estimate the parameters of GARCH type process.

4.3.1 Jump detection

To improve reliability of the estimator, I have separated the jump identification out from the estimation of the spot variance model. This is in different from the Christoffersen et al. [2015] where jump intensity $\lambda(t)$ and diffusion variance $h(t)$ are updated simultaneously using the bipower variance (BV) and realize quadratric variation (RV). My approach is similar, but uses the BV and RV in a first stage cleaning of the jumps. In the empirical part of this chapter, I adopt the method proposed by Tauchen and Zhou [2011] to detect the occurrence and jump size distribution parameters as an example. Jump detection itself is an important and active econometric topic. Notable works include the application of BV and tripower quarticity in jump identification proposed by Barndorff-Nielson and Shephard [2004] and Barndorff-Nielson and Shephard [2006], the jump regression method by Li et al. [2014] and the comparison of different techniques by Huang and Tauchen [2005]. Other jump detection techniques such as Lee and Mykland [2008] and Jacod et al. [2018] can also be applied into my framework for parameter estimation, but I will refer the application of these techniques in future works.

Denoting the intraday logarithm return for day t as $R_{intra,j}(t) = \log(x(t + j\bar{\eta})) - \log(x(t + (j-1)\bar{\eta}))$, where $\bar{\eta}$ is the intraday time step and j is the intraday index. Barndorff-Nielson and Shephard [2004] show that when the intraday time step $\bar{\eta} \to 0$, the realized variance $RV(t)$ and realized bipower variance $BV(t)$

converge to the following

$$RV(t) = \sum_{j=1}^{n} R^2_{intra,j}(t) \to \int_{t-1}^{t} \sigma_s^2 ds + \int_{t-1}^{t} J_s^2 dN_t$$
$$BV(t) = \frac{\pi}{2}\frac{n}{n-1}\sum_{j=2}^{n} |R_{intra,j}(t)||R_{intra,j-1}(t)| \to \int_{t-1}^{t} \sigma_s^2 ds,$$

where σ_t, J_t and N_t are the diffusion and jump terms of a continuous jump-diffusion process

$$dx_t = \mu_t dt + \sigma_t dW_t + J_t dN_t.$$

According to Huang and Tauchen [2005], where they document the jump detecting accuracy that the following ratio statistics converges to a standard normal distribution

$$ZJ(t) \equiv \frac{RJ(t)}{\sqrt{[(\frac{\pi}{2})^2 + \pi - 5]\frac{1}{n}\max(1, \frac{TP(t)}{BV^2(t)})}} \to \mathcal{N}(0,1), \tag{4.16}$$

where

$$RJ(t) \equiv \frac{RV(t) - BV(t)}{RV(t)},$$

and $TP(t)$ is the tripower quarticity defined by

$$TP(t) \equiv n\mu_{4/3}^{-3}\frac{n}{n-2}\sum_{j=3}^{n} |R_{intra,j-2}|^{4/3}|R_{intra,j-1}|^{4/3}|R_{intra,j}|^{4/3} \to \int_{t-1}^{t} \sigma_s^4 ds$$

with

$$\mu_k \equiv 2^{k/2}\Gamma((k+1)/2)/\Gamma(1/2), \quad k > 0.$$

Following Tauchen and Zhou [2011] and Andersen et al. [2007]'s significant

jump assumption that there is at most one significant jump per day (per normal time-step η), the realised jumps are filtered by

$$J(t) = sign(R(t))\sqrt{(RV(t) - BV(t))I_{ZJ(t)\geqslant\Phi_a^{-1}}},$$

where Φ_a is the cumulative density function of standard normal distribution with probability level a, and $I_{ZJ(t)\geqslant\Phi_a^{-1}}$ is an indicator function. $sign(\cdot)$ here is the function to extract the sign of the real value represented by "$\cdot$". Thus $sign(R(t))$ ensures the jump has the same direction of the return.

I then estimate the jump size distribution by observing the behaviour of $J(t)$ in the estimation window

$$\mu_J(t) = \text{mean of the realized jumps} \tag{4.17a}$$

$$\sigma_J(t) = \text{standard deviation of the realized jumps.} \tag{4.17b}$$

The jump assumption of Tauchen and Zhou [2011] I applied in the jump detection leads to the fact that counting process $N(t)$ is the same as $I_{ZJ(t)\geqslant\Phi_a^{-1}}$, which takes value from $\{0, 1\}$. By construction, here the model does not consider simultaneous small jumps as in Lee and Mykland [2008]. I adopt the estimation of jump size distribution method as in Eq. (4.17), and then use the realised jump counting process $N(t)$ to update the intensity process $\lambda(t)$ instead of calculating the intensity as a proportion of realised jump observations in the total estimation window days. This treatment makes sense in the way that the test statistics $ZJ(t)$ only helps observe the occurrence of a significant jump and then infer the intensity statistically. I will infer the intensity dynamic based on the return

dynamic as in the following sub-section.

4.3.2 Likelihood based estimation

After identifying domestic and foreign factors and jumps $J(t)$, which represents the $\sum_{j=0}^{N(t+\eta)} u_j(t+\eta)$ in the logarithm return dynamic, I have the filtered logarithm return

$$\begin{aligned}\tilde{R}(t+\eta) =& R(t+\eta) - r_d(t) + r_f(t) - J(t) \\ =& \zeta_s h(t+\eta) - \zeta_J \lambda(t+\eta) + \sqrt{h(t+\eta)} z(t+\eta). \end{aligned} \tag{4.18}$$

This implies the variance process $h(t+\eta)$ can be updated by the knowledge of new return and implied new shock. Together with the innovation of jump intensity $\lambda(t+\eta)$ with the identification of jump counting process $N(t)$, I have the following state variables updating dynamic:

$$h(t+\eta) = \omega_s + \beta_s h(t) + \alpha_s \frac{(\tilde{R}(t+\eta) - \zeta_s h(t+\eta) + \zeta_J \lambda(t+\eta) - \gamma h(t+\eta))^2}{h(t+\eta)} \tag{4.19a}$$

$$\lambda(t+\eta) = \omega_J + \beta_J \lambda(t) + \alpha_J N(t). \tag{4.19b}$$

I use their unconditional expectation to be the initial points of these processes, that is

$$\begin{aligned} h(0) \equiv& \mathbb{E}[h(t)] = \frac{\omega_s + \alpha_s}{1 - \beta_s - \alpha_s \gamma_s^2} \\ \lambda(0) \equiv& \mathbb{E}[\lambda(t)] = \frac{\omega_J}{1 - \beta_J - \alpha_J} \end{aligned}$$

Now I have

$$z(t+\eta) = \frac{\tilde{R}(t+\eta) - \zeta_s h(t+\eta) + \zeta_J \lambda(t+\eta)}{\sqrt{h(t+\eta)}} \sim \mathcal{N}(0,1),$$
$$N(t+\eta) \sim Poisson(\lambda(t+\eta)).$$

With these information, I can then write the marginal log-likelihood function $\mathcal{L}(t)$ as the sum of the log-likelihood function for the logarithm return, jump intensity and factors, which are

$$\mathcal{L}_s(t) = -\frac{1}{2}\ln(2\pi) - \frac{1}{2}\ln(h(t+\eta)) - \frac{1}{2h(t+\eta)}(\tilde{R}(t+\eta) - \zeta_s h(t+\eta) + \\ + \zeta_J \lambda(t+\eta))^2, \tag{4.20a}$$
$$\mathcal{L}_J(t) = -\lambda(t+\eta) - \ln(N(t+\eta)!) + \ln(\lambda(t+\eta))N(t+\eta). \tag{4.20b}$$

Then I can get the optimal parameter $\hat{\theta}$ by maximise the aggregate likelihood.

4.4 Adjusted time-step and hidden factors

To use the model to uncover the underlying latent factor structure, I firstly propose a time-step adjustment technique at the beginning of this section. This adjustment is inspired by the time-step adjustment in Chapter 3, where I use monthly time-step for contracts with longer tenor and daily time-step for shorter tenor contracts. In this section, I apply a more flexible time-step size to accelerate the computation speed and improve the option quotes accuracy. Based on these upgrades, I then show how to extract the hidden factors from the OTC FX option market quotes using the proposed model.

4.4.1 MFJ-F model, an adjusted time-step model

For longer tenor options, a GARCH type model suffers from the disadvantage that it tends to significantly increase the computational time ($O(\tau)$) and loss the variation in the option implied volatility as the maturity increases. In Fig. 4.1, I show an example of the market quotes for the at-the-money volatility ($\widetilde{AT}$) of EURUSD options with 1M and 2Y tenors in solid lines. Then I compute the HN model implied $\widetilde{AT}$ for corresponding period and present in the figure as dash lines.

From the figure we can see that the HN model provides good dynamic time-series for 1M tenor option compared with the market $\widetilde{AT}$ movements. But for the 2Y tenor contract, the fluctuation from the HN model decays and the outcome is much more flat compared with the market quotes.

One of the most important reason for this term structure issue is the iteration character of the GARCH based model. The option price engine iterate the state variable from initial value towards maturity, which means longer tenor contracts have more iterations during the calculation. Then the mean reverting variance process tends to converge to its long-term mean level when the number of iterations is sufficiently large, thus losses its dynamic. To handle this, I propose to adjust the size of time-step corresponding to the time to maturity, and I call this the MFJ-F model.

I set 1M tenor FX option contract as benchmark, which has time-step size of 1 day, denoted as **1**. Then the 1-minute intraday return frequency is equivalent to 1440 subsections of a time-step. It is worth pointing that here I use 1-minute just for demonstration, the empirical jump detection part of this chapter is based

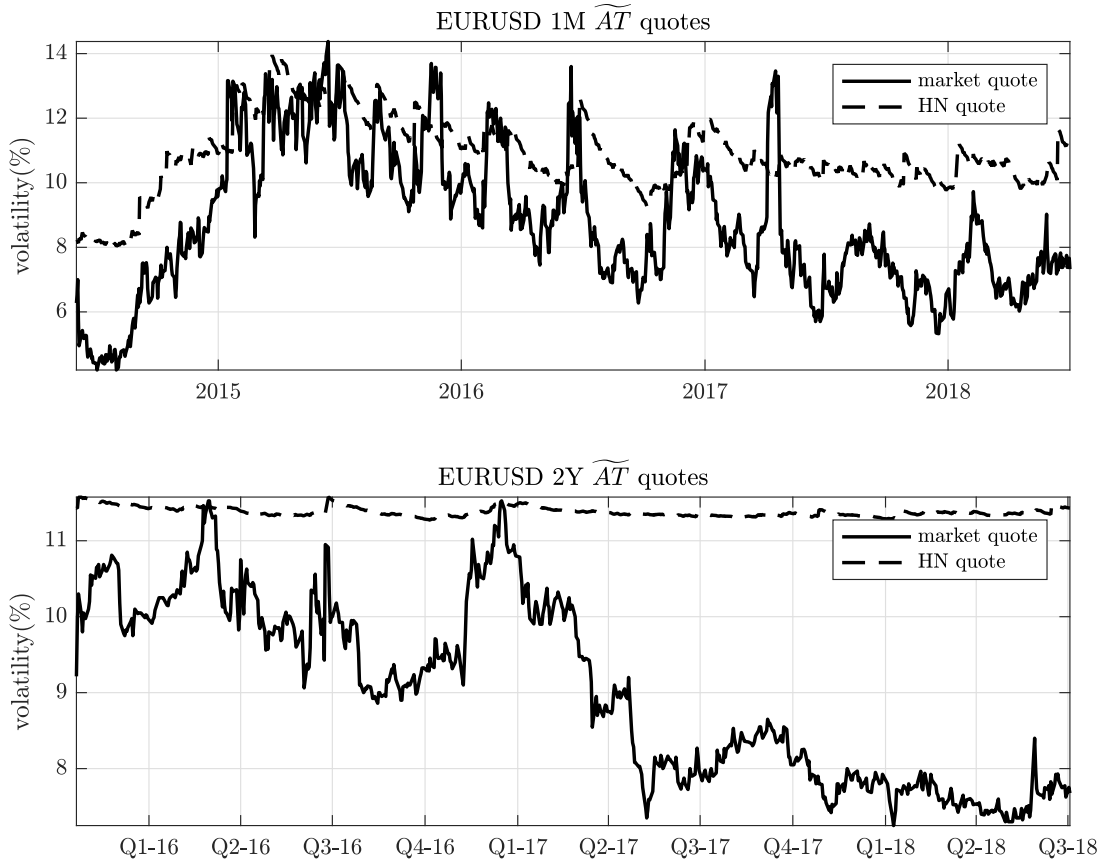

Figure 4.1: $\widetilde{AT}$ market quotes and HN model implied volatility for EURUSD options with 1M and 2Y tenors.

This figure shows the HM model implied $\widetilde{AT}$ for EURUSD with 1M and 2Y tenors. Market quotes are solid lines in the plots and dash lines represent HN quotes. From the plot we can see that the GARCH based HN model provide good dynamic for short-term tenor options. But for the long-term one, the fluctuation of the HN model outcome decays.

on the averaged 5-minute time grid as Liu et al. [2015] suggested. Then for any tenor, τ, longer than 1M, the adjusted return time-step size will be

$$\eta_\tau = \frac{\tau}{1M}\mathbf{1},$$

and accordingly, the intraday frequency is set as

$$\eta_{intra,\tau} = \frac{\tau}{1M}\frac{\mathbf{1}}{1440}.$$

Under this arrangement, take options with 6M tenor as an example, the return process is based on a 6-day time-step size, and the 'intraday' frequency return for realised variance and realised jump detection is based on 6-minute return. Note that the interest rate process should also be adjusted for the modified of time-step size.

4.4.2 MFJ-C model, including hidden factors

I have provided the results from the restricted version of the proposed model, outlined in Section 4.2.2 where interest rate is presumed to be constant. Based on the observation of the interest parity mis-match, I use the multi-factors in interest return to identify the hidden factors in the option price, while muting the fluctuation of the observed interest rates. Therefore I assume both domestic and foreign interest return contains one hidden factor and one fixed observed rate respectively to extract what is driving the future expectation.

To achieve so, I just need to choose the factor number as $n = 2$ and $m = 2$ for domestic and foreign interest rates respectively. While keeping one of the factor as the target hidden factor, I force the dynamic parameter $\beta_{k,2} = 1$ and all other parameters $\theta_{k,2}$ to be zeros. This adjustment fixes the second factor as the constant observed interest rate.

As in Chapter 2, a volatility smile of a FX option at a given time generally includes five volatility quoted strategies describing the smile shape, such as $\widetilde{BF}_{10}$,

$\widetilde{BF}_{25}$, $\widetilde{AT}$, $\widetilde{RR}_{25}$ and $\widetilde{RR}_{10}$. From these five strategies, I am able to back out the five pivotal points, which are Black-Scholes implied volatilities corresponding to 10-put-delta, 25-put-delta, delta-neutral-straddle at-the-money, 25-call-delta and 10-call-delta. I denote these five volatilities as $\sigma_p(10)$, $\sigma_p(25)$, $\widetilde{AT}$, $\sigma_c(25)$ and $\sigma_c(10)$. I then use cubic polynomial to interpolate the volatility smile across a n-point strike price grid, $n = 100$, and denote the interpolated smile as $vol_{market}(K)$.

For a given volatility smile, I calibrate the hidden factor parameter set, which includes ($\theta_{f_d,f_f} = \{f_d(t), f_f(t), \omega_d, \beta_d, \alpha_d, \sigma_d, \omega_f, \beta_f, \alpha_f, \sigma_f\}$), by minimise the quadratic variation between the market volatility smile (vol_{market}) and the model quoted smile (vol_{MFJ-C})

$$\theta_{f_d,f_f} := \underset{\theta_{f_d,f_f}}{\arg\min} \sum_{i=1}^{n} (vol_{market}(K_i) - vol_{MFJ-C}(K_i))^2. \tag{4.21}$$

Then for every volatility smile, there will be a corresponding hidden factor parameter set θ_{f_d,f_f}. I specify the model including the calibrated hidden factors as MFJ-C model.

4.5 Empirical study on six currencies versus the US dollar

4.5.1 Summary of data

I apply the various model specifications mentioned in previous sections for six currencies (G7): Australian dollar (AUD), Euro (EUR), UK pound (GBP), Canadian dollar (CAD), Swiss franc (CHF) and Japanese yen (JPY) versus US dollar

Table 4.1: Sample characteristics

			AUD		
	Obs.	Mean	Std. dev.	Min	Max
Spot	8159041	0.7709	0.1453	0.4776	1.1080
r_1M	7660	4.4635	1.5404	1.5650	7.9250
r_6M	7668	4.6394	1.5377	1.7400	8.2350
r_1Y	7623	4.8382	1.5496	2.0750	8.7950
r_2Y	7592	4.6057	1.6630	1.5950	8.2800
σ_p(10)1M	1384	11.2440	2.5565	6.4500	18.8880
σ_p(25)1M	1384	10.4232	2.3714	6.0115	16.9875
$\widehat{AT}$1M	1384	9.6878	2.2076	5.5550	15.5870
σ_c(25)1M	1384	9.3373	2.0882	5.3645	14.8620
σ_c(10)1M	1384	9.3071	2.0346	5.1520	14.6558
σ_p(10)6M	1330	13.3145	2.1716	8.6400	18.5745
σ_p(25)6M	1330	11.4790	1.8391	7.9440	15.8940
$\widehat{AT}$6M	1330	10.0872	1.6344	6.9000	13.7625
σ_c(25)6M	1330	9.4610	1.5309	6.4125	12.7810
σ_c(10)6M	1330	9.5307	1.5263	6.4120	12.9375
σ_p(10)1Y	1311	14.4847	2.0021	10.0250	18.9995
σ_p(25)1Y	1311	12.1109	1.5963	8.7845	15.7200
$\widehat{AT}$1Y	1311	10.4153	1.3682	7.7175	13.5450
σ_c(25)1Y	1311	9.6908	1.2727	7.0995	12.5200
σ_c(10)1Y	1311	9.8530	1.3020	7.0050	12.8000
σ_p(10)2Y	1305	15.3605	1.9750	10.9380	19.9560
σ_p(25)2Y	1305	12.6427	1.5264	9.4870	16.0335
$\widehat{AT}$2Y	1305	10.8615	1.3103	8.3750	13.8275
σ_c(25)2Y	1305	10.0967	1.2170	7.7625	12.8060
σ_c(10)2Y	1305	10.3134	1.2579	8.0750	13.1995
			CAD		
	Obs.	Mean	Std. dev.	Min	Max
Spot	8157601	1.2596	0.1889	0.9061	1.6164
r_1M	7664	2.4483	1.6299	0.1750	5.9800
r_6M	7681	2.6960	1.5400	0.4000	6.5700
r_1Y	7689	2.9350	1.4816	0.5500	6.4500
r_2Y	4864	2.0368	1.1675	0.2100	5.0315
σ_p(10)1M	1430	7.7551	1.7500	4.0875	12.8750
σ_p(25)1M	1430	7.6393	1.7290	3.9690	12.5750
$\widehat{AT}$1M	1430	7.7709	1.7273	4.0500	12.6250
σ_c(25)1M	1430	8.2427	1.7751	4.4190	13.1185
σ_c(10)1M	1430	8.7574	1.8316	4.8375	13.7500
σ_p(10)6M	1349	7.7633	1.2852	5.0500	11.7065
σ_p(25)6M	1349	7.6016	1.2851	4.8180	11.4250
$\widehat{AT}$6M	1349	7.8830	1.3058	5.0300	11.6750
σ_c(25)6M	1349	8.6973	1.3831	5.6735	12.5185
σ_c(10)6M	1349	9.6591	1.4649	6.5050	13.6500
σ_p(10)1Y	1377	7.9988	1.1399	5.5500	11.5250
σ_p(25)1Y	1377	7.7789	1.1337	5.3240	11.2190
$\widehat{AT}$1Y	1377	8.0879	1.1535	5.5550	11.5250
σ_c(25)1Y	1377	9.0276	1.2306	6.3740	12.5190
σ_c(10)1Y	1377	10.1880	1.3275	7.3500	13.7500
σ_p(10)2Y	1365	8.4171	1.0904	6.4125	11.8630
σ_p(25)2Y	1365	8.1423	1.1021	6.0125	11.5750
$\widehat{AT}$2Y	1365	8.4505	1.1211	6.2250	11.8500
σ_c(25)2Y	1365	9.4188	1.1933	7.0875	12.8500
σ_c(10)2Y	1365	10.6926	1.2719	8.3000	14.1130

Notes: I interpolate the spot exchange rate tick data to a 1 minute grid from 1 millisecond past midnight to 1 millisecond to midnight GMT. For the rest of the 4 currency pairs, see Appendix Table 3.

(USD). Following the market quotation convention, the FX cross rates are denoted as AUDUSD, EURUSD, GBPUSD, USDCAD, USDCHF and USDJPY respectively. I will compute FX option quotes in terms of Black-Scholes implied volatility across the five pivotal delta points ($\sigma_p(10)$, $\sigma_p(25)$, $\widetilde{AT}$, $\sigma_c(25)$ and $\sigma_c(10)$) for tenors out to two years. The HN, MFJ and MFJ-C models are specified over daily data or adjusted frequencies according to maturity (from 1M up to 2Y); I exclude weekends as the quote updates for spot and FX option data are substantially lower.

I collect the tick data from the Tick History database provided by the Thomson Reuters FX feed and warehoused by SIRCA; Table 4.1 provides the sample characteristic for the data. I query both the bid and ask quotes for spot and FX options, and compute the mid-price to use in the models. I am led to believe by the vendor that the quote history for the FX options is complete, in the sense that all of the active broker dealers are included in the survey. For the spot and deposit data the picture is less clear. Certain FX feeds have tighter bid-ask spreads than the quotes from the banks surveyed by Thomson Reuters Tick History. Spot and yield curve data for AUDUSD, GBPUSD, USDCAD, USDCHF and USDJPY exchange rates is taken from January 1, 1996 to July 5, 2018, while for EURUSD the spot and yield curve data starts from February 28, 1998. For the yield curves I use quoted timed deposits for each currency out to one year and quoted swap rates for 2Y tenors. I should note that even though as Du et al. [2018] pointed that CIP condition is typically tested based on interbank offered rates, I use deposit rates in this thesis as the interest rate because this is the rate that OTC FX option market participants undertake to finance their positions.

Table 4.2 provides the MLE estimates for the daily exchange rate variance

Table 4.2: Heston–Nandi parameter estimation.

	ζ_s	ω_s	β_s	α_s	γ_s	$\mathcal{L}$
AUDUSD	0.026	3.446e-12	0.951	2.021e-06	71.649	19944.592
	(0.005)	(1.015)	(0.002)	(0.002)	(0.001)	
EURUSD	-0.005	7.148e-13	0.974	7.893e-07	91.499	18488.754
	(0.006)	(1.718)	(0.002)	(0.002)	(0.001)	
GBPUSD	-0.901	4.227e-13	0.964	9.529e-07	75.573	21437.498
	(0.006)	(2.308)	(0.002)	(0.002)	(0.001)	
USDCAD	0.002	1.783e-13	0.964	8.231e-07	-44.457	22135.470
	(0.007)	(2.136)	(0.002)	(0.002)	(0.001)	
USDCHF	-0.524	1.438e-12	0.946	1.553e-06	-131.019	20008.023
	(0.005)	(3.111)	(0.002)	(0.001)	(0.001)	
USDJPY	0.355	2.089e-11	0.939	2.239e-06	72.872	20239.174
	(0.005)	(0.881)	(0.002)	(0.002)	(0.001)	

Notes: Parameter estimates for the spot exchange rate process: $R(t+\eta) = r_d - r_f - \frac{1}{2}h_s(t+\eta) + \sqrt{h_s(t+\eta)}z^*(t+\eta)$ with spot variance $h_s(t+\eta) = \omega_s + \beta_s h_s(t) + \alpha_s(z^*(t) - \gamma_s^*\sqrt{h_s(t)})^2$. This table reports the parameter estimates as a standard Heston Nandi model via MLE for each currency pair; the final column reports the estimated log-likelihood at the optimum.

process parameters of HN model. Table 4.3 and Table 4.4 present the parameters estimated for MFJ model with fixed daily time-step and the adjusted time-step MFJ-F model, respectively. Here I do not estimate interest factor parameters and use only the restricted version of the MFJ model with constant drift terms. This is because the main purpose of studying the interest bias assume that the stochastic interest factor are hidden from observation.

4.5.2 Empirical results

Compared with the fixed time-step HN model in Fig. 4.1 (The root mean squared error (RMSE) for 2Y $\widetilde{AT}$ being 2.741), the following figure Fig. 4.2 shows that the MFJ-F model with maturity adjusted time-step size preserves some level of

Table 4.3: MFJ parameter estimation

	AUD	EUR	GBP	CAD	CHF	JPY
ζ_s	0.650	-0.634	-0.553	-0.401	1.270	3.024
ζ_J	7.335e-5	2.940e-7	3.826e-7	3.505e-8	3.812e-7	5.490e-4
ω_s	1.952e-11	5.199e-10	1.144e-11	8.276e-13	1.260e-11	2.517e-10
β_s	0.951	0.977	0.965	0.963	0.966	0.931
α_s	1.827e-6	8.288e-7	8.676e-7	7.724e-7	1.177e-6	2.166e-6
γ_s	81.765	1.179	76.306	-50.438	68.003	87.440
ω_J	0.072	0.078	0.080	0.082	0.061	0.084
β_J	0.022	0.021	0.022	3.747e-6	0.038	0.045
α_J	0.834	0.876	0.731	0.917	0.955	0.245
μ_J	3.778e-5	2.459e-5	1.362e-5	-1.266e-5	-3.301e-5	5.60484e-6
σ_J	1.178e-3	1.031e-3	8.799e-4	9.414e-4	2.305e-3	1.231e-3
$\mathcal{L}$	18161.630	16785.240	19462.640	20250.288	18770.097	18174.350

Notes: Parameter estimates for the MFJ model via MLE for each currency pair. The spot exchange rate log-return process is described by $R(t+\eta) = r_d - r_f - \frac{1}{2}h(t+\eta) - (e^{\mu_J+\frac{1}{2}\sigma_J^2} - 1)\lambda^*(t+\eta) + \sqrt{h(t+\eta)}z^*(t+\eta) + \sum_{j=0}^{N^*(t+\eta)} u_j(t+\eta)$, the spot variance is $h(t+\eta) = \omega_s + \beta_s h(t) + \alpha_s(z^*(t) - \gamma_s^*\sqrt{h(t)})^2$ and the jump intensity is $\lambda^*(t+\eta) = \omega_J^* + \beta_J\lambda^*(t) + \alpha_J N^*(t)$. Notice that here I just use the restricted model with constant interest rates because I assume observed interest rates are constant and the stochastic parts come from latent factors. The final row reports the estimated log-likelihood at the optimum.

fluctuation and level of accuracy of its implied volatility even when tenor increases to 2Y (RMSE decreasing to only 0.906).

By adjusting the time-step size, variance process $h(t)$ is changed accordingly. I present EURUSD's $h(t)$ from different time-step size time series in the upper panel of Fig. 4.3. As the tenor grows, the size of time-step grows linearly by the adjustment rule $\eta_\tau = \frac{\tau}{1M}\mathbf{1}$ and $h(t)$ increase its scale in a similar manner. It is reasonable since for a Brownian motion $W_t \sim \mathcal{N}(0,t)$, we should have $W_{nt} \sim \mathcal{N}(0,nt)$. For the 2Y tenor case (the lightest line in the plot), the MFJ-F model is built on a variance process that is much larger in scale (about $\times 24$) compared

Table 4.4: MFJ-F parameter estimation

	AUDUSD				EURUSD			
	1M	6M	1Y	2Y	1M	6M	1Y	2Y
ζ_s	0.65	2.733	2.285	1.883	-0.634	-0.882	0.813	1.204
ζ_J	7.34E-05	8.29E-04	5.71E-04	0.001	2.94E-07	5.78E-10	0.001	2.07E-07
ω_s	1.95E-11	3.52E-06	2.63E-05	2.25E-10	5.20E-10	5.69E-13	4.41E-11	9.39E-07
β_s	0.951	0.916	0.778	0.889	0.977	0.932	0.893	0.866
α_s	1.83E-06	1.93E-05	6.81E-05	1.14E-04	8.29E-07	1.09E-05	2.63E-05	7.21E-05
γ_s	81.765	13.171	27.958	-4.4	1.179	25.233	38.091	17.864
ω_J	0.072	0.234	0.233	0.222	0.078	0.199	0.26	0.31
β_J	0.022	2.61E-05	0.053	0.104	0.021	0.036	3.94E-07	2.03E-05
α_J	0.834	0.234	0.931	5.26E-05	0.876	0.955	0.027	0.352
μ_J	3.78E-05	1.53E-04	-2.63E-04	-6.11E-04	2.46E-05	8.10E-05	.2.720e-4	-3.60E-04
σ_J	0.001	0.005	0.007	0.011	0.001	0.004	0.007	0.011
$\mathcal{L}$	18161.63	1804.823	676.947	212.282	16785.24	1773.036	679.205	237.241

	GBPUSD				USDCAD			
	1M	6M	1Y	2Y	1M	6M	1Y	2Y
ζ_s	-0.553	0.887	-0.506	0.211	-0.401	2.676	-0.068	2.312
ζ_J	3.83E-07	3.65E-08	8.51E-11	8.14E-04	3.51E-08	4.94E-04	1.55E-07	4.95E-08
ω_s	1.14E-11	1.57E-10	1.89E-04	9.42E-05	8.28E-13	2.15E-11	5.98E-10	1.05E-04
β_s	0.965	0.925	0.12	0.171	0.963	0.912	0.85	0.502
α_s	8.68E-07	1.04E-05	7.44E-05	1.04E-05	7.72E-07	1.16E-05	3.46E-05	1.69E-04
γ_s	76.306	30.858	12.297	251.815	-50.438	2.991	19.122	1.032
ω_J	0.078	0.17	0.24	0.303	0.082	0.146	0.178	0.257
β_J	0.022	0.038	0.006	0.018	3.75E-06	0.088	0.068	0.008
α_J	0.731	0.008	5.85E-05	0.315	0.917	0.002	0.003	0.019
μ_J	1.36E-05	-1.54E-04	1.07E-04	2.93E-04	-1.27E-05	-1.21E-04	6.48E-05	-7.28E-04
σ_J	8.80E-04	0.003	0.005	0.01	9.41E-04	0.003	0.004	0.008
$\mathcal{L}$	19462.64	2127.967	832.471	192.479	20250.29	2259.113	938.224	219.833

	USDCHF				USDJPY			
	1M	6M	1Y	2Y	1M	6M	1Y	2Y
ζ_s	1.27	1.851	0.472	1.135	3.024	0.732	0.597	1.355
ζ_J	3.81E-07	3.26E-08	1.29E-07	6.07E-08	5.49	2.47E-06	1.75E-10	9.63E-10
ω_s	1.26E-11	1.68E-09	1.15E-05	1.25E-05	2.52E-10	2.03E-06	3.82E-06	1.11E-04
β_s	0.966	0.955	0.912	0.931	0.931	0.881	0.87	0.742
α_s	1.18E-06	8.28E-06	2.20E-05	4.22E-05	2.17E-06	2.63E-05	5.40E-05	4.26E-06
γ_s	68.003	-24.654	-7.753	1.997	87.44	1.481	1.8	149.687
ω_J	0.061	0.188	0.239	0.229	0.084	0.201	0.281	0.307
β_J	0.038	0.022	0.038	0.056	0.045	0.037	0.015	0.007
α_J	0.955	7.38E-03	0.95	6.28E-04	0.245	0.17	2.17E-05	0.99
μ_J	-3.30E-05	-3.00E-04	-5.07E-05	-0.001	5.61E-06	-2.10E-04	-2.85E-04	1.90E-06
σ_J	0.002	6.77E-04	0.01	0.018	0.001	0.004	0.007	0.011
$\mathcal{L}$	18770.1	1963.499	742.358	136.942	18174.35	1849.138	694.342	234.81

Notes: Following the time-step adjustment rule, $\eta_\tau = \frac{\tau}{1M}\mathbf{1}$, I estimate the parameters for the MFJ-F model and list the parameters in this table.

with the one used in HN model, which is the wider line at the bottom.

In the lower panel of Fig. 4.3, I present the EURUSD's realised jumps for

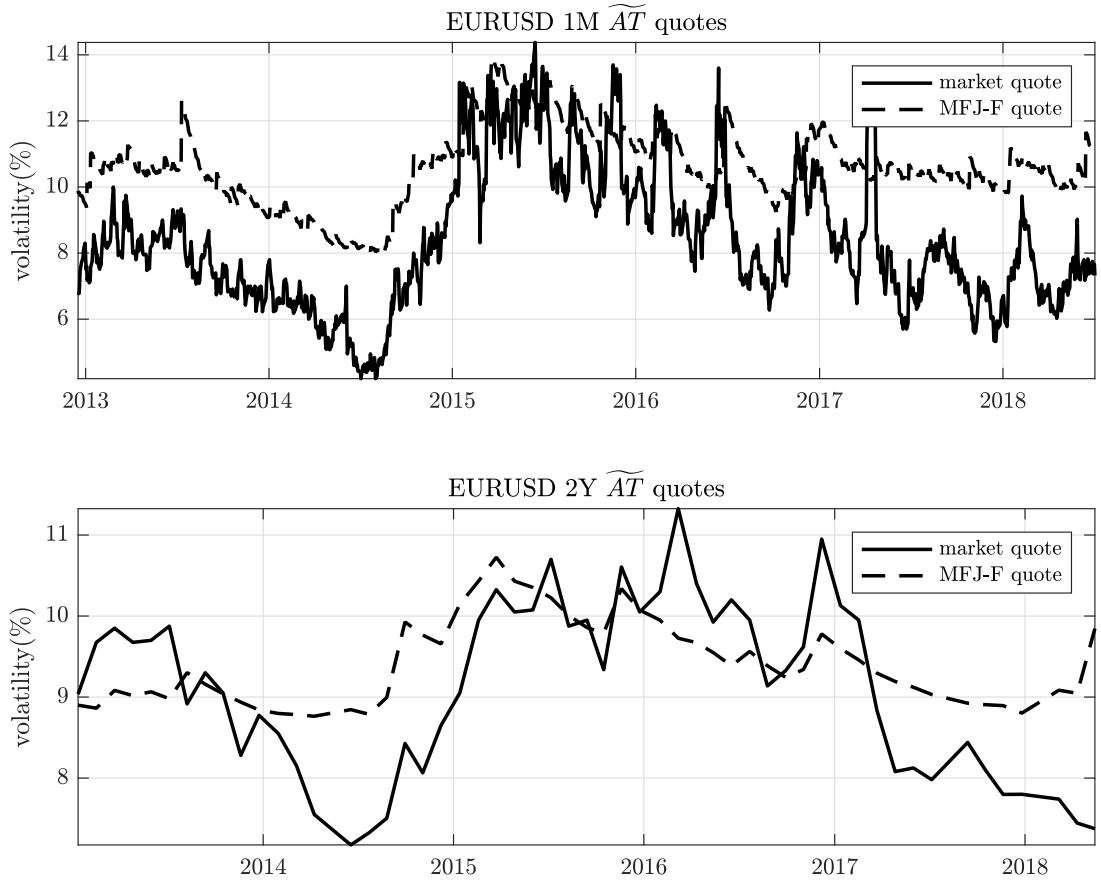

Figure 4.2: $\widetilde{AT}$ market quotes and MFJ-F model implied volatility for EURUSD options with 1M and 2Y tenors.

This figure illustrates the 1M and 2Y $\widetilde{AT}$ quoted by MFJ-F model and the corresponding market quotes. Here solid lines represent market quotes and dash lines are MFJ-F model quotes.

different tenor contracts based on the jump detection method in Tauchen and Zhou [2011] and Section 4.3.1 on different time-step size return processes for the MFJ-F model. From the plot we can observe some jump-clustering property, and the realized jump size tends to be bigger as the time-step size increases. I should note that during the process of generating realized jumps, some short term jumps may be neglected because of the relatively large time-step of data sampling.

Following the Eq. (4.21) to calibrate the hidden factors, I then include the

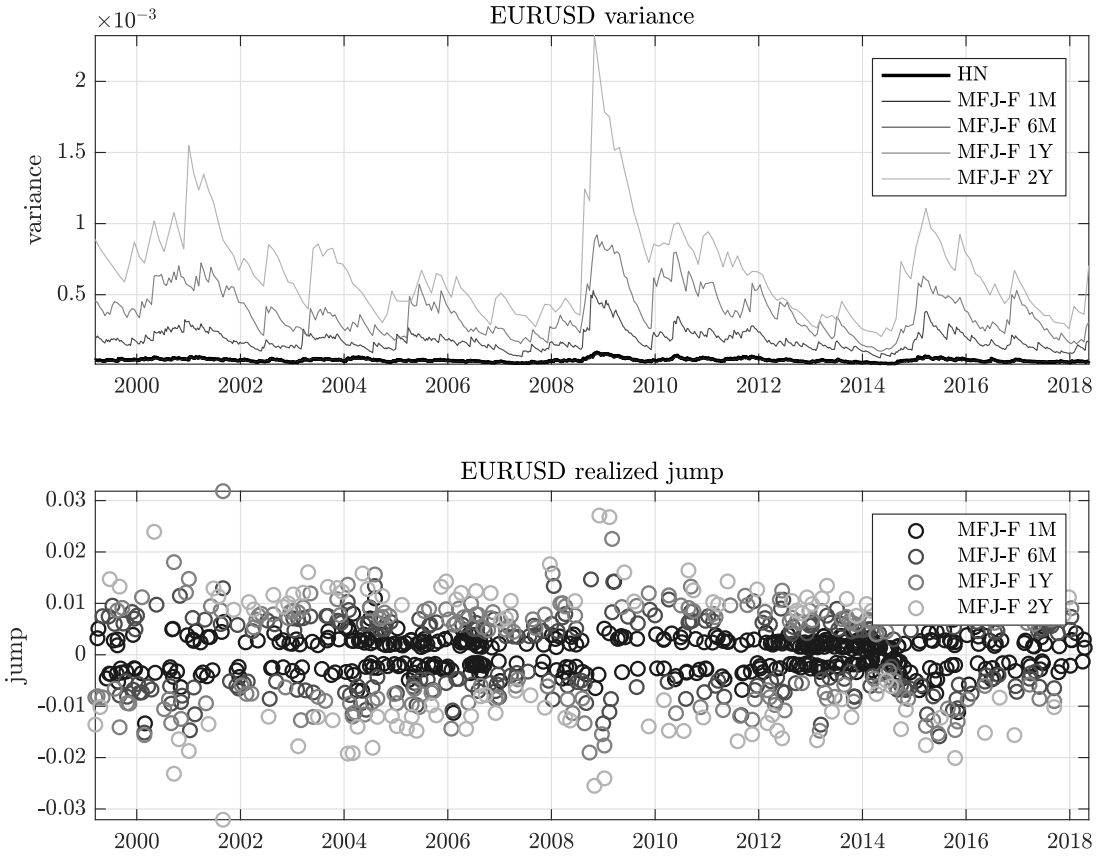

Figure 4.3: The time-series of variance process $h(t)$ and realised jumps with different time-step size.
The time-series of EURUSD's variance process $h(t)$ with different time-step size are shown in the upper panel. Lighter lines represents larger tenor and time-step size. In the lower panel, I plot the realised jumps from different time-step size time series, based on the jump detection method in Section 4.3.1.

hidden factors into the MFJ-C model, which yields a more accurate volatility smile as in Fig. 4.4. The time-series well presents the improvement of the accuracy of the MFJ-C model and the effectiveness of the hidden factors, with the RMSE being only 0.545 (one fourth of the RMSE for HN).

I then collect the implied volatility quotation error for options with 2Y tenor, which losses the most time series dynamic, based on the selected models (HN, MFJ-F and MFJ-C). The results are plotted in Fig. 4.5. The error here is absolute

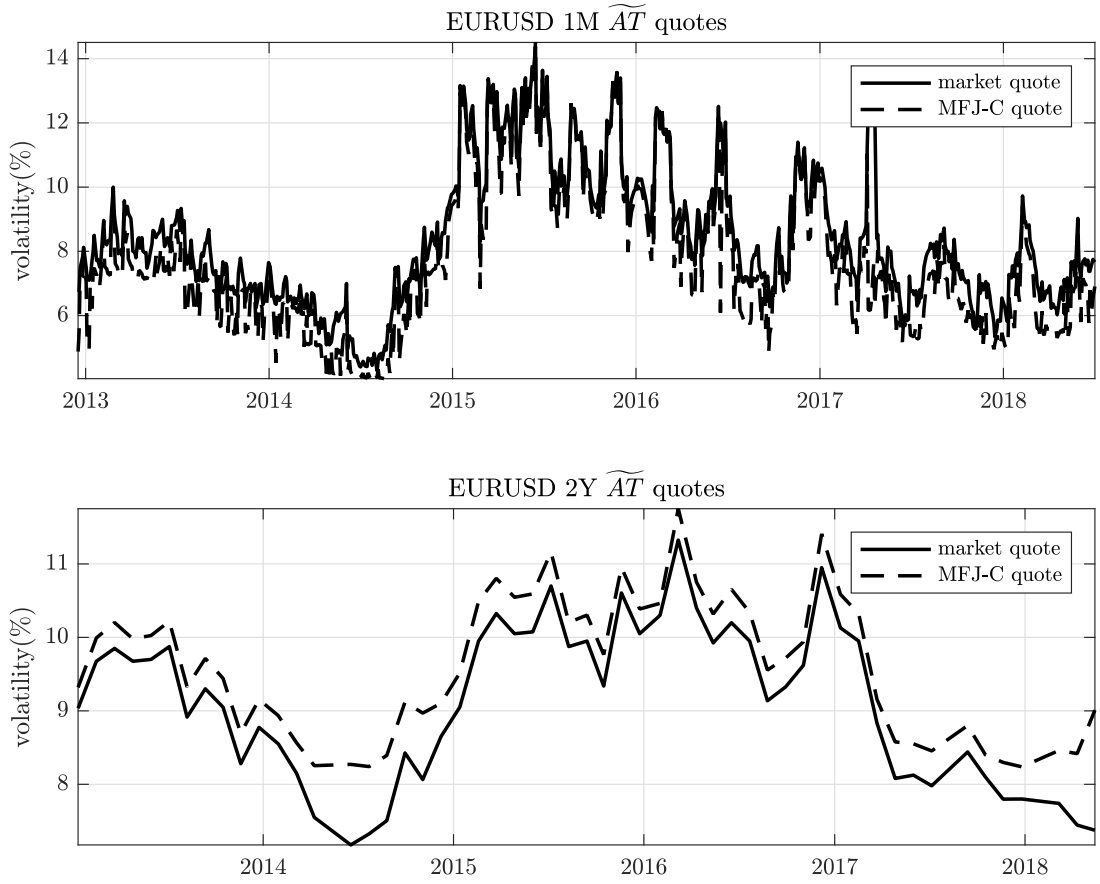

Figure 4.4: $\widetilde{AT}$ market quotes and MFJ-C model implied volatility for EURUSD options with 1M and 2Y tenors.
From the figure we can see that including the hidden factors based on the calibration can improve the accuracy of the volatility smile, compared with HN model in Fig. 4.1 and MFJ-F model in Fig. 4.2.

error as percentage of the market quotes. In this figure, black square marks, representing errors for MFJ-C, are more concentrated at lower level across all the six currency pairs. Among these, MFJ-C works best for the volatility smile of GBPUSD (the lowest RMSE, 0.399) and also for EURUSD (0.545) and USDJPY (0.434). It suggests that GPBUSD's market option quotes are more affected by the latent factors in the interest rate. MFJ-C and MFJ-F both outperform HN for the 2Y tenor contracts.

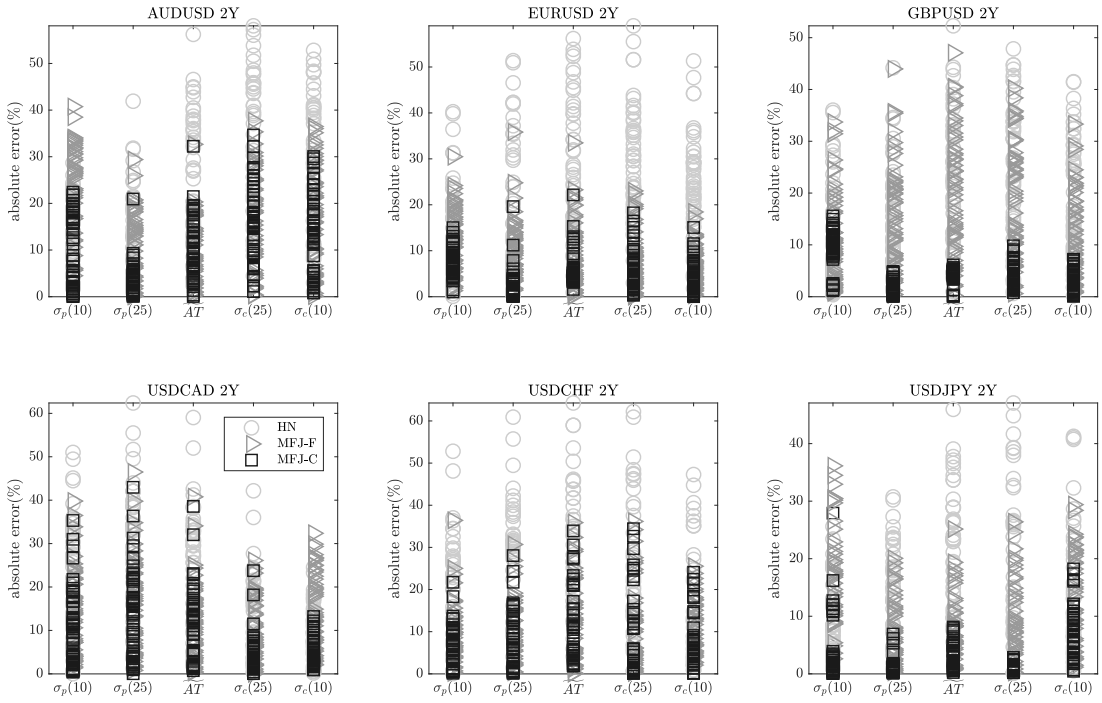

Figure 4.5: Absolute error as a percentage of the market quote among HN, MFJ-F and MFJ-C models
In the figure, I calculate the absolute percentage error of different models compared with the market option quotes. Black square marks, representing errors for MFJ-C, are more concentrated at lower level across all the six currency pairs, especially for GBPUSD. MFJ-C and MFJ-F (triangle marks) both outperform HN (circle marks) for the 2Y tenor volatility smiles.

Further more, I calibrated the hidden factor parameters for tenors from 1M to 2Y across all the six currency pairs, and record the mean value of them in Table 4.5. Based on the hidden factors I quote the HN, MFJ-F and MFJ-C implied option volatility smiles and compared with market quotes. RMSE for each model is shown in Table 4.6, Table 4.7 and Table 4.8.

From Table 4.5 we can see that the hidden factors in the interest return all have large autoregressive parameter $\beta_{d/f}$ (from 0.9418 to 0.9994), which means these hidden factors have dynamic that are very persistent through out of the life circle before option maturity. On the other hand, $\alpha_{d/f}$ shows that these hidden

Table 4.5: Calibrated MFJ-C hidden factor parameters (mean value)

	AUDUSD				EURUSD			
	1M	6M	1Y	2Y	1M	6M	1Y	2Y
f_d	0.005053	0.05758	0.009267	0.005832	0.002038	0.06181	-0.00549	-0.00205
f_f	0.005832	0.05748	0.005788	-0.00459	0.001273	0.06143	-0.0054	-0.00361
ω_d	3.71E-07	2.51E-06	1.06E-07	1.87E-07	4.83E-08	3.08E-06	1.94E-07	1.66E-07
β_d	0.9927	0.9941	0.998	0.9988	0.9985	0.9878	0.9992	0.9932
α_d	3.18E-05	6.97E-05	-6.81E-05	-3.06E-05	1.79E-05	6.24E-05	9.63E-05	2.34E-05
σ_d	2.45E-08	2.93E-07	6.75E-08	4.08E-08	1.06E-08	3.01E-07	1.23E-08	6.35E-08
ω_f	2.78E-07	2.36E-06	6.29E-07	5.92E-07	5.40E-08	2.67E-06	1.52E-07	5.83E-07
β_f	0.9912	0.9803	0.9953	0.9988	0.9959	0.9815	0.9988	0.9933
α_f	-3.05E-05	-6.85E-05	7.16E-05	2.90E-05	-8.76E-06	-4.71E-05	-9.01E-05	3.80E-06
σ_f	3.14E-08	3.11E-07	4.65E-08	5.58E-08	5.14E-09	2.63E-07	2.16E-08	3.54E-08

	GBPUSD				USDCAD			
	1M	6M	1Y	2Y	1M	6M	1Y	2Y
f_d	0.002244	0.06559	0.00412	0.003647	-5.73E-05	0.06397	-0.00332	-0.00225
f_f	0.002699	0.06625	-0.00429	0.008103	0.000252	0.06797	-0.00139	0.004254
ω_d	3.13E-07	2.52E-06	1.00E-07	1.00E-06	1.24E-07	3.18E-06	1.72E-07	2.20E-07
β_d	0.9896	0.9946	0.9993	0.9532	0.9901	0.9953	0.9994	0.999
α_d	2.58E-05	5.63E-05	7.44E-05	-3.64E-05	-9.73E-06	9.53E-05	4.90E-05	5.54E-05
σ_d	2.83E-08	1.64E-07	5.48E-09	7.06E-08	2.03E-08	3.44E-07	2.14E-08	7.14E-09
ω_f	3.50E-07	1.86E-06	1.17E-07	5.47E-07	2.10E-07	2.85E-06	9.38E-08	1.25E-07
β_f	0.987	0.991	0.9989	0.9418	0.9879	0.9905	0.9995	0.9992
α_f	-2.45E-05	-4.67E-05	-7.32E-05	-3.63E-05	1.21E-05	-9.62E-05	-4.61E-05	-5.58E-05
σ_f	3.32E-08	2.15E-07	7.91E-09	8.70E-08	1.52E-08	3.43E-07	2.11E-08	2.78E-08

	USDCHF				USDJPY			
	1M	6M	1Y	2Y	1M	6M	1Y	2Y
f_d	-0.00348	0.03865	-0.00012	-0.00326	-0.00562	0.07759	-0.00093	0.006027
f_f	-0.00202	0.03668	0.002485	-0.00359	-0.00369	0.08343	-0.00367	-0.00623
ω_d	1.86E-07	8.72E-07	1.19E-07	1.04E-07	8.85E-07	4.17E-06	2.89E-07	1.35E-07
β_d	0.9951	0.9871	0.9963	0.9984	0.9835	0.9947	0.9994	0.9937
α_d	2.10E-05	4.77E-05	-6.73E-05	5.71E-05	3.68E-05	3.29E-05	4.57E-05	1.25E-05
σ_d	1.84E-08	1.07E-07	1.72E-08	7.50E-09	9.07E-08	4.54E-07	2.97E-08	1.05E-08
ω_f	1.87E-07	7.15E-07	9.35E-08	8.56E-08	8.12E-07	4.34E-06	3.65E-07	2.31E-07
β_f	0.993	0.9891	0.9992	0.9994	0.9786	0.986	0.9981	0.9939
α_f	-2.25E-05	-6.57E-05	5.86E-05	-5.73E-05	-3.26E-05	-3.00E-05	-5.14E-05	3.71E-06
σ_f	2.07E-08	7.84E-08	1.65E-08	9.06E-09	8.47E-08	4.62E-07	3.43E-08	1.79E-08

Notes: To fit the market quotations of volatility surfaces, I assume there exist one unobservable domestic factor and one foreign factor hidden in the drift dynamics. These laten factors are calibrated under the MFJ-C setting. The estimated parameters' mean value for these factors are listed here.

factors do have certain correlation with the variance process $h(t)$. Notice that α_d and α_f tend to have opposite signs and similar magnitude, for example in AUDUSD 1M α_d is 3.18e-5 and α_f is -3.05e-5. Notice that it is f_d and $-f_f$ that

Table 4.6: RMSE for HM model

		$\sigma_p(10)$	$\sigma_p(25)$	$\widetilde{AT}$	$\sigma_c(25)$	$\sigma_c(10)$
AUDUSD	1M	2.627	2.814	3.034	2.934	2.777
	6M	2.056	2.590	3.370	3.615	3.362
	1Y	2.060	2.016	3.044	3.457	3.140
	2Y	2.615	1.704	2.778	3.332	3.050
EURUSD	1M	2.244	2.376	2.583	2.619	2.539
	6M	2.132	2.475	2.896	2.884	2.563
	1Y	1.842	2.227	2.773	2.877	2.513
	2Y	1.591	1.926	2.471	2.550	2.175
GBPUSD	1M	3.182	2.926	2.741	2.191	1.993
	6M	2.648	2.195	2.258	2.274	2.030
	1Y	2.591	1.864	1.910	1.932	1.603
	2Y	2.084	1.693	2.054	2.159	1.809
USDCAD	1M	1.337	1.375	1.329	1.217	1.214
	6M	1.497	1.622	1.494	1.262	1.465
	1Y	1.472	1.573	1.365	1.168	1.789
	2Y	1.903	2.205	2.010	1.418	1.284
USDCHF	1M	2.879	2.953	2.910	2.553	2.192
	6M	2.889	3.265	3.404	3.043	2.489
	1Y	2.714	3.148	3.248	2.729	2.008
	2Y	2.295	2.785	2.988	2.580	1.858
USDJPY	1M	2.438	2.427	2.438	2.070	1.912
	6M	2.159	2.402	2.690	2.473	2.138
	1Y	1.816	2.032	2.515	2.292	1.910
	2Y	1.977	1.569	2.106	1.935	1.686

Notes: I list the RMSE for HM model compared the the market quotes in this table. RMSE is calculated by $\sqrt{\frac{\sum(HM-MKT)^2}{n}}$, where n is the number of observations.

appear in the return process, thus the correlated shocks in both interest rates merge into the return process.

The RMSE listed in Table 4.6, Table 4.7 and Table 4.8 show the performance improvement of MFJ-C compared with HN model, that MFJ-C has RMSE being about one third of the HN's RMSE for all of the currency pairs and maturities (take $\widetilde{AT}$ of GBPUSD 2Y as an example, HN is 2.054 and MFJ-C is 0.399). On the other hand, MFJ-F has better performance for longer maturities compared

Table 4.7: RMSE for MFJ-F

		$\sigma_p(10)$	$\sigma_p(25)$	$\widetilde{AT}$	$\sigma_c(25)$	$\sigma_c(10)$
AUDUSD	1M	2.780	2.993	3.235	3.146	2.995
	6M	1.990	1.954	2.668	3.065	3.037
	1Y	6.338	4.772	4.033	4.382	5.649
	2Y	4.322	1.910	1.207	1.786	1.957
EURUSD	1M	2.245	2.376	2.584	2.619	2.539
	6M	1.583	1.382	1.535	1.520	1.334
	1Y	1.636	1.954	2.255	2.159	1.711
	2Y	1.723	1.127	0.906	0.782	0.763
GBPUSD	1M	3.182	2.926	2.741	2.192	1.995
	6M	2.390	1.882	1.755	1.635	1.375
	1Y	3.104	2.026	1.660	1.591	1.377
	2Y	1.814	1.690	1.872	1.710	1.222
USDCAD	1M	1.337	1.375	1.329	1.216	1.214
	6M	1.363	1.325	1.138	1.171	1.675
	1Y	1.546	1.407	1.130	1.389	2.307
	2Y	1.316	1.390	1.176	1.240	2.098
USDCHF	1M	2.837	2.914	2.871	2.514	2.154
	6M	2.403	2.584	2.625	2.281	1.984
	1Y	1.611	1.524	1.678	1.573	1.561
	2Y	1.545	1.277	1.360	1.278	1.382
USDJPY	1M	4.028	4.292	4.502	4.065	3.743
	6M	1.802	1.709	2.072	2.151	2.072
	1Y	2.020	1.226	1.470	1.521	1.548
	2Y	3.352	1.634	1.205	1.415	2.284

Notes: I list the RMSE for MFJ-F model compared the the market quotes in this table. RMSE is calculated by $\sqrt{\frac{\sum(MFJ-MKT)^2}{n}}$, where n is the number of observations.

with HN, which benefits from the adjustment of the time-step size (RMSE for GBPUSD 2Y $\widetilde{AT}$ is 1.872). I should note that among these five FX option quotes, $\widetilde{AT}$ is the most important indicator, since it determines the fundamental volatility level, while the other four moneyness points are the relative volatilities affecting the shape of the volatility smile at the out-of-the-money reign. Because the deeply out-of-the-money part of the smile is harder to model and may contains other information, the RMSE for $\sigma_{c/p}(10)$ is higher than that for $\widetilde{AT}$, for example

Table 4.8: RMSE for MFJ-C

		$\sigma_p(10)$	$\sigma_p(25)$	$\widetilde{AT}$	$\sigma_c(25)$	$\sigma_c(10)$
AUDUSD	1M	1.153	0.544	0.723	2.376	2.511
	6M	1.722	1.779	1.094	1.504	2.557
	1Y	1.079	0.194	0.802	0.821	0.902
	2Y	1.894	0.523	1.220	1.676	1.485
EURUSD	1M	1.714	1.800	0.997	1.259	1.998
	6M	1.107	0.861	0.502	1.079	1.003
	1Y	1.175	0.763	1.104	1.227	0.984
	2Y	0.956	0.329	0.545	0.558	0.477
GBPUSD	1M	0.816	0.523	1.611	1.604	1.649
	6M	1.148	0.604	0.527	1.008	0.889
	1Y	0.412	0.593	0.962	1.082	0.890
	2Y	1.219	0.222	0.399	0.390	0.304
USDCAD	1M	1.031	0.884	0.342	0.455	0.468
	6M	1.124	1.093	0.501	0.413	0.701
	1Y	0.996	0.951	0.663	0.630	1.482
	2Y	1.006	1.168	0.968	0.474	0.647
USDCHF	1M	1.307	0.647	0.816	2.245	2.106
	6M	0.796	0.555	0.319	0.506	0.977
	1Y	1.083	1.215	1.429	1.236	1.008
	2Y	0.878	0.938	1.222	1.112	0.932
USDJPY	1M	2.063	1.403	0.911	2.896	3.017
	6M	1.742	1.771	0.747	1.500	1.737
	1Y	1.193	0.924	1.461	1.417	1.312
	2Y	0.602	0.273	0.434	0.167	1.108

Notes: I list the RMSE for MFJ-C model compared the the market quotes in this table. RMSE is calculated by $\sqrt{\frac{\sum(MFJ-MKT)^2}{n}}$, where n is the number of observations.

the MFJ-C model for USDCAD 6M has $\sigma_p(10)$ being 1.124 and $\widetilde{AT}$ being 0.501.

Compared with the ASV-C (average RMSE 0.867) in Chapter 3, the MFJ-C (average RMSE 0.846) model has similar performance. These two model both use the market option quotes to calibrate the parameters but emphasis on different aspects. ASV-C focus on the adjustment of the variance process dynamic and MFJ-C tries to find the hidden interest rate factors that affecting the return dynamic. These observations confirm the argument that the violation of covered

interest parity of the market contributes to the OTC FX option pricing.

4.6 Chapter conclusions

To sum up, in this chapter I specify a new discrete-time model for pricing over-the-counter foreign exchange options with ACP jumps in the return process and multiple stochastic interest factors for domestic and foreign interest rates. Restricting the multi-factor dynamic yields an FX version of the classic Heston and Nandi [2000] GARCH-type model plus an extra jump component in discrete-time. The introduction of multiple interest rate factors help handle the dynamic in the observed market yield data, and can be applied to extract the hidden factors from the market FX option data. The jump component in the model can be estimated non-parametrically from a filtered realised jump process.

I further test the various model specifications and compute the model implied FX option quotes for six actively traded currency pairs over tenors from 1M up-to 2Y. To deal with the over-reverting property of the variance process, I propose to adjust the time-step size according to the tenor of the option.

From the empirical test, I find that applying time-step adjustments help preserve the model implied volatility time series dynamic, which improves the model performance especially for longer tenor options. Then I assume there exist a hidden factor in each of the domestic and foreign drifts, and calibrate the model against market quoted volatility smile to recover the parameters describing these latent factors. The model including these unobservable factors performs well compared with its alternatives for all the option contracts. Theses factors have strong persistence in dynamic and have certain correlation with the spot variance

process. One obvious area to extend my approach is to further generalise the model specification to allow more flexible state variables' correlation structure and more general jumps. Also it is worth to identify the factors and channels explaining such hidden drift terms in future works.

Chapter 5

Pricing Options with Pegged Foreign Exchange Rates

5.1 The problem of pegged FX rates

The preceding chapters focus on cases when the currency is either in a free or partially free float. That is there are no interventions in the currency market to maintain the price of a specific currency relative to a benchmark such as the US dollar. A large number of currencies are however pegged, either by a de-facto or hard peg imposed by the central bank controlling that currency or a de-jour or soft peg, where there are restrictions that amount to a peg and the central bank intervenes to maintain a price band.

Pegged currency pairs account for the major proportion of this less traded category. IMF [2016] reports that by 2016, countries with soft pegs are still the single largest exchange rate arrangement category accounting for 39.6% of all members, compared with 37% members belonging to floating arrangement

category. Ilzetzki et al. [2017] also provide a comprehensive study of the exchange arrangements for 194 countries showing similar statistic.

Currently FX option market for pegged currency pairs barely exist. It is reasonable under normal market condition, considering that the FX rate of such type at expiry is expected to remain the same value with great confidence. Thus there is little demand to trade options on this currency pair. However under some extreme condition such as asset price shocks, or productivity shocks mentioned in Nakatani [2017] for instance, the country authority may abandon the existing pegged currency regime and switch to other exchange rate arrangements, or the currency may be traded with a premium because of liquidity or trading friction issue. Goldberg [2017] provides a literature review on the de-peg event prediction, Guimaraes [2008], Codogno and de Grauwe [2015] and Li [2017] discuss the criteria and probability of certain authorities changing their exchange rate arrangements. From this point, even though there are literature providing risk management techniques such as Lustig and Verdelhan [2007], Reus and Mulvey [2016] and López-Suárez and Razo-Garcia [2017], it is still a big research gap to develop option pricing approaches to hedge the future realignment risk and trading friction risk of these currencies.

Application of econometric models to historical spot prices for pegged currencies is inappropriate. Hence an alternative strategy is needed that collects available information from market prices of various traded contracts to extract the probability structure for any currency realignment through peg breaks or changes in banding limits.

In this chapter, I fill this gap by designing a simple but effective option pricing model under the affine-jump-diffusion (AJD) model family to model a synthetic

spot FX rate, and proposing a corresponding parameter estimation approach given the absence of option market. Using some simple limits to arbitrage restrictions I then derive the closed form solution for a European options contract on the pegged currency pairs. In the empirical part, I test the proposed approach on four classic pegged currency pairs using simulation analysis and calculate their volatility surfaces based on the estimated parameters. Results show the new approach can capture the uncertainty information and provide reasonable option price quotes.

In the work of Lin et al. [2015], a regime switching model with jump shocks is proposed to price foreign exchange option. However this model has constant volatility and fixed parameters estimated from the historical spot FX rate, which is not consistent with the heteroskedasticity character of FX rates and is not suitable for pegged currency pairs. My idea is inspired by Yu [2007], who argues that for a controlled currency, the forward FX rate no longer align with the normal theoretical risk neutral expectation, and uses a stochastic intensity jump model to predict the probability of Chinese yuan's (CNY) realignment, or de-peg event. Yu [2007] documents the mismatch between the Chinese non-deliverable forward rate and covered interest parity implied rate before CNY de-peg with USD, and modelled this phenomenon with a pure jump process with a stochastic up/down jump intensity that follows a Levy process. Yu [2007] shows that the model implied policy realignment distribution responds quickly to the news on the China-US trade.

Forward transaction is available for most of the currencies. Evidences of the forward prices violating interest parity are documented by Hansen and Hodrick [1980], and then studies in detail as forward premium puzzle by Fama [1984],

Bansal [1997], Londono and Zhou [2017] and especially Du et al. [2018], where they provide evidence that all G10 currencies systematically violate covered interest parity after the financial crisis. I make similar argument that for these managed currencies, the existence of trading friction and de-peg risk leads to a market with arbitrage opportunity and implies a synthetic spot FX rate align with the market forward price. And since the model is based on the information of forward market, it naturally contains market's outlook of the future, which surpasses the models that use parameter estimated on historical price information.

AJD type models, including the affine-diffusion models (AD), have been popular and effective for asset pricing since the short rate models of Vasicek [1977] and Cox et al. [1985], and later on the applications in option pricing such as Heston [1993]. Garman and Kohlhagen [1983] specify the model and risk neutral measure to FX option pricing. Hagan et al. [2002]'s SABR model extends the idea to be more suitable for building implied volatility surface. In Duffie et al. [2000]'s work, the general closed-form solution of AJD for option pricing is given, and Pan [2002] applies that to a double jump model and studies the jump-risk premium implicit in S&P 500 index. Da Fonseca et al. [2007] also propose a multi-asset based option pricing model with stochastic correlation.

Estimation of the AJD model parameters is problematic as there are a number of latent, unobserved processes that require parameterisation. This problem is not new and has drawn considerable attention in the extent literature. Given the observable state variables, Yu [2007], Ait-Sahalia et al. [2008], Li et al. [2013] and Li and Chen [2016] derive closed-form (or approximation) likelihood function for AJD model and used maximum likelihood estimation (MLE) or quasi maximum

likelihood estimation to estimate the parameters. Conley et al. [1995], Duffie and Glynn [2004] and Carrasco et al. [2007] propose generalised method of moments type methods. Characteristic function based estimation can be found in Singleton [2001], Jiang and Knight [2002], Da Fonseca et al. [2014] and Carrasco and Kotchoni [2017]. Beside the parametric estimations above, there are also non-parametric estimation techniques suggested by Bandi and Phillips [2003], Zhao and Wu [2009], Bull et al. [2016] and Gourieroux et al. [2017]. There are also more general Levy process estimation techniques such as Jacod et al. [2018], but I will not extend to that in this chapter.

The estimation for process with latent or unobservable state variables, such as the volatility in the stochastic volatility models, is studied in Pan [2002], Aït-Sahalia et al. [2015] and Andersen et al. [2015]. These methods require supplementary information such as derivatives prices. Then the derivatives prices can be converted into information equivalent to unobservable state variables and then techniques above for observable state variables can be used. Other approaches includes simulation of likelihood, efficient method of moments, indirect inference, Markov Chain Monte Carlo or Bayesian estimation, which can be found in Brandt and Santa-Clara [2002], Gallant and Tauchen [1996], Gourieroux and Monfort [1993], Elerian et al. [2001], Andersen et al. [2002], Särkkä et al. [2015], Hurn et al. [2013] and Creel and Kristensen [2015].

By studying the characters of the pegged currencies, I argue that market quoted forward FX rates for the pegged currencies reflect not only the normal risk neutral expectation of the observed pegged spot FX rate, but also market participants' bets[1] on the currency regime rearrangement and trading friction

[1]Such as the betting information in Hanke et al. [2018].

situation in the future. The difference between market quoted forward and theoretical forward is systematically existing and informative of uncertainty outlook, at least in the four currency pairs selected in this chapter. And this leads to a synthetic spot FX rate different from the observed pegged FX rate and gives rise to the adjusted risk neutral measure $\mathbb{Q}$ as proposed in this chapter. I then price the option based on the dynamic of the synthetic spot rate. I also follow the FX option market convention to quote the option in terms of volatility surface.

This chapter is organised as follows. Section 5.2 introduces the synthetic spot FX rate and spot rate bias process. Section 5.3 provides parameter estimation using approximate likelihood based on the segments of the forward information. Section 5.4 describes the data used for empirical study. Then I estimate parameters and simulate forward FX rate based on the proposed model. I present the option pricing model in Section 5.5 and calculate the volatility surfaces following the FX option market convention. Section 5.7 concludes the this chapter.

5.2 The synthetic spot FX rate model

Assuming the filtered probability space $(\Omega, \mathcal{F}, (\mathcal{F}_t)_{t\geqslant 0}, \mathbb{P})$ satisfies the usual conditions (i.e. Protter [2004]), I denote the pegged FX rate as S_t, domestic and foreign interest rates as r_t and q_t respectively. I will make the following assumption on the pegged spot FX rate which helps us focus on the trading and realignment uncertainties in later derivations.

Assumption 11. *Trading and realignment uncertainties are the only sources of pegged currency pairs' spot FX rate risks. Without these two types of uncertainty, the pegged FX rate is then believed to follow a risk neutral process before the future*

time T. Then any domestic investor holding one unit of foreign currency in the money account should expect the future exchange rate to follow:

$$S_t e^{\int_t^T r_\tau - q_\tau d\tau}.$$

This assumption is essentially an analogue to the CIP condition. Therefore the typical theoretical forward FX rate $F_{t,T}$ expiring at T is simply given by

$$F_{t,T} = \mathbb{E}(S_T) = S_t e^{\int_t^T r_\tau - q_\tau d\tau},$$

which demonstrate the fair expected exchange rate for an risk neutral investor holding one unit of foreign currency in the money account, given the risk-free domestic and foreign interest rate. It also shows that the forward FX rate is a function that contains only pegged spot FX rate at current level and interest rate dynamics in order to avoid arbitrage. What is more, the pegged currency pair will remain at its spot FX rate for sure if no other uncertainty is presented.

However, uncertainties do exist in terms of the likelihood of a peg break and these uncertainties can significantly affect the outlook for a pegged currency pair and by extension this uncertainty will be reflected in the forward FX rate. I will then make an interpretation of the forward FX rate similar to Yu [2007] that when the currency is under control, the market quoted forward FX rate $\bar{F}_{t,T}$ does not fully follow its theoretical counterpart $F_{t,T}$, especially for hard pegged currency pair. Yu [2007] shows an example that the forward FX rate's market value of a controlled currency pair, USDCNY, did not agree with its theoretical value before Chinese yuan de-peg with dollar and the difference between these

two forward rates reflects the expectation of the future realignment risk.

This property of forward FX rate of pegged currency pairs implies that the market forward FX rate, $\bar{F}_{t,T}$, contains both information on the parity adjustment and market's views of the currency regime uncertainty. In addition to the currency regime switch risk, pegged currency rates may also be affected by the currency supply and thus has liquidity uncertainty. This type of uncertainty with other trading frictions that might happen in the future should also be priced-in the market forward rate.

Based on these facts that the forward FX rate for pegged currency pairs are more informative than spot rate by including the trading and realignment uncertainty, I will make the following assumption:

Assumption 12. *The market quoted forward FX rate of a controlled currency pair is constructed by the theoretical expectation, trading uncertainty and realignment uncertainty:*

$$\ln \bar{F}_{t,T} = \ln F_{t,T} + \int_t^T -\frac{1}{2} V_\tau d\tau + \int_t^T \sqrt{V_\tau} dW_\tau^s + J_t, \tag{5.1}$$

where $F_{t,T}$ is the theoretical forward FX rate, i.e.

$$F_{t,T} = \mathbb{E}(S_T) = S_t e^{\int_t^T r_\tau - q_\tau d\tau}. \tag{5.2}$$

Stochastic variance V_t and short rates for domestic and foreign interest rates, r_r

and q_t, follow Cox-Ingersoll-Ross (CIR) process,

$$dV_t = \kappa_V(\bar{V} - V_t)dt + \sigma_V\sqrt{V_t}dW_t^V, \tag{5.3}$$

$$dr_t = \kappa_r(\bar{r} - r_t)dt + \sigma_r\sqrt{r_t}dW_t^r, \tag{5.4}$$

$$dq_t = \kappa_q(\bar{q} - q_t)dt + \sigma_q\sqrt{r_t}dW_t^q. \tag{5.5}$$

Each element of the Brownian motions $\mathbf{W} = (W^s, W^V, W^r, W^q)^\top$ are independent and identical distributed. The jump process J_t is also independent:

$$J_t = \sum_{i=0}^{N_t} U_i, \tag{5.6}$$

where N_t is the counting process with intensity λ and U_i is the independent standard normal distributed jump size $U_i \sim^{iid} \mathcal{N}(\mu_J, \sigma_J)$, where constants μ_J and σ_J are the mean and variance of the jump size, respectively.

Notice that in Eq. (5.1), I keep the quadratic term, $\int_t^T -\frac{1}{2}V_\tau d\tau$, to compensate the Brownian motion term. Thus the discounted forward rate $\mathbb{E}[\frac{\bar{F}_{t',T}\exp(\int_t^{t'} q_\tau d\tau)}{\exp(\int_t^{t'} r_\tau d\tau)}], t' \in [t, T]$ is a martingale if we do not consider jumps, i.e. $J_{t'} = 0, \forall t' \in [t, T]$. This setting is made under the belief that the trading uncertainty even though exist and drive the forward rate away from the theoretical value, this kind of uncertainty does not systematically drive the process to a certain direction. On the other hand, the jump process does not have a compensator, thus it will affect the expectation of forward rate with a clear direction. This setting fits the fact that the market normally bet the exchange rate jumping to one of the directions.

Take the market forward rate dynamics above as the foundation, I then infer a potential spot FX rate. In another word, I propose that at a spot time t the

market quoted forward FX rate maturing at T implies a **synthetic spot FX rate**, denoted as $S^*_{t|t,T}$. This synthetic rate is different from the pegged spot FX rate because it is not observable from the market and it contains the uncertainty anticipation information. I define $S^*_{t|t,T}$ as the discounted market quoted forward FX rate:

$$S^*_{t|t,T} = \bar{F}_{t,T} e^{\int_t^T (-r_\tau + q_\tau) d\tau}, \tag{5.7}$$

where $t|t,T$ means the synthetic spot FX rate at time t implied by a forward contract at time t and expiring at T.

Now comparing the synthetic spot FX rate, $S^*_{t|t,T}$, and the pegged rate, $S_t = F_{t,T} \exp(\int_t^T (-r_\tau + q_\tau) d\tau)$ (from Eq. (5.2)), I denote the difference between their logarithm value as **spot rate bias**, which is

$$\begin{aligned} D_{t,T} &= \ln S^*_{t|t,T} - \ln S_t = \ln \bar{F}_{t,T} - \ln F_{t,T} \\ &= \int_t^T -\frac{1}{2} V_\tau d\tau + \int_t^T \sqrt{V_\tau} dW^s_\tau + J_t. \end{aligned} \tag{5.8}$$

Under these definition and assumption, the spot rate bias between the two logarithm spot FX rates is generated by a Levy process including a Brownian motion with stochastic volatility and a jump process with constant jump intensity and normal distributed jump size. To sum up, I use the Brownian motion to represent the trading frictions that diverge theoretical and market forward rates with no preferred direction, and use the non-compensated Poisson process to represent the realignment risk with a expected jump direction. These two components will actually have different roles in the spot rate bias term structure, which I will demonstrate in the following section.

5.3 Short/long-term separated parameter estimation

As mentioned in the introduction, the model process proposed in Section 5.2 could have been easily estimated by methods from various approaches if additional option data is given. However, the tricky part of parameter estimation for pegged currency pairs is that no, or very limited, option data can be observed.

By studying the character of the forward contracts of these currency pairs, I hereby make an novel argument that for pegged FX rates, short term forward contracts contain different information of uncertainty from the long term forward contracts. More specifically, spot rate bias implied by short term, shorter than 1M, forward time series reflects the trading uncertainty, and spot rate bias implied by long term, over 6M, forward term structure hints the realignment uncertainty. Then these two segmented parts on the bias term structure can be used to estimated different set of parameters of the proposed model.

5.3.1 The implied short-term FX bias process

For most of the pegged FX rates, there is very small probability to observe a de-peg event within a short period for most of the time. Thus spot rate bias from short-term maturity forward rate mainly reflects the fluctuation of trading friction, which means we can separate jump process from the model when focusing only on the short-term forward rates. So I firstly emphasis on the spot rate bias process, denoted as $D_{0,d}$, which spans from spot (time zero) to a specific short

maturity date $d \to 0$:

$$D_{0,d} = \int_0^d -\frac{1}{2} V_\tau d\tau + \int_0^d \sqrt{V_\tau} dW_\tau^s + J_d \tag{5.9}$$

I will summarise the preceding arguments in the following assumption:

Assumption 13. *As the maturity date being close to spot date, i.e. $d \to 0$, the probability of observing a jump event is small ($N_d \overset{d\to 0}{=} 0, J_d \overset{d\to 0}{=} 0$), especially for the pegged currency pairs cases we are interested in, then the spot rate bias can be restricted to a Brownian motion as:*

$$D_{0,d} \overset{d\to 0}{=} \int_0^d -\frac{1}{2} V_\tau d\tau + \int_0^d \sqrt{V_\tau} dW_\tau^s. \tag{5.10}$$

The simplified spot rate bias can be further modified. Since the variance process Eq. (5.3) follows a standard CIP process, it has mean reverting property even with the shock W_t^V. Given such reversion trend and neglect the concave/convex property and random shocks as $d \to 0$, I will approximate the stochastic variance V_t using its middle state constant value $V_{d/2}$. This brings the next assumption:

Assumption 14. *As $d \to 0$, the change in the CIR type variance process within a short-term period is of smaller order relative to its middle state at $d/2$ and thus I use a fixed representative state $V_{d/2}$ to approximate the true stochastic V_t for $D_{0,d}$ before the maturity date d. The the approximate short-term spot rate bias is:*

$$\tilde{D}_d \overset{d\to 0}{\equiv} \int_0^d -\frac{1}{2} V_\tau d\tau + \int_0^d \sqrt{V_\tau} dW_\tau^s \approx -\frac{d}{2} V_{d/2} + \sqrt{V_{d/2}} W_d^s. \tag{5.11}$$

With the assumptions above, we can now calculate the approximate distribution of the spot rate bias with a certain parameter vector, $(\kappa_V, \bar{V}, \sigma_V)'$ and initial variance V_0. For the variance process at time $d/2$, $V_{d/2}$ is a Cox-Ingersoll-Ross process thus the transition probability density function (p.d.f) $f_{V_{d/2}}$ is

$$f_{V_{d/2}}(V_{d/2}; V_0, \kappa_V, \bar{V}, \sigma_V) = ce^{-u-\omega}(\frac{\omega}{u})^{q/2} I_q(2\sqrt{u\omega}), \tag{5.12}$$

where

$$\begin{aligned} c =& \frac{2\kappa_V}{(1-e^{-\kappa_V d/2})\sigma_V^2}, \\ q =& \frac{2\kappa_V \bar{V}}{\sigma_V^2} - 1, \\ u =& cV_0 \exp(-\kappa_V d/2), \\ \omega =& cV_{d/2}, \end{aligned}$$

and $I_q(2\sqrt{u\omega})$ is modified Bessel function of the first kind of order q. A useful transform $2cV_{d/2}$ will follow non-central χ^2 distribution, with $2q+2$ degrees of freedom and non-centrality parameter $2u$.

Then $\sqrt{2cV_{d/2}}$ follows the non-central χ distribution. And the distribution of $v_{d/2} = \sqrt{V_{d/2}}$ can be calculated applying transformation of density function:

$$\begin{aligned} f_{v_{d/2}}(v_{d/2}) =& f_{\sqrt{2cV_{d/2}}}(\sqrt{2cV_{d/2}}) \frac{d\sqrt{2cV_{d/2}}}{dv_{d/2}} \\ =& \sqrt{2c}\chi(\sqrt{2c}v_{d/2}; 2q+2, \sqrt{2u}) \\ =& 2\sqrt{cu}e^{-u-cv_{d/2}^2}(\frac{\sqrt{c}v_{d/2}}{\sqrt{u}})^{q+1} I_q(2\sqrt{cu}v_{d/2}) \end{aligned} \tag{5.13}$$

I also denote the probability density function of the Wiener process at d as

$$f_{W_d} \equiv f_W(W_d; W_0 = 0) = \mathcal{N}(0, d) \tag{5.14}$$

When the variance process is independent with the W_t^s of the spot rate bias process, using change of variable transformation, we can have the probability density function of $\tilde{D}_d$

$$\begin{aligned} f_{\tilde{D}_d}(\tilde{D}_d) &= \int_{0+}^{\infty} f_{v_{d/2}}(v_{d/2}) f_{\tilde{D}_d}(\tilde{D}_d | v_{d/2}) dv_{d/2} \\ &= \int_{0+}^{\infty} f_{v_{d/2}}(v_{d/2}) f_{W_d}\left(\frac{\tilde{D}_d + \frac{d}{2}v_{d/2}^2}{v_{d/2}}\right) \left| \frac{\partial(\tilde{D}_d + \frac{d}{2}v_{d/2}^2)/v_{d/2}}{\partial \tilde{D}_d} \right| dv_{d/2} \\ &= \int_{0+}^{\infty} f_{v_{d/2}}(v_{d/2}) f_{W_d}\left(\frac{\tilde{D}_d + \frac{d}{2}v_{d/2}^2}{v_{d/2}}\right) \frac{1}{v_{d/2}} dv_{d/2}. \end{aligned} \tag{5.15}$$

Substitute the probability density functions Eq. (5.13) and Eq. (5.14) into Eq. (5.15), we will have the probability density function for the short-term approximate spot rate bias as in the following proposition.

Proposition 3. *When the bias shock W_t^s and the variance process are independent, the probability density function of the short-term spot rate bias is (omitting the parameters in notations for short):*

$$\begin{aligned} & f_{\tilde{D}_d}(\tilde{D}_d = -\frac{d}{2}V_{d/2} + \sqrt{V_{d/2}} W_d^s) \\ &= \int_{0+}^{\infty} f_{v_{d/2}}(v_{d/2}) f_{W_d}\left(\frac{\tilde{D}_d + \frac{d}{2}v_{d/2}^2}{v_{d/2}}\right) \frac{1}{v_{d/2}} dv_{d/2} \\ &= \int_{0+}^{\infty} \sqrt{\frac{2cu}{\pi v_{d/2}^2 d}} e^{-u - cv_{d/2}^2 - \frac{(\tilde{D}_d + \frac{d}{2}v_{d/2}^2)^2}{2v_{d/2}^2 d}} \left(\frac{cv_{d/2}^2}{u}\right)^{\frac{q+1}{2}} I_q(2\sqrt{cuv_{d/2}^2}) dv_{d/2}. \end{aligned} \tag{5.16}$$

This p.d.f can be calculated numerically, and then the logarithm likelihood function $\ln \mathcal{L}_{short}(\kappa_V, \bar{V}, \sigma_V, V_0 | \tilde{D}_d)$ can also be calculated. Therefore the trading uncertainty parameters, $\kappa_V, \bar{V}$ and σ_V, can be estimated using maximum likelihood estimation (MLE) on the historical short-term spot rate bias of a collection of points on the time series with the same tenor d,

$$(\widehat{V_0}, \widehat{\kappa_V}, \widehat{\bar{V}}, \widehat{\sigma_V})' = \underset{\kappa_V^*, \bar{V}^*, \sigma_V^*, V_0^*}{\arg\max} \sum_{i=1}^{n} \ln \mathcal{L}_{short}(\kappa_V, \bar{V}, \sigma_V, V_0 | \tilde{D}_{d,i}),$$

where the subscript $i \in [1, n]$ indicates the sample points on the time series of spot rate bias with the specified short-term maturity d.

5.3.2 The implied long-term FX bias process

Unlike in the short-term assumption where spot rate bias mainly contains trading uncertainty and jump events are neglected because of small possibility, I assume that the outlook of jump events, the realignment uncertainty such as de-peg changes, dominate the spot rate bias term structure implied by long-term forward rates at a given time, and the premium the bias caused by the trading uncertainty is expected to be irrelevant for large tenors. Based on these, I form the following assumption for long-term spot rate bias:

Assumption 15. *For an increasing series of long-term tenors, denoted as* $\mathbf{d} = [d_1, d_2, ..., d_n]$ *and* $d_i > d_j$ *if* $i > j$*, the long-term term structure of spot rate bias at a specific time* t *is dominated by the jump process* $J_{\mathbf{d}}$ *to reflect market's expectation of de-peg events, while the continuous part of the process representing*

trading friction is expected to be neglected, that is

$$\hat{D}_{d_m} \equiv \sum_{i=1}^{N_{d_m}} U_i, \tag{5.17}$$

where $d_m \in \mathbf{d}$.

Under this assumption, $\hat{D}_{d_m}$ is a non-compensated compound Poisson process. Since jump size and the counting process are independently distributed, the joint probability density of $\hat{D}_{d,m}$ is

$$f_{\hat{D}_{d_m}}(J_{d_m} = \hat{D}_{d_m}) = \sum_{n=1}^{\infty} f_J(\sum_{i=1}^{N_{d_m}} U_i = \hat{D}_{d_m} | N_{d_m} = n) f_{N_t}(N_{d_m} = n), \tag{5.18}$$

where $f_J(\cdot)$ is the probability density of the aggregate size of N_{d_m} jumps with normal distributed jump sizes, and $f_{N_t}(\cdot)$ is the Poisson density function with intensity λ. I should note that when jump times $n = 0$, the compound Poisson process $J_{dm} = 0$ since no jump is observed, and thus the conditional jump size distribution becomes a degenerate distribution with in this function. Also it is almost impossible to observe J_{dm} being exactly zero in the real world, I will skip the distribution point mass at $\hat{D}_{dm} = 0$.

With Eq. (5.18), we can now substitute the p.d.f of Poisson distribution can get the following proposition.

Proposition 4. *Under the assumption of long-term term structure at a given time point* t*, the probability density of the spot rate bias with tenor* $d_m \in \mathbf{d}$ *is*

given by

$$
\begin{aligned}
f_{\hat{D}_{d_m}}(J_{d_m} = \hat{D}_{d_m}) &= \sum_{n=1}^{\infty} f_J(\sum_{i=1}^{n} U_i | N_{d_m} = n) \frac{(\lambda d_m)^n e^{-\lambda d_m}}{n!} \\
&= \sum_{n=1}^{\infty} \mathcal{N}(n\mu_J, n\sigma_J^2) \frac{(\lambda d_m)^n e^{-\lambda d_m}}{n!} \\
&= \sum_{n=1}^{\infty} \frac{(\lambda d_m)^n e^{-\lambda d_m - \frac{(\hat{D}_{d_m} - n\mu_J)^2}{2n\sigma_J^2}}}{n!\sqrt{2\pi n\sigma_J^2}}
\end{aligned} \tag{5.19}
$$

This also need to be calculated numerically. Now the logarithm likelihood, $\ln \mathcal{L}_{long}(\mu_J, \sigma_J, \lambda | \hat{D}_{d_m})$, for each long-term tenor on the spot rate bias term structure $d_m \in \mathbf{d}$ can be computed and used to estimate the realignment uncertainty parameters,

$$
(\widehat{\mu_J}, \widehat{\sigma_J}, \widehat{\lambda})' = \underset{\mu_J, \sigma_J, \lambda}{\arg\max} \sum_{m=1}^{n} \ln \mathcal{L}_{long}(\mu_J, \sigma_J, \lambda | \hat{D}_{d_m}) \tag{5.20}
$$

5.4 Market observations and simulations

Before going to price any option, I hereby estimate the model on selected market data to test the model performance in this section. Firstly I will introduce the currency data used in this chapter.

5.4.1 Synthetic spot FX rates

For the empirical application of my model, I select four representative currencies, Danish krone (DKK), Saudi riyal (SAR), Qatar riyal (QAR) and Nigerian naira (NGN). Except DKK, which is pegged with euro (EUR) within the framework of European Exchange Rate Mechanism (ERM II), the other three currencies

are pegged to US dollar (USD). DKK and the two Gulf Cooperation Council (GCC) currencies SAR and QAR are under the conventional peg category and NGN is under the stabilised arrangement according to IMF [2016]. EURDKK has been a relatively stable peg with no sudden changes in the FX rate. On the contrary, USDNGN had a major de-peg event in 2016 and jumped from one peg rate to a much higher peg level. USDQAR and USDSAR are hard pegs and has similar economic situations. But USDQAR experienced a FX rate fluctuation in 2016. These characters makes the four currency pairs have unique characters and suitable for the study in this chapter.

I collect the tick-by-tick spot FX rates, forward FX rates and their corresponding domestic and foreign interest rates with various maturities of the four pegged currency pairs from Thomson Reuters Tick History database and pick the end of day value from the time series. By market convention, EUR and USD are the foreign currencies in the targeting currency pairs.

Note that USDNGN also have a non-deliverable forward (NDF) market. Subjecting to the currency restriction, NDF contracts of USDNGN provides more information of this currency's outlook. Thus I will separate the NDF outright data and normal forward outright data. To be more specific, in the Thomson Reuters Tick History database, normal forward and NDF have different identity tickers, such as "NGN1MV=" and "NGN1MNDFOR=" for USDNGN.

The starting dates of my dataset for EURDKK, USDSAR, USDQAR, USDNGN are July 16th, 2013, June 24th, 2014, September 28th, 2014 and September 28th, 2014, respectively. The ending point for all my datasets is February 23rd, 2018. I summarise the details of the data in Table 5.1. Panel A of the table shows the number of maturities and the shortest and longest tenors for each mar-

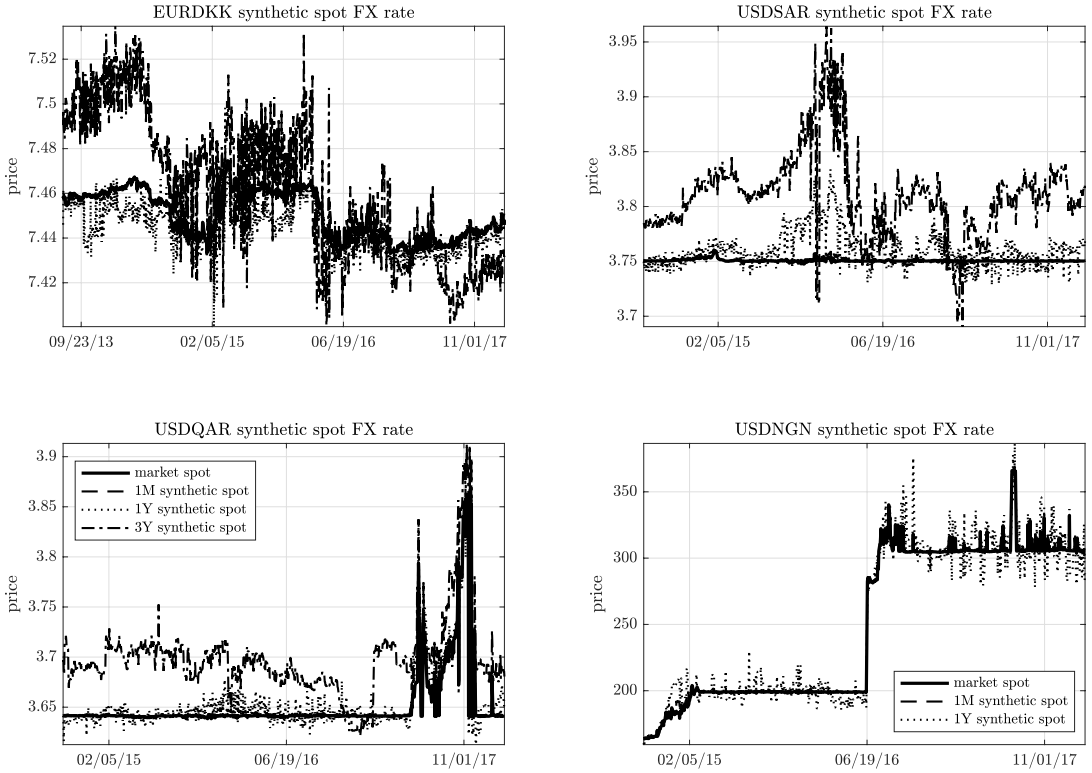

Figure 5.1: Market spot FX rates compared with synthetic spot FX rate implied by forward prices with different maturities
In these plots, I show the synthetic spot FX rates implied by forward prices with 1M (dash line), 1Y (dot line) and 3Y (dash-dotted line) tenors, compared with the market spot FX rates (solid line), for the four currency pairs. We can observe that the difference between any synthetic rate and corresponding market rate increases as the maturity grows. The biases exist and being consistent among all the selected currency pairs within the data periods.

ket forward FX rate and interest rate term structure. For the interest rates, I use the deposit rates for each currency, and I use the forward FX outright instead of base points for each forward FX rate to avoid the transformation process . Panel B provides a descriptive statistics for the spot FX rate and forward FX rate time series for selective maturities.

To demonstrate the synthetic spot FX rate and the spot rate bias, I plot Fig. 5.1 and highlight the synthetic spot implied by NDF in Fig. 5.2. Each

Table 5.1: Data summary

Panel A: Number of maturities of domestic and foreign interest rates and market forward FX rates

		Tenor No.	Min	Max			Tenor No.	Min	Max
EURDKK	r_d	23	SW	10Y	USDQAR	r_d	9	SW	10Y
	r_f	21	SW	10Y		r_f	24	SW	10Y
	F	25	SW	10Y		F	20	SW	5Y
USDSAR	r_d	18	SW	7Y	USDNGN	r_d	8	SW	1Y
	r_f	24	SW	10Y		r_f	24	SW	10Y
	F	17	SW	5Y		F	12	SW	5Y
						NDF	6	1M	1Y

Panel B: Descriptive statistics for spot FX rates and forward FX rates time series (selective maturities)

		Obs.	Mean	Std. dev.	Min	Max	Skewness	Kurtosis
EURDKK	Spot	1162	7.4503	0.0108	7.4328	7.4746	0.0271	1.4581
	SW	1162	7.4500	0.0106	7.4328	7.4735	0.0149	1.4463
	1M	1162	7.4489	0.0101	7.4319	7.4696	-0.0116	1.4403
	6M	1162	7.4423	0.0101	7.3815	7.4622	-0.9827	6.5219
	1Y	1162	7.4367	0.0120	7.3586	7.4613	-1.7026	10.5567
	3Y	1162	7.4374	0.0218	7.3062	7.4864	-1.2929	7.7037
USDSAR	Spot	925	3.7507	0.0012	3.7475	3.7605	3.5677	22.2399
	SW	925	3.7510	0.0012	3.7478	3.7603	3.0150	17.5033
	1M	925	3.7519	0.0020	3.7478	3.7622	1.6625	6.2326
	6M	925	3.7587	0.0087	3.7476	3.8018	1.4399	5.6065
	1Y	925	3.7733	0.0196	3.7507	3.8511	1.0164	3.7338
	3Y	925	3.8502	0.0711	3.7505	4.0762	0.6899	2.6342
USDQAR	Spot	858	3.6508	0.0329	3.6384	3.8635	4.3500	23.2935
	SW	858	3.6512	0.0329	3.6386	3.8635	4.3454	23.2584
	1M	858	3.6526	0.0327	3.6392	3.8634	4.3239	23.0934
	6M	858	3.6606	0.0332	3.6402	3.8660	3.9182	19.9144
	1Y	858	3.6717	0.0363	3.6435	3.8717	3.1390	14.2197
	3Y	858	3.7105	0.0440	3.6537	3.9124	1.6872	7.5679
USDNGN	Spot	858	250.3745	57.7367	163.6150	366.3000	0.0391	1.2127
	SW	858	250.9289	57.9516	163.8250	367.0500	0.0398	1.2120
	1M	858	253.0309	58.6372	164.6250	372.3954	0.0430	1.2084
	6M	858	267.3803	63.5221	170.5600	405.2696	0.0527	1.2273
	1Y	858	287.3378	70.9601	179.1650	447.2658	0.1038	1.3040
	1M–NDF	858	265.4417	64.4165	164.5100	354.5000	-0.0398	1.1491
	6M–NDF	858	296.4558	69.3979	170.4800	408.4250	-0.0869	1.4106
	1Y–NDF	858	323.0643	76.3641	178.3250	448.5000	-0.0909	1.5299

Notes: The data used in this chapter is summarized in this table. I collect deposit rate with maturity from SW up to 10Y. Foreign rates (EUR, USD) of the four currency pairs have more points on the yield curve than the domestic rates. For each currency pair, I intersect the cross-section data to have the same time-stamp. From Panel B we can see that the spot rate of USDNGN, which experienced a de-peg event within the data period, has large standard deviation (50%+) compared with others (<4%).

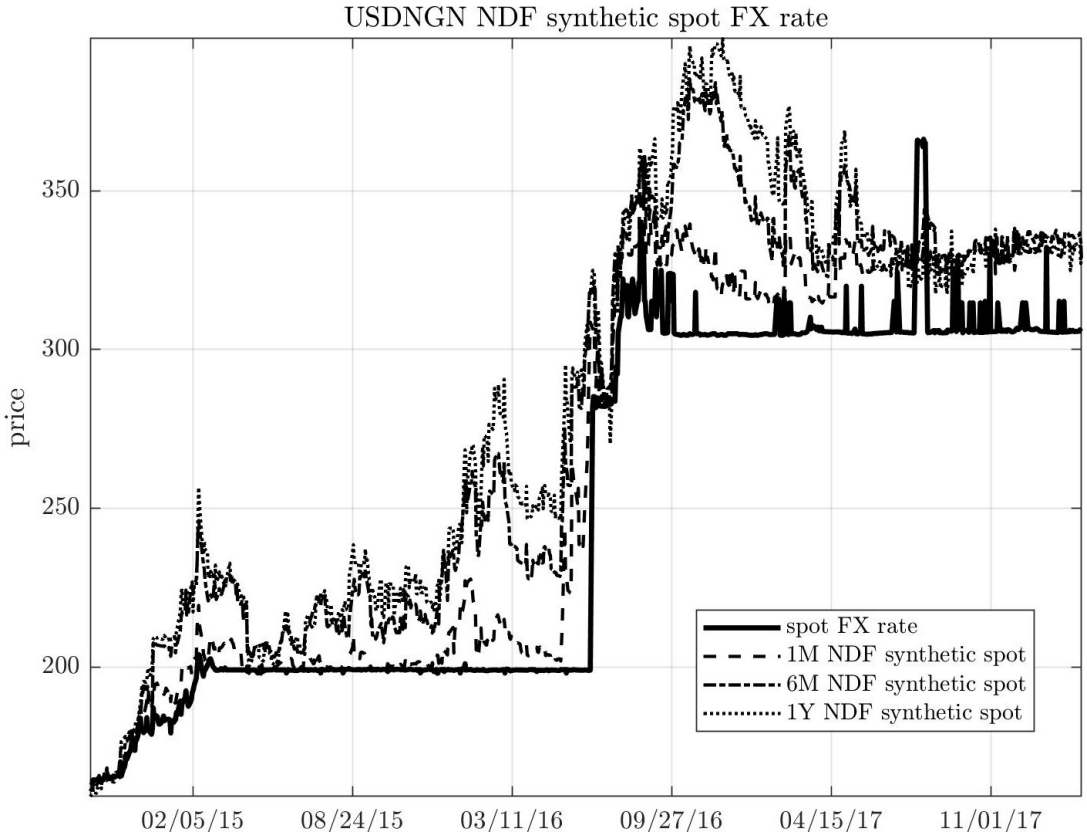

Figure 5.2: NGNUSD market spot FX rate compared with synthetic spot FX rate implied by NDF with different maturities
This figure shows the difference between NGNUSD market spot rate and NDF implied synthetic spot FX rate. Since for NGNUSD, NDF is a more actively traded asset, it reflect more information about market's outlook than normal forwards, thus the biases are more obvious in this plot than the one in Fig. 5.1.

panel of the first figure represents one of the four selected currency pairs. The solid lines are the market spot FX rates. The spot FX rate of EURDKK and USDSAR are generally bounded with in a small range, while USDQAR had a major fluctuation after May 2017. After the peak in November 2017, which is about 5.8% higher than its average rate, the spot rate dropped back to the normal peg level. USDNGN acts differently from the others that it firstly increased to its first peg level in March 2015 and stayed around 199 naira per dollar until June

17th, 2016. Then it de-pegged and jumped to a new peg level on June 20th, 2016 with more volatility around 304 naira per dollar. The dash lines in the figures are the synthetic spot FX rates calculated using Eq. (5.7) based on forward FX rates with tenors ranging from 1M to 3Y (or 1Y for USDNGN because of the deposit rate data limitation). It is clearly observed that as the maturity increases, the spot rate bias from Eq. (5.8) becomes more significant.

Note that for USDNGN, NDF is more actively traded than standard forward rate, therefore NDF is a better indicator of the market's opinion. Different from the last plot in Fig. 5.1, Fig. 5.2 shows that the synthetic spot rates rocketed much earlier than the de-peg event, showing that the de-peg jump in June 2017 was anticipated by the NDF. This evidence can be used for carry trade strategies and can reflect market participants' outlook of the trading and realignment uncertainties.

5.4.2 Estimation procedure

In this section, I apply the proposed approximate likelihood estimation approach as described in Section 5.2 to estimate the bias process parameters. To be more specific, I choose SW forward contracts for the short term trading uncertainty estimation, and use the first 600 days in the time series of each currency pair as their estimation window.

The estimated trading uncertainty parameters are listed in Panel A of Table 5.2. From the parameters we can see that all of these currency pairs have relative smaller long term unconditional mean of volatilities, $\bar{v}$, than what normally observed from other equity assets, such as in Pan [2002]. Based on the normal

Table 5.2: Estimated parameters

Panel A: Trading uncertainty parameters based on 600 days' SW forward implied spot rate bias

	κ_v	$\bar{v}$	σ_v	v_0		κ_v	$\bar{v}$	σ_v	v_0
EURDKK	0.018	4.344e-4	0.004	1.490e-8	USDQAR	0.045	0.001	0.009	1.490e-8
USDSAR	0.058	9.532e-4	0.011	9.443e-8	USDNGN	0.836	0.003	0.022	0.002

Panel B: Realignment uncertainty parameters based on 6M–5Y forward implied spot rate biass on 23 February 2018

	λ	μ_J	σ_J		λ	μ_J	σ_J
EURDKK	0.895	-4.965e-4	6.813e-4	USDQAR	1.504	0.003	9.622e-4
USDSAR	1.983	0.003	8.756e-4	USDNGN	9.912	-0.006	7.369e-4
				USDNGN–NDF	1.852	0.083	0.005

Panel C: Interest rate term structure parameters based on CIR model on 23 February 2018

	κ_r	$\bar{r}$	σ_r	r_0		κ_r	$\bar{r}$	σ_r	r_0
DKK	16.034	1.599e-4	0.004	8.648e-7	QAR	14.833	5.754e-4	0.494	0.027
SAR	0.080	0.135	0.338	0.021	NGN	2.704	0.068	0.256	0.107
USD	10.186	0.001	0.499	0.021	EUR	13.434	1.981e-4	0.005	1.079e-6

Notes: This table documents selected estimated parameters of the model for different currency pairs. I use the likelihood based estimation in Section 5.3 to estimated the parameters for trading and realignment (just for February 23rd, 2018 here) uncertainties, as listed in panel A and panel B, respectively. In panel C, I pick one day's interest term structure and estimate the parameters for the CIR processes. Summary of the parameters for all the term structures in the data period is presented in Table 5.3.

forward outright data, USDNGN has the largest $\bar{v}$, which is only 0.003. The mean reversion speed parameters, κ_v, are generally small indicating the volatility process for the trading uncertainty are more vulnerable to the disturbances, except for USDNGN being 0.836. USDNGN spot FX rate changes more sharply in direction and bigger in magnitude compared with the other three because of the bigger κ_v and $\bar{v}$. The volatility of volatility parameters, σ_v being less than 0.022, and short volatility, v_0 being less than 0.002, also reflect that trading uncertainty of the pegged currency pairs has effects on the spot FX rate, but the effects are less significant than the natural fluctuation of free floating currencies. The parameters overall indicate that EURDKK has less trading friction or liquidity issue

than the other currency pairs. Since the NDF data for USDNGN starts from 1M, I do not estimate the trading uncertainty based on NDF.

Then to estimate the realignment uncertainty parameters for each day in the rest days in the data, I calculate every day's spot rate bias term structure implied by forward contracts with maturities from 6M up to 5Y (for USDNGN the estimation is based on 1M–1Y forward implied spot rate bias because of the limitation of the interest rate data). I use cubic polynomial to interpolate this term structure on a 300-points uniformly distributed grid with the same maturity range. The interpolation stabilises the likelihood level and provides a natural weighting for different maturities, thus bias implied by longer maturity forward FX rates has more influences on the likelihood.

Panel B of Table 5.2 lists the long term uncertainty estimation for the realignment parameters on February 23rd, 2018, the last day of my sample data, as an example. The parameters estimated for February 23rd, 2018 shows that USDNGN has the largest realignment uncertainty, with the biggest jump intensity, λ, being 9.912, while DKK has the lowest jump intensity 0.895. And the mean size of jumps of DKK, μ_J, is just -4.965e-4 showing there is no clear jump direction. The two GCC currencies has similar μ_J around 0.003, showing the market expecting similar jump direction and jump size for these two currencies, while USDNGN is expected to jump to an opposite direction with μ_J being -0.006. Notice that NDF of USDNGN behaves differently compared with its normal forward counterpart. NDF implies larger jumps in size (0.083) and lower frequency (1.852), which is in-line with the figures before that the NDF implied spot bias is more consistent and large.

I use the standard CIR model to fit the interest rate term structure of each day.

Table 5.3: Descriptive statistics for realignment uncertainty parameters

		Obs.	Mean	Std. dev.	Min	Max	Skewness	Kurtosis
EURDKK								
	λ	1162	0.8622	0.0448	0.7344	1.1101	0.2109	3.2182
	μ_J	1162	0.0019	0.0010	-0.0007	0.0044	-0.1674	2.3361
	σ_J	1162	0.0022	0.0007	0.0006	0.0052	0.3152	4.3235
USDSAR								
	λ	925	1.9217	0.3046	0.5522	2.7693	-0.2644	4.3316
	μ_J	925	0.0023	0.0013	-0.0019	0.0118	1.3389	9.3130
	σ_J	925	0.0014	0.0008	0.0001	0.0069	1.7597	9.1822
USDQAR								
	λ	858	1.6827	0.1636	0.7646	2.2811	-0.2883	6.3201
	μ_J	858	0.0027	0.0009	0.0001	0.0054	-0.7073	3.6566
	σ_J	858	0.0019	0.0010	0.0003	0.0056	0.3199	2.2199
USDNGN								
	λ	858	5.8151	2.8974	1.3333	12.9496	0.1136	2.1375
	μ_J	858	0.0024	0.0131	-0.0691	0.1401	3.2959	40.7038
	σ_J	858	0.0023	0.0031	0.0000	0.0172	2.3289	8.7562
USDNGN–NDF								
	λ	858	6.6678	4.3132	1.6000	14.9033	0.2359	1.4997
	μ_J	858	0.0488	0.0587	-0.1024	0.4647	2.6435	13.8117
	σ_J	858	0.0057	0.0066	0.0001	0.0495	3.0895	15.7439

Notes: Different from panel B in Table 5.2, this table summarise the descriptive statistics for the realignment uncertainty parameters of all the dates outside of the short-term estimation window. Overall the NDF implied USDNGN has the most significant jump process with the largest intensity and mean jump size. And EURDKK on the other hand has the smallest jump intensity and jump size.

The parameters listed in Panel C of Table 5.2 are the parameters on February 23rd, 2018 for all the domestic and foreign interest rates. Specifically, USD interest rates are the foreign counterpart for USDSAR, USDQAR and USDNGN by market convention, and EUR interest rates are the foreign counterpart for EURDKK. The 4 currencies I study in this chapter are on the domestic side.

Table 5.3 and Table 5.4 record the descriptive statistics for the realignment and interest rate term structure parameters for all the days outside of short-term estimation window. In general, the NDF of USDNGN implies the largest jump intensity and mean jump size on the dates my data covers.

Table 5.4: Descriptive statistics for interest rate term structures parameters

Panel A: Domestic interest rate term structure parameters

		Obs.	Mean	Std. dev.	Min	Max	Skewness	Kurtosis
DKK								
	κ_r	1162	11.2324	8.8783	0.3399	27.7511	0.3435	1.6537
	$\bar{r}$	1162	0.0013	0.0024	0.0000	0.0136	2.8992	11.4924
	σ_r	1162	0.0497	0.0757	0.0005	0.3146	1.5462	4.2175
	r_0	1162	0.0005	0.0007	0.0000	0.0026	1.2783	3.2616
SAR								
	κ_r	925	0.9039	1.8623	0.0265	17.2821	3.5860	19.2205
	$\bar{r}$	925	0.1475	0.1851	0.0002	0.5000	1.0600	2.4175
	σ_r	925	0.2594	0.1435	0.0012	0.5000	-0.2239	2.4619
	r_0	925	0.0122	0.0060	0.0000	0.0243	-0.3406	1.7748
QAR								
	κ_r	858	1.7257	4.4304	0.0165	23.0646	3.0564	11.2884
	$\bar{r}$	858	0.0682	0.1073	0.0004	0.4999	2.6541	10.0811
	σ_r	858	0.3650	0.0826	0.0121	0.5000	-0.4447	6.4242
	r_0	858	0.0168	0.0057	0.0045	0.0278	-0.2917	1.6995
NGN								
	κ_r	858	2.0820	3.4498	0.0000	29.9042	6.0122	42.5976
	$\bar{r}$	858	0.1152	0.1313	0.0003	0.5000	2.4135	7.2543
	σ_r	858	0.2805	0.0960	0.0002	0.5000	0.6758	5.3053
	r_0	858	0.0952	0.0231	0.0042	0.1929	-0.9255	4.5047

Panel B: Foreign interest rate term structure parameters

		Obs.	Mean	Std. dev.	Min	Max	Skewness	Kurtosis
EUR								
	κ_q	1162	8.9574	8.7702	0.0157	29.7474	0.7464	2.1984
	$\bar{q}$	1162	0.0104	0.0363	0.0000	0.2734	4.4735	23.6385
	σ_q	1162	0.0564	0.0761	0.0001	0.4996	2.3466	11.3879
	q_0	1162	0.0010	0.0014	0.0000	0.0053	1.1207	3.0285
USD								
	κ_q	925	0.8166	1.9772	0.0236	12.7602	3.8234	17.5405
	$\bar{q}$	925	0.1080	0.1415	0.0009	0.4999	1.6419	4.5949
	σ_q	925	0.3607	0.0983	0.0083	0.5000	-0.2604	3.6754
	q_0	925	0.0101	0.0061	0.0000	0.0215	-0.2185	1.7423

Notes: Similar to Table 5.3, this table describes the properties of the domestic and foreign interest rate CIR process parameters of all the dates in my data periods. Based on the market convention, DKK, SAR, QAR and NGN are the domestic currencies of the four currency pairs, while EUR and USD are the foreign currencies. Also since EUR and USD are the conventional premium currencies, I apply the premium adjusted deltas as the moneyness.

5.4.3 Calibration exercise and simulations

Using the estimated parameters above, I run a Monte Carlo simulation, and the results are shown in Fig. 5.3. The left panels contain simulations for short term

trading uncertainty. I generate 10000 simulations of the possible spot rate bias in the 1 month future, and then add these biases as corrections to the theoretical 1M forward FX rates to get the uncertainty adjusted 1M forward FX rates. Upper and lower boundary dot lines record the 90% and 10% quantile of these simulations, respectively. The thinner solid lines are the traditional theoretical 1M forward FX rates. From the plots we can see that for these pegged currency pairs, the differences between theoretical and market quotes forward FX rates are less than 0.5%. Therefore it shows that trading uncertainty though exists, yet it is not the main reason for the big difference between the observed market forward FX rates and theoretical values especially for longer tenors.

For the long term realignment uncertainty, I use the estimated jump parameters to simulate 10000 bias on the selected term structure, i.e. from 6M to 5Y (1Y for USDNGN) on February 23rd, 2018. These values again are added to the theoretical forward FX rates with the corresponding maturities. The circles on the right panels of Fig. 5.3 are the mean values constructed by the adjusted forward FX rate term structure. It illustrates that the adjustments of spot rate bias lead to closer fits to the market forward FX rate term structure, while the theoretical forward FX rate diverges from the market values at longer maturities. In Fig. 5.3, such difference between the adjusted forward and theoretical forward can be 4.4% as in USDNGN.

Further, to show that the bias contains market's outlook of the de-peg event, I present similar simulation exercise for USDNGN NDF term structure from May 13th, 2016 to June 30th, 2016, which covers the de-peg jump event on June 20th. In Fig. 5.4, I illustrate the models analysis of a de-peg event for USDNGN on June 20th, 2016. Before June 20th, 2016, the difference between market

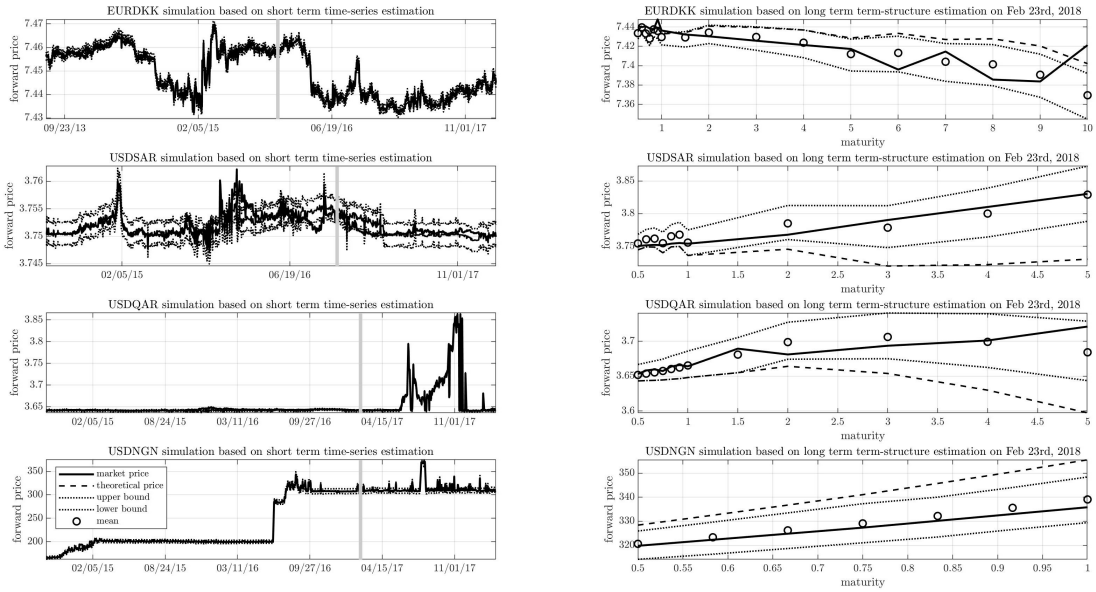

Figure 5.3: Simulations for short and long term forward adjusted by bias with upper and lower boundary on February 23rd, 2018
Based on the estimated parameters as in Table 5.2, I simulate 10000 times possible short (left panel) and long (right panel) term adjusted forwards. For the short term, the forward bias is not as significant as the long term counterparts. In the right panel, I list the market forward term structure in solid line, the theoretical forward in dash line, 90% and 10% quantile in the simulation as upper and lower bounds in dot lines and mean of the simulations in circles. It is clear that the bias adjusted forwards are more close to the market term structure than the theoretical forwards.

quoted NDF and theoretical forward started from 75 for 1Y contract and were significant and increasing. Market NDF were much higher than the theoretical forward indicating market's expectation of the de-peg event, and the difference peaked on June 17th, 2016 in this figure (the difference for 1Y contract is 132). The mean of bias adjusted forward from the proposed model tracks the market value. After the realignment, the market NDF and theoretical forward converged together, showing the risk-off after the de-peg, and the difference for 1Y contract dropped to 13 on June 30th.

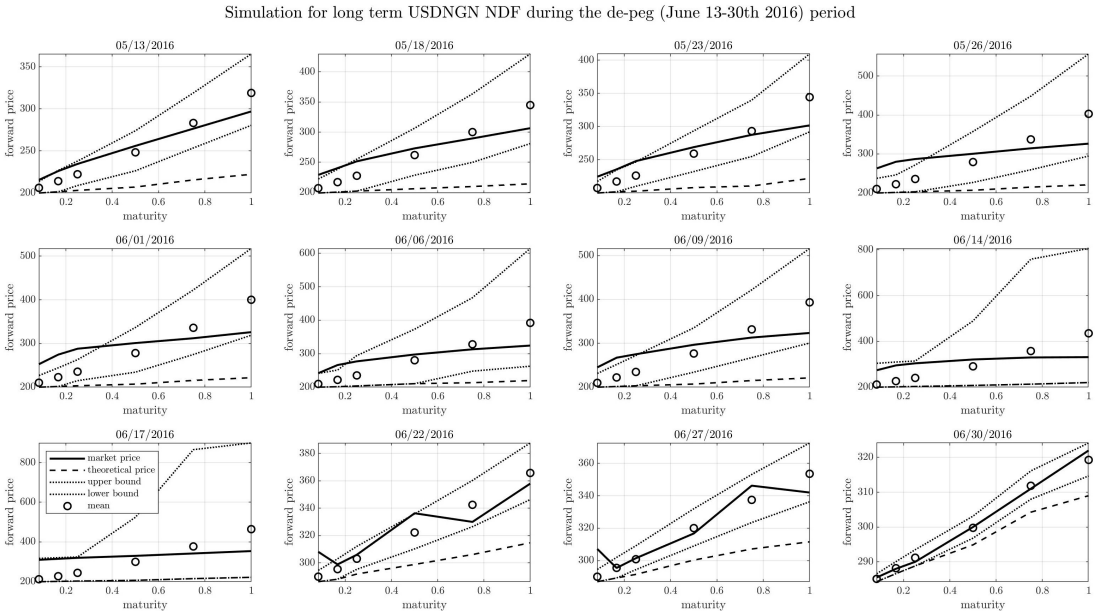

Figure 5.4: Simulations for USDNGN NDF adjusted by bias during the de-peg (June 13-30th, 2016) period
This figure shows the difference between market NDF (solid line) and theoretical forward rate (dash line) are growing since May 13th, and reach its pick on June 17th, 2016 (Friday, the last business date of the week), and then decrease after the realignment on June 20th. These plots show that the estimated parameters (circles) capture the synthetic spot bias and thus contains the information of future realignment risks that reflected by the NDF rate.

5.5 Pricing under an adjusted risk neutral measure

As pointed out by Hanke et al. [2018] that FX options generally containing betting information, I will include the bias extracted from forward market into FX option pricing model to reflect the market's outlook of trading and realignment uncertainties. Firstly I need to introduce an adjusted risk neutral measure.

5.5.1 Correcting the spot rate bias

Given the assumptions in Section 5.2, we now need to revise and interpret the meaning of risk neutral under the restricted market of the controlled currencies. Under the traditional circumstance, the risk neutral expectation of holding a foreign currency bond should be equal to holding S_t shares of the domestic risk-free bonds. Then the ratio of these therefore should be a martingale, such as

$$\mathbb{E}(\frac{S_T B^f_{t,T}}{B^d_{t,T}}|\mathcal{F}_{T-1}) = \frac{S_{T-1} B^f_{t,T-1}}{B^d_{t,T-1}},$$

where $B^d_{t,T} = \exp(\int_t^T r_\tau \tau)$ and $B^f_{t,T} = \exp(\int_t^T q_\tau \tau)$ are the money account of domestic and foreign investors respectively. This is already implied in Assumption 11 as the theoretical forward FX rate. However, this expectation will not match the real market forward quotes because of the existence of trading and realignment uncertainties. These components shift the market's belief of spot FX rates in the future, yet can not be reflected by conventional risk-free rate dynamics. As a result, fundamental valuation of the FX rate may alter with the expectation of the risks. Then such differences needs to be compensated in order to achieve non-arbitrage.

When I take the spot rate bias into consideration, the synthetic spot rates will replace the market quoted pegged spot FX rates in order to match the real market anticipations of the future since the difference mentioned above is embedded within the synthetic spot rates. Then holding one unit of the risky synthetic foreign bond should be considered to be holding risk-free domestic bonds adjusted by the spot rate bias, which is not reflected by the risk-free rates. Thus the ratio

being a local martingale is

$$\frac{S^*_{t|t,T}B^f_{t,T}}{B^d_{t,T}e^{D_{t|t,T}}}, \tag{5.21}$$

remind from Eq. (5.8) that $D_{t|t,T}$ is the spot rate bias. We can see that

$$\mathbb{E}(\frac{S^*_{T|t,T}B^f_{t,T}}{B^d_{t,T}e^{D_{T|t,T}}}|\mathcal{F}_{T-1}) = \mathbb{E}(\frac{S_TB^f_{t,T}}{B^d_{t,T}}|\mathcal{F}_{T-1}) = \frac{S_{T-1}B^f_{t,T-1}}{B^d_{t,T-1}}$$

is the same as

$$\frac{S^*_{T-1|t,T}B^f_{t,T-1}}{B^d_{t,T-1}e^{D_{T-1|t,T}}} = \frac{S_{T-1}B^f_{t,T-1}}{B^d_{t,T-1}},$$

This results in the expectation of the future value under the restricted market setting and allows trading uncertainty and re-alignment uncertainty to be taken into consideration and embedded in $e^{D_{T-1|t,T}}$. Thus the expected return is not only the interest rates, but also the terms that adjust the expectation bias. Then to achieve the non-arbitrage assumption, contingents claims on the controlled currency should expect the spot rate bias adjusted risk-free return as well. I refer to this the new adjusted risk neutral measure, under the peg constraint, as $\mathbb{Q}$. FX option on pegged currency pairs will be priced under this new measure.

5.5.2 The recovered option prices

Under the spot rate bias adjusted risk neutral measure $\mathbb{Q}$, the synthetic process is then

$$dx_t = (r_t - q_t - \frac{1}{2}V_t)dt + \sqrt{V_t}dW_t^s + dJ_t, \tag{5.22}$$

$$dV_t = \kappa_v(\bar{v} - V_t)dt + \sigma_v\sqrt{V_t}dW_t^v, \tag{5.23}$$

$$dr_t = \kappa_r(\bar{r} - r_t)dt + \sigma_r\sqrt{r_t}dW_t^r, \tag{5.24}$$

$$dq_t = \kappa_q(\bar{q} - q_t)dt + \sigma_q\sqrt{q_t}dW_t^q, \tag{5.25}$$

where $x_t = \ln S^*_{t|t,T}$ is the logarithm synthetic spot FX rate at time t. I denote $\mathbb{D}$ as the space of *cádlág* processes with filtration $\mathcal{F}_t$ on $\mathbb{R}^4$, and $\mathbf{X} = (x, V, r, q)^\top \in \mathbb{D}$ is the tuple of the state variables on the probability space $(\Omega, \mathcal{F}, \mathcal{F}_t, \mathbb{Q})$.

Following Duffie et al. [2000]'s work, the transition function $\Psi : \mathbb{C} \times \mathbb{D} \times \mathbb{R}_+ \times \mathbb{R}_+ \to \mathbb{C}$ is defined as

$$\Psi(c, \mathbf{X}, t, T) = \mathbb{E}[\exp(\int_t^T -r_\tau d\tau)e^{cx_T}], \tag{5.26}$$

Duffie et al. [2000] prove that this function can be written as exponential affine term

$$\Psi(c, \mathbf{X}, t, T) = \exp(\alpha + \boldsymbol{\beta}\mathbf{X}_t^\top) \tag{5.27}$$

where $\alpha \in \mathbb{C}$ and $\boldsymbol{\beta} = (\beta_x, \beta_v, \beta_r, \beta_q)^\top \in \mathbb{C}^4$ are the coefficients of state variables at time t. When $c \in \mathbb{C}$, $\Psi(c, \mathbf{X}, t, T)$ is the discounted characteristic function of x_T. From the terminal condition, $\Psi(c, \mathbf{X}, T, T) = \exp(cx_T)$, we can get that $\beta_x = c$.

Proposition 5. *The coefficients of the transition function* $\Psi(c, \mathbf{X}, t, T) = \exp(\alpha + \boldsymbol{\beta}\mathbf{X}_t^\top)$ *is given by:*

$$
\begin{aligned}
\beta_q &= -\frac{2c\left(1-e^{-\gamma_q(T-t)}\right)}{2\gamma_q-(\gamma_q-\kappa_q)(1-e^{-\gamma_q(T-t)})} \\
\beta_r &= -\frac{2(1-c)\left(1-e^{-\gamma_r(T-t)}\right)}{2\gamma_r-(\gamma_r-\kappa_r)(1-e^{-\gamma_r(T-t)})} \\
\beta_v &= -\frac{(c-c^2)\left(1-e^{-\gamma_v(T-t)}\right)}{2\gamma_r-(\gamma_v-\kappa_v)(1-e^{-\gamma_c(T-t)})} \\
\alpha &= -\frac{\kappa_r\bar{r}}{\sigma_r^2}\left((\gamma_r-\kappa_r)(T-t)+2\ln\left[1-\frac{\gamma_r-\kappa_r}{2\gamma_r}(1-e^{-\gamma_r(T-t)})\right]\right) \\
&\quad -\frac{\kappa_q\bar{q}}{\sigma_q^2}\left((\gamma_q-\kappa_q)(T-t)+2\ln\left[1-\frac{\gamma_q-\kappa_q}{2\gamma_q}(1-e^{-\gamma_q(T-t)})\right]\right) \\
&\quad -\frac{\kappa_v\bar{v}}{\sigma_v^2}\left((\gamma_v-\bar{\kappa}_v)(T-t)+2\ln\left[1-\frac{\gamma_v-\bar{\kappa}_v}{2\gamma_v}(1-e^{-\gamma_v(T-t)})\right]\right) \\
&\quad +\lambda_s(T-t)\left(\exp(c\mu_J+\frac{c^2\sigma_J^2}{2})-1\right),
\end{aligned}
\tag{5.28}
$$

The derivation of Proposition 5 is based on Ito's lemma as follows.

Proof. For convenience, I will expand Eq. (5.27) and assume the discounted characteristic function for x_t is of the affine type:

$$
f(c;t,x,V,r,q) = \exp(\alpha(c,t)+\beta_x(c,t)x_t+\beta_v(c,t)V_t+\beta_r(c,t)r_t+\beta_q(c,t)q_t), \tag{5.29}
$$

where $c \in \mathbb{C}$, and $\alpha(c,t)$ and $\beta_{v/r/q}(c,t)$ are functions of c and t. Define x_t^c, V_t^c, r_t^c

and q_t^c are the continuous parts of corresponding processes, i.e.

$$dx_t^c = (r_t - q_t - \frac{1}{2}V_t)dt + \sqrt{V_t}dW_t^s, \tag{5.30}$$

$$dV_t^c = \kappa_v(\bar{v} - V_t)dt + \sigma_v\sqrt{V_t}dW_t^v, \tag{5.31}$$

$$dr_t^c = dr_t, \tag{5.32}$$

$$dq_t^c = dq_t. \tag{5.33}$$

Apply Ito's formula to the characteristic function,

$$\begin{aligned} df(c;t,x,V,r,q) =& f_t'dt + f_x'dx_t^c + f_V'dV_t^c + f_r'dr_t^c + f_q'dq_t^c + f_{x,V}''dx_t^c dV_t^c \\ &+ f_{x,r}''dx_t^c dr_t^c + f_{x,q}''dx_t^c dq_t^c + f_{V,r}''dV_t^c dr_t^c + f_{V,q}''dV_t^c dq_t^c \\ &+ f_{r,q}''dr_t^c dq_t^c + \frac{1}{2}f_{x,x}''dx_t^c dx_t^c + \frac{1}{2}f_{V,V}''dV_t^c dV_t^c \\ &+ \frac{1}{2}f_{r,r}''dr_t^c dr_t^c + \frac{1}{2}f_{q,q}''dq_t^c dq_t^c + \Delta f(c;t,x_t,V_t,r_t,q_t) \end{aligned} \tag{5.34}$$

Then we can list the relative derivatives,

$$\begin{aligned} f_t'(c) =& (\alpha' + \beta_v'V_t + \beta_r'r_t + \beta_q'q_t)f(c), \\ f_i'(c) =& \beta_i f(c), \\ f_{i,j}''(c) =& \beta_i\beta_j f(c), \end{aligned} \tag{5.35}$$

where $i, j \in [x, V, r, q]$ and $\beta_x = c$. Substitute the derivatives in Eq. (5.35)] into

Eq. (5.34), we have

$$\begin{aligned}\frac{df(c;t,x,V,r,q)}{f(c;t,x,V,r,q)} =&(\alpha' + \beta'_v V_t + \beta'_r r_t + \beta'_q q_t)dt + cdx_t^c + \beta_v dV_t^c + \beta_r dr_t^c + \beta_q dq_t^c \\ &+ c\beta_v dx_t^c dV_t^c + c\beta_r dx_t^c dr_t^c + c\beta_q dx_t^c dq_t^c + \beta_v\beta_r dV_t^c dr_t^c \\ &+ \beta_v\beta_q dV_t^c dq_t^c + \beta_r\beta_q dr_t^c dq_t^c + \frac{1}{2}c^2 dx_t^c dx_t^c + \frac{1}{2}\beta_v^2 dV_t^c dV_t^c \\ &+ \frac{1}{2}\beta_r^2 dr_t^c dr_t^c + \frac{1}{2}\beta_q^2 dq_t^c dq_t^c + \Delta f(c;t,x_t,V_t,r_t,q_t). \end{aligned} \tag{5.36}$$

The discrete parts, which comes from the jump processes, denoted as $\Delta f(c;t,x_t,V_t,r_t,q_t)$, is calculated by

$$\begin{aligned}\Delta f(c;t,x_t,V_t,r_t,q_t) =&f(c;t,x_t,V_t,r_t,q_t) - f(c;t-,x_{t-},V_{t-},r_{t-},q_{t-}) \\ =&\lambda_s \int (e^{cU^s} - 1)p_s(U^s)dU^s dt, \end{aligned} \tag{5.37}$$

where $p_s(\cdot)$ here is the p.d.f of the jump size distribution.

Since $\mathbf{W_t}$ are independent, the cross terms $dx_t^c dV_t^c$, $dx_t^c dr_t^c$, $dV_t^c dr_t^c$, $dx_t^c dq_t^c$, $dV_t^c dq_t^c$, $dr_t^c dq_t^c$ are all equal to 0. Then we have

$$\begin{aligned}\frac{df(c;t,x,V,r,q)}{f(c;t,x,V,r,q)} =&(\alpha' + \beta'_v V_t + \beta'_r r_t + \beta'_q q_t)dt + c(r_t - q_t - \frac{1}{2}V_t)dt \\ &+ c\sqrt{V_t}dW_t^s + \beta_v\kappa_v(\bar{v} - V_t)dt + \beta_v\sigma_v\sqrt{V_t}dW_t^v \\ &+ \beta_r\kappa_r(\bar{r} - r_t)dt + \beta_r\sigma_r\sqrt{r_t}dW_t^r + \beta_q\kappa_q(\bar{q} - q_t)dt + \beta_q\sigma_q\sqrt{q_t}dW_t^q \\ &+ \frac{1}{2}c^2 V_t dt + \frac{1}{2}\sigma_v^2\beta_v^2 V_t dt + \frac{1}{2}\beta_r^2\sigma_r^2 r_t dt + \frac{1}{2}\beta_q^2\sigma_q^2 q_t dt \\ &+ \lambda_s \int (e^{cU^s} - 1)p_s(U^s)dU^s dt \end{aligned}$$

$f(c;t,x,V,r,q)$ being a martingale requires $\mathbb{E}[df] = r_t f dt$, that is

$$
\begin{aligned}
&(\alpha' + \beta_v' V_t + \beta_r' r_t + \beta_q' q_t)dt + c(r_t - q_t - \frac{1}{2}V_t)dt \\
&+ \beta_v \kappa_v (\bar{v} - V_t)dt + \beta_r \kappa_r (\bar{r} - r_t)dt + \beta_q \kappa_q (\bar{q} - q_t)dt \\
&+ \frac{1}{2}c^2 V_t dt + \frac{1}{2}\sigma_v^2 \beta_v^2 V_t dt + \frac{1}{2}\beta_r^2 \sigma_r^2 r_t dt + \frac{1}{2}\beta_q^2 \sigma_q^2 q_t dt \\
&+ \lambda_s \int (e^{cU^s} - 1) p_s(U^s) dU^s dt \\
&= r_t dt,
\end{aligned}
$$

which can be arranged as the ordinary differential equations (ODEs) form as the following

The ODEs for β

$$
\begin{aligned}
\dot{\beta} = &\begin{bmatrix} 0 \\ 0 \\ 1 \\ 0 \end{bmatrix} - \begin{bmatrix} 0 & 0 & 0 & 0 \\ -\frac{1}{2} & -\kappa_v & 0 & 0 \\ 1 & 0 & -\kappa_r & 0 \\ -1 & 0 & 0 & -\kappa_q \end{bmatrix} \begin{bmatrix} \beta_x \\ \beta_v \\ \beta_r \\ \beta_q \end{bmatrix} \\
&- \frac{1}{2} \begin{bmatrix} 0 \\ \beta_x^2 + 2\sigma_v \rho \beta_x \beta_v + \sigma_v^2 \beta_v^2 \\ \sigma_r^2 \beta_r^2 \\ \sigma_q^2 \beta_q^2 \end{bmatrix} - \begin{bmatrix} 0 \\ 0 \\ 0 \\ 0 \end{bmatrix}
\end{aligned}
\tag{5.38}
$$

and the ODE for α

$$
\dot{\alpha} = -\kappa_v \bar{v} \beta_v - \kappa_r \bar{r} \beta_r - \kappa_q \bar{q} \beta_q - \lambda_s (\theta(\beta_x) - 1) \tag{5.39}
$$

The terminal condition is $\beta_x(T,c) = c$, $\beta_{v/r/q}(T,c) = 0$, thus we have $\beta_x(t,c) = c$. Firstly derive $\beta_q(t,c)$.

$$\begin{aligned}\dot{\beta}_q(t,c) &= \beta_x + \kappa_q\beta_q - \frac{1}{2}\sigma_q^2\beta_q^2 \\ &= c + \kappa_q\beta_q - \frac{1}{2}\sigma_q^2\beta_q^2 \end{aligned} \tag{5.40}$$

Set $\mathcal{S} = -\sigma_q^2 c/2$ and $\mathcal{R} = \kappa_q$ and $y'' - \mathcal{R}y' + \mathcal{S}y = 0$. Then we have the solution to the function $y^2 - \kappa_q y - \sigma_q^2 c/2 = 0$ is

$$\frac{\kappa_q \pm \sqrt{\kappa_q^2 + 2\sigma_q^2 c}}{2} = \frac{\kappa_q \pm \gamma_q}{2}$$

where $\gamma_q = \sqrt{\kappa_q^2 + 2\sigma_q^2 c}$. The general solution for the linear ODE is of the form

$$y = a_1 e^{\frac{\kappa_q+\gamma_q}{2}t} + a_2 e^{\frac{\kappa_q-\gamma_q}{2}t}$$

for some constant a_1 and a_2. The derivative of y should be 0 when $t = T$

$$y'(T,c) = \frac{\kappa_q + \gamma_q}{2} a_1 e^{\frac{\kappa_q+\gamma_q}{2}T} + \frac{\kappa_q - \gamma_q}{2} a_2 e^{\frac{\kappa_q-\gamma_q}{2}T} = 0$$

Thus we have the relationship between these constants

$$\frac{\kappa_q + \gamma_q}{2} a_1 e^{\frac{\kappa_q+\gamma_q}{2}T} = -\frac{\kappa_q - \gamma_q}{2} a_2 e^{\frac{\kappa_q-\gamma_q}{2}T}$$

We can choose

$$a_1 = \frac{2m}{\kappa_q + \gamma_q} e^{-\frac{\kappa_q + \gamma_q}{2} T}, \quad a_2 = -\frac{2m}{\kappa_q - \gamma_q} e^{-\frac{\kappa_q - \gamma_q}{2} T}$$

where m is a constant number. Then we set the solution to be

$$\frac{2m}{\kappa_q + \gamma_q} e^{-\frac{\kappa_q + \gamma_q}{2} T + \frac{\kappa_q + \gamma_q}{2} t} - \frac{2m}{\kappa_q - \gamma_q} e^{-\frac{\kappa_q - \gamma_q}{2} T + \frac{\kappa_q - \gamma_q}{2} t},$$

which is

$$\begin{aligned} y &= \frac{2m}{\kappa_q + \gamma_q} e^{-\frac{\kappa_q + \gamma_q}{2}(T-t)} - \frac{2m}{\kappa_q - \gamma_q} e^{-\frac{\kappa_q - \gamma_q}{2}(T-t)} \\ y' &= m e^{-\frac{\kappa_q + \gamma_q}{2}(T-t)} - m e^{-\frac{\kappa_q - \gamma_q}{2}(T-t)}. \end{aligned}$$

Thus we have

$$\begin{aligned}
\beta_q &= -\frac{y'}{-\frac{\sigma_q^2}{2}y} \\
&= \frac{2}{\sigma_q^2}\frac{me^{-\frac{\kappa_q+\gamma_q}{2}(T-t)} - me^{-\frac{\kappa_q-\gamma_q}{2}(T-t)}}{\frac{2m}{\kappa_q+\gamma_q}e^{-\frac{\kappa_q+\gamma_q}{2}(T-t)} - \frac{2m}{\kappa_q-\gamma_q}e^{-\frac{\kappa_q-\gamma_q}{2}(T-t)}} \\
&= \frac{2}{\sigma_q^2}\frac{e^{-\frac{\gamma_q}{2}(T-t)} - e^{-\frac{-\gamma_q}{2}(T-t)}}{\frac{2}{\kappa_q+\gamma_q}e^{-\frac{\gamma_q}{2}(T-t)} - \frac{2}{\kappa_q-\gamma_q}e^{-\frac{-\gamma_q}{2}(T-t)}} \\
&= \frac{2}{\sigma_q^2}\frac{(\kappa_q^2-\gamma_q^2)\left(e^{-\frac{\gamma_q}{2}(T-t)} - e^{-\frac{-\gamma_q}{2}(T-t)}\right)}{2(\kappa_q-\gamma_q)e^{-\frac{\gamma_q}{2}(T-t)} - 2(\kappa_q+\gamma_q)e^{-\frac{-\gamma_q}{2}(T-t)}} \\
&= \frac{2}{\sigma_q^2}\frac{(\kappa_q^2-\kappa_q^2-2\sigma_q^2 c)\left(e^{-\frac{\gamma_q}{2}(T-t)} - e^{\frac{\gamma_q}{2}(T-t)}\right)}{2(\kappa_q-\gamma_q)e^{-\frac{\gamma_q}{2}(T-t)} - 2(\kappa_q+\gamma_q)e^{\frac{\gamma_q}{2}(T-t)}} \\
&= -\frac{2c\left(e^{-\gamma_q(T-t)} - 1\right)}{(\kappa_q-\gamma_q)e^{-\gamma_q(T-t)} - (\kappa_q+\gamma_q)} \\
&= -\frac{-2c\left(1 - e^{-\gamma_q(T-t)}\right)}{-(\kappa_q-\gamma_q)(1-e^{-\gamma_q(T-t)}) + (\kappa_q-\gamma_q) - (\kappa_q+\gamma_q)} \\
&= -\frac{-2c\left(1 - e^{-\gamma_q(T-t)}\right)}{-(\kappa_q-\gamma_q)(1-e^{-\gamma_q(T-t)}) - 2\gamma_q} \\
&= -\frac{2c\left(1 - e^{-\gamma_q(T-t)}\right)}{2\gamma_q - (\gamma_q-\kappa_q)(1-e^{-\gamma_q(T-t)})}.
\end{aligned} \tag{5.41}$$

For the ODE for β_r, the derivation is similar except that c is replaced with $1-c$ because the ODE is of the form

$$\begin{aligned}
\dot{\beta}_r(t,c) &= -\beta_x + \kappa_r\beta_r - \frac{1}{2}\sigma_r^2\beta_r^2 \\
&= 1 - c + \kappa_r\beta_r - \frac{1}{2}\sigma_r^2\beta_r^2.
\end{aligned}$$

So the result is then

$$\beta_r = -\frac{2(1-c)\left(1-e^{-\gamma_r(T-t)}\right)}{2\gamma_r-(\gamma_r-\kappa_r)(1-e^{-\gamma_r(T-t)})},$$

where $\gamma_r = \sqrt{\kappa_r^2 + 2(1-c)\sigma_r^2}$.

Then the ODE for the variance process, the β_v is then of the form:

$$\begin{aligned}\dot{\beta}_v &= \frac{\beta_x}{2} + \kappa_v\beta_v - \frac{1}{2}\left(\beta_x^2 + \sigma_v^2\beta_v^2\right) \\ &= \frac{c-c^2}{2} + \kappa_v\beta_v - \frac{1}{2}\sigma_v^2\beta_v^2\end{aligned}$$

Denote $\gamma_v = \sqrt{\kappa_v^2 + (c-c^2)\sigma_v^2}$, which leads to:

$$\beta_v = -\frac{(c-c^2)\left(1-e^{-\gamma_v(T-t)}\right)}{2\gamma_r-(\gamma_v-\kappa_v)(1-e^{-\gamma_c(T-t)})}$$

Then we can integrate the ODE of α to get the solution for α

$$\dot{\alpha} = -\kappa_v\bar{v}\beta_v - \kappa_r\bar{r}\beta_r - \kappa_q\bar{q}\beta_q - \lambda_s(\theta(c)-1)$$

Now we consider the integration of $-\kappa_q\bar{q}\beta_q$

$$\begin{aligned}
\int_0^\tau -\kappa_q\bar{q}\beta_q(s)ds &= -\kappa_q\bar{q}\int_0^\tau \beta_q(s)ds \\
&= -\kappa_q\bar{q}\int_0^\tau -\frac{y(s)'}{-\frac{\sigma_q^2}{2}y(s)}ds \\
&= -\frac{2\kappa_q\bar{q}}{\sigma_q^2}\ln(y(s))|_0^\tau \\
&= -\frac{2\kappa_q\bar{q}}{\sigma_q^2}\ln\frac{y(\tau)}{y(0)} \\
&= -\frac{\kappa_q\bar{q}}{\sigma_q^2}\left((\gamma_q-\kappa_q)\tau + 2\ln\left[1-\frac{\gamma_q-\kappa_q}{2\gamma_q}(1-e^{-\gamma_q\tau})\right]\right)
\end{aligned}$$

Thus

$$\begin{aligned}
\alpha = &-\frac{\kappa_r\bar{r}}{\sigma_r^2}\left((\gamma_r-\kappa_r)(T-t) + 2\ln\left[1-\frac{\gamma_r-\kappa_r}{2\gamma_r}(1-e^{-\gamma_r(T-t)})\right]\right) \\
&-\frac{\kappa_q\bar{q}}{\sigma_q^2}\left((\gamma_q-\kappa_q)(T-t) + 2\ln\left[1-\frac{\gamma_q-\kappa_q}{2\gamma_q}(1-e^{-\gamma_q(T-t)})\right]\right) \\
&-\frac{\kappa_v\bar{v}}{\sigma_v^2}\left((\gamma_v-\bar{\kappa}_v)(T-t) + 2\ln\left[1-\frac{\gamma_v-\bar{\kappa}_v}{2\gamma_v}(1-e^{-\gamma_v(T-t)})\right]\right) \\
&+\lambda_s(T-t)\left(\exp(c\mu_J+\frac{c^2\sigma_J^2}{2})-1\right). \qquad (5.42)
\end{aligned}$$

Gather the information above, we have the coefficients of the characteristic function as

$$
\begin{aligned}
\beta_q =& -\frac{2c\left(1-e^{-\gamma_q(T-t)}\right)}{2\gamma_q-(\gamma_q-\kappa_q)(1-e^{-\gamma_q(T-t)})}\\
\beta_r =& -\frac{2(1-c)\left(1-e^{-\gamma_r(T-t)}\right)}{2\gamma_r-(\gamma_r-\kappa_r)(1-e^{-\gamma_r(T-t)})}\\
\beta_v =& -\frac{(c-c^2)\left(1-e^{-\gamma_v(T-t)}\right)}{2\gamma_r-(\gamma_v-\kappa_v)(1-e^{-\gamma_c(T-t)})}\\
\alpha =& -\frac{\kappa_r\bar{r}}{\sigma_r^2}\left((\gamma_r-\kappa_r)(T-t)+2\ln\left[1-\frac{\gamma_r-\kappa_r}{2\gamma_r}(1-e^{-\gamma_r(T-t)})\right]\right)\\
&-\frac{\kappa_q\bar{q}}{\sigma_q^2}\left((\gamma_q-\kappa_q)(T-t)+2\ln\left[1-\frac{\gamma_q-\kappa_q}{2\gamma_q}(1-e^{-\gamma_q(T-t)})\right]\right)\\
&-\frac{\kappa_v\bar{v}}{\sigma_v^2}\left((\gamma_v-\bar{\kappa}_v)(T-t)+2\ln\left[1-\frac{\gamma_v-\bar{\kappa}_v}{2\gamma_v}(1-e^{-\gamma_v(T-t)})\right]\right)\\
&+\lambda_s(T-t)\left(\exp(c\mu_J+\frac{c^2\sigma_J^2}{2})-1\right),
\end{aligned}
$$

where $\gamma_q = \sqrt{\kappa_q^2+2\sigma_q^2 c}$, $\gamma_r = \sqrt{\kappa_r^2+2\sigma_r^2(1-c)}$, $\gamma_v = \sqrt{\kappa_v^2+(c-c^2)\sigma_v^2}$. The derivation comes from the application of Ito's lemma on the discounted characteristic function.

End of proof. □

For a specific strike price K, I denote $k_t = K/S_t$ as the moneyness at time t, and then the European FX call option expiring at T is given by,

$$C_t = S_t(P_1 - k_t P_2), \tag{5.43}$$

where

$$P_1 = \frac{\Psi(1, \mathbf{X}, t, T)}{2} - \frac{1}{\pi}\int_0^\infty \frac{\Im(\Psi(1-iu, \mathbf{X}, t, T))e^{iu\ln k_t}}{u}du,$$
$$P_2 = \frac{\Psi(0, \mathbf{X}, t, T)}{2} - \frac{1}{\pi}\int_0^\infty \frac{\Im(\Psi(-iu, \mathbf{X}, t, T))e^{iu\ln k_t}}{u}du,$$

and $\Im(\cdot)$ is the imaginary part of a complex number. Put option price can be calculated easily by the put-call parity.

Note that under $\mathbb{Q}$, the transition function $\Psi(1, \mathbf{X}, t, T)$ with $c = 1$ is an analogue of the 'discounted forward FX rate' since

$$\Psi(1, \mathbf{X}, t, T) = \mathbb{E}[\exp(\int_t^T -r_t d\tau)e^{X_T}].$$

Also when $c = 0$ we have

$$\Psi(0, \mathbf{X}, t, T) = \mathbb{E}[\exp(\int_t^T -r_t d\tau)],$$

which can then applied in the put-call parity as the foreign bond price. With Eq. (5.28) being the closed form of the coefficients for the discounted characteristic function Eq. (5.27) and the option price in Eq. (5.43), we can then compute the model implied FX option quotes.

5.6 Model implied FX option quotes

For the selected four currency pairs, I will apply spot percentage delta convention since I only compute FX option with tenor up to 1Y and the foreign currencies (EUR or USD) are the premium currency of the four currency pairs. In this

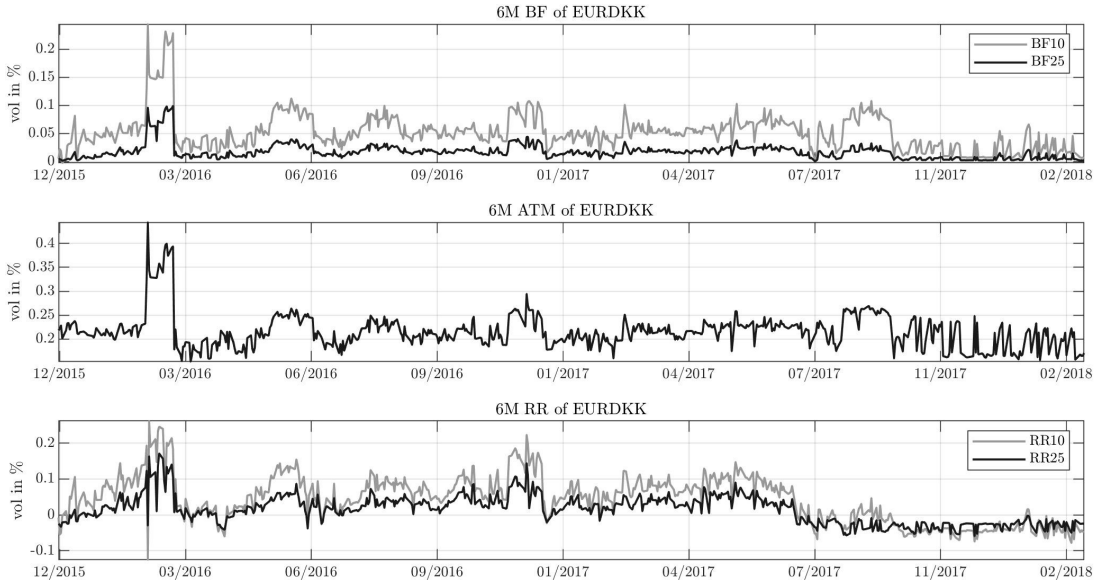

Figure 5.5: Synthetic spot FX rate implied FX option quotes with 6M maturity. In this figure, I calculate the five pivot quotes for 6M tenor FX option based on the synthetic spot FX rates for EURDKK. Appendix Fig. 1 is for USDSAR, USDQAR and USDNGN. The top panel contains model implied 10 and 25 delta BF, the middle panel contains delta-neutral ATM and the bottom panel is for 10 and 25 delta RR. In each plot, the lighter lines are for 10-delta strategies and darker lines are for 25-delta strategies.

section, I use the estimated parameters in previous section and calculate the 5 typical types of FX option quotes, i.e. butterflies ($BF10$, $BF25$), delta-neutral at-the-money (ATM) and risk reversals ($RR25$, $RR10$), for the 4 currency pairs through all the dates out of the short-term estimation window. Fig. 5.5 (with Appendix Fig. 1) and Fig. 5.6 (with Appendix Fig. 2) illustrate the model implied quotes for FX options expiring in 6M and 1Y, respectively. Each set of sub-plot represents one of the chosen currency pairs. Table 5.5 and Table 5.6 provide a more detail descriptive statistics of the model implied quotes.

The first rows of the plots present the time series of $BF25$ and $BF10$. In the plots, $BF10$ is always higher than $BF25$ for all the currency pairs through out the chosen periods, which is commonly observed from normal FX option market and

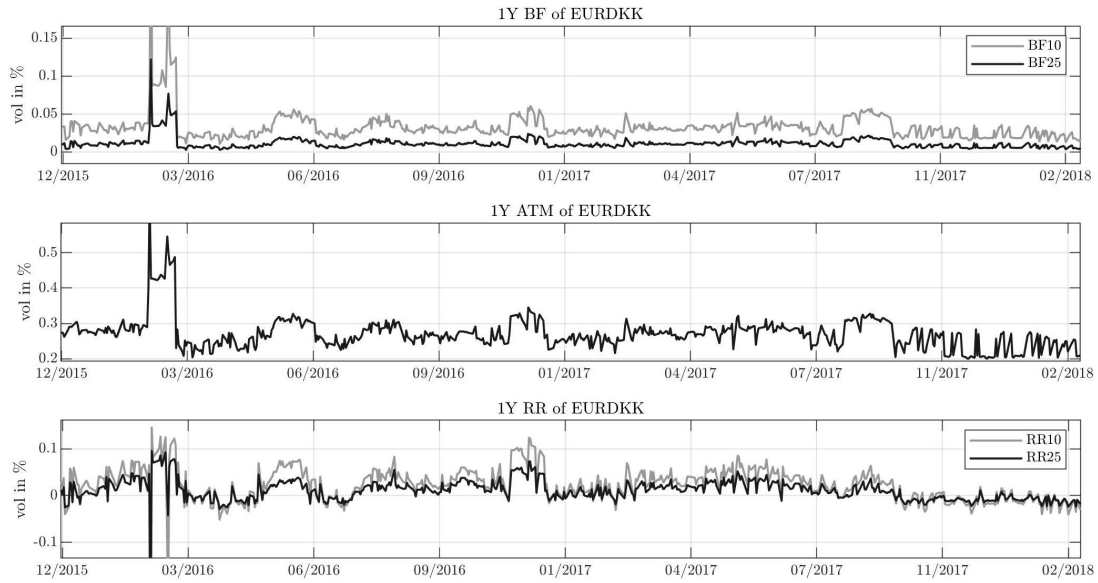

Figure 5.6: Synthetic spot FX rate implied FX option quotes with 1Y maturity
Similar to Fig. 5.5, this figure and Appendix Fig. 2 are the model implied FX option quotes but for 1Y maturity. Again, the lighter lines are for 10-delta strategies and darker lines are for 25-delta strategies. From the figure we can see that the 10-delta strategies are normally larger in magnitude compared with the 25-delta strategies.

means the distributions have more mass at the tails than normal distribution and the shape of volatility smiles are convex. USDSAR and USDQAR generally have higher BF (1Y mean value in percentage are 0.0558 and 0.0873, respectively) than the rest 2 currency pairs (1Y mean value is 0.0158 for EURDKK and 0.0107 for USDNGN) showing their synthetic spot FX rates are less concentrated at the pegged level compared with normal distribution, and the volatility surfaces should be less flat. The second rows illustrate the behaviour of ATM within the periods. USDNGN has the overall highest mean volatility level (6M being 5.5869 and 1Y being 6.0981) and EURDKK remains at the lowest volatility level (6M being 0.2243 and 1Y being 0.2833). Time series of RR in the third rows shows the direction of the slop of volatility surfaces are not always the same. For example USDQAR 1Y has $RR10$ from -3.2423 to 4.3184. All the currency

Table 5.5: Descriptive statistics for 6M FX option quotes

		Obs.	Mean	Std. dev.	Min	Max	Skewness	Kurtosis
EURDKK								
	$BF10$	562	0.0509	0.0320	0.0070	0.2338	2.1558	11.2107
	$BF25$	562	0.0158	0.0123	0.0005	0.0926	2.8863	16.4019
	ATM	562	0.2243	0.0363	0.1619	0.4497	1.9007	10.6401
	$RR25$	562	0.0143	0.0381	-0.0561	0.1713	0.5884	3.7988
	$RR10$	562	0.0409	0.0632	-0.1209	0.2590	0.3077	2.9484
USDSAR								
	$BF10$	325	0.2160	0.1498	0.0146	0.7859	1.3964	5.0199
	$BF25$	325	0.0558	0.0623	-0.0383	0.3194	1.4041	5.9937
	ATM	325	1.3994	0.3250	0.6713	2.3255	0.2260	2.7783
	$RR25$	325	-0.2124	0.2825	-1.0308	0.6262	-0.2682	3.7404
	$RR10$	325	-0.3780	0.5215	-1.7954	1.3254	-0.0453	3.7801
USDQAR								
	$BF10$	258	0.2668	0.1127	0.0384	0.6341	0.7448	3.9354
	$BF25$	258	0.0873	0.0394	-0.0024	0.2281	0.5738	3.8434
	ATM	258	1.5391	0.4132	0.5507	2.4656	-0.6703	2.5880
	$RR25$	258	0.0432	0.2457	-0.5962	0.8973	0.4082	4.2447
	$RR10$	258	0.0870	0.4595	-1.2559	1.6112	0.3221	4.1930
USDNGN								
	$BF10$	258	0.0470	0.0690	0.0206	0.4425	4.5713	23.9796
	$BF25$	258	0.0107	0.0123	-0.0561	0.0851	2.4294	24.1641
	ATM	258	5.5869	0.8118	4.7823	11.6211	4.4301	29.3505
	$RR25$	258	0.0576	0.4262	-1.4081	3.5000	4.5976	42.0696
	$RR10$	258	0.0976	0.7470	-2.6711	5.8952	3.8372	37.0228
USDNGN–NDF								
	$BF10$	858	0.2540	0.9222	-0.3132	12.3339	8.2980	87.9506
	$BF25$	858	0.1456	0.6994	-0.4574	9.6083	8.7385	95.7332
	ATM	858	9.5820	4.2257	4.6922	34.7252	2.0256	8.9166
	$RR25$	858	1.9932	4.0240	-3.7201	40.1916	4.7364	33.6054
	$RR10$	858	3.1984	5.6373	-5.8391	53.0278	4.1059	26.7439

Notes: Corresponding to Fig. 5.5, this table documents the summary statistics of the model implied quotes for the 6M tenor FX option quotes. It also contains the data for Fig. 5.7, which is based on the NDF of USDNGN. I should note that in the table USDNGN-NDF has 600 more observation than the normal forward counterpart. This is because for the USDNGN-NDF, I take the short-term parameters estimated from the normal forward rate bias as given, thus do not exclude this estimation window from the option computation.

pairs experienced positive and negative risk reversals. The sudden changes on the quotes indicate the inconsistency of the market's anticipation.

In Fig. 5.7 and Fig. 5.8, I show the strategies implied by the USDNGN-NDF for the whole dataset period with 6 month and 1 year maturity, respectively. I should note that in the table USDNGN-NDF has 600 more observations than the

Table 5.6: Descriptive statistics for 1Y FX option quotes

		Obs.	Mean	Std. dev.	Min	Max	Skewness	Kurtosis
EURDKK								
	$BF10$	562	0.0332	0.0204	0.0126	0.3368	7.7886	97.4944
	$BF25$	562	0.0109	0.0072	0.0024	0.0996	5.6579	53.2469
	ATM	562	0.2833	0.0450	0.2142	0.6659	2.6693	17.6885
	$RR25$	562	0.0091	0.0239	-0.2829	0.0929	-2.7327	42.3836
	$RR10$	562	0.0183	0.0463	-0.7353	0.1406	-7.5436	126.1996
USDSAR								
	$BF10$	325	0.6503	0.4516	0.0129	2.3324	1.3101	4.9721
	$BF25$	325	0.1762	0.2080	-0.1203	0.9725	1.2011	5.0067
	ATM	325	2.3884	0.7030	0.7392	4.1814	-0.1142	2.6983
	$RR25$	325	-0.5236	0.6826	-2.4532	1.2199	-0.2450	3.3918
	$RR10$	325	-0.8904	1.3562	-4.4067	3.3659	0.1090	3.6232
USDQAR								
	$BF10$	258	0.8712	0.3941	0.0270	2.0483	0.1218	3.6963
	$BF25$	258	0.3003	0.1617	0.0052	0.6884	0.0297	2.5044
	ATM	258	2.4385	0.8873	0.6127	4.1655	-0.5042	2.0052
	$RR25$	258	0.2391	0.6588	-1.3025	2.2409	0.4079	3.7027
	$RR10$	258	0.4170	1.3053	-3.2423	4.3184	0.2959	3.6907
USDNGN								
	$BF10$	258	0.0581	0.0447	0.0246	0.2936	2.5912	10.3167
	$BF25$	258	0.0158	0.0090	0.0085	0.0591	2.6002	10.3733
	ATM	258	6.0981	0.8666	5.0460	12.3018	4.2083	27.3144
	$RR25$	258	0.0670	0.2654	-0.9056	2.1099	3.5713	33.8126
	$RR10$	258	0.1134	0.4984	-1.6947	3.8334	3.2071	30.5312
USDNGN–NDF								
	$BF10$	858	0.2945	0.5249	-0.4579	5.8482	5.9789	52.8188
	$BF25$	858	0.1075	0.3206	-0.2455	5.1205	10.7173	139.2258
	ATM	858	10.6075	4.7322	4.8842	41.3973	2.2418	10.7230
	$RR25$	858	1.0531	2.4446	-2.1082	23.6532	4.3675	30.0622
	$RR10$	858	1.7036	3.6424	-3.8257	30.8596	3.3778	19.5235

Notes: Corresponding to Fig. 5.6, this table documents the summary statistics of the model implied quotes for the 1Y tenor FX option quotes. It also contains the data for Fig. 5.8, which is based on the NDF of USDNGN. The table structure is similar to Table 5.5.

normal forward counterpart. This is because for the USDNGN-NDF, I take the short-term parameters estimated from the normal forward rate bias as given, thus do not exclude this estimation window from the option computation. Clearly in these two figures, the peaks of all strategies appear at the de-peg day. Before the announcement of realignment, NDF implied volatility is high, with maximum 1Y ATM being 41.3973, and heavily skewed, with maximum 1Y $RR10$ being over 30, because of the market's firm confidence of future peg break. Notice that 1Y tenor

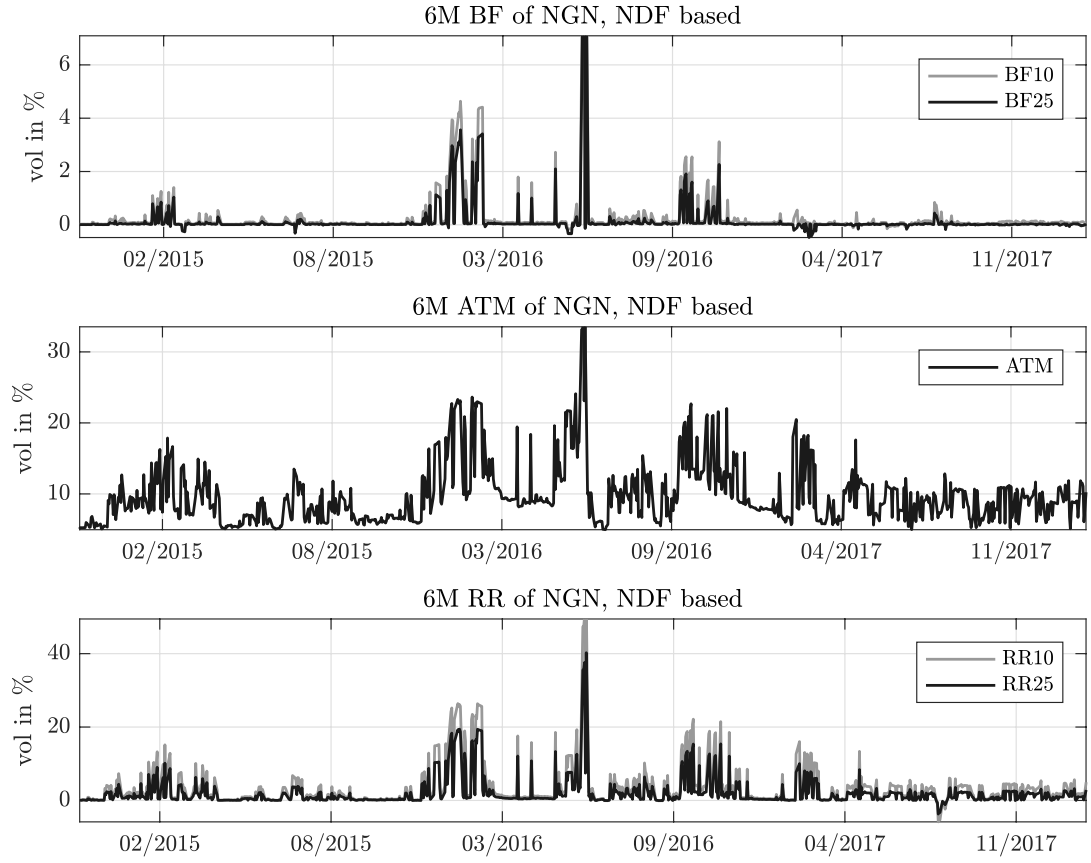

Figure 5.7: USDNGN NDF implied FX option quotes with 6M maturity
Different from the ones in Fig. 5.5 and Fig. 5.6, I use the NDF to estimate the bias and implied 6M FX option quotes for USDNGN. The three panels are BF, ATM and RR quotes respectively. Lighter lines in the first and last plots are for 10 delta quotes, while the darker lines are for 25 delta quotes. Compared with the normal forward, NDF implied option quotes show more clear patterns of the the volatility surfaces dynamics.

BF (maximum 5.1205) and RR (maximum 23.6532) are smaller compared with 6M ones (9.6083 and 40.1916 respectively), while 1Y ATM (maximum 41.3973) is higher than 6M ATM (maximum 34.7252). This shows 1Y tenor option has higher overall volatility smile, but with a more flat smile curve. This is consistent with the fact that farther future is more unpredictable.

Fig. 5.9 contains the synthetic spot FX rate implied volatility surfaces for the four currency pairs on February 23rd, 2018 with 6M, 9M and 1Y maturities.

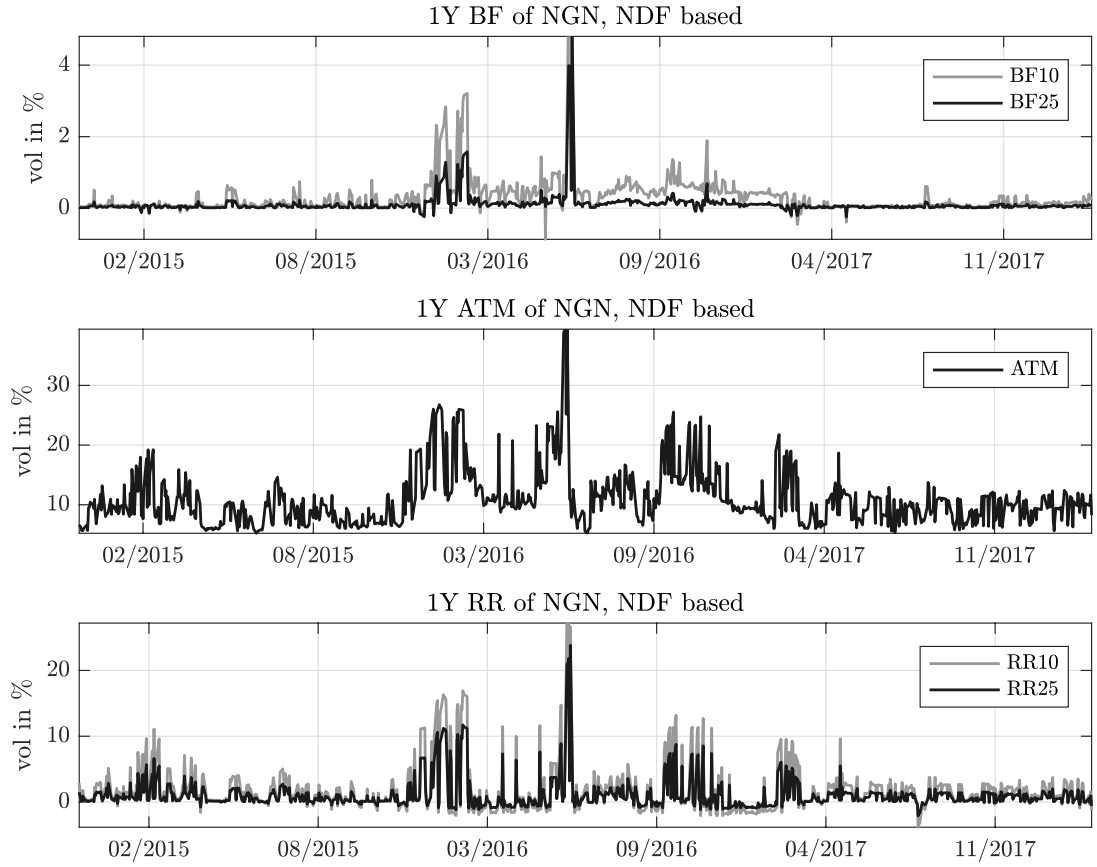

Figure 5.8: USDNGN NDF implied FX option quotes with 1Y maturity. Similar to Fig. 5.7, this figure use the NDF to compute the implied FX option quotes but with 1Y maturity for USDNGN. Notice that 1Y tenor BF and RR are smaller compared with 6M ones, while 1Y ATM is higher than 6M ATM. This shows 1Y tenor option has higher overall volatility smile, but with a more flat smile curve.

In the figure, the x-axis represents call delta from 0.1 to 0.9, which is the spot percentage delta by convention. From the figure we observe that all the currency pairs have an overall increasing volatility surface as the maturity grows at all the deltas (or moneyness). EURDKK and USDNGN have more flat smiles than the two GCC currency pairs, which is also reflected by the smaller BF in Fig. 5.5 and Fig. 5.6. EURDKK and USDQAR on this date skew to a opposite direction compared with USDSAR, consistent with the sign of their RR.

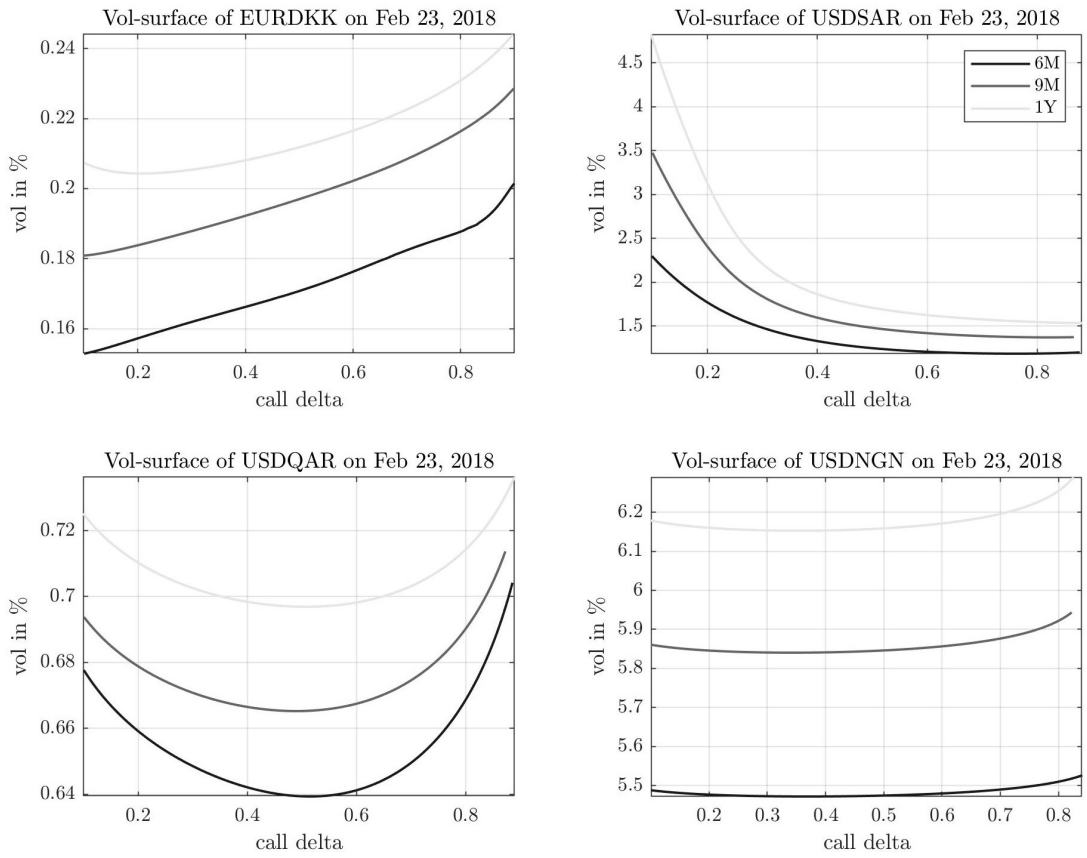

Figure 5.9: Synthetic spot FX rate implied volatility surfaces on February 23rd, 2018. I select the model implied volatility surface on February 23rd, 2018 for the EURDKK, USDSAR, USDQAR and USDNGN. The x-axis is call delta from 0.1 to 0.9, and y-axis is Black-Scholes implied volatility in percentage. Lightest lines represent for 1Y tenor volatility smiles and darkest lines are for 6M tenor smiles.

I also provide the implied volatility surfaces of USDNGN based on NDF on June 16th, 2016 and June 21st, 2016 in Fig. 5.10, which represent the volatility surfaces before and after the realignment jump and illustrate the effectiveness of the model. Volatility level on June 16th, 6M ATM being 23.10, is much higher than that after the de-peg (6M ATM equals 10.25), and so is the slop of the surface. The RR of the volatility surface is thus higher before de-peg (6M RR being 7.44) than after the event (6M RR being 1.17), meaning that call options

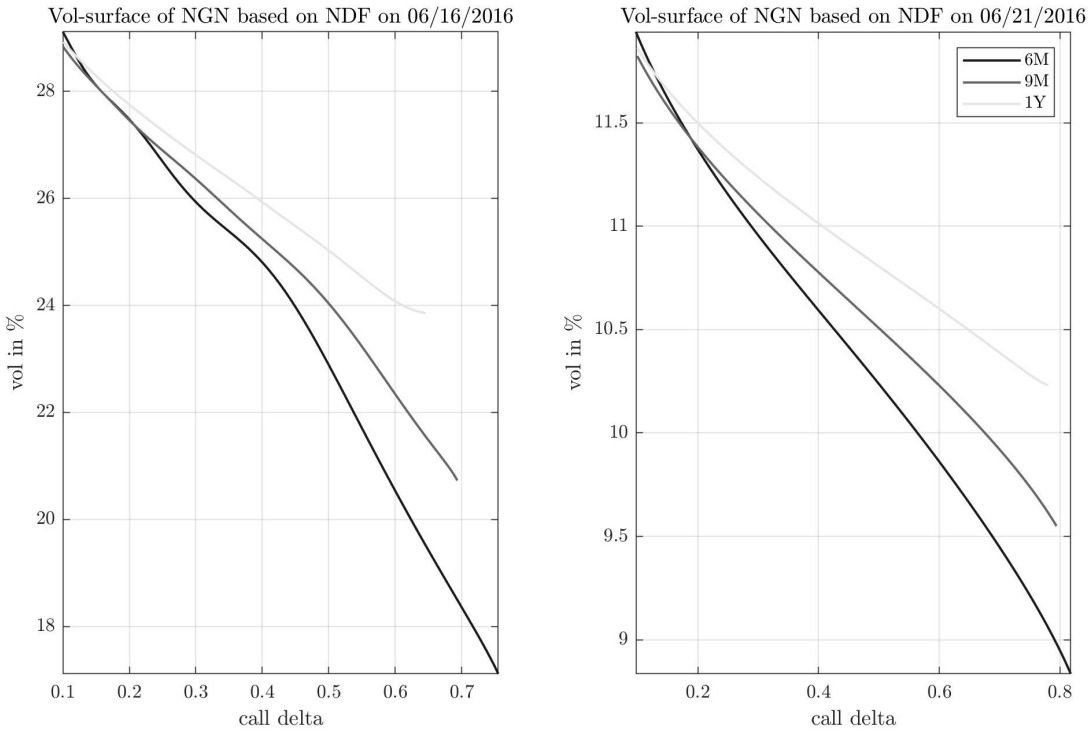

Figure 5.10: Implied volatility surfaces of USDNGN based on NDF before and after the de-peg (June 16th and 21st, 2016)
Addition to Fig. 5.9, I pick the model implied volatility surface before and after the de-peg event of USDNGN based on the NDF bias and present in this figure. The x-axis is call delta from 0.1 to 0.9, and y-axis is Black-Scholes implied volatility in percentage. Lightest lines represent for 1Y tenor volatility smiles and darkest lines are for 6M tenor smiles.

are more expensive or in-favour than put options. This indicates the shift of volatile outlook of the market before and after the major shock and the market's expectation of NGN's sudden depreciation.

These exercises show the proposed model can capture the uncertainty information that embedded in the forward rates, and the model implies an fair FX option price that can be used to manage such risk.

5.7 Chapter conclusions

In this chapter, I fill the option pricing gap for pegged FX rates. By studying their character, I identify the synthetic spot FX rate and spot rate bias implied by the forward FX rate deviation evidence. Spot rate bias information are divided into two parts by maturity and I then propose to use an affine jump diffusion model to capture the trading uncertainty and realignment uncertainty embedded in these two parts of the spot rate bias. Given the fact that FX option transactions for such currency pairs are currently rare and there are very limited data available, I design a novel approach to estimate the model parameters from forward market data. Then under an adjusted risk neutral measure, I provide the FX option price model based on the forward looking information.

In the empirical part of this chapter, I apply the proposed approach on four representative pegged currency pairs (EURDKK, USDSAR, USDQAR and USDNGN) and provide model implied volatility quotes under the FX option market convention. The volatility surfaces generated by the proposed model do reflect the market's anticipation of the future uncertainties, thus offer an alternative way to manage the FX rate risk of pegged currency pairs. This also contributes to the literature on asset pricing with consistent prices, their associated forward price puzzles and carry trade opportunities. This chapter can also be extended on improving the parameter estimation method, and upgrade the model to fit the synthetic spot FX rate process better.

Chapter 6

Conclusions

6.1 Summary and remarks

This thesis provides an extensive analysis of the OTC FX option pricing. Previous works tend to focus only on the actively traded FX option contracts and ignore the numerous currency pairs that have relatively small option market. Literature in this area, such as Beber et al. [2010], Chalamandaris and Tsekrekos [2010] and Hanke et al. [2018], generally are based on mature FX option markets and presume the existence of the whole updated volatility surfaces. In this thesis, I fill such research gap by proposing models to price FX options with inactive market quotes.

In Chapter 3 I introduce and modify the discrete time model by Heston and Nandi [2000] to the FX world and allow a multi-factor structure. The GARCH based processes can be estimated from spot rate observations by MLE, without the requirement of option data. I further test various specifications of the model and generate model implied volatility quotes out-of-sample for five actively traded currencies over different tenors. I show that the model provides a good first pass for generating volatility level when option data is absent, and by the calibration to

a few market volatility quotes, which is the case for sparsely updated FX option market, the fitting performance improves significantly. The main strengths of the proposed model is then 1) it can contain multiple NGARCH type of factors in the mean return process, which allows the model to have more general and complex dynamic structure; 2) The parameter estimation is simple and can be improved to have much better time-series performance with only few option data for calibration; 3) It generates accurate ATM volatility level and dynamic. One of the main limitations of such discrete time type model is the computational time. Even with a closed-form solution, this model is still slower than the continuous models. Based on the empirical analysis in Section 3.6.2, the proposed model has better performance at the ATM, but still need to be improved at the deeply out-of-the-money part of the implied volatility surface.

This works is useful for industry practitioners because it allows the market maker to provide FX options on more currency pairs that were sparsely traded. Therefore investors hold such currencies have more tools to hedge their currency risk.

These GARCH type model based results suggest that even though spot FX rate and interest rates do share similar information with the FX option, the OTC FX option still contains extra information that diverge the level and shape of the implied volatility surface.

To address this issue, in Chapter 4 I extend the model in Chapter 3 to include ACP jump component in the return process and allow multiple factors in both domestic and foreign interest rates to capture the hidden interest factors. The jump process can be estimated by non-parametric methods from high frequency spot FX rate data. To improve the performance, I design a time-step size adjust-

ment rule so that different frequency return data is applied to price options with different tenors. I find that this adjustment helps reduce the over mean reverting property of the variance process and thus preserve the implied volatility dynamic, especially for longer maturity contacts which require large number of iteration in the calculation. Further I assume there is one hidden factor in each of the domestic and foreign drift terms, and calibrate these factors against the market option quotes.

The empirical test of this chapter shows that using the hidden factors calibrated from the market option data improves the model performance. These extracted factors show strong persistence dynamic character with large β_k. The improvement of the performance also comes from the correlated shock terms among the hidden factors and variance process. This correlation affect the skewness of the spot rate distribution thus influence the shape of the implied volatility surface. The test also shows the adjusted time-step size overcomes over mean reverting of the variance process and improves the performance for longer maturity options. The main limitation of this chapter is that the extracted hidden factors are not identified thus it is not studied in this chapter that what are the economic factors that causes these hidden dynamics.

The takeaway of this chapter is that the spot rate process can be modified by 1) including hidden interest factor 2) including correlation between the state variables and 3) adjusting the time-step size to yield better option pricing performance.

Chapter 5 focuses on option pricing for pegged FX rates, which has been neglected in the literature. By carefully studying the character of pegged FX rates and their forward rates, I identify the synthetic spot FX rates and spot rate bias

implied by the forward rate deviation. I formulate an affine jump diffusion model to capture the information reflected by the spot rate bias. Such information is categorised into trading uncertainty and policy realignment uncertainty, which are modelled by the diffusion and jump part of the model respectively. In the empirical analysis, I test the model on four representative pegged currency pairs. The simulation experiments based on the estimated parameters show that the model generated bias can adjust the process to be align with the market forward expectation. Then based on these parameters I calculated the implied volatility quotes under the market convention. These generated volatility surfaces has ideal skewness and kurtosis property and illustrates dynamics that reflect the market's anticipation of the future uncertainties. Therefore these synthetic volatility quotes offer an new way to manage the FX risk of the pegged currency pairs.

This chapter can benefit the industry by providing new tools to price FX options for the majority currency pairs that were not able to be priced. It helps market makers to generate benchmark quotes for these pegged currency pairs and provides instruments for investors holding assets denominated by these currencies to hedge their currency risk. The main limitation of the chapter is its model setting that it currently can not handle the volatility jumps that may happen along with the regime switch. Solving this issue requires different source of information that implies the volatility distribution after de-peg events.

6.2 Future work

This thesis can be further improved in various ways. From the option pricing model perspective, the proposed models have potential to be more generalised,

such as to include stochastic variance jump components and more flexible and general form of return, variance and interest rate dynamic. State variables also can be allowed to have correlations with each others. One of the obvious example is to allow volatility jumps in the peg currency synthetic spot rate process, which models the variance distribution changes along with the policy realignment. Non-parametrically models can be mixed into the FX option pricing, such as empirical characteristic function estimated from high frequency spot data. And for more general models, it is then a research question that how to estimate these models, especially given limited market derivatives data.

Based on the empirical works in this thesis, the OTC FX option markets contains unique information compared with their underlying spot markets. I contribute part of these differences to the hidden factors that affect the money account rate of return as in Chapter 4. And then use the bias information from forward contracts to price options for pegged currency pairs in Chapter 5. An possible extension is to find out what are the factors that contribute to such anticipation differences, and whether we can use these factors to improve the option pricing performance.

Appendix

The supplementary tables and figures of the main chapters are provided in this appendix. Appendix Fig. 1 corresponding to Fig. 5.5 and Appendix Fig. 2 corresponding to Fig. 5.6 in Chapter 5 illustrate the model implied quotes for FX options on the selected four currency pairs with maturity from 6M to 1Y, respectively. Each set of sub-plot represents one of the chosen currency pairs. These supplementary figures covers the currency pairs including USDSAR, USDQAR and USDNGN.

Appendix Table 1 documents the estimated parameters for the ASTSV model on AUDUSD, EURUSD, USDCAD and USDJPY, as an extension to the Table 3.4 in Chapter 3. More data sample characteristic of EUR, CHF, GBP and JPY for Chapter 4 can refer to Appendix Table 3 as the extension to the Table 4.1.

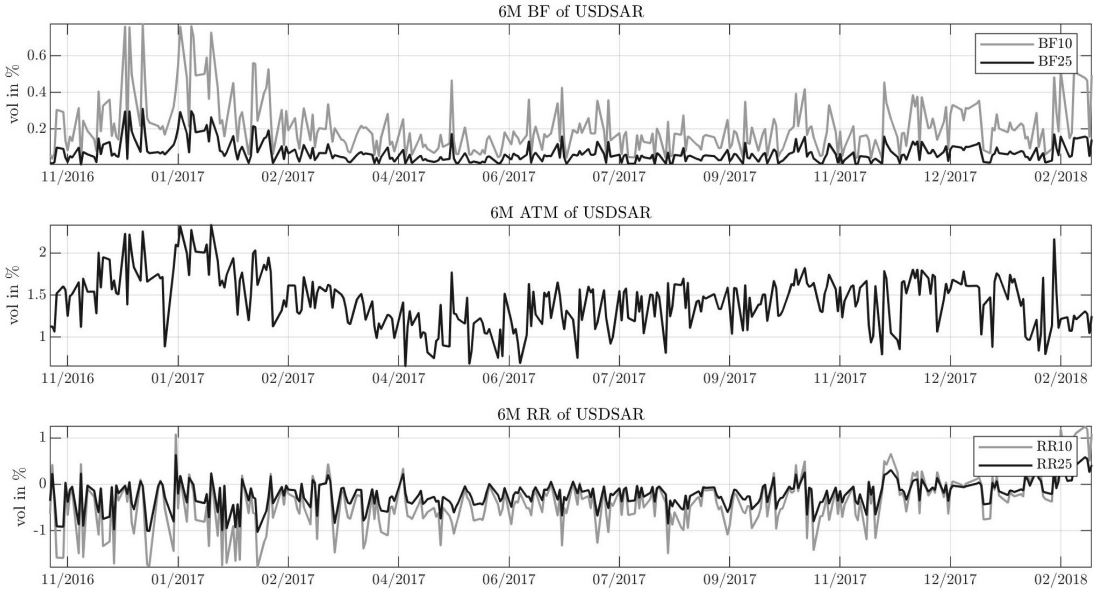

Figure 1: Synthetic spot FX rate implied FX option quotes with 6M maturity (Cont.). In this figure, I calculate the five pivot quotes for 6M tenor FX option based on the synthetic spot FX rates for USDSAR, USDQAR and USDNGN. The top panel contains model implied 10 and 25 delta BF, the middle panel contains delta-neutral ATM and the bottom panel is for 10 and 25 delta RR. In each plot, the lighter lines are for 10-delta strategies and darker lines are for 25-delta strategies. Note that for USDNGN, the quotes here are based on normal forwards.

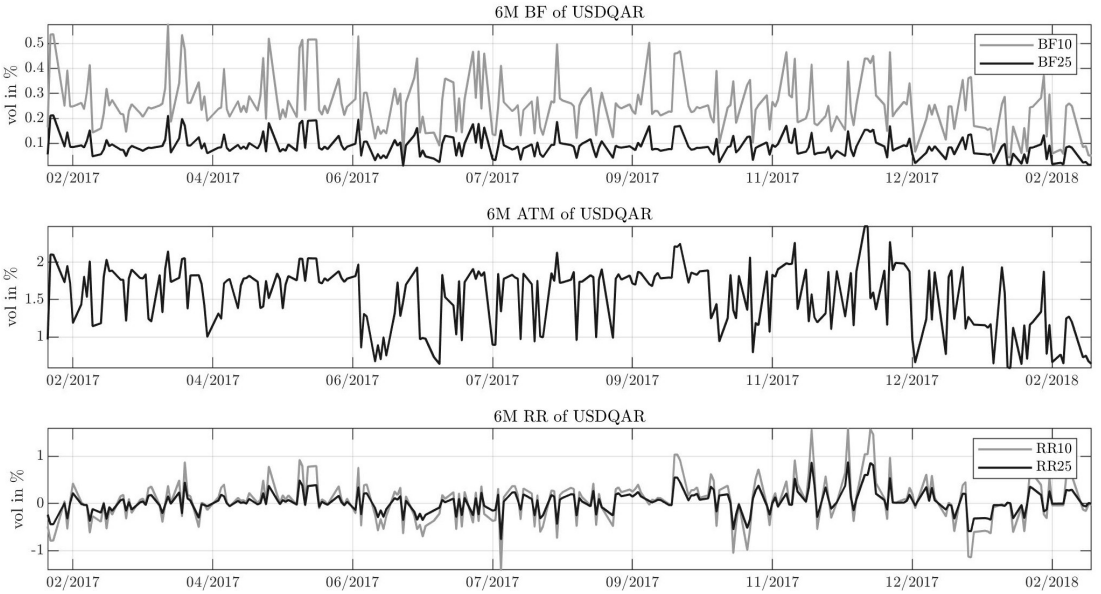

Figure 1: Synthetic spot FX rate implied FX option quotes with 6M maturity (Cont.).

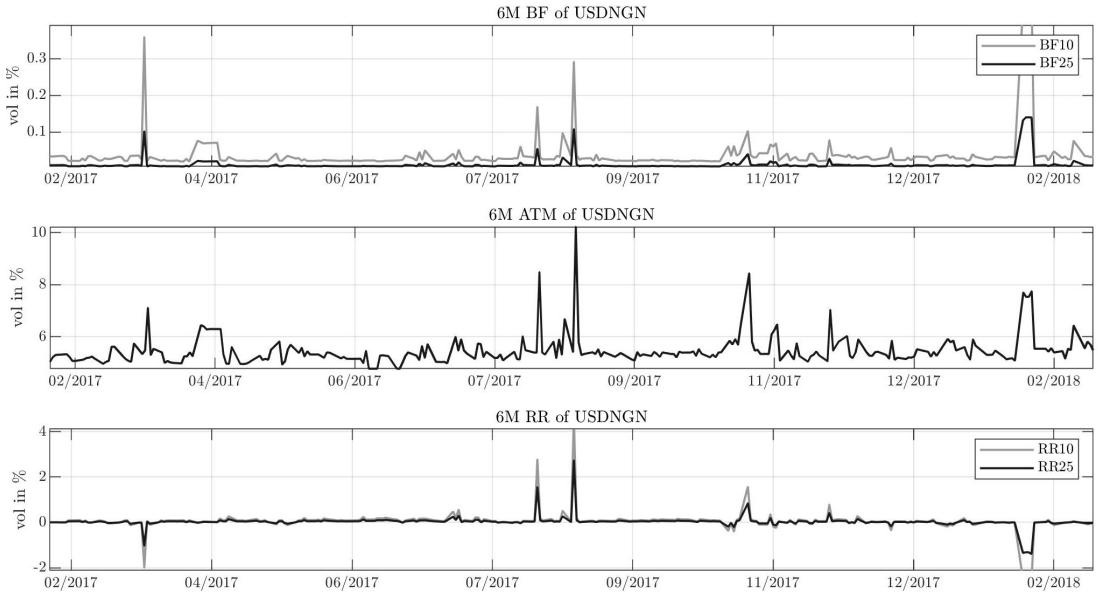

Figure 1: Synthetic spot FX rate implied FX option quotes with 6M maturity (Cont.).

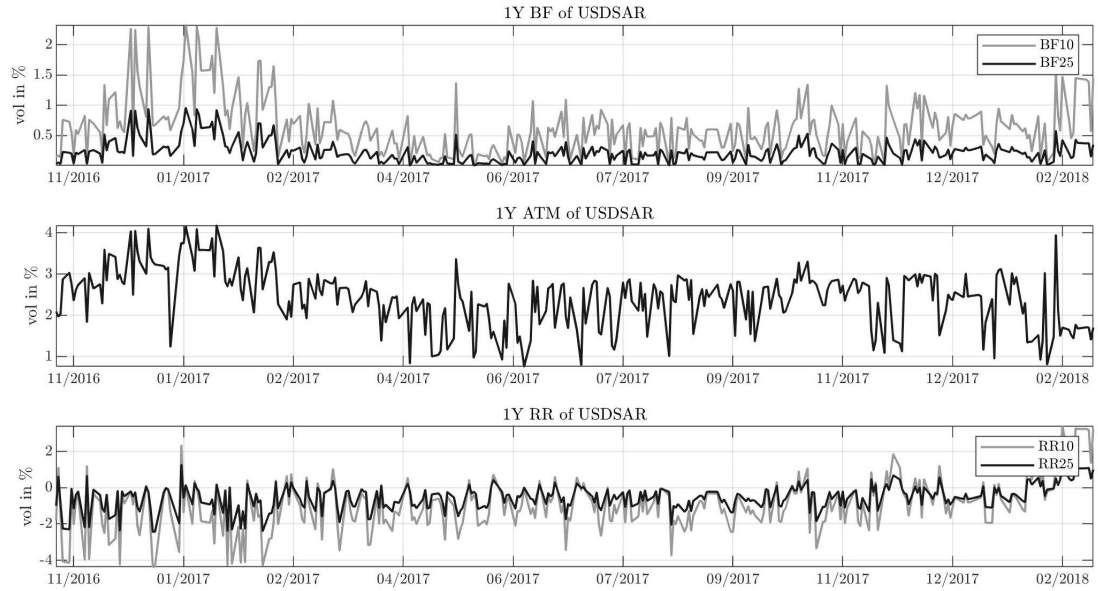

Figure 2: Synthetic spot FX rate implied FX option quotes with 1Y maturity (Cont.). Similar to Fig. 5.5, this figure is the model implied FX option quotes but for 1Y maturity. Again, the lighter lines are for 10-delta strategies and darker lines are for 25-delta strategies. From the figure we can see that the 10-delta strategies are normally larger in magnitude compared with the 25-delta strategies.

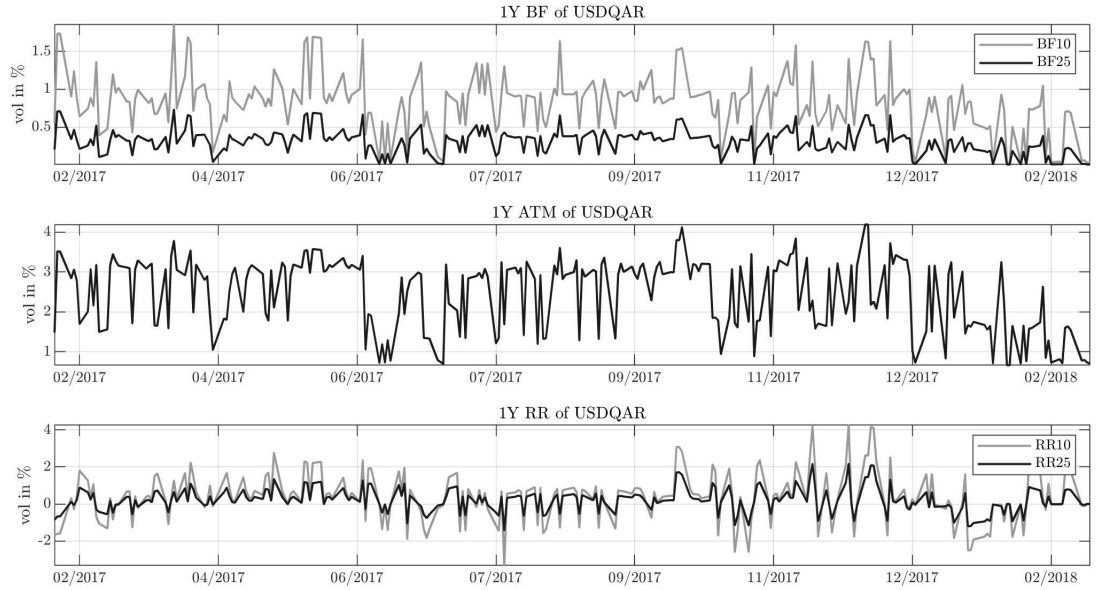

Figure 2: Synthetic spot FX rate implied FX option quotes with 1Y maturity (Cont.).

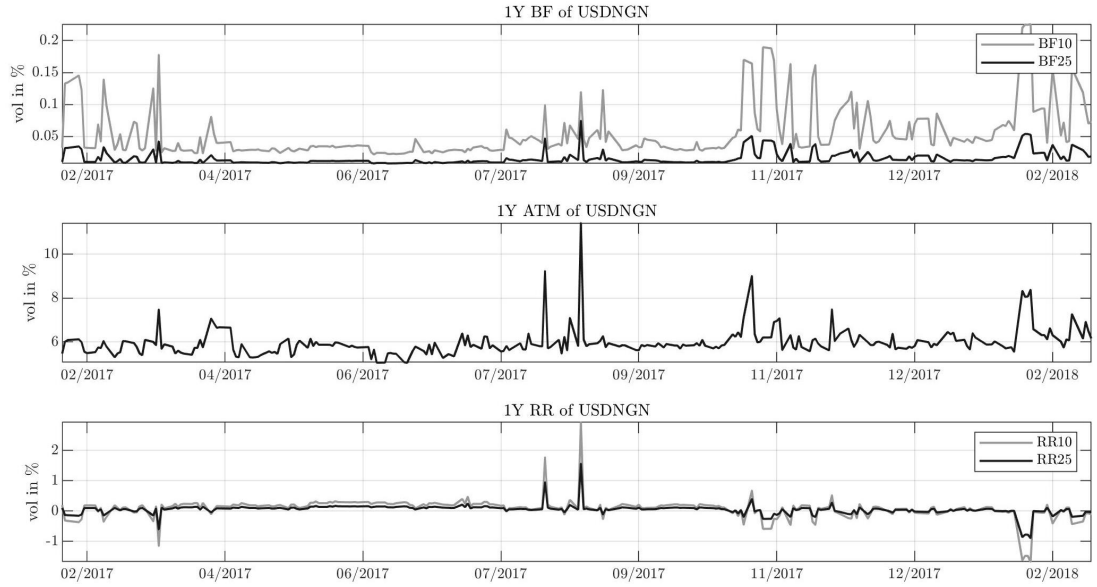

Figure 2: Synthetic spot FX rate implied FX option quotes with 1Y maturity (Cont.).

Table 1: ASTSV parameter estimation (Cont.)

	AUDUSD				
	6M	1Y	2Y	3Y	5Y
μ_{0f}	7.40E-05	3.51E-05	3.03E-05	3.16E-05	4.01E-05
μ_{1f}	0.98	0.99	0.99	0.99	0.99
λ_f	-9.99	10.00	9.92	9.97	10.00
ω_f	3.45E-94	2.69E-08	5.90E-10	6.59E-267	1.30E-10
β_f	0.52	0.80	0.84	0.86	0.91
α_f	3.13E-08	2.02E-08	6.29E-09	5.95E-09	3.49E-09
γ_f	-500.00	500.00	500.00	500.00	500.00
$\mathfrak{L}(\hat{\theta}_s)$	1.67E+03	1.61E+03	1.61E+03	1.61E+03	1.61E+03
μ_{0d}	-1.68E-06	2.05E-04	3.57E-07	7.71E-06	1.69E-05
μ_{1d}	0.99	0.91	0.99	0.99	0.99
λ_d	9.99	-0.46	10.00	10.00	10.00
ω_d	2.48E-09	5.27E-08	6.67E-248	1.72E-57	4.80E-32
β_d	0.73	0.87	0.89	0.89	0.92
α_d	8.08E-09	3.95E-07	3.83E-09	4.86E-09	3.68E-09
γ_d	500.00	-63.75	500.00	500.00	500.00
$\mathfrak{L}(\hat{\theta}_s)$	1.70E+03	1.45E+03	1.64E+03	1.61E+03	1.60E+03
λ_s	0.98	0.76	0.72	0.65	0.54
ω_s	2.76E-4	1.81E-04	1.87E-04	1.91E-04	1.95E-04
β_s	0.90	0.71	0.70	0.70	0.69
α_s	1.10E-04	1.40E-04	1.40E-04	1.39E-04	1.37E-04
γ_s	12.66	18.94	19.89	20.71	21.80
$\mathfrak{L}(\hat{\theta}_s)$	457.25	436.06	435.98	436.19	436.55
	EURUSD				
	6M	1Y	2Y	3Y	5Y
μ_{0f}	3.41E-06	1.10E-03	1.55E-03	-9.19E-06	-1.25E-05
μ_{1f}	0.99	0.87	0.82	1.00	1.00
λ_f	-9.90	-0.96	-10.00	10.00	9.96
ω_f	5.75E-10	6.43E-08	2.31E-07	1.18E-37	2.09E-16
β_f	0.91	0.85	0.87	0.87	0.94
α_f	1.48E-09	4.68E-07	3.54E-07	3.18E-09	1.20E-09
γ_f	-500.00	334.82	385.72	500.00	-500.00
$\mathfrak{L}(\hat{\theta}_s)$	1.54E+03	8.52E+02	1.15E+03	1.48E+03	1.48E+03
μ_{0d}	1.90E-06	1.47E-05	-5.61E-07	6.58E-06	1.45E-05
μ_{1d}	0.99	0.97	0.99	0.99	0.99
λ_d	10.00	9.96	10.00	10.00	10.00
ω_d	3.01E-09	3.57E-53	0.00E+00	1.72E-57	4.80E-32
β_d	0.69	0.77	0.90	0.90	0.92
α_d	1.04E-08	6.70E-09	3.66E-09	3.91E-09	3.48E-09
γ_d	500.00	500.00	500.00	500.00	500.00
$\mathfrak{L}(\hat{\theta}_s)$	1.49E+03	1.06E+03	1.45E+03	1.42E+03	1.41E+03
λ_s	-0.10	-0.40	-0.44	-0.56	-0.69
ω_s	4.73E-05	3.42E-05	4.01E-05	4.02E-05	4.07E-05
β_s	0.84	0.82	0.85	0.85	0.85
α_s	6.25E-05	7.72E-05	6.99E-05	6.82E-05	6.75E-05
γ_s	22.82	26.38	21.32	22.31	23.15
$\mathfrak{L}(\hat{\theta}_s)$	438.36	307.34	424.34	424.42	424.60

Notes: The short rate dynamics $r_k(t+\eta) = \mu_{0k} + \mu_{1k} r_k(t) + \lambda_k h_k(t+\eta) + \sqrt{h_k(t+\eta)} u_k(t+\eta)$ and $h_k(t+\eta) = \omega_k + \beta_k h_k(t) + \alpha_k (u_k(t) - \gamma_k \sqrt{h_k(t)})^2$ are calibrated to the historical yield curve data. We apply the short rate estimated dynamics to the one-month quoted timed deposit rate and return the observed log-likelihoods $\mathfrak{L}(\hat{\theta}_k)$ for comparison with $\mathfrak{L}(\hat{\theta}_s)$ the log-likelihoods of the spot exchange rate returns at the monthly frequency.

Table 1: ASTSV parameter estimation (Cont.)

	USDCAD				
	6M	1Y	2Y	3Y	5Y
μ_{0f}	-1.59E-06	2.02E-04	9.26E-07	1.45E-07	1.30E-05
μ_{1f}	0.99	0.91	0.99	0.99	0.99
λ_f	9.98	-0.47	10.00	9.96	9.93
ω_f	2.68E-09	5.77E-08	0.00E+00	9.62E-265	4.80E-32
β_f	0.71	0.87	0.89	0.87	0.92
α_f	8.59E-09	3.99E-07	2.57E-09	3.88E-09	3.13E-09
γ_f	500.00	-87.82	500.00	500.00	500.00
$\mathfrak{L}(\hat{\theta}_s)$	1.70E+03	1.50E+03	1.04E+03	8.95E+02	8.78E+02
μ_{0d}	2.30E-05	3.11E-05	5.69E-06	8.21E-06	2.13E-05
μ_{1d}	0.98	0.98	0.99	0.99	0.98
λ_d	0.05	9.99	10.00	10.00	9.99
ω_d	2.88E-09	4.69E-09	8.82E-09	9.61E-09	1.26E-08
β_d	0.66	0.75	0.56	0.60	0.55
α_d	1.30E-08	8.03E-09	3.67E-09	3.24E-09	4.14E-09
γ_d	209.23	500.00	500.00	500.00	500.00
$\mathfrak{L}(\hat{\theta}_s)$	1.68E+03	1.65E+03	1.03E+03	8.88E+02	8.79E+02
λ_s	-0.27	-0.39	0.02	0.54	0.68
ω_s	5.23E-06	5.19E-06	4.91E-05	4.94E-05	4.91E-05
β_s	1.00	1.00	0.85	0.82	0.82
α_s	1.66E-07	2.52E-07	4.21E-05	5.78E-05	5.88E-05
γ_s	136.91	97.77	-36.14	-36.25	-36.12
$\mathfrak{L}(\hat{\theta}_s)$	551.82	551.90	300.44	260.29	260.30
	USDJPY				
	6M	1Y	2Y	3Y	5Y
μ_{0f}	-1.69E-06	2.49E-04	-2.47E-06	3.41E-06	9.63E-06
μ_{1f}	0.99	0.89	1.00	0.99	0.99
λ_f	9.99	-10.00	10.00	10.00	9.94
ω_f	2.82E-09	1.26E-07	0.00E+00	1.72E-57	4.80E-32
β_f	0.70	0.87	0.89	0.89	0.92
α_f	8.86E-09	1.41E-06	3.91E-09	4.83E-09	3.57E-09
γ_f	500.00	-499.98	500.00	500.00	500.00
$\mathfrak{L}(\hat{\theta}_s)$	1.70E+03	1.31E+03	1.70E+03	1.67E+03	1.66E+03
μ_{0d}	2.60E-05	1.06E-05	1.41E-05	1.59E-05	2.02E-05
μ_{1d}	0.88	0.96	0.96	0.96	0.96
λ_d	-9.91	-9.93	-10.00	-9.97	-9.80
ω_d	1.04E-267	0.00E+00	0.00E+00	0.00E+00	2.18E-19
β_d	0.80	0.91	0.91	0.95	0.88
α_d	2.32E-09	1.27E-10	2.39E-10	1.46E-10	1.13E-09
γ_d	-500.00	-500.00	-500.00	-500.00	-500.00
$\mathfrak{L}(\hat{\theta}_s)$	1.85E+03	1.90E+03	1.98E+03	1.92E+03	1.85E+03
λ_s	2.81	2.53	2.98	3.03	3.16
ω_s	1.10E-05	2.41E-5	1.09E-05	9.13E-06	1.13E-05
β_s	0.94	0.95	0.93	0.94	0.94
α_s	5.04E-05	5.72E-05	5.52E-05	5.03E-05	5.04E-05
γ_s	-3.99	-3.66	-2.27	-2.85	-2.33
$\mathfrak{L}(\hat{\theta}_s)$	485.75	443.78	489.05	485.91	486.29

Table 2: ASV calibration adjustments (Cont.)

Currency	Strategy	1Y			2Y		
		α	γ	ζ	α	γ	ζ
AUDUSD	$\widetilde{BF}_{10}$	3.06E-06	122.5541	0.3966	3.41E-06	127.3123	1.0167
	$\widetilde{BF}_{25}$	5.49E-05	23.9143	-9.9772	5.75E-05	20.3219	-11.3734
	$\widetilde{AT}$	1.04E-06		5.6356	1.16E-06		9.735
	$\widetilde{RR}_{25}$	3.28E-07	114.3564	1.0343	9.64E-07	227.4117	17.6237
	$\widetilde{RR}_{10}$	3.29E-06	114.4447	1.0329	3.28E-06	118.2591	0.9433
EURUSD	$\widetilde{BF}_{10}$	1.96E-06	82.1613	0.3387	1.43E-06	121.7796	0.6686
	$\widetilde{BF}_{25}$	2.07E-05	28.1478	-9.1389	4.49E-06	74.3001	-2.0642
	$\widetilde{AT}$	3.87E-07		3.5461	4.45E-07		5.2167
	$\widetilde{RR}_{25}$	2.48E-07	322.4567	3.0285	2.04E-07	342.2352	7.4177
	$\widetilde{RR}_{10}$	2.53E-06	72.9664	7.3971	5.67E-07	190.0486	26.082
GBPUSD	$\widetilde{BF}_{10}$	8.62E-07	161.5054	1.0769	1.47E-06	140.922	1.1438
	$\widetilde{BF}_{25}$	1.06E-05	54.5887	-15.6857	2.59E-05	25.3295	-17.5142
	$\widetilde{AT}$	3.88E-07		3.7122	4.27E-07		6.1962
	$\widetilde{RR}_{25}$	1.38E-07	484.3177	4.2012	1.14E-07	522.9823	6.6826
	$\widetilde{RR}_{10}$	1.08E-07	558.8289	2.8041	2.38E-06	90.2603	9.3116
USDCAD	$\widetilde{BF}_{10}$	2.57E-06	-117.678	-1.7279	1.90E-06	-136.629	0.5732
	$\widetilde{BF}_{25}$	1.86E-06	-133.948	-0.7267	1.83E-06	-131.055	-0.631
	$\widetilde{AT}$	4.87E-07		5.8318	5.31E-07		11.8408
	$\widetilde{RR}_{25}$	3.84E-07	-301.22	-301.22	1.99E-06	-118.375	-0.5716
	$\widetilde{RR}_{10}$	1.85E-06	-113.337	0.6285	1.94E-06	-118.001	0.5831
USDJPY	$\widetilde{BF}_{10}$	2.32E-06	-173.846	4.8506	1.86E-06	-193.303	4.3697
	$\widetilde{BF}_{25}$	3.48E-06	-130.652	8.5358	1.42E-06	-216.099	4.2324
	$\widetilde{AT}$	1.37E-06		10.3351	1.65E-06		16.3169
	$\widetilde{RR}_{25}$	2.28E-05	4.9698	-0.9289	1.04E-06	190.6999	-83.6336
	$\widetilde{RR}_{25}$	1.05E-05	14.2869	-13.5317	3.53E-06	88.5417	0.7993

Notes: To fit the market quotation of $\widetilde{AT}$, α and ζ are calibrated though $\{\hat{\alpha}, \hat{\zeta}\} := \arg\min_{\{\hat{\alpha},\zeta\}} \sum_{d=1}^{D} (\widetilde{AT}_{0,d}(\tau) - \widetilde{AT}_{0,d}(\alpha, \zeta|\theta))^2$ while γ is also adjusted to model the quotations of $\widetilde{BF}_{\Delta}$ and $\widetilde{RR}_{\Delta}$. Then we fix the parameters $\hat{\theta}$ and carried through the entire evaluation window out-of-sample. The useful aspect of this adjustment is the degree of stability in the model fit given these parameters over the evaluation window, which is useful for the application on sparsely quoted FXOs.

Table 3: Sample characteristics (Cont.)

	Obs.	Mean	Std. dev.	Min	Max
			EUR		
Spot	7308001	1.2062	0.1682	0.8232	1.6035
r_1M	7204	1.7831	1.7047	-0.4550	5.8887
r_6M	7189	1.9954	1.6875	-0.4650	7.3700
r_1Y	7201	2.1391	1.6593	-0.3400	6.3335
r_2Y	6656	2.2514	1.5983	-0.0900	5.5600
σ_p(10)1M	1459	9.3863	2.4697	4.8750	18.1500
σ_p(25)1M	1459	8.8472	2.2601	4.5370	15.8873
$\widehat{AT}$1M	1459	8.3974	2.0680	4.2000	14.3750
σ_c(25)1M	1459	8.3073	1.9599	4.0880	14.0000
σ_c(10)1M	1459	8.4588	1.9528	4.1565	14.0880
σ_p(10)6M	1443	10.5385	2.1473	6.6255	15.4680
σ_p(25)6M	1443	9.4394	1.8253	5.8625	13.4425
$\widehat{AT}$6M	1443	8.5648	1.5036	5.2500	11.6800
σ_c(25)6M	1443	8.2715	1.2807	5.1375	11.2310
σ_c(10)6M	1443	8.4896	1.2251	5.4005	11.6190
σ_p(10)1Y	1428	11.0577	1.8991	7.6700	16.7550
σ_p(25)1Y	1428	9.7480	1.5827	6.7190	15.5960
$\widehat{AT}$1Y	1428	8.7646	1.2471	6.0000	14.3050
σ_c(25)1Y	1428	8.4526	1.0128	5.8810	13.9960
σ_c(10)1Y	1428	8.7335	0.9565	6.2125	13.8050
σ_p(10)2Y	1408	11.3114	1.6601	8.1255	14.9600
σ_p(25)2Y	1408	9.9825	1.3653	7.3625	13.0965
$\widehat{AT}$2Y	1408	9.0470	1.0772	6.6250	11.7775
σ_c(25)2Y	1408	8.7877	0.8854	6.4875	11.3965
σ_c(10)2Y	1408	9.0973	0.8490	6.8625	11.5375
			CHF		
	Obs.	Mean	Std. dev.	Min	Max
Spot	8159041	1.2065	0.2535	0.7103	1.8296
r_1M	7684	0.7232	1.1618	-3.4750	4.1400
r_6M	7733	0.8876	1.2046	-1.7950	4.2750
r_1Y	7748	1.0574	1.2030	-1.3950	4.7150
r_2Y	3937	0.4154	1.0221	-1.0500	3.6750
σ_p(10)1M	1253	9.2004	2.4204	4.6875	32.5765
σ_p(25)1M	1253	8.7512	2.2674	4.5125	30.0450
$\widehat{AT}$1M	1253	8.5504	2.1854	4.5750	27.9825
σ_c(25)1M	1253	8.8043	2.2265	4.9875	26.9450
σ_c(10)1M	1253	9.2850	2.3518	5.2875	28.1313
σ_p(10)6M	1220	9.8316	1.9580	6.2560	22.0450
σ_p(25)6M	1220	9.0910	1.6368	5.8310	19.1515
$\widehat{AT}$6M	1220	8.8275	1.5072	5.9000	17.1575
σ_c(25)6M	1220	9.2645	1.6162	6.3375	16.4015
σ_c(10)6M	1220	10.1372	1.8375	6.6625	17.4200
σ_p(10)1Y	1235	10.3591	1.7760	7.0313	19.4380
σ_p(25)1Y	1235	9.4378	1.3876	6.6190	16.4440
$\widehat{AT}$1Y	1235	9.1115	1.2554	6.6750	14.4880
σ_c(25)1Y	1235	9.5981	1.4202	6.8625	13.8440
σ_c(10)1Y	1235	10.6470	1.6763	7.4130	15.2130
σ_p(10)2Y	1155	10.8832	1.6155	7.8125	18.7375
σ_p(25)2Y	1155	9.8431	1.2337	7.3000	15.6000
$\widehat{AT}$2Y	1155	9.4385	1.1099	7.1150	13.7000
σ_c(25)2Y	1155	9.8160	1.2468	7.1475	13.1000
σ_c(10)2Y	1155	10.7737	1.4127	7.7250	14.6625

Notes: I interpolate the spot exchange rate tick data to a 1 minute grid from 1 millisecond past midnight to 1 millisecond to midnight GMT.

Table 3: Sample characteristics (Cont.)

			GBP		
	Obs.	Mean	Std. dev.	Min	Max
Spot	8159041	1.6131	0.1782	1.2038	2.1159
r_1M	7697	3.0832	2.4206	0.1600	7.6800
r_6M	7696	3.3111	2.3498	0.3400	8.1850
r_1Y	7694	3.5138	2.2655	0.4300	8.3100
r_2Y	5347	2.7952	1.6567	0.8400	6.8100
σ_p(10)1M	1404	9.4805	3.5278	4.7250	39.0375
σ_p(25)1M	1404	8.8289	3.0843	4.4565	34.0685
$\widetilde{AT}$1M	1404	8.2917	2.6521	4.3250	29.2000
σ_c(25)1M	1404	8.1466	2.3139	4.3940	25.0935
σ_c(10)1M	1404	8.2920	2.1841	4.5500	23.3125
σ_p(10)6M	1393	10.8891	2.7580	6.5685	20.7938
σ_p(25)6M	1393	9.6099	2.2928	5.9940	17.8940
$\widetilde{AT}$6M	1393	8.6162	1.8520	5.6000	15.1500
σ_c(25)6M	1393	8.2676	1.5509	5.5750	13.5435
σ_c(10)6M	1393	8.4717	1.4422	5.8750	13.4530
σ_p(10)1Y	1371	11.5133	2.3751	7.5505	19.5150
σ_p(25)1Y	1371	9.9641	1.9402	6.7625	16.0275
$\widetilde{AT}$1Y	1371	8.8280	1.5470	6.3000	13.5000
σ_c(25)1Y	1371	8.4418	1.2881	6.4250	12.4225
σ_c(10)1Y	1371	8.7126	1.2051	6.8438	12.5540
σ_p(10)2Y	1354	11.9339	2.0459	8.3375	18.7605
σ_p(25)2Y	1354	10.3368	1.6876	7.3935	15.5600
$\widetilde{AT}$2Y	1354	9.2261	1.3974	6.8750	13.4000
σ_c(25)2Y	1354	8.8523	1.2162	6.9685	12.5750
σ_c(10)2Y	1354	9.1358	1.1483	7.2995	12.5630
			JPY		
	Obs.	Mean	Std. dev.	Min	Max
Spot	8159041	108.4896	13.9679	75.6124	147.6081
r_1M	7618	0.1685	0.2722	-0.7950	1.7000
r_6M	7709	0.2798	0.3472	-0.3950	2.4250
r_1Y	7616	0.3829	0.3692	-0.2500	2.7750
r_2Y	7549	0.4481	0.3837	-0.1800	1.8500
σ_p(10)1M	1395	11.1883	2.7867	5.0685	20.0940
σ_p(25)1M	1395	10.4149	2.5787	4.7370	18.2795
$\widetilde{AT}$1M	1395	9.8337	2.4502	4.5180	17.4980
σ_c(25)1M	1395	9.7916	2.4765	4.5190	17.7545
σ_c(10)1M	1395	10.0204	2.5541	4.7313	18.3920
σ_p(10)6M	1392	12.0610	2.1635	7.2850	18.4150
σ_p(25)6M	1392	10.7809	1.8214	6.5350	16.0590
$\widetilde{AT}$6M	1392	9.9842	1.6682	6.0500	14.9900
σ_c(25)6M	1392	10.0230	1.7633	6.0005	15.3090
σ_c(10)6M	1392	10.5709	1.9947	6.3050	16.4650
σ_p(10)1Y	1393	12.7467	1.8789	5.2788	17.9365
σ_p(25)1Y	1393	11.0801	1.5024	3.8100	15.5615
$\widetilde{AT}$1Y	1393	10.1360	1.3581	2.9600	14.3800
σ_c(25)1Y	1393	10.2584	1.5002	2.8850	14.6865
σ_c(10)1Y	1393	11.0800	1.8293	3.4412	16.4615
σ_p(10)2Y	1362	13.6036	1.8162	10.7800	19.1560
σ_p(25)2Y	1362	11.5316	1.3762	9.2615	15.9380
$\widetilde{AT}$2Y	1362	10.4620	1.2364	8.2020	14.6500
σ_c(25)2Y	1362	10.5729	1.4080	7.8800	14.9380
σ_c(10)2Y	1362	11.5891	1.7886	7.7875	16.2690

References

Ait-Sahalia, Y. et al. (2008). Closed-form likelihood expansions for multivariate diffusions. *The Annals of Statistics 36*(2), 906–937. 101, 145

Aït-Sahalia, Y., D. Amengual, and E. Manresa (2015). Market-based estimation of stochastic volatility models. *Journal of Econometrics 187*(2), 418–435. 6, 146

Amin, K. I. and R. A. Jarrow (1991). Pricing foreign currency options under stochastic interest rates. *Journal of International Money and Finance 10*(3), 310–329. 34, 43, 106

Andersen, T. G., L. Benzoni, and J. Lund (2002). An empirical investigation of continuous-time equity return models. *The Journal of Finance 57*(3), 1239–1284. 146

Andersen, T. G., T. Bollerslev, and F. X. Diebold (2007). Roughing it up: Including jump components in the measurement, modeling and forecasting of return volatility. *The Review of Economics and Statistics 89*(4), 701–720. 119

Andersen, T. G., N. Fusari, and V. Todorov (2015). Parametric inference and

dynamic state recovery from option panels. *Econometrica 83*(3), 1081–1145. 6, 101, 146

Backus, D. K., S. Foresi, and C. I. Telmer (2001). Affine term structure models and the forward premium anomaly. *The Journal of Finance 56*(1), 279–304. 11

Bandi, F. M. and P. C. Phillips (2003). Fully nonparametric estimation of scalar diffusion models. *Econometrica 71*(1), 241–283. 146

Bansal, R. (1997). An exploration of the forward premium puzzle in currency markets. *The Review of Financial Studies 10*(2), 369–403. 145

Barndorff-Nielson, O. and N. Shephard (2004). Power and bipower variation with stochastic volatility and jumps. *Journal of Financial Econometrics 2*(1), 1–48. 118

Barndorff-Nielson, O. and N. Shephard (2006). Econometrics of testing for jumps in financial economics using bipower variation. *Journal of Financial Econometrics 4*(1), 1–30. 118

Barone-Adesi, G., R. F. Engle, and L. Mancini (2008). A GARCH option pricing model with filtered historical simulation. *Review of Financial Studies 21*(3), 1223–1258. 31, 35, 101

Bauwens, L., S. Laurent, and J. V. Rombouts (2006). Multivariate garch models: a survey. *Journal of Applied Econometrics 21*(1), 79–109. 35, 101

Beber, A., F. Breedon, and A. Buraschi (2010). Differences in beliefs and currency risk premiums. *Journal of Financial Economics 98*(3), 415–438. 6, 194

Black, F. and M. Scholes (1973). The pricing of options and corporate liabilities. *The Journal of Political Economy*, 637–654. 29

Bollen, N. P. and R. E. Whaley (2004). Does net buying pressure affect the shape of implied volatility functions? *The Journal of Finance 59*(2), 711–753. 6

Brandt, M. W. and P. Santa-Clara (2002). Simulated likelihood estimation of diffusions with an application to exchange rate dynamics in incomplete markets. *Journal of Financial Economics 63*(2), 161–210. 146

Brockwell, P., E. Chadraa, A. Lindner, et al. (2006). Continuous-time GARCH processes. *The Annals of Applied Probability 16*(2), 790–826. 37

Bull, A. D. et al. (2016). Near-optimal estimation of jump activity in semimartingales. *The Annals of Statistics 44*(1), 58–86. 146

Carr, P. and L. Wu (2007). Stochastic skew in currency options. *Journal of Financial Economics 86*(1), 213–247. 28, 29

Carr, P. and L. Wu (2016). Analyzing volatility risk and risk premium in option contracts: A new theory. *Journal of Financial Economics 120*(1), 1–20. 5

Carrasco, M., M. Chernov, J.-P. Florens, and E. Ghysels (2007). Efficient estimation of general dynamic models with a continuum of moment conditions. *Journal of Econometrics 140*(2), 529–573. 146

Carrasco, M. and R. Kotchoni (2017). Efficient estimation using the characteristic function. *Econometric Theory 33*(2), 479–526. 146

Casella, G. and R. L. Berger (2002). *Statistical inference*, Volume 2. Duxbury Pacific Grove, CA. 64

Castagna, A. and F. Mercurio (2007). Option pricing: The Vanna-Volga method for implied volatilities. *Risk 20*(1), 106. 20, 33

Chalamandaris, G. and A. E. Tsekrekos (2010). Predictable dynamics in implied volatility surfaces from otc currency options. *Journal of Banking & Finance 34*(6), 1175–1188. 194

Christoffersen, P., B. Feunou, K. Jacobs, and N. Meddahi (2014). The economic value of realized volatility: using high-frequency returns for option valuation. *Journal of Financial and Quantitative Analysis 49*(03), 663–697. 34, 47

Christoffersen, P., B. Feunou, and Y. Jeon (2015). Option valuation with observable volatility and jump dynamics. *Journal of Banking & Finance 61*, S101–S120. 100, 101, 103, 118

Christoffersen, P., S. Heston, and K. Jacobs (2006). Option valuation with conditional skewness. *Journal of Econometrics 131*(1), 253–284. 34

Christoffersen, P., S. Heston, and K. Jacobs (2013). Capturing option anomalies with a variance-dependent pricing kernel. *The Review of Financial Studies 26*(8), 1963–2006. 101

Christoffersen, P. and K. Jacobs (2004a). The importance of the loss function in option valuation. *Journal of Financial Economics 72*(2), 291–318. 34

Christoffersen, P. and K. Jacobs (2004b). Which garch model for option valuation? *Management science 50*(9), 1204–1221. 34

Christoffersen, P., K. Jacobs, and K. Mimouni (2010). Volatility dynamics for

the S&P500: evidence from realized volatility, daily returns, and option prices. *Review of Financial Studies 23*(8), 3141–3189. 34

Clark, I. J. (2011). *Foreign exchange option pricing: a practitioner's guide*. John Wiley & Sons. 20

Codogno, L. and P. de Grauwe (2015). Why denmark should either abandon its peg to the euro or join the single currency. *LSE European Politics and Policy (EUROPP) Blog*. 143

Conley, T., L. P. Hansen, E. Luttmer, and J. Scheinkman (1995). Estimating subordinated diffusions from discrete time data. *The Review of Financial Studies 10*, 525–577. 146

Cox, J. C., J. E. Ingersoll Jr, and S. A. Ross (1985). An intertemporal general equilibrium model of asset prices. *Econometrica: Journal of the Econometric Society*, 363–384. 25, 145

Creel, M. and D. Kristensen (2015). Abc of sv: Limited information likelihood inference in stochastic volatility jump-diffusion models. *Journal of Empirical Finance 31*, 85–108. 146

Da Fonseca, J., M. Grasselli, and F. Ielpo (2014). Estimating the wishart affine stochastic correlation model using the empirical characteristic function. *Studies in Nonlinear Dynamics & Econometrics 18*(3), 253–289. 146

Da Fonseca, J., M. Grasselli, and C. Tebaldi (2007). Option pricing when correlations are stochastic: an analytical framework. *Review of Derivatives Research 10*(2), 151–180. 145

Diebold, F. X. and R. S. Mariano (1995). Comparing predictive accuracy. *Journal of Business & Economic Statistics 13*(3), 253–263. 77, 90

Ding, Z., C. W. Granger, and R. F. Engle (1993). A long memory property of stock market returns and a new model. *Journal of Empirical Finance 1*(1), 83–106. 31

Doust, P. (2012). The stochastic intrinsic currency volatility model: a consistent framework for multiple fx rates and their volatilities. *Applied Mathematical Finance 19*(5), 381–445. 33, 97

Du, D. (2013). General equilibrium pricing of currency and currency options. *Journal of Financial Economics 110*(3), 730–751. 28, 29

Du, W., A. Tepper, and A. Verdelhan (2018). Deviations from covered interest rate parity. *The Journal of Finance 73*(3), 915–957. 6, 128, 145

Duan, J.-C. (1995). The GARCH option pricing model. *Mathematical finance 5*(1), 13–32. 28, 34

Duan, J.-C. (1997). Augmented GARCH(p, q) process and its diffusion limit. *Journal of Econometrics 79*(1), 97–127. 34, 35, 101

Duffie, D. and P. Glynn (2004). Estimation of continuous-time markov processes sampled at random time intervals. *Econometrica 72*(6), 1773–1808. 146

Duffie, D., J. Pan, and K. Singleton (2000). Transform analysis and asset pricing for affine jump-diffusions. *Econometrica 68*(6), 1343–1376. 108, 145, 173

Dupoyet, B. V. (2006). Information content of cross-sectional option prices: A comparison of alternative currency option pricing models on the japanese yen. *The Journal of Futures Markets 26*(1), 33–59. 29

Elerian, O., S. Chib, and N. Shephard (2001). Likelihood inference for discretely observed nonlinear diffusions. *Econometrica 69*(4), 959–993. 146

Engle, R. and I. Ishida (2002). Forecasting variance of variance: The square-root, the affine, and the cev garch models. *Department of Finance Working Papers, New York University*. 31

Engle, R., T. Ito, and W.-L. Lin (1990). Meteor showers or heat waves? heteroskedastic intra-daily volatility in the foreign exchange market. *Econometrica 58*(3), 525–42. 30

Engle, R. F. and C. Mustafa (1992). Implied arch models from options prices. *Journal of Econometrics 52*(1-2), 289–311. 28

Engle, R. F. and V. K. Ng (1993). Measuring and testing the impact of news on volatility. *The Journal of Finance 48*(5), 1749–1778. 35, 100

Eraker, B. (2004). Do stock prices and volatility jump? Reconciling evidence from spot and option prices. *The Journal of Finance 59*(3), 1367–1403. 101

Eraker, B., M. Johannes, and N. Polson (2003). The impact of jumps in volatility and returns. *The Journal of Finance 58*(3), 1269–1300. 101

Fama, E. F. (1984). Forward and spot exchange rates. *Journal of Monetary Economics 14*(3), 319–338. 144

Fleming, J. and C. Kirby (2003). A closer look at the relation between GARCH and stochastic autoregressive volatility. *Journal of Financial Econometrics 1*(3), 365–419. 37

Gallant, A. R. and G. Tauchen (1996). Which moments to match? *Econometric Theory 12*(4), 657–681. 146

Garman, M. B. and S. W. Kohlhagen (1983). Foreign currency option values. *Journal of International Money and Finance 2*(3), 231–237. 27, 37, 40, 58, 145

Giacomini, R. and B. Rossi (2016). Model comparisons in unstable environments. *International Economic Review 57*(2), 369–392. 77, 90

Giacomini, R. and H. White (2006). Tests of conditional predictive ability. *Econometrica 74*(6), 1545–1578. 77, 90

Gil-Pelaez, J. (1951). Note on the inversion theorem. *Biometrika 38*(3-4), 481–482. 54

Goldberg, D. (2017). Predicting pegged exchange rate currency collapse: A literature review. 143

Gourieroux, C. and A. Monfort (1993). Simulation-based inference: A survey with special reference to panel data models. *Journal of Econometrics 59*(1-2), 5–33. 146

Gourieroux, C., H. T. Nguyen, and S. Sriboonchitta (2017). Nonparametric estimation of a scalar diffusion model from discrete time data: a survey. *Annals of Operations Research 256*(2), 203–219. 146

Guimaraes, B. (2008). Vulnerability of currency pegs: evidence from brazil. 143

Hagan, P. S., D. Kumar, A. S. Lesniewski, and D. E. Woodward (2002). Managing smile risk. *The Best of Wilmott 1*, 249–296. 30, 100, 145

Hanke, M., R. Poulsen, and A. Weissensteiner (2018). Event-related exchange rate forecasts combining information from betting quotes and option prices. *Journal of Financial and Quantitative Analysis*. 6, 146, 170, 194

Hansen, L. P. and R. J. Hodrick (1980). Forward exchange rates as optimal predictors of future spot rates: An econometric analysis. *Journal of Political Economy 88*(5), 829–853. 144

Hansen, P. R. and A. Lunde (2005). A forecast comparison of volatility models: does anything beat a garch (1, 1)? *Journal of Applied Econometrics 20*(7), 873–889. 77

Heston, S. L. (1993). A closed-form solution for options with stochastic volatility with applications to bond and currency options. *Review of Financial Studies 6*(2), 327–343. 24, 30, 100, 145

Heston, S. L. and S. Nandi (1999). A discrete-time two-factor model for pricing bonds and interest rate derivatives under random volatility. Technical report, FRB Atlanta Working Paper Series No. 99-20; Robert H. Smith School Research Paper No. RHS 2491281. Available at SSRN: http://ssrn.com/abstract=2491281. 34, 35, 47, 53

Heston, S. L. and S. Nandi (2000). A closed-form garch option valuation model.

Review of Financial Studies 13(3), 585–625. 7, 25, 28, 33, 34, 35, 47, 51, 53, 58, 59, 96, 140, 194

Huang, X. and T. Tauchen (2005). The relative contribution of jumps to total price variance. *Journal of Financial Econometrics 3*(3), 456–499. 118, 119

Hurn, A., K. Lindsay, and A. McClelland (2013). A quasi-maximum likelihood method for estimating the parameters of multivariate diffusions. *Journal of Econometrics 172*(1), 106–126. 146

Ilzetzki, E., C. M. Reinhart, and K. S. Rogoff (2017, February). Exchange arrangements entering the 21st century: Which anchor will hold? Working Paper 23134, National Bureau of Economic Research. 143

IMF (2016). Annual report on exchange arrangements and exchange restrictions. Technical report, International Monetary Fund. 142, 159

Ingersoll, J. E. (1987). *Theory of Financial Decision Making*, Volume 3. Rowman & Littlefield. 53, 54

Jacod, J., V. Todorov, et al. (2018). Limit theorems for integrated local empirical characteristic exponents from noisy high-frequency data with application to volatility and jump activity estimation. *The Annals of Applied Probability 28*(1), 511–576. 6, 118, 146

Jain, A. and M. Stafford (2006). DB guide to risk reversals: How to value risk reversal contracts and identify relative value trading opportunities. Technical report, Deutsche Bank. 28

Jiang, G. J. and J. L. Knight (2002). Estimation of continuous-time processes via the empirical characteristic function. *Journal of Business & Economic Statistics 20*(2), 198–212. 146

Lee, S. and P. A. Mykland (2008). Jumps in financial markets: A new nonparametric test and jump dynamics. *Review of Financial Studies 21*(6), 2535–2563. 118, 120

Lévy, P. (1925). *Calcul des probabilités*, Volume 9. Gauthier-Villars Paris. 54

Li, C. et al. (2013). Maximum-likelihood estimation for diffusion processes via closed-form density expansions. *The Annals of Statistics 41*(3), 1350–1380. 145

Li, C. and D. Chen (2016). Estimating jump–diffusions using closed-form likelihood expansions. *Journal of Econometrics 195*(1), 51–70. 145

Li, J., V. Todorov, and G. Tauchen (2014). Jump regressions. Technical report, Technical report, Duke Univeristy. 118

Li, K. (2017). Weakness in hk currency board system and trading opportunities in betting a de-peg of the hong kong dollar. *International Finance and Banking 4*(1), 95–107. 143

Lin, C.-H., S.-K. Lin, and A.-C. Wu (2015). Foreign exchange option pricing in the currency cycle with jump risks. *Review of Quantitative Finance and Accounting 44*(4), 755–789. 101, 144

Liu, L. Y., A. J. Patton, and K. Sheppard (2015). Does anything beat 5-minute

rv? a comparison of realized measures across multiple asset classes. *Journal of Econometrics 187*(1), 293–311. 124

Londono, J. M. and H. Zhou (2017). Variance risk premiums and the forward premium puzzle. *Journal of Financial Economics 124*(2), 415–440. 145

López-Suárez, C. F. and R. Razo-Garcia (2017). Speculative attacks in a two-peg model. *Journal of International Money and Finance 70*, 234–256. 143

Lustig, H. and A. Verdelhan (2007). The cross section of foreign currency risk premia and consumption growth risk. *American Economic Review 97*(1), 89–117. 143

Melino, A. and S. M. Turnbull (1990). Pricing foreign currency options with stochastic volatility. *Journal of Econometrics 45*(1), 239 – 265. 30

Nakatani, R. (2017). Real and financial shocks, exchange rate regimes and the probability of a currency crisis. *Journal of Policy Modeling*. 143

Ornthanalai, C. (2014). Levy jump risk: Evidence from options and returns. *Journal of Financial Economics 112*(1), 69–90. 100, 101, 103

Pagliarani, S. and A. Pascucci (2012). Local stochastic volatility with jumps. *Preprint available on SSRN*. 30, 100

Pan, J. (2002). The jump-risk premia implicit in options: Evidence from an integrated time-series study. *Journal of Financial Economics 63*(1), 3–50. 100, 101, 145, 146, 163

Protter, P. E. (2004). Stochastic integration and differential equations. 104, 147

Reghai, A., V. Klaeyle, and A. Boukhaffa (2012). LSV models with a mixing weight. *Available at SSRN 2008207*. 30, 100

Reus, L. and J. M. Mulvey (2016). Dynamic allocations for currency futures under switching regimes signals. *European Journal of Operational Research 253*(1), 85–93. 143

Rubinstein, M. (1976). The valuation of uncertain income streams and the pricing of options. *The Bell Journal of Economics*, 407–425. 37

Särkkä, S., J. Hartikainen, I. S. Mbalawata, and H. Haario (2015). Posterior inference on parameters of stochastic differential equations via non-linear gaussian filtering and adaptive mcmc. *Statistics and Computing 25*(2), 427–437. 146

Sercu, P. and R. Uppal (1995). *International financial markets and the firm*. South-Western Publishing/Chapman & Hall; Ohio/London. 11

Shastri, K. and K. Tandon (1986). Valuation of foreign currency options: some empirical tests. *Journal of Financial and Quantitative Analysis 21*(02), 145–160. 30

Shiraya, K. and A. Takahashi (2013). Pricing basket options under local stochastic volatility with jumps. *Available at SSRN 2372460*. 30, 100

Singleton, K. J. (2001). Estimation of affine asset pricing models using the empirical characteristic function. *Journal of Econometrics 102*(1), 111–141. 146

Sundaresan, S. M. (2000). Continuous-time methods in finance: A review and an assessment. *The Journal of Finance 55*(4), 1569–1622. 101

Tauchen, G. and H. Zhou (2011). Realized jumps on financial markets and predicting credit spreads. *Journal of Econometrics 160*(1), 102–118. 118, 119, 120, 132

Vasicek, O. (1977). An equilibrium characterization of the term structure. *Journal of Financial Economics 5*(2), 177–188. 145

Yu, J. (2007). Closed-form likelihood approximation and estimation of jump-diffusions with an application to the realignment risk of the chinese yuan. *Journal of Econometrics 141*(2), 1245–1280. 144, 145, 148

Zhao, Z. and W. B. Wu (2009). Nonparametric inference of discretely sampled stable lévy processes. *Journal of Econometrics 153*(1), 83–92. 146